UNIVERSITÀ
DEGLI STUDI
FIRENZE

DOTTORATO DI RICERCA IN SCIENZE CLINICHE
Indirizzo in Fisiopatologia Clinica e dell'Invecchiamento

CICLO XXVII

COORDINATORE Prof. Giacomo Laffi

Role of Transient Receptor Potential Ankyrin 1 (TRPA1) channel in anticancer drugs-induced peripheral neuropathy and pain

Settore Scientifico Disciplinare MED/09

Dottoranda
Dr.ssa Camilla Fusi

Tutore
Prof. Pierangelo Geppetti

Coordinatore
Prof. Giacomo Laffi

Anni 2012/2014

Index

Chapter I – Introduction

1.1 The primary afferent nociceptors

According to the International Association for the Study of Pain (IASP), pain is defined as "an unpleasant sensory and emotional experience associated with actual or potential tissue damage, or described in terms of such damage". The sensory experience begins in the periphery, where the peripheral terminals of primary afferent fibers respond to a myriad of stimuli and translate this information into the dorsal horn of the spinal cord, where the central ends of these fibers terminate. Nearly a century ago, Sherrington proposed the existence of the nociceptor, a primary sensory neuron that is activated by stimuli capable of causing tissue damage [1]. According to this model, nociceptors have characteristic thresholds or sensitivities that distinguish them from other sensory nerve fibers. Electrophysiological studies have, in fact, shown the existence of primary sensory neurons that can be excited by noxious heat, intense pressure or irritant chemicals, but not by innocuous stimuli such as warming or light touch [2]. Primary afferent fibers have a unique morphology, called pseudo-unipolar, wherein both central and peripheral terminals emanate from a common axonal stalk. Primary sensory neurons have the cell somata in sensory ganglia, dorsal root and trigeminal ganglia (DRG and TG, respectively). The peripheral axon of these neurons innervates tissue, such as skin and whose terminals react to sensory stimuli, and the central axon enters the spinal cord, where it forms synapse with second order neurons to transfer information to the central nervous system (CNS). Many neurons innervating the viscera are located in the nodose ganglia and their peripheral fibers travel with the vagus nerve whereas their central axons project to the area postrema. All sensory system form an anatomic connection between the potentially harmful external and internal milieu and the CNS and convert all the stimuli into electro-chemical signals. The heterogeneous population of sensory fibers originated from the ganglia can be distinguished into three main groups based on anatomical and functional criteria (Fig. I-

1). Cell bodies with the largest diameters give rise to myelinated, rapidly conducting Aβ primary sensory fibers. Most, but not all, Aβ fibers detect innocuous stimuli applied to skin, muscle and joints and thus do not contribute to pain. By contrast, small- and medium-diameter cell bodies give rise to most of the nociceptors, including unmyelinated, slowly conducting C-fibers and thinly myelinated, more rapidly conducting Aδ fibers (Fig. I-1a). It has long been assumed that Aδ and C nociceptors mediate "first" and "second" pain, respectively, namely the rapid, acute, sharp pain and the delayed, more diffuse, dull pain evoked by noxious stimuli (Fig. I-1b). There are two main classes of Aδ nociceptor and both respond to intense mechanical stimuli, but can be distinguished by their differential responsiveness to intense heat or how they are affected by tissue injury. The Aδ and C nociceptive fibers either respond to one type of physical stimulus (unimodal nociceptors), or more commonly integrate and generate a response to potentially damaging thermal, mechanical and/or chemical stimuli (polymodal nociceptors) [2].

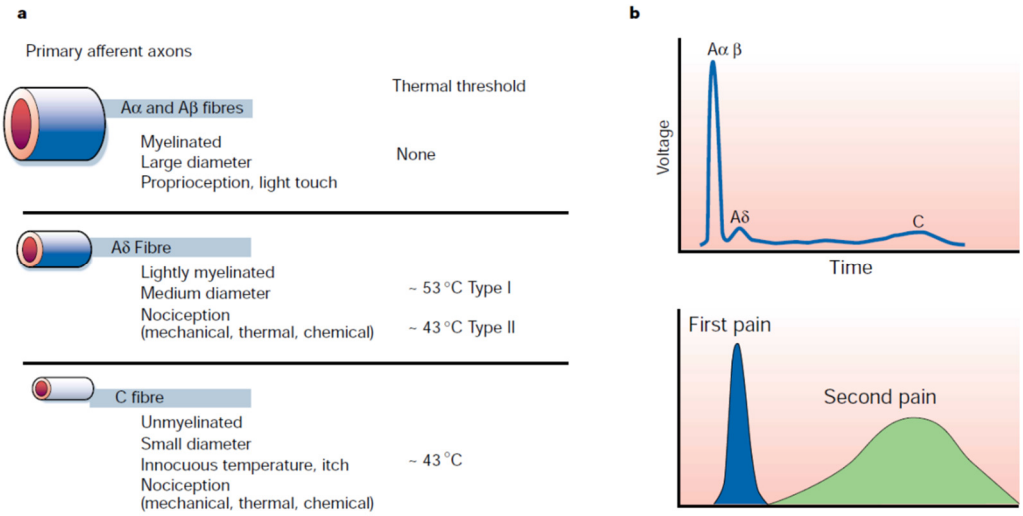

Figure I-1. Different nociceptors detect different types of pain. a Peripheral nerves include small-diameter (Aδ) and medium- to large-diameter (Aα,β) myelinated afferent fibres, as well as small-diameter unmyelinated afferent fibres (C). **b** Conductive velocity is related to fiber diameter. Aδ and C nociceptors mediate "first" and "second" pain. From [1].

As described, primary sensory neurons are the interface of the nervous system with the external and internal environment of our body. A major function of the sensory apparatus is to detect potentially damaging stimuli and warn of the risk of injury. All primary sensory nociceptors make synaptic connections with neurons in the grey matter (dorsal horn) of the spinal cord. Subsets of dorsal horn neurons, in turn, project axons and transmit pain messages to higher brain centers, including the reticular formation,

thalamus and ultimately the cerebral cortex (Fig. I-2). Primary afferent nerve fibers project to the dorsal horn of the spinal cord, which is organized into anatomically and electrophysiological distinct laminae. For example, the spinal cord neurons within lamina I and II are generally responsive to noxious stimulation (*via* Aδ and C fibers), neurons in laminae III and IV are primarily responsive to innocuous stimulation (*via* Aβ), and neurons in lamina V receive a convergent non-noxious and noxious input *via* direct (monosynaptic) Aδ and Aβ inputs and indirect (polysynaptic) C fiber inputs [3] (Fig. I-2). In animal model, the expression of c-Fos protein is a useful marker for monitoring neural activities in the central pathways of the sensory system, particularly in the pain pathway including thermal, mechanical and chemical stimuli [4]. Spinal neurons that express c-Fos after noxious stimulation are located in laminae I and II, and laminae V and VI of the dorsal horn.

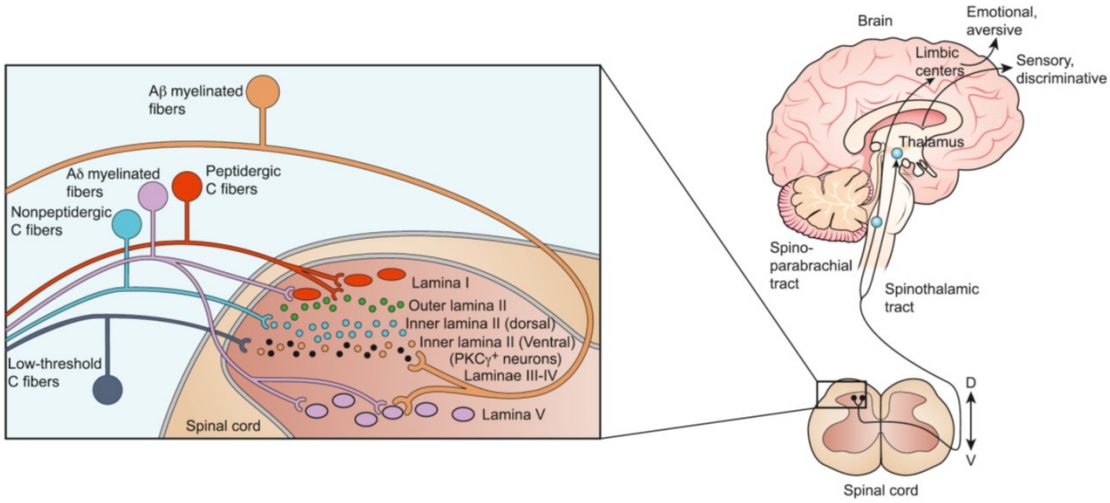

Figure I-2. Spinal Cord Neuroanatomy: inputs and projections. Different populations of primary afferent fibers target different regions of the dorsal horn of the spinal cord, with the input from C nociceptors concentrated in the superficial dorsal horn (laminae I and II). The small myelinated Aδ nociceptors target both laminae I and V. The low-threshold C mechanoreceptors, in contrast, target neurons in the ventral part of inner lamina II, which contains many PKCγ-expressing populations of interneurons. The right side of the Fig. illustrates the major ascending pathways that derive from the spinal cord dorsal horn. From [292].

Most C-fibers nociceptors respond to noxious chemical stimuli such as capsaicin, the pungent ingredient in hot chili peppers, and for this reason they are defined as capsaicin-sensitive sensory neurons. Histochemical studies of adult DRG reveal two broad classes of unmyelinated C-fiber. The so-called peptidergic population contains the peptide neurotransmitter substance P (SP), and expresses TrkA, the high-affinity tyrosine kinase receptor for nerve growth factor (NGF) [5]. The second

population does not express SP or TrkA, but can be labelled selectively with the α-D-galactosyl-binding lectin IB4, and expresses P2X3 receptors, a specific subtype of ATP-gated ion channel. This categorization is a first approximation at best, as additional molecular markers become available, new subsets are likely to be recognized. The ability of sensing and transmitting noxious stimuli and nociceptive information is intrinsically associated to the release of neuropeptides from their peripheral terminals. The ionic event, gating by noxious stimuli, results in an excitatory effect with the subsequent depolarization of the nerve fibers and the initiation of an action potential propagation. Ca^{2+} influx into the peptidergic nerve endings causes the local release of neuropeptides, including calcitonin gene-related peptide (CGRP) and the tachykinins, SP and neurokinin A (NKA). Activation of CGRP and tachykinin receptors (NK1, NK2 and NK3) on effector cells, particularly at the vascular levels, causes a series of inflammatory responses, collectively referred to as neurogenic inflammation [6]. Sir Thomas Lewis in his pioneering studies [7] precisely defined the dual "nocifensor" role of these neurons as characterized by the capacity of one portion of the widely branching sensory fiber to respond to the injury, and to generate action potentials, which are carried, antidromically, to other branches of the fiber, where they release a chemical substance that causes the flare and increases the sensitivity of other sensory axons responsible for pain. There is now a bulk of information suggesting that this phenomenon, firstly described at the somatic (skin) level, occurs in a variety of visceral organs. In addition, sensory neuropeptide release may occur not only from collateral fibers invaded antidromically by action potentials, through a tetrodotoxin-sensitive axon reflex, but also, as in the case of capsaicin, by the stimulated terminal itself *via* a tetrodotoxin-insensitive mechanism [8].

1.1.1 **Neurogenic inflammation**

The term neurogenic inflammation refers to a series of responses that occur at peripheral level following the activation of capsaicin-sensitive sensory neurons, mainly present at the vascular level. These events also occur in other tissues and organs with a large variability according to the mammal species under investigation. At the vascular level, the release of CGRP, SP and NKA induces vasodilatation, mediated by CGRP, plasma protein extravasation and leukocyte adhesion to the vascular endothelium of postcapillary venules, mediated by SP/NKA and the NK1 receptor [6]. In non-vascular

tissues, neurogenic inflammatory responses include cardiac positive chronotropic effects (CGRP-mediated), contraction of the smooth muscle of the iris sphincter (SP/NKA, NK2 receptor), ureter, bladder neck and urethra (SP/NKA, NK2/NK1 receptors), relaxation of bladder dome (CGRP), exocrine gland secretion (SP/NKA, NK1 receptor). Species-related variations in neurogenic inflammatory responses are clearly illustrated by the motor effect produced by sensory nerve activation and tachykinins in the airways. The release of SP/NKA from capsaicin-sensitive nerve terminals causes direct bronchoconstriction in the guinea-pig, indirect and nitric oxide/prostanoid-mediated bronchodilatation in the rat and mouse. In humans, as in guinea-pigs, activation of both NK2 and, in part, NK1 receptors mediates a robust bronchoconstriction in human isolated bronchi [9]. Of particular interest is the ability of tachykinins (NK1) to stimulate seromucous secretion [10] from bronchial glands, and to excite (NK3) postganglionic cholinergic nerve terminals in the human bronchus [11]. Neurogenic inflammation markedly contributes to inflammatory responses both at the somatic and visceral levels in different mammal species. In the human skin there is strong evidence that capsaicin or histamine cause a flare response that is blocked by local anesthetics or by repeated application of topical capsaicin (capsaicin desensitization), is mediated by stimulation of terminals of capsaicin-sensitive neurons and the subsequent release of neuropeptides. Less clear is, however, whether in man, neurogenic inflammation plays a pathophysiological role at the visceral level. There is evidence that CGRP is released by capsaicin from human tissues *in vitro* [12] and during migraine attacks [13]. A major role of CGRP released from trigeminal perivascular nerve fibers derived from the observation that BIBN 4096BS, a peptoid with high affinity for the CGRP receptor [14] that does not cross the blood brain barrier, reduces the pain and other symptoms associated with migraine attacks [15]. This finding supports the hypothesis that sensory CGRP is released from terminals of primary sensory neurons and exerts a pathophysiological role in human disease.

1.2 **Pain classification**

Pain is a multidimensional sensory experience that is intrinsically unpleasant and associated with hurting and soreness. It may vary in intensity (mild, moderate, or severe), quality (sharp, burning, or dull), duration (transient, intermittent, or persistent), and referral (superficial or deep, localized or diffuse). Although it is essentially a

sensation, pain has strong cognitive and emotional components; it is linked to, or described in terms of, suffering. It is also associated with avoidance motor reflexes and alterations in autonomic output. All of these traits are inextricably linked to the experience of pain. Pain can be essentially divided into two broad categories: adaptive and maladaptive. Adaptive pain contributes to survival by protecting the organism from injury or promoting healing when injury has occurred. Maladaptive pain, in contrast, is an expression of the pathologic operation of the nervous system; it is pain as disease. The sensory experience of acute pain caused by a noxious stimulus is mediated by the nociceptive system. To prevent damage to tissue, we have learnt to associate certain categories of stimuli with danger that must be avoided if at all possible. This association is formed by linking noxious stimuli with a sensation that is intense and unpleasant: that is, pain. The sensation of pain must be strong enough that it demands immediate attention. This nociceptive pain system is a key early warning device, an alarm system that announces the presence of a potentially damaging stimulus. Nociceptive pain must be controlled only under specific clinical situations, such as during surgery or medical procedures that damage tissue and after trauma. It is important that this system not be chronically disabled, because loss of its protective function inevitably leads to tissue damage, including self-induced mutilation of the tongue and lips, destruction of joints, loss of the tips of fingers, and pressure ulcers. Nociceptive pain is therefore a vital physiologic sensation. Lack of it in patients with congenital insensitivity to pain due to a mutation of the NGF tyrosine kinase A receptor, which results in a loss of high-threshold sensory neurons, reduces life expectancy [16]. If tissue damage occurs despite the nociceptive defensive system (for example, through trauma, surgery, or inflammatory diseases), the body shifts from protecting against noxious, potentially damaging stimuli to promoting healing of the injured tissue. The term inflammatory pain is used to accomplish this goal. In this state, sensitivity is increased such that stimuli to the affected part that would normally not cause pain now do so. Peripheral sensitization is produced when nociceptor terminals become exposed to products of tissue damage and inflammation, referred to collectively as the “inflammatory soup” [2]. Some of the main components of the “inflammatory soup” include peptides (bradykinin, BK), lipids (prostaglandins), neurotransmitters (serotonin and ATP) and neurotrophins (NGF). The acidic nature of the “inflammatory soup” is also an important factor. Each of these factors sensitize or excite the terminals of the nociceptor by interacting with cell-surface receptors expressed by nociceptor neurons [2]. As a result,

we prevent contact with or movement of the injured part until repair is complete, minimizing further damage. Inflammatory pain typically decreases as the damage and inflammatory response resolve.

Maladaptive pain is uncoupled from a noxious stimulus or healing tissue. Such pain may occur in response to damage to the nervous system (neuropathic pain) or result from abnormal operation of the nervous system (functional pain). Maladaptive pain is the expression of abnormal sensory processing and usually is persistent or recurrent. This is an area of enormous unmet clinical need because treatment options are limited and our understanding incomplete. Essentially, in maladaptive pain, the fire alarm system is constantly switched on even though there is no emergency, or repeated false alarms occur. Neuropathic pain may result from lesions to the peripheral nervous system, as in patients with diabetic or AIDS polyneuropathy, post-herpetic neuralgia, or lumbar radiculopathy, or to the central nervous system, such as in patients with spinal cord injury, multiple sclerosis, or stroke [17]. Functional pain is an evolving concept. In this form of pain sensitivity, no neurologic deficit or peripheral abnormality can be detected. The pain is due to an abnormal responsiveness or function of the nervous system, in which heightened gain or sensitivity of the sensory apparatus amplifies symptoms. Several common conditions have features that may place them this category: for example, fibromyalgia, irritable bowel syndrome, some forms of noncardiac chest pain, and tension-type headache [18-20]. It is not known why the central nervous system of patients with functional pain displays abnormal sensitivity or hyperresponsiveness. Although inflammatory, neuropathic, and functional pain each have different causes, they share some characteristics. The pain in these syndromes may arise spontaneously in the apparent absence of any peripheral stimulus, or it may be evoked by stimuli. Evoked pain may arise from a low-intensity, normally innocuous stimulus, such as a light touch to the skin in a patient with post-herpetic neuralgia or vibration during an acute attack of gout, or it may be an exaggerated and prolonged response to a noxious stimulus. The former condition is called allodynia and the latter hyperalgesia. Spontaneous pain and changes in sensitivity to stimuli are fundamental features of clinical pain, distinguishing it from nociceptive pain, in which pain occurs only in the presence of an intense or noxious stimulus.

Classic migraine is in a category of its own. It is an episodic neurologic condition that has been related to abnormal cortical activity that alters sensory input from dural and cerebrovascular sensory fibers and is associated with an abnormal

sensory processing in the brainstem. It possesses features of inflammatory and functional pain, as well as of objective neurologic dysfunction [287, 21].

Pain caused by cancer varies greatly in character and source; it depends on the tumor, its location, and its proximity to other tissues. In some cases, tumor cells produce chemical signals that contribute directly to the pain, as in osteosarcomas. In other tumors, the pain may be due to mechanical compression or invasion of a nerve, distention of an organ, ischemia, or an inflammatory reaction to tissue necrosis. It may also represent a neurotoxic side effect of chemotherapy [22].

1.2.1 Chemotherapy-induced peripheral neuropathy

Chemotherapy-induced peripheral neuropathy (CIPN) is a potentially dose limiting side effect of commonly used chemotherapeutic agents like taxanes, vinca-alkaloids, platinum compounds, bortezomib and thalidomide. Symptoms are predominantly sensory, ranging from a mild tingling sensation to spontaneous burning pain and hypersensitivity to stimuli. These symptoms often affect both hands and feet and may spread into a “glove and stocking” distribution. Sometimes there are motor symptoms like weakness, autonomic neuropathy and incidentally cranial nerve involvement. CIPN leads to a lower quality of life and often causes patients to discontinue chemotherapy [23]. The incidence of CIPN depends on the dose, mainly cumulative, the type of agent, and concomitant use of other neurotoxic agents. Moreover, the development of chemotherapy side effects may be influenced by the age of the patients and preexisting conditions that potentially cause nerve damages, such as diabetes and use of alcohol [23]. CIPN can begin weeks to months after initial treatment and reach a peak at, or after, the end of treatment and it is most frequently associated with axonal degeneration. Usually, this axonopathy occurs weeks to months after exposure to the medication, may continue despite withdrawal of the drug, and may be irreversible. If the degree of axonal degeneration is mild, then complete regeneration may occur. However, if there is injury to the dorsal root ganglion resulting in neuronal apoptosis, then the sensory neuropathy is severe and usually irreversible [24]. The toxic effects of chemotherapy target the structures and functions of the peripheral nervous system, including neuronal cell bodies, axons, myelin sheath, and supporting glial cells. Most toxic neuropathies affect axons, resulting in an axonopathy and causing distal, symmetric, sensory-predominant neuropathy that exhibits a “dying-back” pattern. The

most distal portions of axons are usually the first that undergo degeneration, and axonal atrophy advances slowly towards the cell body. These effects lead to sensory disturbances with a symmetrical "glove and stocking" distribution. In its most severe form, it will lead to wallerian (or secondary) degeneration of the surrounding nerve sheath (i.e., demyelination) distal to the injury. Neuronal cell body damage results in neuronopathies and manifests as global nerve cell failure. Patients will first notice paresthesias, pain, or both, in the toes and feet that with time and continued insult will advance proximally. By the time the fingertips are affected, a tear-drop pattern of sensory loss and dysesthesias appears the abdominal wall, and sensory distortion will have migrated proximally up the leg, approaching or passing the knee. Myalgias are another presentation of neuropathic pain, and patients complain of muscle cramps and aching that are frequently exacerbated by activity.

1.2.1.1 Paclitaxel-induced neuropathic pain

Paclitaxel (Taxol) belongs to the taxane family and it is active against a broad range of solid neoplasms that are generally considered to be refractory to conventional chemotherapy. Paclitaxel is a microtubule targeting agent. Microtubules are composed of polymers of tubulin in dynamic equilibrium with tubulin heterodimers composed of alpha and beta protein subunits. Although their principal function is the formation of the mitotic spindle during cell division, microtubules are also involved in many vital interphase functions, including the maintenance of shape, motility, signal transmission, and intracellular transport. Unlike other antimicrotubule drugs, such as vinca-alkaloids, which induce the disassembly of microtubules, paclitaxel promotes the polymerization of tubulin. At subnanomolar concentrations, paclitaxel inhibits the disassembly of microtubules, whereas it increases their mass and numbers at higher, albeit clinically achievable, concentrations. The microtubules formed in the presence of paclitaxel are extraordinarily stable and dysfunctional, thereby causing the death of the cell by disrupting the normal microtubule dynamics required for cell division and vital interphase processes. Paclitaxel binds to the N-terminal 31 aminoacids of the beta-tubulin subunit in the microtubule, rather than to tubulin dimers.

Paclitaxel-induced neurotoxicity typically presents a sensory neuropathy with the most common complaints being numbness, tingling and burning pain. More pronounced symptoms are tingling and allodynia that typically occur in a "glove and

stocking" distribution. Sensory symptoms usually start symmetrically in the feet, but also appear simultaneously in both hands and feet [25]. Many cases resolve briefly after paclitaxel discontinuation, but the sensory abnormalities and pain can be long-lasting [26]. Symptoms may begin as soon as 24 to 72 hours after treatment with higher doses (> 250 mg per square meter) but usually occur only after multiple courses at conventional doses (135 to 250 mg per square meter). Severe neurotoxicity precludes the administration of paclitaxel doses above 250 mg per square meter over a period of 3 or 24 hours, but severe neurotoxicity is rare at conventional doses (< 200 mg per square meter), even in patients who have previously received other neurotoxic agents, such as cisplatin. Motor and autonomic dysfunction may also occur, especially at high doses and in patients with preexisting neuropathies caused by diabetes mellitus and alcoholism. Transient myalgia, usually noted two to five days after therapy, is also common at doses above 170 mg per square meter, and myopathy has been noted with high doses of paclitaxel (> 250 mg per square meter) in combination with cisplatin.

1.2.1.2 Bortezomib-induced neuropathic pain

Bortezomib (BTZ) is a modified dipeptidyl boronic acid authorized for the treatment of multiple myeloma and mantle cell lymphoma [27-29]. Bortezomib is a 20S proteasome complex inhibitor that acts by disrupting various cell signaling pathways, thereby leading to cell cycle arrest, apoptosis, and inhibition of angiogenesis. The hallmark of bortezomib action is the inhibition of NF-κB, thereby interfering with NF-κB-mediated cell survival, tumor growth, and angiogenesis [30]. Peripheral neuropathy is a significant dose-limiting toxicity of bortezomib that typically occurs within the first courses of bortezomib, reaches a plateau at cycle 5, and thereafter does not appear to increase [31, 32] (Fig. I-3).

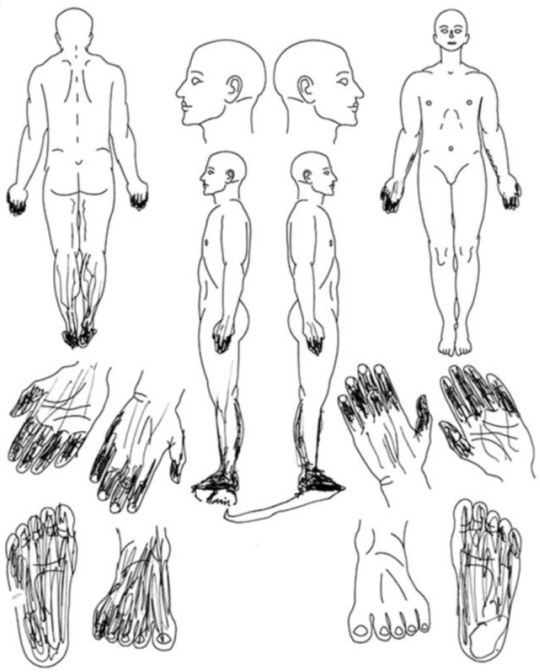

Figure I-3. Representative pain diagram completed by a patient with bortezomib-induced neuropathic pain. Darkly shaded areas show where the patient complained of ongoing pain. This area was described as "burning" and "numb." Lightly shaded area shows the border area of altered sensibility. This area was described as "tingling." A typically sharp boundary between the areas affected and "normal" skin was indicated by the lack of drawing above the wrists. From [293].

According to the results of major phase 2/3 clinical trials, the incidence of bortezomib-induced peripheral neuropathy (BIPN) ranges from 31 to 45%. Pre-treatment with other neurotoxic antineoplastic drugs, such as vincristine and thalidomide, is associated with even higher percentages (18-37%) of clinically significant BIPN. Dose reduction or treatment discontinuation occurs in up to 12% of BTZ-treated patients, mostly occurring in those with pre-existing neuropathy due to exposure to other neurotoxic chemotherapies [32, 33]. BTZ therapy can also evoke autonomic dysfunction in 12-50% of patients, with constipation (12%) and orthostatic hypotension (50%) being the most frequent symptoms [33, 34]. The improvement or resolution of BIPN is normally observed in up to 85% of patients between 2 and 3.5 months after discontinuation of BTZ treatment [31-33]. To date, several agents, including various opioids, tricyclic antidepressants, anticonvulsants, serotonin-norepinephrine reuptake inhibitors, non-steroidal anti-inflammatory agents, vitamins and nutritional supplements, have been tested for their efficacy to symptomatically treat the neuropathic pain component in the context of BIPN [35]. However, based on results

from randomized controlled trials, only duloxetine, a serotonin-norepinephrine reuptake inhibitor, appears effective and well tolerated enough to alleviate BTZ-associated neuropathic pain.

1.2.2 Third-generation aromatase inhibitors-induced painful states

Third-generation aromatase inhibitors (AIs) are currently recommended for adjuvant endocrine treatment as primary, sequential, or extended therapy with tamoxifen, for postmenopausal women diagnosed with estrogen receptor-positive breast cancer [36-38]. Estrogen is the main hormone involved in the development and growth of breast tumors; oophorectomy was first shown to cause regression of advanced breast cancer, and estrogen deprivation remains a key therapeutic approach. Tamoxifen inhibits the growth of breast tumors by competitive antagonism of estrogen at its receptor site. Its actions are complex and it also has partial estrogen-agonist effects. These partial agonist effects can be beneficial, since they may help prevent bone demineralization in postmenopausal women, but also detrimental, since they are associated with increased risks of uterine cancer and thromboembolism. In addition, they may play a part in the development of tamoxifen resistance. In contrast, AIs markedly suppress plasma estrogen levels in post-menopausal women by inhibiting or inactivating aromatase, the enzyme responsible for the synthesis of estrogens from androgenic substrates (specifically, the synthesis of estrone from the preferred substrate androstenedione and estradiol from testosterone). Unlike tamoxifen, AIs have no partial agonist activity.

AIs are described as first-, second-, and third-generation inhibitors according to the chronologic order of their clinical development, and they are further classified as type 1 or type 2 inhibitors according to their mechanism of action. Type 1 inhibitors are steroidal analogue of androstenedione and bind to the same site on the aromatase molecule, but unlike androstenedione they bind irreversibly. Therefore, they are commonly known as enzyme inactivators. Type 2 inhibitors are non-steroidal and bind reversibly to the heme group of the enzyme by way of a basic nitrogen atom; anastrozole and letrozole, both third-generation inhibitors, bind at their triazole groups. The third-generation AIs, developed in the early 1990s, include the triazoles anastrozole (Arimidex) and letrozole (Femara) and the steroidal agent exemestane (Aromasin). They are administered orally; anastrozole and letrozole have similar pharmacokinetic

properties, with half-lives approximating 48 hours, allowing a once-daily dosing schedule. The half-life of exemestane is 27 hours. Pharmacokinetic interactions between some inhibitors and tamoxifen have been described. The levels of anastrozole and letrozole are reduced (by a mean of 27 percent and 37 percent, respectively) when they are coadministered with tamoxifen, but these reductions are not associated with impaired suppression of plasma estradiol levels.

The use of AIs is associated with a series of relevant side effects which are reported in 30-60% of treated patients [39, 40]. Among these, the AI-associated musculoskeletal symptoms (AIMSS) are characterized by morning stiffness and pain of the hands, knees, hips, lower back, and shoulders [41, 42]. In addition to musculoskeletal pain, pain symptoms associated with AIs have recently been more accurately described with the inclusion of neuropathic, diffused, and mixed pain [43]. The whole spectrum of painful conditions has been reported to affect up to 40% of patients, and to lead 10-20% of patients to non-adherence or discontinuation of treatment [41-46]. Although it has been proposed that estrogen deprivation and several other factors, including a higher level of anxiety, may contribute to the development of AIMSS and related pain symptoms, none of these hypotheses has been confirmed [43, 47].

1.2.3 Chemotherapy-induced peripheral neuropathy mechanisms

Although the underlying mechanisms involved in the induction of chemotherapy side effects are still under debate, various mechanisms possibly involved in development of CIPN have been explored and suggested. Several mitochondrial pathways, including regulation of intracellular calcium [48], generation of reactive oxygen species (ROS) [49] and apoptotic signaling [50], have been proposed to play a critical role in the development of CIPN. Indeed, paclitaxel-evoked painful peripheral neuropathy is associated with increased swollen and vacuolated axonal mitochondria [51]). Moreover, paclitaxel appears to gate the multi-molecular complex containing the voltage-dependent anion channel, defined as mitochondrial permeability transition pore (mPTP), [51] causing a toxic calcium release from the mitochondria. Indeed, calcium chelating agents are able to reverse paclitaxel-evoked pain [52] and acetyl-l-carnitine, which prevents mPTP opening [53], reduces the development of paclitaxel-induced neuropathic pain [54]. Administration of BTZ leads to the intracytoplasmic vacuolation

in DRG satellite cells, probably due to mitochondrial and endoplasmic reticulum enlargement [55]. All these intracellular modifications are probably related to the ability of BTZ to induce the mitochondrial-based apoptotic pathway including activation of caspases [56] and dysregulation of calcium homeostasis [57]. Disregulation of neurotrophins has also been proposed as another important mechanism of BTZ-induced peripheral neuropathy genesis, since the main action of BTZ is the inhibition of NF-κB activation, thereby blocking the transcription of nerve growth factor-mediated neuron survival. The inhibitors of mitochondrial electron transport chain (mETC) produce CIPN antinociception and attenuate TNF-α-induced mechanical hyperalgesia [50]. The critical role of mETC in peripheral pain mechanisms is further corroborated by the effect of inhibitors of ATP synthesis to attenuate neuropathic pain [50]. Moreover, it has been demonstrated that α-lipoic acid, by regulating essential mitochondrial proteins with antioxidant and chaperone properties [58], exerts neuroprotective effects against chemotherapy-induced neurotoxicity in sensory neurons. Finally, significant changes in the expression of various genes, including those controlling the mitochondrial dysfunction due to vincristine- and BTZ-associated peripheral neuropathy, have been demonstrated in a clinical study [56].

Impaired mitochondrial calcium uptake or increased leakage of mitochondrial calcium could exaggerate calcium signals and, eventually, calcium-dependent processes which participate to neuropathy mechanism. It has been proposed that administration of vincristine and paclitaxel, by raising neuronal calcium levels in the nerves, induces mitochondrial changes, associated with neuronal hyperexcitability. Accordingly, drugs which reduce intracellular calcium levels are able to reverse the negative effects of altered mitochondrial calcium regulation and neuropathic pain [52, 59]. Furthermore, paclitaxel- and vincristine-evoked neuropathic pain is reduced by both the T-type channel calcium blocker, ethosuximide, and the α2δ-1 calcium channel subunit antagonist, gabapentin [60, 61]. In addition, paclitaxel has been reported to increase the expression level of α2δ-1 mRNA in the dorsal spinal cord [60, 62]. Accordingly, it is proposed that of α2δ-1 subunit in the spinal dorsal horn and DRG is a main site of inhibitory action of gabapentin on paclitaxel-induced allodynia [63]. Thus, different lines of evidence indicate that dysregulation of intracellular calcium levels represents an additional factor contributing to the pathogenesis of CIPN.

A number of studies suggest a role of sodium channels in CIPN. Exposure of DRG neurons to oxaliplatin increases sodium currents which are antagonized by the

sodium channel blocker, carbamazepine [64]. The oxaliplatin metabolite oxalate probably alters the functional properties of voltage-gated sodium channels, resulting in a prolonged open state of the channels and, finally, in the hyperexcitability of sensory neurons [65]. Further, oxaliplatin administration has been described to slow sodium channel inactivation kinetics [64, 66]. A change in sodium channel properties may predispose to ectopic activity leading to paresthesia and fasciculations [67]. Cold exposure affects sodium channel kinetics [68] and, accordingly, sodium channel dysfunction is aggravated by cold temperatures [69]. Cold hypersensitivity is a typical feature observed in acute oxaliplatin-induced neurotoxicity. It has been shown that acute modulation of sodium channel influences the severity of oxaliplatin-induced neurotoxicity [70, 71]. The involvement of sodium channels is also reported in paclitaxel-induced neuropathic pain where low doses of tetrodotoxin result able to prevent pain induced by taxane [72]. However, the role of the sodium channels in the neuropathy induced by different chemotherapeutic agents is challenged by the finding that administration of antisense oligodeoxynucleotides targeting the $Na_V1.8$ channel does not interfere with vincristine-induced neuropathic pain [73].

An important role of inflammatory mediators has been described in models of CIPN [74, 75]. A recent study demonstrated a correlation between the increase in IL-6 and the appearance of BTZ-induced neuropathic pain [76]. Further, the administration of the prostaglandin E1 (PGE_1) analog, limaprost, attenuated mechanical allodynia induced by paclitaxel and oxaliplatin (but not by vincristine) [62]. The increase in skin Langerhans cells (LC) has been associated with the development of pain in vincristine- and paclitaxel-evoked neuropathy [52]. LC cells may contribute to pain development by different mechanisms including release of nitric oxide (NO) [77], pro-inflammatory cytokines and neurotrophic factors [78], that in turn cause spontaneous neuronal discharge, nociceptor sensitization and mechano-hypersensitivity. It has also been demonstrated that paclitaxel-induced neuropathic pain is associated with the induction of TNF-α and IL-1β in lumbar DRGs [79]. Glial cell inhibitors attenuate paclitaxel- and vincristine-induced neuropathic pain [80, 81], supporting a role for activated glial cells in this condition.

In vincristine- and paclitaxel-evoked neuropathy [52], and more recently in oxaliplatin-induced neuropathy [82], a loss of intraepidermal nerve fibers in plantar hind paw skin region of the sensory neuron peripheral terminal arbors, similar to that documented in other neuropathic pain syndromes, has been shown. Neuropathy seems

also to be characterized by a loss of the cutaneous Aδ and C fibers (cool- and warm-specific) [83] and of Aδ cool-specific fibers which seem to contribute to cold allodynia [84].

Oxidative stress has been repeatedly proposed to play a central role in the mechanism of CIPN. The effect of antioxidants, including acetyl-l-carnitine, α-lipoic acid and vitamin C, which seem to partially reverse the hyperalgesia, represents an indirect proof of oxidative stress role in oxaliplatin-induced neuropathy [85, 86]. Recently, administration of the free radicals scavenger phenyl N-tert-butylnitrone has been shown to reduce mechanical allodynia in paclitaxel-induced neuropathic pain in rats [290]. Moreover, it has been demonstrated that BTZ increases ROS in DRG neurons [87] and that vitamin C or N-acetyl-l-cysteine administration alleviates the cytotoxicity in Schwann cells, but not in myeloma cells treated with BTZ [88]. This observation suggests that treatment with antioxidant agents could afford neuroprotection without modifications of the antineoplastic activity [88]. Recent evidence also supports the role for other biological effectors in CIPN. For instance, paclitaxel-induced peripheral neuropathy is characterized by the activation of calcium-activated proteases, such as calpains and caspases or MAPK [50]. Furthermore, the prolonged exposure to oxaliplatin induces early activation of p38 and ERK1/2 in DRG neurons, eventually provoking neuronal apoptosis. Contrasting data have been reported on the role of neuropeptides, such as CGRP or SP [287, 288]. The role of NO has been also evaluated, and there is indication that NO contributes to vincristine- and oxaliplatin-induced neuropathy. Finally, a number of other mediators or effector mechanisms have been implicated in the genesis of CIPN, including NMDA and 5HT receptors, potassium channels, protein kinase C (PKC) or l-serine [89].

Although the mechanism underlying the acute neuronal hyperexcitability and the subsequent peripheral neuropathy and pain induced by chemotherapeutic agents remains still to be established, in the recent years remarkable interest has been paid to the different ion channels located to neuronal membrane. In particular, due to their specific and abundant expression on peripheral sensory neurons, research on Transient Receptor Potential (TRP) channels represents a promising area of investigation. Emerging and compelling data have shown the contribution of several members of this channel family to the mechanism of CIPN.

1.3 Transient Receptor Potential (TRP) channels

The TRP ion channels are a large class of channel subunits united by a common primary structure and permeability to monovalent cations and Ca^{2+} ions. The first gene encoding a TRP channel was discovered in the fruit-fly *Drosophila melanogaster* where mutants for that gene exhibited impaired vision due to the lack of a specific Ca^{2+} influx pathway into photoreceptors [90]. Phototransduction in the fruit-fly involves activation of membrane cation channels leading to a depolarizing current. *Drosophila* photoreceptors contain the light-sensitive G protein-coupled receptor rhodopsin, whose activation results in stimulation of phospholipase C-β (PLC-β). Resolving components of the light-induced current (LIC) led to the identification of a *Drosophila* mutant displaying a transient LIC in response to light, in contrast to the sustained LIC in wild-type flies. This mutant strain was termed *trp*, for transient receptor potential. Mutations in this gene led to a disruption of a Ca^{2+} entry channel in the photoreceptors, indicating that TRP, the protein encoded by the *trp* gene, forms all, or part, of a Ca^{2+} influx channel [91].

More than 50 members of the TRP family have been characterized in many tissues and cell types in both vertebrates and invertebrates making them one of the largest groups of ion channels [92]. A unifying theme in this group is that TRP proteins play critical roles in sensory physiology, which include contributions to vision, taste, olfaction, hearing, touch, and thermo- and osmosensation. TRP cation channels are unique cellular sensors characterized by a promiscuous activation mechanism [93]. For example, yeasts use a TRP channel to perceive and respond to hypertonicity [94], nematodes use TRP channels at the tips of neuronal dendrites in their “noses” to detect and avoid noxious chemicals [95], and male mice use a pheromone-sensing TRP channel to tell males from females [96]. Humans use TRP channels to appreciate sweet, bitter and umami (amino acid) [97] and to discriminate warmth, heat and cold. In each of these cases, TRPs mediate sensory transduction, not only in a classical sense, for the entire multicellular organism, but also at the level of single cells.

1.3.1 Classification and structural features

TRPs are classified essentially according to their primary amino acid sequence rather than selectivity or ligand affinity, because their properties are heterogenous and their regulation is complex. The 28 mammalian TRPs channel superfamily can be divided into six families [98, 99] (Fig. I-4). The TRPC (Canonical) and TRPM (Melastatin) subfamilies consist of seven and eight different channels, respectively (i.e. TRPC1-TRPC7 and TRPM1-TRPM8). The TRPV (Vanilloid) subfamily presently comprises six members (TRPV1-TRPV6). The most recently identified subfamily, TRPA (Ankyrin), has only one mammalian member (TRPA1). The TRPP (Polycystin) and TRPML (mucolipin) families, each containing three mammalian members, are not sufficiently characterized, but gain increasing interest because of their involvement in several human diseases.

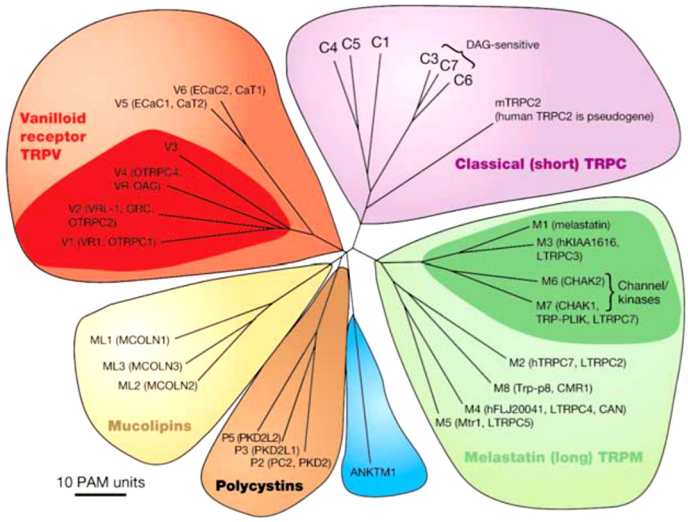

Figure I-4. Mammalian TRP family tree. The evolutionary distance is shown by the total branch lengths in point accepted mutations (PAM) units, which is the mean number of substitutions per 100 residues. Adapted from [98].

All TRP channels comprise six transmembrane domains (S1-S6) and a pore region formed by a short, hydrophobic stretch between S5 and S6 to form cation-permeable pores. Both the N- and C-termini are located intracellularly (Fig. I-5). Despite the topographic similarities between the TRPs and the voltage-gated potassium channels, the TRPs are actually only distantly related to these channels. Voltage-gating refers to channel opening results from movement of the charged S4 segment in K_V/Na_V/Ca_V channels upon a change in transmembrane voltage. In TRPs channels, S4

lacks the complete set of positively charged residues necessary for the voltage sensor in many voltage-gated ion channels [100]. In general, TRP channel gating is not dominated by voltage but rather is effected by the energy differences accompanying changes in temperature, binding, and voltage. Functional TRP channels consist of either homo- or heteromultimers of four TRP subunits (Fig. I-5). Whereas the C-terminus is a highly conserved residue, most TRP channels contain N-terminus ankyrin repeats, which are 33-residue motifs with a conserved backbone and variable residues that mediate specific protein-protein interactions [101]. It is notable that ankyrin repeats are prominent in the assembly of macromolecular complexes between the plasma membrane and the cytoskeleton. It is also possible that the ankyrin repeats play a functional role in transmitting mechanical forces to the gate of the channels.

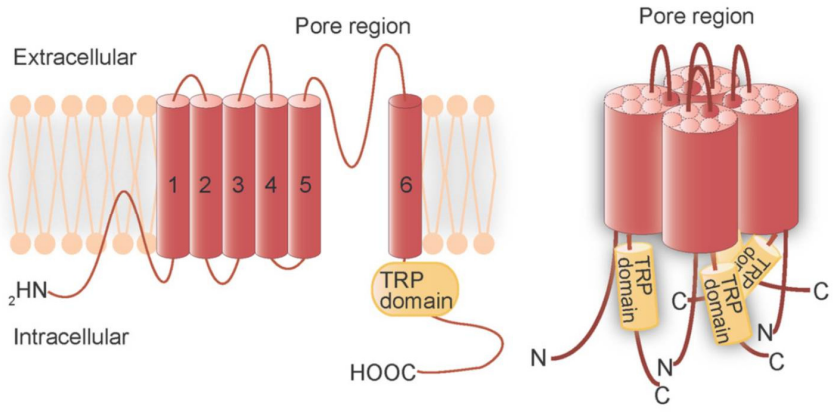

Figure I-5. Transmembrane topology of TRP channels. Transmembrane topology (left) and the quaternary structure of TRP channels (right). The TRP protein has six putative transmembrane domains, a pore region between the fifth and sixth transmembrane domains and a TRP domain in the C-terminal region. The TRP protein assembles into homotetramers or heterotetramers to form channels. From [294].

Although a single defining characteristic of TRP channels function has not yet emerged, TRPs may be generally described as calcium-permeable cation channels with polymodal activation properties. By integrating multiple concomitant stimuli and coupling their activity to downstream cellular signal amplification *via* Ca^{2+} permeation and membrane depolarization, TRP channels appear well adapted to function in cellular sensation. Indeed, their localization in the plasma membranes of neurons or other cells and a large body of evidence collected using a plethora of stimuli, indicates that they are sensors of chemical, mechanical and thermal stimuli. All functionally characterized TRP channels mediate the transmembrane flux of cations down their electrochemical gradients, thereby raising intracellular Ca^{2+} and Na^{+} concentrations and depolarizing the

cell. As they are widely expressed in mammalian tissues, TRPs are well positioned to regulate intracellular Ca^{2+} and Na^{+}, and transmembrane voltage in both excitable and non-excitable cells. Most Ca^{2+}-permeable TRP channels are only poorly selective for Ca^{2+}, with permeability ratio relative to Na^{+} (P_{Ca}/P_{Na}) in the range between 0.3 and 10. Exceptions are TRPV5 and TRPV6, two highly Ca^{2+}-selective TRP channels with P_{Ca}/P_{Na} >100. TRP channels are gated by different stimuli that include the binding of intracellular and extracellular messengers, changes in temperature, and chemical and/or mechanical (osmotic) stress. Sensitivity to polymodal activation suggests that the physiologically relevant stimulus for any given TRP will be governed by the specifics of cellular context (i.e., phosphorylation status, lipid environment, interacting proteins, and concentrations of relevant ligands). Ligands that activate TRP channels may be classified as (a) exogenous small organic molecules, including synthetic compounds and natural products; (b) endogenous lipids or products of lipid metabolism; (c) purine nucleotides and their metabolites; (d) inorganic ions, with Ca^{2+} and Mg^{2+} being the most likely to have physiological relevance [296]. In addition, from their first identification, several members of other TRP subfamilies have been described as store operated channels (SOCs). Store-operated Ca^{2+} entry channels are considered channels that are activated whenever intracellular Ca^{2+} stores become depleted. In many cases, the classification of TRP channels as SOCs is mainly based on the results of Ca^{2+} imaging protocols, in which store-dependent Ca^{2+} influx is estimated from the rise in intracellular Ca^{2+} concentration that occurs in cells to which extracellular Ca^{2+} is readded after artificial store depletion. However, most TRP are not gated by the usual mechanism defined as activating store-operated Ca^{2+} entry. Thus it is not accurate to refer to TRP channels as store-operated channels, although it may turn out that one or more of these channels participate to this process [102].

1.3.2 The TRPC subfamily

The mammalian TRP channels most closely related to Drosophila TRP are classified in the TRPC subfamily. TRPC channels are nonselective, Ca^{2+}-permeable cation channels, but the permeability ratio (P_{Ca}/P_{Na}) varies significantly between different members of the family. In general, TRPC members can be considered as channels activated subsequent to stimulation of receptors that activate different isoforms

of PLC. A recent study reported that TRPC1 is directly activated by membrane stretch, independent of PLC activity [103].

1.3.3 The TRPV subfamily

The TRPV family includes six mammalian members divided into two group: TRPV1-TRPV4 and TRPV5-TRPV6. The vanilloid receptor TRPV1 is the best characterized ion channel in this class. Members of the TRPV family contain three to five ankyrin repeats in their cytosolic NH_2-termini. TRPV1-TRPV4 are all heat-activated channels that are non-selective for cations and modestly permeable to Ca^{2+}. In addition, they also function as chemosensors for a broad array of endogenous and synthetic ligands. Recently, it has been described that TRPV4 is also activated upon cell swelling [104]. Interestingly, these different chemical and physical activator stimuli mostly have an additive, or even supra-additive, effect on the gating of TRPV channels, which endows these channels with the ability to act as signal integrators. This form of signal integration is of great importance to several pathological states. The properties of the two other members of this subfamily, TRPV5 and TRPV6, are quite different from those of TRPV1-TRPV4. They are the only highly Ca^{2+}-selective channels in the TRP family, and both are tightly regulated by intracellular Ca^{2+} [105]. These properties allow TRPV5 and TRPV6 to play a crucial role as gatekeepers in epithelial Ca^{2+} transport, and as selective Ca^{2+} influx pathways in non-excitable cells [106]. In addition, in contrast to the other TRPVs, the temperature sensitivity of TRPV5 and TRPV6 is relatively low.

TRPV1, originally named vanilloid receptor 1 (VR1) and commonly referred as the capsaicin receptor, was first described as a polymodal receptor activated by vanilloid compounds (capsaicin, resiniferatoxin), moderate heat (≥43 °C) and low pH (<5.9) [107, 108]. Since then, TRPV1 has been reported to be also activated by camphor [109], allicin [110, 111], nitric oxide [112], spider toxins [113], potentiated by ethanol [114] and modulated by extracellular cations [115]. TRPV1 was initially described in a subpopulation of small- to medium-diameter neurons in dorsal root, trigeminal and nodose ganglia [107, 108]. While TRPV1 has been described in many other neuronal and non-neuronal cells [116], its highest expression level is in sensory neurons. Several studies have demonstrated that inflammatory mediators, such as BK, prostaglandin E_2, extracellular ATP, glutamate and NGF indirectly sensitize TRPV1 [291, 117]; following exposure of sensory neurons to inflammatory mediators, responses to capsaicin or heat

are dramatically enhanced to the extent that body temperature can be sufficient to activate nociceptors [108]. Inflammatory mediators sensitize TRPV1 function by various mechanisms; they may increase TRPV1 expression levels in the membrane [118, 119], induce TRPV1 phosphorylation by protein kinases [120] or release the inhibition of TRPV1 by phosphatidylinositol 4,5-bisphosphate, which render the channel more responsive to agonist stimulation [121]. In addition, these inflammatory mediators act on receptors that are coupled to G proteins or tyrosine kinase pathways thus activating PLC and/or PLA2 which, in turn, induce the release of arachidonic acid metabolites. Several amide derivatives of arachidonic acid (anandamide) and lipoxygenase products of arachidonic acid, such as 12-(S)-HPETE, are agonists of TRPV1 and therefore are candidates for endogenous capsaicin like substances [122]. In addition to inflammatory mediators, proteases released during inflammation or nerve injury, such as trypsins and mast cell tryptase, can also sensitize TRPV1; these proteases cleave the protease activated receptor 2 (PAR2) to sensitize TRPV1 to induce thermal hyperalgesia through PKA and PKCε second messenger pathways [123, 124]. These findings demonstrate that TRPV1 not only participates in pain evoked by chemical and moderate heat but that TRPV1 contributes to peripheral sensitization, acting as the final substrate for multiple inflammatory mediators that operate *via* distinct intracellular signaling pathways.

TRPV4 channel is a polymodal receptor with a wide expression pattern and a corresponding variety of physiological roles [125]. TRPV4 is widely expressed on nervous and non-nervous organs, tissues and cells, including urinary bladder, kidney, vascular endothelium, keratinocytes, cochlear hair cells, and Merkel cells [126-128]. TRPV4 activation on sensory neurons, TG and DRG neurons [125, 129] causes SP and CGRP release, thus evoking neurogenic inflammation in peripheral tissues [130]. TRPV4 was firstly identified as an osmo-transducer activated by decrease in osmolarity, suggesting a role in the regulation of cell swelling [125, 131]. Later studies demonstrated that TRPV4 is activated by shear stress [132], innocuous warmth (27-35 °C) [129, 133], low pH, citrate [128], endocannabinoids and arachidonic acid (AA) metabolites [92, 134], NO [112] and synthetic selective agonists, such as the phorbol ester 4α-phorbol 12,13-didecanoate (4α-PDD) [133]. The mechanosensitive nature of TRPV4 and its implication in sensing shear stress suggest a role in flow-sensitive cells, such as vascular endothelial and renal tubular epithelial cells. The mechanism through which TRPV4 is activated by mechanical stress is still under debate. Two transduction

pathways have been proposed to regulate TRPV4 activation: the PLC/diacylglycerol (DAG) pathway and the PLA2/AA pathway [135, 136]. Some evidence suggests that activation of TRPV4 by hypotonicity involves its phosphorylation by Src family of tyrosine kinase [137]. Although the molecular mechanism of hypotonicity-induced TRPV4 activation should be further investigated, studies addressing the gating mechanism of the channel by cell swelling exclude that it is directly gated by mechanotransduction since it does not respond to membrane stretch [131]. It was shown that hypotonicity becomes painful to the animals when nociceptive fibers are sensitized by the PGE_2, whose levels increase during inflammation or in response to mechanical, chemical and thermal injury. TRPV4 also plays a crucial role in mechanical hyperalgesia elicited by exposure to inflammatory mediators. Indeed, PGE_2 and serotonin, can act synergistically through cAMP/PKA and PKCε to engage TRPV4 in hyperalgesia to mechanical and osmotic stimuli [138]. In addition, PAR2 agonists may sensitize TRPV4 through the activation of multiple second messenger pathways, such as PKA, PKC, PKD, PLCβ [130]. Proteases generated during inflammation activate PAR2 thus leading to TRPV4-mediated release of SP and CGRP in the spinal cord and TRPV4-induced mechanical hyperalgesia [139].

1.3.4 The TRPM subfamily

Members of the TRPM family fall into three subgroups on the basis of sequence homology: TRPM1/3, TRPM4/5, and TRPM6/7, with TRPM2 and TRPM8 representing structurally distinct channels. In contrast to TRPCs and TRPVs, TRPMs do not contain ankyrin repeats within their NH_2-terminal domain. TRPM channels exhibit highly variable permeability to Ca^{2+} and Mg^{2+}, ranging from Ca^{2+} impermeable (TRPM4 and TRPM5) to highly Ca^{2+} and Mg^{2+} permeable (TRPM6, TRPM7 and specific splice variants of TRPM3).

1.3.5 The TRPML subfamily

The TRPML family consists of three mammalian members (TRPML1–3) that are relatively small proteins consisting of ~600 amino acid residues. TRPML1 is widely expressed and appears to reside in late endosomes/lysosomes. Recently, TRPML1 has

been described as a H^+ channel that may act as a H^+ leak in lysosomes preventing overacidification in these organelles [140].

1.3.6 The TRPP subfamily

The TRPP family is very heterogeneous and can be divided, on structurally criteria, into PKD1-like (TRPP1-like) and PKD2-like (TRPP2-like) proteins. PKD1-like members comprise TRPP1 (previously termed PKD1), PKDREJ, PKD1L1, PKD1L2, and PKD1L3. TRPP1 consists of 11 transmembrane domains, a very longand complex ~3,000 amino acid extracellular domain, and an intracellular COOH-terminal domain that interacts with the COOH-terminal of TRPP2 through a coiled-coil domain. The PKD2-like members structurally resemble other TRP channels. There is considerable evidence that TRPP1 and TRPP2 physically couple to act as a signaling complex at the plasma membrane to which TRPP2 is recruited by TRPP1 [141].

1.3.7 The TRPA subfamily

The TRPA family currently comprises one mammalian member, TRPA1, which is expressed in DRG and TG neurons and in hair cells [142, 143]. TRPA1 consists of at least 14 N-terminal ankyrin repeat domains (ARDs), an unusual structural feature that may be relevant to the proposed role of the channel as a mechanosensor. TRPA1 receptor is activated by various stimuli including exogenous (natural compound) but also endogenous compound. TRPN is a channel that is closely homologous to TRPA1. It is characterized by 29 ankyrin repeats within the N-terminus. To date, this subfamily comprises only one member in *C. elegans*, *Drosophila*, and zebrafish. TRPN1 probably acts as a mechanotransduction channel that is involved in hearing. Currently available genome information indicates that mammals have no TRPN orthologs.

1.4 The TRPA1 channel

TRPA1 is the only member of the ankyrin subfamily found in mammals. This receptor was originally cloned from human pulmonary fibroblasts [144], and was found selectively expressed in a subpopulation of unmyelinated nociceptors that also express the capsaicin receptor TRPV1, suggesting an important role in nociception [93, 143, 145]. The TRPA1 is a non-selective cation channel permeable to both monovalent and divalent ions, including Ca^{2+}, Na^{+}, K^{+}. TRPA1 has a high Ca^{2+} permeability compared to most other TRP channels and a unitary conductance ~70 pS to ~110 pS in the inward and outward directions, respectively, under physiological conditions when the channel is constitutively open [146, 147]. In presence of TRPA1 activators the pore of the channel, with a size of 11.0 Å, can undergo dilation increasing Ca^{2+} permeability and allowing larger charged molecules to pass through the channel [148, 149].

Like all other TRP proteins, TRPA1 has six predicted transmembrane domains (S1-S6), a pore loop between S5 and S6 and the N- and C-termini located intracellulary. Although there is no apparent voltage sensor in S4, as shown for voltage-gated K^{+} channels, TRPA1 displays some voltage dependency although less pronounced compared to TRPM8 and TRPV1 [150, 151]. A distinguish features of TRPA1 receptor is its long N-terminus with 14 to 18 ankyrin repeats which are important for protein-protein interactions and insertion of the channel into the plasma membrane [152] (Fig. I-6 a,b). The N-terminus contains a large numbers of cysteine residues, some of which can form a network of protein disulfide bridges within or between monomers [153] (Fig. I-6 c). N-terminal cysteine and lysine residues are key targets for electrophilic TRPA1 activators, but cysteines outside the N-terminus region may also contribute to channel gating [153]. Furthermore, the potent TRPA1 activator Zn^{2+} may bind to cysteine and histidine residues in the C-terminus [154, 155]. The N- and C-termini have been suggested to contain binding sites for Ca^{2+} that can both sensitize or desensitize TRPA1 [145, 156, 157]. Ca^{2+} strikingly modulates TRPA1 activity. Indeed micromolar intracellular Ca^{2+} concentrations ($[Ca^{2+}]_i$) activate TRPA1, and also elevation of extracellular Ca^{2+} concentration can transiently increase the channel activity. It has been suggested that activation may depend on Ca^{2+} binding to an N-terminal EF-hand motif [158, 159]. The putative EF-hand motif involved in $[Ca^{2+}]_i$-dependent activation of TRPA1 is located between ARD11 and ARD12 [158, 159] (Fig. I-6 a,b). The importance of this EF-hand site is questionable, since point mutations in this region

have only modest effects on $[Ca^{2+}]_i$-dependent activation mechanism, while deletions impair trafficking of the truncated channel to the plasma membrane [146]. Another putative Ca^{2+}-binding domain is composed of a cluster of acidic residues in the distal C-terminus of TRPA1 [157]. Four conserved residues in human TRPA1, Glu1077, Asp1080, Asp1081 and Asp1082, have strong effects on the Ca^{2+}- and voltage-dependent potentiation and/or inactivation of agonist-induced responses. Truncation of the C-terminus by only 20 residues selectively slowed down the Ca^{2+}-dependent inactivation without affecting other functional parameters. The only direct structural insights on TRPA1 channel are those available from a 16 Å resolution structure of purified, amphipol-stabilized, TRPA1 proteins analyzed by single-particle electron microscopy (EM) [160]. This structural model suggests that the critical N-terminal cysteine residues involved in electrophilic activation are located at the interface between neighboring subunits and form a ligand-binding pocket, allowing disulfide bonding between the cysteine residues [153]. Covalent modifications by thiol-reactive compounds within such pockets may alter interactions between subunits and promote conformational changes that translate to modification of the gating mechanism [153, 160].

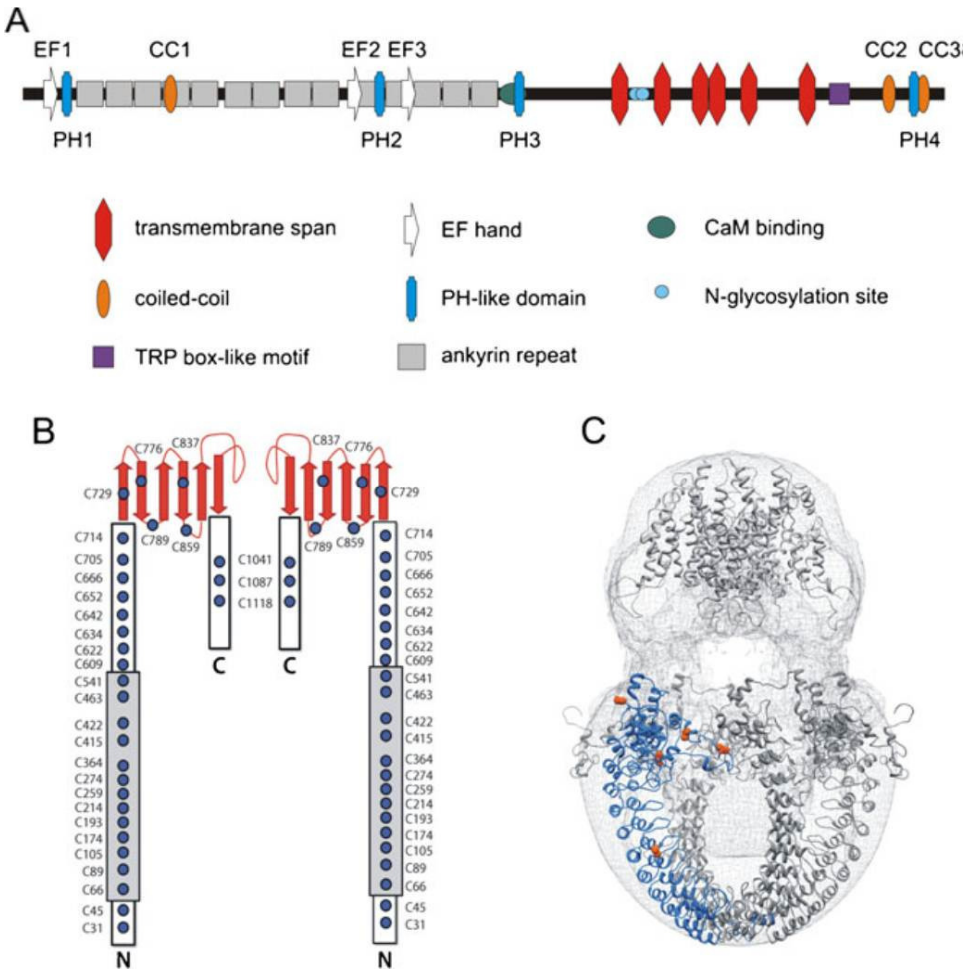

Figure I-6. Predicted structural topology of human TRPA1 channel. **a** Positions of major domains and motifs are annotated. **b** Schematic representation of a TRPA1 dimer with annotations of all 31 cysteine residues (blue circles). The position of ankyrin repeat domains is represented by a gray box. **c** Reconstruction of electron microscopy density and N-terminal model of TRPA1 (blue ribbon). The cysteines involved in disulfide bonding are displayed in orange (adapted from [160, 146]).

1.4.1 Localization of TRPA1 channel

Shortly after the identification of TRPA1 receptor in human pulmonary fibroblast (Jaquemar, 1999) and in hairy cells of the auditory system [142], abundant expression of TRPA1 have been localized in a subpopulation of peptidergic primary sensory neurons (with C and Aδ fibers) where it signals nociceptive/painful responses. TRPA1-expressing neurons contain and release the neuropeptides, SP, NKA and CGRP. TRPA1 is mostly found in a subpopulation of TRPV1-positive neurons, but non-TRPV1-containig neurons expressing TRPA1 also exist, including a small population of myelinated Aβ-fibers, which are activated by innocuous mechanical force [161]. By using radial stretch in combination with live-cell calcium imaging different mechano-

sensitive or -insensitive sensory neuronal categories were identified [163]. A group of small-diameter stretch-sensitive cells could be further subdivided in a cluster of small-diameter cells, sensitive to hydroxy-α-sanshool (a two pore K^+ channel antagonist) and the TRPV1 agonist, capsaicin, and a second one which comprises large-diameter cells that respond to hydroxy-α-sanshool, but not capsaicin. The former neuron type likely corresponds to high threshold nociceptors and the latter to low threshold proprioceptors. Moreover, stretch insensitive neurons fall into two groups of small-diameter cells. A first group is composed by petidergic neurons sensitive to capsaicin and to the TRPA1 selective agonist, mustard oil, and a second group by a small cohort of menthol-sensitive cells [163]. Thus, TRPA1 expressing neurons which obligatory co-express TRPV1, are those apparently insensitive to mechanical stimulation and that, because they contain neuropeptides, bring about neurogenic inflammation.

More recently extraneuronal localization of TRPA1 has been identified. TRPA1 activation inhibited the repair of the epithelial wound in the stomach, probably by the suppression of cell migration, and suggested the involvement of TRPA1 in the mechanism of gastric epithelial restitution [164]. TRPA1, highly expressed in the bladder epithelium, might be involved in the bladder sensory transduction and the induction process of overactive bladder by bladder outlet obstruction [165]. The localization of TRPA1 to nerves that also express TRPV1 and CGRP, and in urothelial cells and interstitial cells, as well as the findings that TRPA1 agonists can modify tone of human urethral preparations, propose a role for TRPA1 in afferent and efferent sensory signaling of the human outflow region [166]. TRPA1 is highly expressed in rat enterochromaffin cells (EC), and TRPA1 agonists, including allyl isothiocyanate and cinnamaldehyde, stimulate EC cell functions, such as increasing intracellular Ca^{2+} levels and 5-HT release. By this mechanism TRPA1 regulates intestinal motility [167]. Finally, and more importantly for the present research proposal there is evidence that TRPA1 expressed in endothelial cells of rat cerebral vessels regulates vascular tone by nitric oxide and cyclooxigenase-independent pathways [168]. The relaxing mechanism activated by TRPA1 agonists is mediated by endothelial cell Ca^{2+}-activated K^+ channels and inwardly rectifying K^+ channels in arterial myocytes [168]. TRPA1 is found in melanocytes, mast cells, fibroblasts, odontoblasts [169-172].

1.4.2 TRPA1: more than just a spice receptor

Many different stimuli have been reported to either directly or indirectly activate the TRPA1 receptor channels, including cold, mechanical displacement and exogenous pungent compound and irritants, BK and other endogenous proalgesic agents.

TRPA1 and thermosensation. The molecular basis of thermosensation has made great strides with the discovery that several members belonging to the TRP cation channel family exhibit highly temperature-sensitive gating and are expressed in cells of the sensory system. Among the TRP channels expressed in sensory neurons, TRPM8, activated by cold temperatures and cooling compounds, such as menthol, plays a major role in cold sensing [173]. TRPA1 was originally reported to be a potential candidate to mediate detection of noxious cold, based on its expression in nociceptive neurons, and on the finding that heterologously expressed TRPA1 in CHO cells is activated by cold temperatures with a lower temperature threshold for activation than TRPM8 [143]. Whether or not TRPA1 is a noxious cold sensor, *via* either direct or indirect mechanism, is not well explained. On one hand, some studies have shown that when TRPA1 is expressed in heterologous systems, human embryonic kidney (HEK) cells or chinese hamster ovary (CHO) cells, it is activated by cold temperatures, ~17 °C and below that are in the noxious range [143, 174, 175]. Alternatively, other studies have shown that exogenously expressed TRPA1 is not activated by noxious cold [142, 145, 176]. A more recently report suggests that cold-induced activation of TRPA1 in overexpression systems is an indirect effect caused by Ca^{2+} release from intracellular stores by a direct activation of the receptor, mediated by intracellular Ca^{2+}, *via* an EF-hand domain in its N-terminus domain [159]. These contradictory findings appear to have been resolved by subsequent work, where TRPA1 null mice were still able to sense cold, but that also indicated that the behavioral response to noxious cold was significantly reduced in the absence of TRPA1 [177]. Furthermore, mice in which $Na_V1.8$-expressing sensory neurons were eliminated by diphtheria toxin A exhibit a strongly reduced expression of TRPA1 in DRG neurons and lack TRPA1-mediated nociceptive responses to formalin and cold [178]. Thus, noxious cold sensing *in vivo* requires somatosensory neurons that express both $Na_V1.8$ and TRPA1.

TRPA1 and mechanotransduction. TRPA1 receptor has also been proposed to be involved in mechanotransduction adding further diversity to its potential

physiological roles. Mice with a deletion of the pore domain of TRPA1 exhibit decreased behavioral responses to intense mechanical force in the noxious range [179], although behavioral deficits to mechanical stimuli were not observed in a similar TRPA1 mutant mouse [180]. A small molecule inhibitor of TRPA1 reverses mechanical hyperalgesia induced by inflammation in mice [181]. No cellular studies have provided clear evidence that TRPA1 is directly gated by mechanical force, although a recent study shows that heterologously-expressed TRPA1 is activated by hypertonic saline, suggesting that TRPA1 is sensitive to osmotic stimuli [182]. However, it should be noted that the nature of osmotic stimuli and how it activates channels in a cell membrane may differ substantially from that of punctuate mechanical force applied to a localized region of the neuronal membrane.

TRPA1 and chemical irritants. The TRPA1 channel is best characterized as a chemosensor activated in response to many chemical agents, a large number produced by plants or some others synthetic that cause neurogenic inflammation and pain. It has been established that TRPA1 acts as a detector of thiol-reactive electrophiles and oxidants in addition to non-electrophiles compounds as well as being indirectly regulated by G-protein coupled receptor signaling.

Electrophilic activators. Electrophilic TRPA1 ligands of environmental-, dietary- or endogenous origin modify nucleophilic cysteine and lysine residue(s) in the N-terminus of the channel [183]. Allyl isothiocyanate (AITC) from mustard oil is one of the most efficient electrophilic activators of TRPA1 (Fig. I-7a). In human TRPA1, electrophilic agonists modify cysteines Cys619, Cys639 and Cys663 (and to a lesser extent K708) [184]. In the mouse TRPA1 homologue the most reactive cysteine residues are Cys415 and Cys422 and Cys622 [185]. Other electrophiles, such as methyl, isopropyl-, benzyl-, phenylethyl-isothiocyanate, cinnamaldehyde (in cinnamon), iodoacetamide, and 2-(trimethylammonium)ethyl methane-thiosulfonate bromide (MTSEA; used for cysteine scanning), are capable of reacting with cysteine residues and act as TRPA1 activators [93, 145] (Fig. I-7a).

TRPA1 has been also recognized as the target of a series of endogenous α,β-unsaturated aldehydes, which are produced by lipid peroxidation in response to oxydative stress at sites of inflammation and tissue injury [111, 180, 186] (Fig. I-7a). These aldehydes include 4-hydroxy-2-nonenal (HNE) which is produced by peroxidation of omega 6-polyunsaturated fatty acids, such as linoleic acid and arachidonic acid [187, 188] or 4-oxononenal [189] that has been reported to cause

nociceptive behavior *via* a selective action at TRPA1. 4-HNE is an α,β-unsaturated hydroxyalkenal which is produced in inflammed tissues during peroxidation of membrane phospholipids by ROS. It evokes release of SP and CGRP from nerve endings, causing extravasations of plasma proteins into the surrounding tissue. 4-HNE acts *via* covalent modification of the cysteine/lysine residues in the TRPA1 N-terminus [186].

More recently, mediators of oxidative and nitrative stress have been identified as activators of the TRPA1 channel. These include the ROS hydrogen peroxide (H_2O_2) [175, 190, 191], superoxide (O^{2-}), hypochlorite (ClO^-) [191] and the reactive nitrative species (RNS) peroxynitrite ($ONOO^-$) [175]. Also nitrooleic acid, a byproduct nitrative stress, is a TRPA1 activator [192]. It has been reported that ROS cause cysteine oxidation or disulfide formation, RNS, like nitric oxide (NO), mediate S-nitrosylation, and reactive carbonyl species (RCS), like electrophilic prostaglandins (PG) and α,β-unsaturated aldehyde, alkylatively modify cysteine activating TRPA1. Cyclopentenone PGs have been reported to produce pain and neurogenic inflammation by TRPA1 stimulation [193, 194]. Also the cyclopentenone isoprostane (IP), 8-iso-PGA2, which forms from E-isoprostane that does not require for its synthesis activation of cyclooxygenases, stimulates sensory nerve terminals by targeting TRPA1 [193]. Altogether these findings suggest that TRPA1 is an unspecific sensor for a plethora of stimuli (exogenous and metabolites generated by both oxidative and nitrative stress), that use the TRPA1 channel to alert of inflammation and tissue injury.

Hydrogen sulfide (H_2S) is a malodorous gas that functions as an endogenous gasotransmitter in humans and is involved in a wide variety of processes including nociceptive processes [195]. H_2S evokes CGRP release from sensory neurons of isolated rat tracheae through TRPA1 activation.

It has been reported that high concentrations of carbon dioxide (CO_2) evoke a stinging sensation that depends on the activation TG nociceptors that express TRPA1 and innervate the respiratory, nasal, and oral epithelia. CO_2 diffuses into cells and produce intracellular acidification thereby gating TRPA1 [196]. Alkaline pH also causes pain *via* activation of TRPA1. Two N-terminal residues, Cys422 and Cys622, are responsible for high pH perception. Pain behaviors evoked by intraplantar injection of ammonium chloride are completely reduced in *Trpa1*$^{-/-}$ mice [197].

N-acetyl-p-benzoquinoneimine (NAPQI), the metabolite of N-Acetyl-p-aminophenol (paracetamol, acetaminophen, APAP), is another example of TRPA1

electophilic agonist. NAPQI, like other TRPA1 activators, stimulates TRPA1 causing airway neurogenic inflammation. This inflammatory responses evoked by NAPQI can be abolished by TRPA1 antagonists [198].

The monoterpene ketone umbellulone, the major volatile constituent of the leaves of *Umbellularia californica*, known as the "headache tree" because the inhalation of its vapours can cause severe headache crises, has been shown to activate TRPA1 channel [199]. It has been demonstrated that umbellulone acts on TRPA1 as a partial electrophilic agonist [200].

Although it is now generally accepted that TRPA1 is activated through covalent modification of specific cysteines, the precise mechanism and the chemistry of this covalent modification with unsaturated carbonyl-containing compounds is unclear. Channel activation occurs with chemicals that react with cysteine residues *via* alkylative conjugate addition [201], but unravelling of the molecular details underlying activation and deactivation of TRPA1 *via* covalent modifications still remains an exciting challenge. TRPA1 electrophilic agonists, that are structurally diverse, are unified in their ability to form covalent adduct with thiol group, a moiety that confers them the ability to activate TRPA1 receptor. A variety of known TRPA1 agonists, including acrolein and other α,β-unsaturated aldehydes, possess an electrophilic carbon or sulphur atom that is subject to nucleophilic attack (Michael addition) [202] by cysteine, lysine or histidine of TRPA1. Indeed, mutagenesis studies have clarified that such reactivity promotes channel gating through covalent modification of residues within the cytoplasmic N-terminal domain of the channel [184-186]. In human TRPA1 crucial residues for channel activation by AITC include a cluster of cysteines (Cys619, Cys639 and Cys663) and Lys708 [184]. The ability to form Michael adducts with cysteine is virtually shared by all α,β-unsaturated aldehydes, including the highly electrophilic compound, 4-oxononenal [189].

Non-electrophilic activators. Beside the huge number of electrophilic activators, TRPA1 can also be modulated by other compounds that are unlikely to induce covalent modifications of the channel proteins. Anesthetic agents can induce an activation and sensitization of TRPA1. Propofol (2,6-diisopropylphenol), a commonly used intravenous anesthetic, elicits intense pain upon injection *via* TRPA1 activation [203]. Lidocaine, inhibits cellular excitability by blocking voltage-gated Na^+ channels, but can activate TRPA1 in a concentration-dependent manner. Lidocaine can also act as an inhibitor of TRPA1, an effect more evident with rodent than human TRPA1. This

species-specific difference is probably linked to the pore region (S5 and S6) [204]. Fenamate nonsteroidal anti-inflammatory drugs (NSAIDs) can also activate and sensitize TRPA1. Several non-electrophilic NSAIDs, including flufenamic, niflumic, and mefenamic acid, as well as flurbiprofen, ketoprofen, diclofenac, and indomethacin, reversibly activate TRPA1.

TRPA1 is a non-covalent sensor of polyunsaturated fatty acids (PUFAs), which contain at least 18 carbon atoms and three unsaturated bonds. Those PUFAs activate TRPA1 to excite primary sensory neurons and enteroendocrine cells. They act non-covalently binding domains located in the N-terminus [205].

Many non-covalent modulators of TRPA1 function in a bimodal fashion, i.e. they activate the channel at low concentration, and inhibit it at higher concentrations. Menthol from *Mentha piperita*, a known TRPM8 activator, is also a bimodal modulator of TRPA1. Low-micromolar concentrations of menthol cause channel activation, whereas higher concentrations lead to a reversible channel inactivation [206]. This is only true for human TRPA1, indeed mouse TRPA1 is blocked by menthol. Similarly to menthol, the super-cooling synthetic compound icilin activates not only TRPM8 as but also TRPA1 [207, 208]. Another non-electophilic TRPA1 agonist is caffeine from *Coffea Arabica*. This compound activates mouse TRPA1 but suppresses its human version. Similarly, nicotine from *Nicotinia tabacum* or its analogue, anabasin from *Nicotiana glauca*, are bimodal TRPA1 modulators. Topical application of nicotine causes irritation of the mucosa and skin due to TRPA1 activation. In contrast, higher concentrations inhibit the channel.

Zinc, an essential biological trace element, is required for the structure or function of over 300 proteins. High concentrations of zinc have cytotoxic effects and can cause pain and inflammation. Surprisingly, zinc activates TRPA1 through a unique mechanism that requires zinc influx through TRPA1 channels and subsequent activation *via* specific intracellular cysteine and histidine residues. TRPA1 is highly sensitive to intracellular zinc, as low nanomolar concentrations activate TRPA1 and modulate its sensitivity [209].

TRPA1 is also activated by Δ9THC, the psychoactive compound in marijuana. Also two non-psychoactive cannabinoids, cannabidiol (CBD) and cannabichromene (CBC), are known to modulate TRPA1.

In addition to being directly gated by physical or chemical stimuli, many TRP channels are activated or modulated downstream of neurotransmitter or growth-factor

receptors that stimulate phospholipase C (PLC) (Fig. I-7b). *In vitro* studies have shown that TRPA1 can be activated in this manner, raising the possibility that it functions as a ‘‘receptor-operated’’ channel that depolarizes nociceptors in response to proalgesic or proinflammatory agents that activate PLC [174]. One such agent is BK, a proalgesic and proinflammatory nonapeptide produced endogenously in response to tissue injury, inflammation, or ischemia, which binds to PLC coupled BK receptors (BK2) on sensory neurons [210]. BK elicits acute pain through immediate excitation of nociceptors, followed by a longer lasting sensitization to thermal and mechanical stimuli [211]. Indeed, mice with a mutation in TRPA1 did not develop hyperalgesia after exposure to BK [180]. More interestingly, there are many other proalgesic and proinflammatory agents that activate the PLC pathway, suggesting that may exert they action via TRPA1 receptor [145]. Finally, TRPA1 appears to be sensitized by NGF and PAR2 [212, 213], both of which are known to play a role in infiammatory pain.

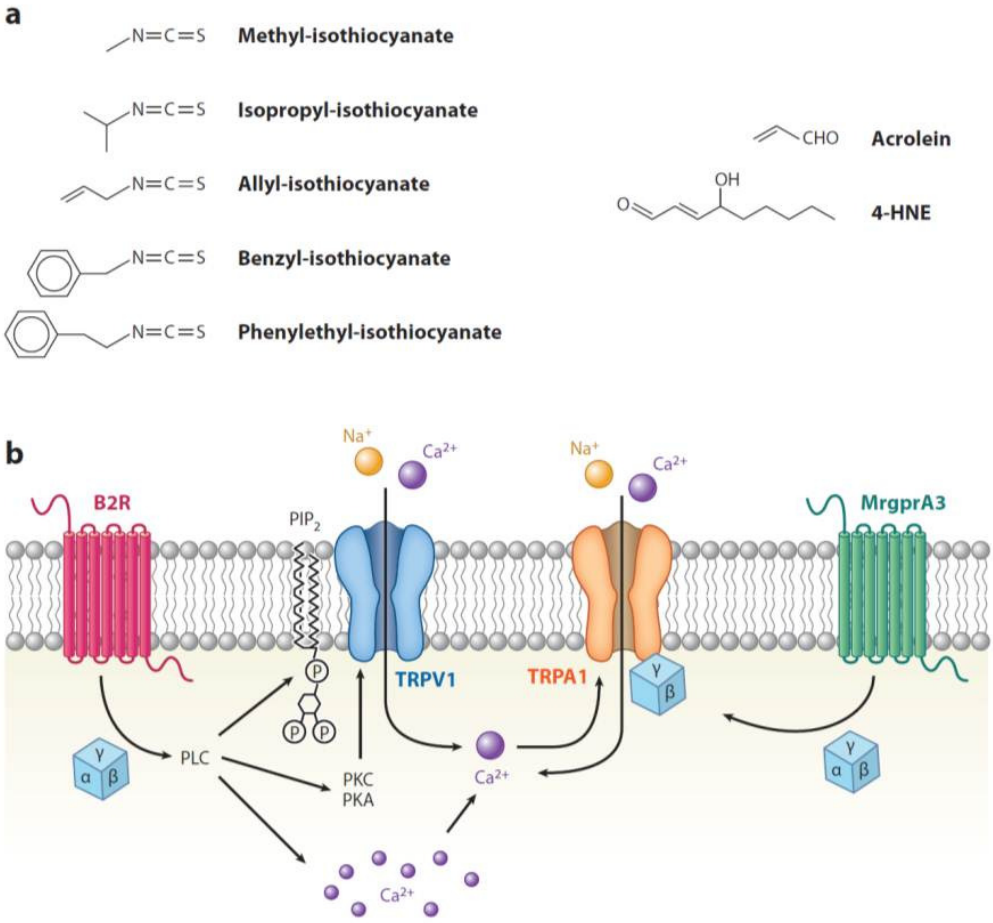

Figure I-7. TRPA1, is a detector of chemical irritants. a A variety of compounds activate TRPA1, including exogenous irritants and endogenous products of tissue injury and inflammation. The agents shown here include isothiocyanates and α,β-unsaturated aldehydes, both of which exhibit strong electrophilic reactivity as the functional attribute underlying their ability to activate TRPA1 channels. **b** In addition to direct activation by electrophilic irritants, TRPA1 functions as a receptor-operated channel that can be activated or sensitized by G protein-coupled signaling pathways. Two such mechanisms have been proposed: (i) A GPCR, such as the B2R bradykinin receptor, activates phospholipase C (PLC) to mobilize release of intracellular calcium. Increased cytoplasmic calcium then activates TRPA1. (ii) Activation of a GPCR, such as the MrgprA3 puritogen receptor, promotes the release of free Gβγ, which serves as the downstream cytoplasmic activator of TRPA1. In addition to these proposed mechanisms, TRPA1 can be activated or sensitized by other events that enhance cytoplasmic calcium levels, such as activation of TRPV1 or other calcium-permeable channels. (Adapted from [295]).

1.4.3 Pharmacology of TRPA1 receptor

In addition to various pain-producing chemicals described as TRPA1 agonists, some molecules have been studied as TRPA1 receptor antagonist: ruthenium red, gentamicin, gadolinium and amiloride. Ruthenium red and gentamicin are very similar, both of them are pore blockers that plug into the channel pore, and differ from amiloride and gadolinium, that block by interacting with an extracellular site of the channel that is outside of the electric field of the pore [142]. However, each of these antagonists also blocks other type of TRP channels, as well as other ion channels. More recently has been identified a TRPA1 selective antagonist, HC-030031 [214]. The first pharmacological evidence implicating the TRPA1 receptor in mediating pain under inflammatory conditions came from the discovery of this new molecule. Indeed, HC-030031 has been an instrumental to determine the role of the channel in the first and second phase of the nociceptive and inflammatory response to formaldehyde [214]. Further studies showed that HC-030031 reduced somatic and visceral nociceptive response [215] or BK-induced mechanical hyperalgesia [181]. Along with TRPA1-decficient mice, this antagonist is currently being used to identify novel roles of TRPA1 in health and disease. Additional TRPA1 antagonists have been more recently identified, including AP18 [181] and Chembridge5861528 [216]. AP18 is a small molecule that blocks TRPA1 through a competitive mechanism displacing the receptor agonists from the binding site. The *in vivo* analgesic activity of AP18 was tested in well-established animal models of inflammation, such as the complete Freund adjuvant (CFA) and the BK-induced mechanical hyperalgesia [181]. Moreover, AP18 is a selective TRPA1 antagonist that inhibits both the mouse and human receptor. Chembridge5861528 is an analogue of HC-030031 and has been shown to display mechanical anti-hyperalgesic activity in vivo in diabetic mice [216].

1.5 Role of TRP channels in chemotherapy-induced peripheral neuropathy

Pharmacological and genetic studies using animal models of CIPN induced by different chemotherapeutic agents indicate that the mechanisms underlying mechanical and thermal hyperalgesia behaviours are multiple. Notwithstanding, recent evidence has emphasized a primary role for several members of the TRP family, in particular TRPV1, TRPV4, TRPA1 and TRPM8 [217-219].

1.5.1 TRPV1 in chemotherapy-induced peripheral neuropathy

The invertebrate relatives of TRPV1 are essential to sensory transduction (phototransduction, thermosensation, mechanosensation, osmosensation) [92], while in mammals TRPV1 seems to contribute to hypersensitivity to thermal, chemical and mechanical stimuli associated with peripheral inflammation and neuronal damage. Among various adverse reactions, heat hypersensitivity has been often reported by patients treated with platinum-based anticancer drugs [220]. Thus, the hypothesis that TRPV1 may play a role in such reactions has been advanced. Treatment with cisplatin has been found to produce up-regulation of TRPV1 mRNA in cultured DRG neurons [221]. A similar up-regulation occurs also after *in vivo* treatment with cisplatin, although cisplatin-treated mice showed no change in the proportion of TRPV1-immunopositive trigeminal ganglia neurons [222]. TRPV1 up-regulation was associated with increased nociceptors responsiveness and contributed to cisplatin-evoked thermal, but not mechanical hyperalgesia in mice [222]. In addition, acute exposure to oxaliplatin induces TRPV1 sensitization, which may cause neuronal damage [221]. The mechanism through which oxaliplatin/cisplatin-induced neuropathy results in TRPV1 sensitization is unclear. However, enhanced TRPV1 protein trafficking, consequent of mRNA overexpression, to peripheral nerve processes, or channel phosphorylation by different kinases, leading to enhanced TRPV1 sensitivity, have been proposed as a general mechanism contributing to pathological pain states [223].

1.5.2 TRPV4 in chemotherapy-induced peripheral neuropathy

Recent evidence has proposed a role for TRPV4 in mechanical allodynia in rodent models of CIPN [224]. In models of painful peripheral neuropathy induced by chemotherapy, alcoholism, diabetes, and human virus/acquired immunodeficiency syndrome therapy, mechanical hyperalgesia was markedly reduced by spinal intrathecal administration of oligodeoxynucleotides antisense to TRPV4 [218]. TRPV4-decificient mice showed reduced mechanical hyperalgesia induced by anticancer drugs, paclitaxel and vincristine, or in a diabetic model [218]. TRPV4 plays a major role in mechanical hyperalgesia and it also contributes to enhanced nociception to hypo-osmotic stimuli in paclitaxel-treated rats. TRPV4-mediated hypersensitivity by paclitaxel is not attributable to increased mRNA levels, but rather it may be related to a specific interaction with second messenger pathways [224]. Similarly to paclitaxel, treatment with vincristine has been reported to produce mechanical allodynia in rodents through a TRPV4-dependent mechanism [218]. Authors suggest that TRPV4 is not directly activated by these agents, but plays a role in mechanotransduction, as a component of a molecular complex that functions only in presence of inflammation or nerve injury phenomena. This complex pathway results in the activation of a signaling cascade initiated by integrins that, *via* Src tyrosine kinase, induces membrane insertion and/or activation of the TRPV4 channel in sensory neurons. Tyrosine kinases are known to regulate trafficking of ion channels and receptors. Recent reports demonstrate that Src tyrosine kinases participate in the modulation of TRP channel function [137, 225, 226], and this mechanism could be responsible for TRPV4 sensitization. In paclitaxel-induced peripheral neuropathy TRPV4-mediated mechanical hyperalgesia results essentially dependent on integrin/Src tyrosine kinase signaling [224]. Another recent paper demonstrates that paclitaxel may release mast cell tryptase, which activate PAR2 receptor expressed in primary sensory neurons [227]. PAR2 activation and the downstream enzymes, PKA, PKCε and PLC, cause sensitization of TRPV1, TRPV4, and TRPA1, thereby leading to mechanical allodynia and thermal hyperalgesia. Targeting the signaling pathways of PAR2 seems to effectively attenuate paclitaxel-induced mechanical, heat, or cold hypersensitivity [227]. The contribution of TRPV4 to CIPN, as more in general to models of inflammatory pain, corroborates the hypothesis that TRPV4 plays a role in sensitization of nociceptors and makes it a novel target for the development of an innovative class of analgesics.

1.5.3 TRPM8 in chemotherapy-induced peripheral neuropathy

TRPM8 is expressed by a non-peptidergic subpopulation of nociceptors and responds to mild and noxious cold (<25°C) temperatures. TRPM8, together with TRPA1, is involved in the induction of hypersensitivity to cold stimuli [207]. An increase in TRPM8 receptor expression occurs in some sensory neurons after nerve injury [228], possibly contributing to enhanced cooling sensation. Similarly, oxaliplatin increased the expression of TRPM8 mRNA in mouse DRG when cold hypersensitivity peaked, suggesting that cold hypersensitivity is at least partly due to the increased expression of TRPM8 in primary sensory neurons [62]. In addition, wet-dog shake and jumping behaviors elicited by icilin, a non-selective TRPM8 activator, were significantly increased in mice treated with oxaliplatin [62]. Furthermore, oxaliplatin seems to affect TRPA1 rather than TRPM8, because oxaliplatin-treatment induces a sensitization to icilin, which activates TRPA1 expressing neurons, but not the response to a TRPM8 specific ligand, WS12 [221]. A recent paper has reported a possible contribution of TRPM8 expressing fibres to cold hypersensitivity induced by oxaliplatin [229].

Paradoxically, a case report indicates that topical menthol application has an analgesic effect in CIPN induced by bortezomib [230]. In addition, topical application of menthol was able to significantly reverse CIPN induced by carboplatin and its prolonged application during chemotherapy appears to prevent neuropathy worsening [231]. Thus, more basic and clinical investigations are required to identify and clarify the role of TRPM8 in CIPN.

1.5.4 TRPA1 in chemotherapy-induced peripheral neuropathy

Recently, our research group demonstrated that TRPA1 acts as a major player in models of CIPN [232]. By both genetic and pharmacological approaches, we showed that TRPA1 entirely mediates mechanical and cold hypersensitivity induced by oxaliplatin and cisplatin [232] in mice and rats. Our recent work (Nassini, 2011), however, indicates that oxaliplatin does not directly gate TRPA1, as it does not cause any calcium response in primary culture of mouse or rat DRG neurons. However, CHO cells transfected with the cDNA codifying for the mouse TRPA1 channel respond, with a glutathione-sensitive intracellular calcium mobilization, upon challenge with

oxaliplatin, whereas untransfected CHO cells do not respond. Thus, we have proposed that calcium response by oxaliplatin requires that the cell expresses TRPA1 and generates sufficient oxidative stress.

1.6 Aim of the study

Peripheral neuropathy represents a common side effect of different chemotherapeutic treatments. Recent evidence advocates a primary role for members of the TRP channels family, expressed on nociceptive primary sensory neurons, in particular TRPV1 and TRPV4, TRPA1 and TRPM8 in painful side effects induced by different chemotherapeutic drugs [221, 222, 224, 218, 62, 232]. In particular, the TRPA1 member, originally cloned from human fetal lung fibroblasts [144], is a nonspecific calcium-permeable cationic channel expressed in primary sensory neurons of the dorsal root, trigeminal and vagal ganglia, where it co-localizes with the TRPV1 channel. Whereas the role of TRPA1 in mechano- and cold-transduction remains to be better clarified, it has been extensively demonstrated that TRPA1 plays a key role in the detection of chemical irritants. In fact, TRPA1 is activated by a wide range of pungent and irritant compounds [174]. Compelling evidence indicates that TRPA1 can be activated by endogenous products generated at sites of inflammation and tissue injury from metabolism and oxidative stress-derived substances. More importantly for the main aim of this thesis, recently it has been demonstrated that TRPA1 acts as a major player in mechanical and cold hypersensitivity induced by the platinum-based chemotherapeutic drugs, oxaliplatin and cisplatin [232].

CIPN is a common major dose-limiting side effect of many chemotherapeutic treatments, including the taxane derivative PXL [25], and the first-in-class proteasome inhibitor BTZ [31, 32]. Among CIPN sensory symptoms, neuropathic pain is prominent and important for many patients, and its severity is often dose-limiting. Inflammation [74, 75], oxidative stress [49], loss of intraepidermal nerve fibers, modifications of both mitochondria and various ion channels function [51, 52, 64] are only some of the several mechanisms mentioned as possibly participating in CIPN development and progression. Following the evidence that TRPA1 acts as a major oxidant sensor [191] and that the chemotherapeutic treatment is associated with the generation of oxidative stress and its by-products, we hypothesized that chemotherapeutic drugs could directly

or indirectly target the TRPA1 channels through the generation of oxidative stress inducing painful states.

Pain symptoms are also associated with the treatment with the third-generation AIs, that include the triazoles anastrozole (Arimidex) and letrozole (Femara), and the steroidal agent exemestane (Aromasin), currently recommended for adjuvant endocrine treatment as primary, sequential, or extended therapy with tamoxifen, for postmenopausal women diagnosed with estrogen receptor-positive breast cancer [36, 37, 38]. Among these, the AI-associated musculoskeletal symptoms (AIMSS) are characterized by morning stiffness and pain of the hands, knees, hips, lower back, and shoulders [41, 42]. In addition to musculoskeletal pain, pain symptoms associated with AIs have recently been more accurately described with the inclusion of neuropathic, diffused, and mixed pain [43]. The chemical structure of exemestane includes a system of highly electrophilic conjugated Michael acceptor groups, which might react with the thiol groups of reactive cysteine residues [277]. Michael addition reaction with specific cysteine residues is a major mechanism that results in TRPA1 activation by a large variety of electrophilic compounds [186, 184, 185]. In addition, aliphatic and aromatic nitriles can react with cysteine to form thiazoline derivatives and accordingly the tear gas 2-chlorobenzylidene malononitrile (CS) has been identified as a TRPA1 agonist [280]. We noticed that both letrozole and anastrozole possess nitrile moieties. Thus, we hypothesized that exemestane, letrozole and anastrozole may produce neurogenic inflammation, nociception and hyperalgesia by targeting TRPA1.

The work described in this thesis is aimed at defining the role of TRPA1 in several painful states induced by the chemotherapeutic agents PXL, BTZ and third-generation AIs. To this purpose both *in vitro* and *in vivo* assays have been used. Calcium imaging experiments were performed in order to explore whether PXL, BTZ and third-generation AIs were able to directly gate the TRPA1 channel evoking painful states. Furthermore, several animal models of chemotherapy-evoked painful side effects were developed and the involvement of TRPA1 was investigated through the use of *Trpa1*$^{+/+}$ and *Trpa1*$^{-/-}$ mice or *via* the administration of TRPA1 selective antagonist.

Chapter II - TRPA1 and TRPV4 mediate paclitaxel-induced peripheral neuropathy in mice via a glutathione-sensitive mechanism

2.1 Materials and methods

Animals. Animal experiments were carried out according to Italian legislation (DL 116/92) and European Communities Council Directive (86/609/EEC). Studies were conducted under the permit (number 143/2008-B and 204/2012-B, University of Florence, Florence, Italy) approved by the Italian National Committee for Animal Research. C57BL/6 mice (male, 25-30 g; Harlan Laboratories), wild-type (*Trpa1*$^{+/+}$), or TRPA1-deficient mice (*Trpa1*$^{-/-}$; 25-30 g; Jackson Laboratories) were used. Animals were housed in a temperature- and humidity-controlled vivarium (12-hour dark/light cycle, free access to food and water). Behavioral experiments were done in a quiet, temperature controlled room (20-22°C) between 10 a.m. and 4 p.m., and were conducted by an operator blinded to the genotype and the status of drug treatment. Animals were sacrificed with a high dose of intraperitoneal (i.p.) sodium pentobarbital (200 mg/kg).

Paclitaxel-induced painful neuropathy models and drugs administration. After habituation and baseline measurements of pain sensitivity, animals were randomized into treatment groups. C57BL/6, *Trpa1*$^{+/+}$, or *Trpa1*$^{-/-}$ mice were treated with a single i.p. administration of paclitaxel (6 mg/kg) or its vehicle (ethanol and Cremophore EL, 50:50, *v/v*) [218]. No weight loss was observed in mice throughout the duration of the experiments after paclitaxel treatment. Paclitaxel was formulated at a concentration of 1 mg/ml and was first dissolved in a vehicle containing absolute ethanol and Cremophore EL (50:50, *v/v*) because of its poor aqueous solubility. Final solution (10% of this stock solution) was made in sterile saline (NaCl 0.9%) at the time

of injection, and the volume was adjusted to 10 ml/kg for the i.p. administration [224]. Intragastric (i.g.) HC-030031 (300 mg/kg) or its vehicle (0.5% carboxymethyl cellulose, CMC), and HC-067047 (10 mg/kg, i.p.) or its vehicle (2.5% DMSO), were administered at day 8 after the administration of paclitaxel or its vehicle. In another experimental setting, HC-030031 (300 mg/kg, i.g.) or its vehicle (0.5% CMC), and HC-067047 (10 mg/kg, i.p.) or its vehicle (2.5% DMSO), were coadministered at day 8 after the administration of paclitaxel or its vehicle.

Tactile allodynia (Von Frey hair test). Paclitaxel-induced mechanical allodynia was measured in C57BL/6, *Trpa1*$^{+/+}$, or *Trpa1*$^{-/-}$ mice by using the up-and-down paradigm [233]. Mechanical nociceptive threshold was determined before (basal level threshold) and after drug administration. The effect of paclitaxel was tested for 20 days after treatment. Data are expressed as the mean threshold values (in grams).

Cold stimulation. Cold allodynia was assessed in C57BL/6, *Trpa1*$^{+/+}$, or *Trpa1*$^{-/-}$ by measuring the acute nocifensive responses to the acetone-evoked evaporative cooling as previously described [62]. Briefly, the animal was held in the hand and a droplet (50 μl) of acetone, formed on the flat-tip needle of a syringe, was gently touched to the plantar surface of the hind paw. The mouse was immediately put in a cage with a transparent floor, and the time spent in elevation and licking of the plantar region over a 60-s period was measured. Acetone was applied three times at a 10-15-min interval, and the average of elevation/licking time was calculated. Cold allodynia was measured in mice before (baseline) and for 20 days after drug treatment.

Isolation of primary sensory neurons. Primary dorsal root ganglia (DRG) from *Trpa1*$^{+/+}$ or *Trpa1*$^{-/-}$ adult mice were cultured as previously described [193]. Briefly, lumbosacral (L5–S2) ganglia were bilaterally excised under a dissection microscope. Ganglia were digested using 2 mg/ml of collagenase type 1A and 1 mg/ml of papain in HBSS (25 min, 37°C). Neurons were pelleted and resuspended in Ham's-F12 containing 10% FBS, 100 U/ml of penicillin, 0.1 mg/ml of streptomycin, and 2 mM glutamine, dissociated by gentle trituration, and plated on glass coverslips coated with poly-L-lysine (8.3 μM) and laminin (5 μM). Neurons were cultured for 3-4 days.

Calcium imaging experiments. Cells were incubated with 5 μM Fura-2 AM ester for 30 min at 37°C. Intracellular calcium mobilization was measured on Nikon Eclipse TE2000U microscope. Fluorescence was measured during excitation at 340 and 380 nm for 5 min before and 10 min after stimulus administration, and after correction for the individual background fluorescence signals, the ratio of the fluorescence at both excitation wavelengths (F_{340}/F_{380}) was monitored. Experiments were performed using a buffer solution containing (in millimolars): 150 NaCl, 6 KCl, 1 $MgCl_2$, 1.5 $CaCl_2$, 10 glucose, and 10 HEPES and titrated to pH 7.4 with 1 N NaOH. Cells were exposed to paclitaxel (10 and 50 μM), allyl isothiocyanate (AITC, 30 μM), or their respective vehicles (0.1%, 0.5%, and 0.03% DMSO). DRGs were challenged with capsaicin (0.1 μM) and by KCl (50 mM) to identify nociceptive neurons and at the end of each experiment with ionomycin (5 μM).

Calcitonin gene-related peptide release. Slices (0.4 mm) of esophagus taken from C57/BL6, *Trpa1*$^{+/+}$, or *Trpa1*$^{-/-}$ were superfused with paclitaxel (10-30-50 μM), or the vehicle (2.5% DMSO), dissolved in a modified Krebs solution at 37°C, and oxygenated with 95% O_2 and 5% CO_2, containing (in millimolars): 119 NaCl, 25 $NaHCO_3$, 1.2 KH_2PO_4, 1.5 $MgSO_4$, 2.5 $CaCl_2$, 4.7 KCl, 11D-glucose, 0.1% BSA, phosphoramidon (1 μM), and captopril (1 μM). Some tissues were preexposed to capsaicin (10 μM) for 20 min to desensitize TRPV1-expressing sensory nerve terminals. Some experiments were performed in a calcium-free medium, containing EDTA (1 mM). Other experiments were performed in the presence of HC-030031 (30 μM) and HC-067047 (3 μM) or in the presence of the unsaturated aldehyde and ROS scavenger, glutathione monoethylester (GSH, 1 mM). Calcitonin gene-related peptide (CGRP) immunoreactivity (CGRP-IR) was assayed in 10-min fractions (two before, one during, and one after exposure to the stimulus) according to the methods previously reported [186]. The detection limit was 5 pg/ml. CGRP-IR release was calculated by subtracting the mean pre-stimulus value from those obtained during or after stimulation. Stimuli did not cross react with CGRP antiserum.

Reagents. If not otherwise indicated, all reagents were from Sigma-Aldrich (Milan, Italy). HC-030031 was synthesized as previously described [234]. HC-067047 was from Tocris Bioscience (Bristol, United Kingdom), and paclitaxel was from Ascent Scientific Ltd (Bristol, UK).

Statistical analysis. Data are presented as mean ± SEM. Statistical analyses were performed by the unpaired two-tailed Student's t test for comparisons between two groups, the one-way analysis of variance, followed by the post-hoc Bonferroni's test for comparisons of multiple groups. $p<0.05$ was considered statistically significant.

2.2 Results

2.2.1 TRPA1 and TRPV4 receptors activation contributes to the mechanical allodynia evoked by paclitaxel in mice

We first investigated the involvement of TRPA1 in the mechanical allodynia induced by paclitaxel in mice. As previously reported [218], administration of a single dose of paclitaxel (6 mg/kg, i.p.) produced a delayed reduction in mechanical nociceptive threshold as assayed by the Von Frey hair test in C57BL/6 mice. Reduction from baseline value was significant at day 2, peaked at day 8, and returned to baseline about 20 days after paclitaxel administration (Fig. II-1a). A role for the TRPV4 channel in paclitaxel induced sensory hypersensitivity has been previously reported by using TRPV4 knockout mice and antisense mediated TRPV4 knockdown [139, 218]. Here we confirm that administration of the selective TRPV4 antagonist, HC-067047 (10 mg/kg, i.p.) [235], 8 days after paclitaxel injection partially reverted paclitaxel-evoked mechanical allodynia. In agreement with previous reports in a different pain model [235], maximum inhibition by HC-067047 was evident 30 min post dosing. HC-067047 did not affect the baseline threshold for mechanical stimulation in naïve animals (Fig. II-1c). In the present study, we also investigated TRPA1 contribution to mechanical allodynia induced by paclitaxel. Eight days after paclitaxel administration, systemic administration of the TRPA1 selective antagonist, HC-030031 (300 mg/kg, i.g.) [214], reverted partially mechanical allodynia. In keeping with previous data obtained in different models of hyperalgesia [236], the effect of HC-030031 was evident 60 min post dosing. HC-030031 did not affect the threshold in mechanical allodynia in naïve animals (Fig. II-1b). Finally, we found that treatment with a combination of the TRPA1 antagonist, HC-030031 (300 mg/kg, i.g.), and the TRPV4 antagonist, HC-067047 (10 mg/kg, i.p.), 8 days after paclitaxel injection completely reverted paclitaxel-evoked mechanical allodynia (Fig. II-1d).

In another series of experiments, we treated *Trpa1*$^{+/+}$ and *Trpa1*$^{-/-}$ mice following the same protocol used in C57BL/6 mice (one single dose of paclitaxel, 6 mg/kg, i.p.). In *Trpa1*$^{+/+}$ mice, the reduction in mechanical nociceptive threshold from baseline value was already significant at day 2, peaked at day 8, and returned to baseline about 20 days after paclitaxel administration. *Trpa1*$^{-/-}$ mice treated with paclitaxel developed a similar, although less pronounced, mechanical allodynia than that observed

in *Trpa1*$^{+/+}$ mice. In particular, at days 7, 8, and 9 after paclitaxel administration, the threshold in the mechanical nociceptive response was significantly reduced in *Trpa1*$^{+/+}$ compared to *Trpa1*$^{-/-}$ mice (Fig. II-1e). To further investigate the relative contribution of TRPV4 and TRPA1 in mechanical allodynia induced by paclitaxel, the effect of HC-067047 was studied in *Trpa1*$^{-/-}$ mice at day 8 after drug injection. Thirty minutes after treatment with HC-067047 (10 mg/kg, i.p.), mechanical allodynia induced by paclitaxel was completely reverted (Fig. II-1f). Thus, present pharmacological and genetics data indicate that, in addition to TRPV4 [218], TRPA1 contributes to paclitaxel-evoked mechanical allodynia.

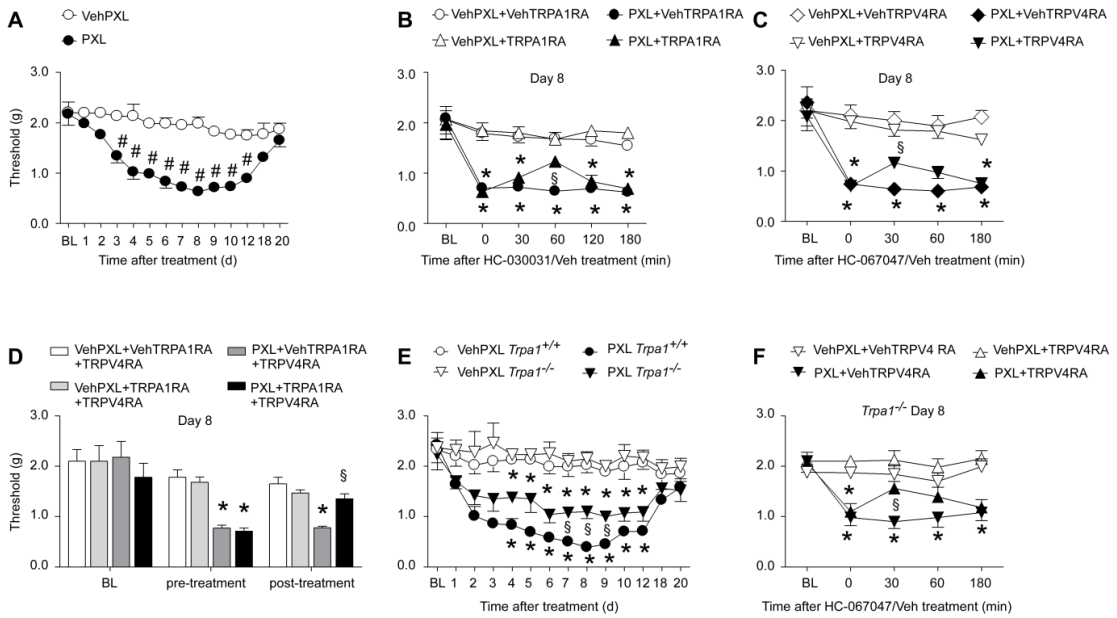

Figure II-1 Paclitaxel induces mechanical allodynia via TRPA1 and TRPV4 activation in mice. (a) The administration of a single dose of paclitaxel (PXL; 6 mg/kg, i.p.) in C57BL/6 mice induces a time-dependent reduction in mechanical nociceptive threshold (Von Frey test), with a maximum effect at day (*d*) 8 after PXL administration. At day 8 after PXL administration, treatment with TRPA1 receptor antagonist, HC-030031 (TRPA1RA; 300 mg/kg i.g), significantly reduces mechanical allodynia 60 min post dosing (b). A similar significant reduction in mechanical allodynia is visible after treatment with the TRPV4 receptor antagonist, HC-067047 (TRPV4RA; 10 mg/kg, i.p.), 30 min post dosing (c). At day 8 after PXL, treatment with a combination of TRPA1 and TRPV4 receptor antagonists HC-030031 and HC-067047 (TRPA1RA+TRPV4RA) completely reverses the mechanical allodynia at the time of the maximum effect of inhibition for each antagonist (post-treatment; 60 and 30 min post HC-030031 and HC-067047 administration, respectively) (d). The administration of the same dose of PXL (6 mg/kg, i.p.) induces a time-dependent reduction in mechanical nociceptive threshold $Trpa1^{+/+}$ mice (e). The development of mechanical allodynia observed in $Trpa1^{+/+}$ mice after PXL treatment is not completely absent in $Trpa1^{-/-}$ mice. A significant difference in the reduction of mechanical nociceptive threshold between $Trpa1^{+/+}$ and $Trpa1^{-/-}$mice is visible at days 7, 8, and 9 after PXL treatment. At day 8 after PXL administration, treatment with the TRPV4 antagonist HC-067047 (TRPV4RA; 10 mg/kg, i.p.) significantly reduces mechanical allodynia developed by $Trpa1^{-/-}$ mice after PXL treatment (f). Values are mean ± SEM of n=8-10mice. #p<0.05 vs. VehPXL in a; Student'st test; *p<0.05 vs. VehPXL-VehTRPA1RA and VehPXL-TRPA1RA in b, or VehPXL-VehTRPV4RA and VehPXLTRPV4RA in c or VehPXL-VehTRPA1 + TRPV4RA and VehPXLTRPA1RA + TRPV4RA in d or VehPXL-$Trpa1^{+/+}$ and Veh PXL$Trpa1^{-/-}$ in e or VehPXL-Veh TRPV4RA and VehPXL-TRPV4RA in f; §p<0.05 vs. PXL-Veh TRPA1RA in b, or PXL-VehTRPV4RA in c and f, or PXL-Veh TRPA1RA + TRPV4RA in d or PXL $Trpa1^{-/-}$ in e; oneway ANOVA and Bonferroni's test. BL baseline withdrawal threshold.

2.2.2 TRPA1 activation mediates the paclitaxel-induced cold hypersensitivity in mice

Next, by using the same treatment protocol, we addressed whether paclitaxel produced cold hypersensitivity by assaying the time spent licking the hind paw following acetone application for cooling stimulation, and the relative contribution of TRPA1 and TRPV4 activation in this response. A single dose of paclitaxel (6 mg/kg, i.p.) significantly increased the behavioral responses evoked following acetone application for cooling stimulation in C57BL/6 mice from day 4 to day 12 after paclitaxel administration (Fig. II-2a). Peak increase was seen at day 8 (Fig. II-2a). This effect of paclitaxel was completely reverted by treatment with HC-030031 (300 mg/kg, i.g.), 60 min post dosing. It should be underlined that time course of inhibition by HC-030031 of either mechanical or cold hypersensitivity was similar. HC-030031 did not affect cold sensitivity in naïve animals (Fig. II-2b). Treatment with HC-067047 (10 mg/kg, i.p.) 8 days after paclitaxel injection did not affect the cold allodynia induced by the drug (Fig. II-2c). Like C57BL/6 mice, *Trpa1*$^{+/+}$ mice treated with paclitaxel developed a cold hypersensitivity that started at day 2, peaked at day 8, and returned to baseline 18 days after paclitaxel administration (Fig. II-2d). The increased response to the cold stimulus observed in *Trpa1*$^{+/+}$mice was completely absent in *Trpa1*$^{-/-}$ mice, which responded to the stimulus in a manner superimposable to vehicle-treated animals. Pharmacological and genetic findings indicate that TRPA1, but not TRPV4, contributes to paclitaxel-evoked cold allodynia.

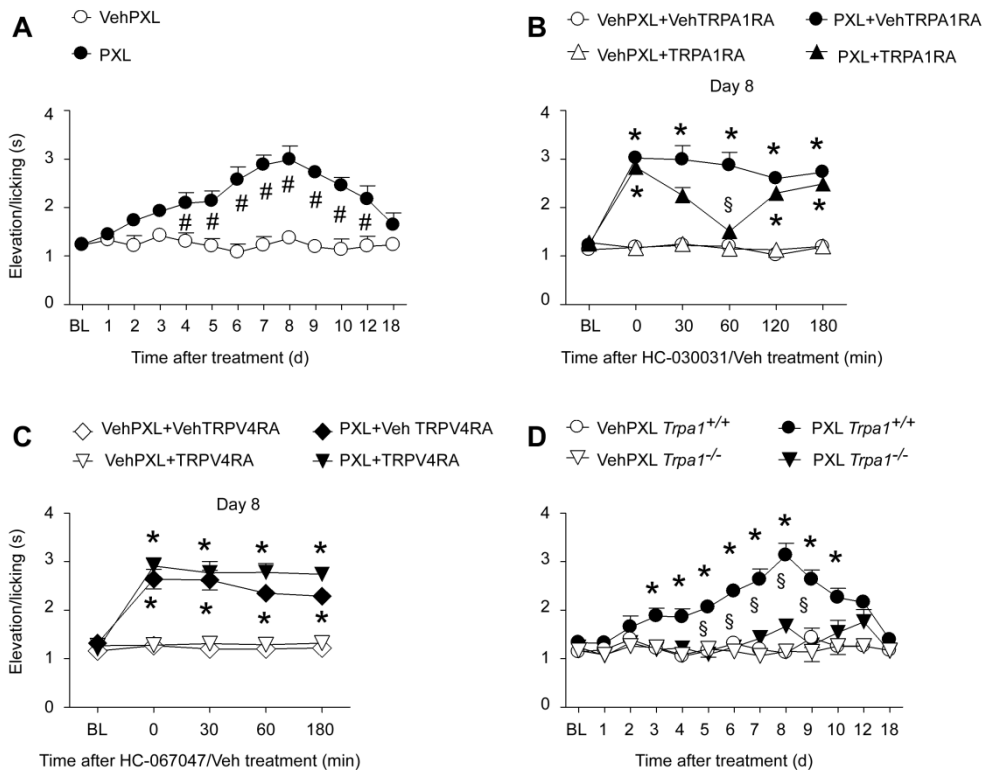

Figure II-2 Paclitaxel-induced cold hypersensitivity is mediated by TRPA1 activation in mice. (a) The administration of paclitaxel (PXL; 6 mg/kg, i.p.) induces in C57BL/6 mice a time-dependent increase in cold hypersensitivity (acetone test) with maximum effect at day (*d*) 8 after PXL administration. At day 8 after PXL treatment, TRPA1 receptor antagonist HC-030031 (TRPA1 RA; 300 mg/kg, i.g.) completely reverses the cold allodynia 60 min post dosing (b). Treatment with the TRPV4 receptor antagonist HC-067047 (TRPV4 RA; 10 mg/kg, i.p.) does not affect the cold allodynia induced by PXL (c). The development of cold allodynia observed in *Trpa1*$^{+/+}$ mice after PXL (6 mg/kg, i.p.) treatment is completely absent in *Trpa1*$^{-/-}$ mice (d). Values are mean ± SEM of n=8–10 mice. #p<0.05 vs. Veh PXL in a; Student'st test; *p<0.05 vs. VehPXLVehTRPA1RA and VehPXL-RPA1RA in b, or VehPXL-VehTRPV4RA and VehPXL-TRPV4RA in c or VehPXL- *Trpa1*$^{+/+}$ in d; §p<0.05 vs. PXL-VehTRPA1RA in b or PXL- *Trpa1*$^{-/-}$ in e; one-way ANOVA and Bonferroni's test. BL baseline withdrawal threshold.

2.2.3 Paclitaxel does not directly activate TRPA1 or TRPV4 in dorsal root ganglion neurons but releases CGRP from peripheral nerve endings *via* glutathione-sensitive mechanism

Exposure to AITC (30 μM) of mouse DRG evoked a calcium response in neurons obtained from *Trpa1*$^{+/+}$ mice (24 cells of the 48 capsaicin (0.1 μM) sensitive neurons responded to AITC), an effect that was completely absent in DRG neurons taken from *Trpa1*$^{-/-}$ mice (0 cells of the 52 responding to capsaicin). Exposure to paclitaxel (50 μM) failed to evoke any significant calcium response in the 68 neurons tested, taken from *Trpa1*$^{+/+}$.

TRPA1 activation of peripheral terminals of capsaicin-sensitive primary sensory neurons is associated with the release of sensory neuropeptides, including CGRP [6]. Several peripheral tissues, including the esophagus [114], have been previously used to study the release of sensory neuropeptides. Paclitaxel increased the basal outflow of CGRP from slices of C57BL/6 mouse esophagus in a concentration-dependent manner (Fig. II-3a), a response that was markedly reduced (>80% inhibition) by preexposure of the tissue to a high capsaicin concentration (a procedure known to cause desensitization of sensory nerve terminals) or by removal of extracellular calcium ions from the bath solution (Fig. II-3a). Thus, paclitaxel evokes a calcium-dependent neurosecretory process of CGRP from capsaicin-sensitive sensory neurons. Paclitaxel-evoked CGRP-IR release was reduced, but not abolished, in the presence of each individual antagonist of TRPA1 (HC-030031) or TRPV4 (HC-067047) channel (Fig. II-3b). However, pretreatment of the tissue with GSH (1 mM) abated completely the paclitaxel-evoked increase in CGRP-IR outflow (Fig. II-3b).

Exposure to paclitaxel increased the CGRP-IR outflow from slices of esophagus obtained from *Trpa1*$^{+/+}$ mice. This response was significantly, but not completely, reduced in preparations obtained from *Trpa1*$^{-/-}$ mice (Fig. II-3c). To further investigate the contribution of the oxidative stress byproducts that eventually target TRPV4 receptor, esophageal slices from *Trpa1*$^{-/-}$ mice were exposed to paclitaxel in the presence of GSH. Under these circumstances, GSH further decreased paclitaxel-evoked CGRP-IR release (Fig. II-3c). Thus, paclitaxel evokes a calcium-dependent neurosecretory process from capsaicin-sensitive neurons by a dual TRPA1 and TRPV4 dependent mechanism and in a manner entirely sensitive to GSH.

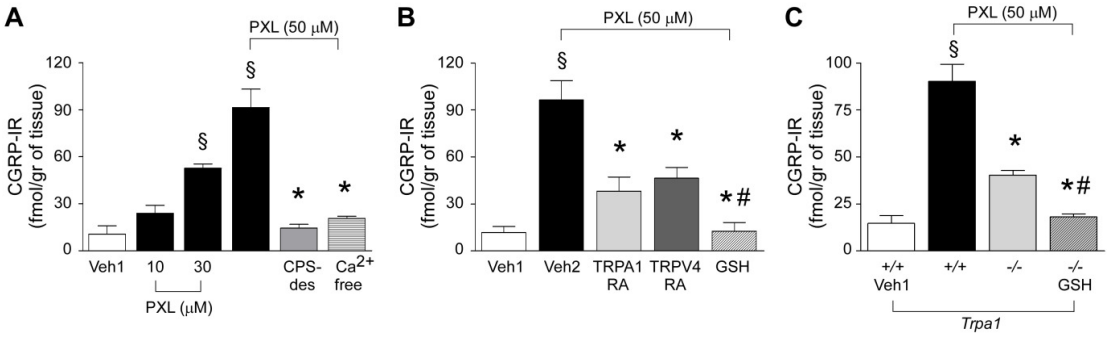

Figure II-3. Paclitaxel releases calcitonin gene-related peptide (CGRP) from mouse esophagus peripheral nerve endings. a Paclitaxel (PXL) increases the outflow of CGRP immunoreactivity (CGRP-IR) from slices of C57BL/6 mice esophagus in a concentration-dependent manner. CGRPIR release evoked by PXL is abolished by capsaicin desensitization (CPSdes) or calcium removal (Ca2+-free). b CGRP-IR evoked by PXL in peripheral tissues is significantly reduced by pretreatment with TRPA1, HC-030031 (TRPA1 RA, 30 μM), or TRPV4, HC-067047 (TRPV4 RA, 3 μM) selective antagonists and by glutathione (GSH, 1 mM). c Paclitaxel increases the release of CGRP-IR from esophageal slices obtained from *Trpa1*$^{+/+}$ mice, an effect significantly reduced in preparations taken from *Trpa1*$^{-/-}$ mice. Pretreatment of the esophageal slices taken from *Trpa1*$^{-/-}$ mice with GSH (1 mM) abated the CGRP-IR release induced by paclitaxel. Veh1 is the vehicle of PXL and Veh2 is a combination of vehicles of the various treatments. Values are mean ± SEM of n05 experiments. §p<0.05 vs. Veh1; *p<0.05 vs. Veh2 or PXL-*Trpa1*$^{+/+}$, #p<0.05 vs. TRPA1 RA and TRPV4 RA or PXL-*Trpa1*$^{-/-}$.

2.3 Discussion

Sensory peripheral neuropathy (PN) affects a proportion of patients treated with the anticancer drug, paclitaxel, and this adverse reaction is often the cause for drug discontinuation [25]. The experimental counterpart of this clinical condition has been described in a large series of studies in rodents showing that paclitaxel causes mechanical and cold allodynia. Among the various mechanisms proposed as causing the paclitaxel sensory neuropathy, recent evidence proposed a role for the TRPV4 channel in mechanical allodynia in mouse and rat models [218, 224]. Here, we confirm in a mouse model that TRPV4 contributes to mechanical allodynia induced by paclitaxel. We also show that TRPA1 accounts for the remaining TRPV4-resistant component of the mechanical hypersensitivity produced by the anticancer drug. This conclusion is derived from either pharmacological study, using selective TRPA1 and TRPV4 antagonists, or genetic study, using TRPA1-deficient mice. The TRPV4 antagonist, HC-067047, abated completely the component of the paclitaxel-evoked mechanical allodynia that was resistant to TRPA1 pharmacological blockade or genetic deletion.

Paclitaxel administration to rodents evokes a typical cold hypersensitivity, reminiscent of the clinical condition caused by the drug in treated patients [61]. In contrast, with mechanical allodynia, either pharmacological or genetic studies indicate a primary and unique role of TRPA1 in the present mouse model of cold hypersensitivity evoked by paclitaxel. This conclusion is derived from the observation that, either after treatment with HC-030031, or in TRPA1-deficient mice, paclitaxel-induced cold allodynia was completely abated, and that HC-067047 failed to affect the increased response to acetone after paclitaxel treatment. Thus, under the present circumstances, cold hypersensitivity is completely mediated by TRPA1, whereas both TRPA1 and TRPV4 contribute to mechanical allodynia.

There is compelling evidence obtained both *in vitro* or *in vivo*, both in experimental animals and in humans, that paclitaxel treatment is associated with production of oxidative stress [237, 238]. Indeed, accumulation of hydrogen peroxide is an early and crucial step for paclitaxel-induced cancer cell death [237]. In general, induction of oxidative stress as a mechanism that may contribute to the antineoplastic effect of several chemotherapeutic agents has been gaining acceptance [239]. Antioxidants, such as N-acetylcysteine, have been shown to inhibit both paclitaxel-evoked decreases in cell viability and increases in intracellular levels of ROS and

apoptosis, [240]. N-acetylcysteine has been reported to prevent completely paclitaxel-evoked mechanical hypersensitivity [51]. Thus, the proapototic effects on one side, and the establishment of the sensory PN on the other side, seem to be dependent on one single mechanism, e.g., the ability of paclitaxel to generate oxidative stress. We have recently identified the primary role of TRPA1 in mediating mechanical and cold hypersensitivity to oxaliplatin and its ability to target TRPA1, not directly, but rather via oxidative stress generation [232]. In fact, we showed that, in contrast with the selective TRPA1 agonist, AITC, oxaliplatin per se does not activate TRPA1 in cultured DRG neurons, as measured by the ability to evoke an early calcium response [232]. However, in a more complex preparation, such as the isolated guinea pig pulmonary artery, oxaliplatin caused a TRPA1- and CGRP-dependent relaxation that mechanistically was indistinguishable from the relaxation evoked by AITC [232]. This finding suggested that oxaliplatin, like AITC, targets TRPA1 on sensory nerve endings, thereby releasing the sensory neuropeptide CGRP, which eventually relaxes the artery [232]. Of interest for the present discussion is the finding that oxaliplatin-evoked, but not AITC-evoked, arterial relaxation was completely abated by GSH. These findings imply that oxaliplatin does not directly gate TRPA1, but rather probably exerts this action indirectly via the generation by neighboring cells of oxidative stress byproducts that eventually target the channel in sensory nerve terminals, through direct formation of disulfide bridges.

Following this hypothesis, we tested whether paclitaxel could target sensory nerve terminals in a manner similar to that of oxaliplatin by measuring the release of the sensory neuropeptide, CGRP. Previous papers [217, 241] reported that paclitaxel releases substance P (SP) from airway sensory nerves, another neuropeptide co-expressed with CGRP in a subset of primary sensory neurons [242]. The mechanism of action of paclitaxel on sensory neurons remained unknown, although inhibition of paclitaxel-evoked SP release from DRG neurons by ruthenium red [219], a nonspecific TRP channels inhibitor [93], suggests the involvement of this type of channels. Here, we confirm that paclitaxel releases neuropeptides from terminals of capsaicin-sensitive primary sensory neurons, and for the first time we show, by using both pharmacological and genetic data, that the action of paclitaxel is mediated in part by TRPA1 activation and in part by TRPV4 activation. In addition, the ROS and reactive aldehydes, scavenger, GSH, completely abolished paclitaxel-evoked CGRP release from esophageal slices of either wild type or TRPA1-deficient mice. These findings indicate

that GSH-sensitive compounds are generated by paclitaxel and finally target TRPA1 and TRPV4.

Additional issues remain to be determined. Although release experiments indicate that paclitaxel is apparently able to acutely stimulate both TRPA1 and TRPV4, it is only after a significant time delays (days) that mechanical allodynia (mediated by both TRPA1 and TRPV4) and cold hypersensitivity (mediated by TRPA1) develop. The time dependent mechanism(s), which from early stimulation leads to the delayed and enduring hypersensitivity, is unknown. Pathophysiological functions of TRPV4 and TRPA1 are not completely understood; although TRPV4 is considered to mediate osmomechanical stimuli [125], TRPA1 has been proposed as a sensor of chemical irritants [243], and both may play a role in hyperalgesia [236]. Our present data are in agreement with recent findings reporting a contribution of TRPA1 and TRPV4 in paclitaxel-evoked hypersensitivity [227]. However, in our study, pharmacological inhibition and, more importantly, TRPA1 genetic deletion, reduced mechanical allodynia only partially, and it was only after TRPV4 inhibition that paclitaxel-evoked response was completely abated. The difference may be due to the diverse protocols of paclitaxel administration used in the present study (one single administration) as compared to the other study (repeated administrations) [227]. In the latter paper, antagonism in the central nervous system of the proteinase-activated receptor 2 (PAR2) completely inhibited heat, cold, and mechanical hypersensitivity, three sensory modalities that, at different degrees, were mediated by TRPV1, TRPV4, and TRPA1, respectively. TRPV4 has been reported to induce thermal and mechanical hyperalgesia [244]. There is evidence that TRPA1 and TRPV4 can be sensitized by PAR2 [130, 212]. Thus, it is possible that PAR2 orchestrates the mechanism that eventually results in TRP channel-mediated hypersensitivity. However, the mechanism of the interaction between PAR2 and TRP channels, and the anatomo-functional site where the interaction occurs, remain to be determined.

A number of studies reported that antioxidants protect against the sensory neuropathy induced by paclitaxel [238, 245]. Present evidence shows that GSH inhibits TRPA1 and TRPV4 targeting on sensory nerves induced by paclitaxel. However, whereas endogenous oxidative stress byproducts capable of activating TRPA1 are well identified, little information [246] is available regarding activation of TRPV4 by oxidative stress byproducts, and no evidence exists that oxidative stress may activate PAR2. Thus, further studies are required to define upstream (oxidative stress) or

downstream (PAR2) mechanisms apparently associated to paclitaxel-induced and TRPA1/TRPV4-mediated hypersensitivity. Irrespective of the underlying mechanism, previous [139, 218, 224, 232] and present findings support the hypothesis of using TRPA1 and TRPV4 antagonists to treat patients with PN evoked by anticancer medicines, such as paclitaxel or oxaliplatin.

This work has been published in Pflügers Archiv - European Journal of Physiology

Materazzi S, Fusi C, Benemei S, Pedretti P, Patacchini R, Nilius B, Prenen J, Creminon C, Geppetti P, Nassini R (2012). "TRPA1 and TRPV4 mediate paclitaxel-induced peripheral neuropathy in mice via a glutathione-sensitive mechanism." Pflugers Arch 463(4):561-9.

Chapter III - Novel therapeutic strategy to prevent chemotherapy-induced persistent sensory neuropathy by TRPA1 blockade

3.1 Materials and methods

Animals. Animal experiments were carried out according to Italian legislation (DL116/92) and European Communities Council Directive (86/609/EEC). Studies were conducted under the permit (number143/2008-Band204/2012-B, University of Florence, Florence, Italy) approved by the Italian National Committee for Animal Research. C57BL/6 mice (male, 25-30 g; Harlan Laboratories), wild-type (*Trpa1*$^{+/+}$), or TRPA1-deficient mice (*Trpa1*$^{-/-}$; 25-30 g; Jackson Laboratories) were used. Animals were housed in a temperature- and humidity-controlled vivarium (12 hour dark/light cycle, free access to food and water). Behavioral experiments were done in a quiet, temperature-controlled room (20-22°C) between 9 a.m. and 5 p.m., and were conducted by an operator blinded to the genotype and the status of drug treatment. Animals were sacrificed with a high dose of intraperitoneal (i.p.) sodium pentobarbital (200 mg/kg).

Reagents. If not otherwise indicated, all reagents were from Sigma-Aldrich. HC-030031 [2-(1,3-Dimethyl-2,6-dioxo-1,2,3,6-tetrahy-dro-7H-purin-7-yl)-N-(4-isopropylphenyl) acetamide] was synthesized as previously described (15). HC-067047 (2-Methyl-1-[3-(4-morpholinyl) propyl]-5-phe-nyl-N-[3-(trifluoromethyl) phenyl]-1H-pyrrole-3-carboxamide) was obtained from Tocris Bioscience, and bortezomib was purchased from LC Laboratories.

Chemotherapy-induced painful neuropathy models. Previous studies have described rat and mouse models of peripheral neuropathy induced by repeated and prolonged administration of bortezomib [55, 247-249]. On the basis of these findings, in

the first series of experiments, we explored whether a single administration of bortezomib produced mechanical and cold hypersensitivity in mice, as observed for different chemotherapeutic agents including oxaliplatin, paclitaxel, and vincristine [62, 232, 250]. After habituation and baseline measurements of pain sensitivity, animals were randomized into treatment groups. C57BL/6, *Trpa1*$^{+/+}$, or *Trpa1*$^{-/-}$ mice were treated with a single intraperitoneal administration of different doses of bortezomib (0.2, 0.5, and 1 mg/kg), or vehicle (dimethylsulfoxide, DMSO1%; ref. [248]). Bortezomib, formulated at a concentration of 1 mg/mL, was first dissolved in a vehicle containing DMSO, and the volume was adjusted to 10 mL/kg to a final concentration of 1% DMSO, then diluted in isotonic saline (NaCl 0.9%) to obtain lower doses. A different group of C57BL/6 mice was treated with a single administration of oxaliplatin (3 mg/kg, i.p.) or its vehicle (isotonic saline, NaCl 0.9%; ref. [232]). No weight loss was observed in mice after bortezomib or oxaliplatin treatment throughout the duration of the experiments. Effects induced by bortezomib and oxaliplatin were tested for 14 and 30 days (starting 6 hours after drug administration), respectively. Baseline values for nociceptive tests were observed before chemotherapy treatment.

Nociceptive tests.

Von frey hair test. Mechanical threshold was measured in C57/BL6, *Trpa1*+/+, or *Trpa1*$^{-/-}$ mice after a single administration of bortezomib or oxaliplatin by using the up-and-down paradigm [233]. Mechanical nociceptive threshold was determined before (basal level threshold) and after different treatments. The 50% mechanical paw withdrawal threshold (ing) response was then calculated from these scores, as previously described [233, 251].

Hot plate test. The paw thermal hyperalgesia was assessed in C57/BL6, *Trpa1*$^{+/+}$, or *Trpa1*$^{-/-}$ by placing animals on a hot plate (Ugo Basile) with the temperature adjusted to 50 ± 0.1°C [252]. The latency to the first hindpaw licking or withdrawal was taken as an index of nociceptive threshold. The cut-off time was set at 30 seconds, to avoid damage to the paw. The paw withdrawal latency to the first response was reported as mean of 2 different trials.

***Cold stimulation*.** Cold allodynia was assessed in C57/BL6, *Trpa1*$^{+/+}$, or *Trpa1*$^{-/-}$ by measuring the acute nocifensive response to the acetone-evoked evaporative cooling as previously described [250]. Briefly, a droplet (50 µL) of acetone, formed on the flat-tip needle of a syringe, was gently touched to the plantar surface of the mouse hindpaw,

and the time spent in elevation and licking of the plantar region over a 60-second period was measured. Acetone was applied 3 times at a 10- to 15-minute intervals, and the average of elevation/licking time was calculated.

Chemical hyperalgesia. Nociceptive behavior was assessed by measuring spontaneous nociceptive response induced by intraplantar (i.pl.) injection (20 µL) of subthreshold doses of allyl isothiocyanate (AITC; 1 nmol/paw), capsaicin (0.01 nmol/paw), hypotonic saline (NaCl, 0.45%), or prostaglandin E_2 (PGE_2, 0.3 nmol/paw) at day 7 after the administration of bortezomib or its vehicle. Immediately after the injection, mice were placed inside a Plexiglas chamber and the total time spent licking and lifting the injected hindpaw was recorded for 5 minutes (AITC, capsaicin, and hypotonic saline), or 20 minutes (PGE_2). Previous experiments conducted in our laboratory and previous findings [253, 254] suggested subthreshold doses that do not cause nociception in naïve mice.

Rotarod test. Locomotor function, coordination, and sedation of animals were tested by using a rotarod apparatus (Ugo Basile). The test was done as previously described [255]. Briefly, 24 hours before the experiments, the animals were trained on the rotarod apparatus, programmed at 8 rpm, until they remained without falling for 60 seconds. The day of the experiment, the latency (seconds) to the first fall and the number of falls were recorded. Cut-off time was 240 seconds.

Treatment protocols. In a first set of experiments, intragastric (i.g.) HC-030031 (300 mg/kg) or its vehicle (0.5% carboxymethylcellulose, CMC), HC-067047 (10 mg/kg, i.p.) or its vehicle (2.5% DMSO), or α-lipoic acid (100 mg/kg, i.g.) or its vehicle (0.5% CMC), were administered at day 7 after the administration of bortezomib (1 mg/kg, i.p.) or its vehicle. In a second set of experiments, i.pl. HC-030031 (100 mg/paw, 20 µL; ref. [256]), α-lipoic acid (10 mg/paw, 20µL; ref. [257]), or vehicle (20 µL/paw, 1% DMSO in isotonic saline, NaCl 0.9%) were injected at day 3 or day 7 after the administration of oxaliplatin or bortezomib (see earlier section for dosing), respectively. In a third set of experiments, HC-030031 (300 mg/kg, i.g.), α-lipoic acid (100 mg/kg, i.g.), or their respective vehicles, were administered 15 minutes before the administration of bortezomib, oxaliplatin, or their vehicles and treatment was repeated 3 times at approximately 90-minute intervals each after the administration of bortezomib or oxaliplatin. In a fourth and final set of experiments, a group of mice was treated with HC-030031 or its vehicle 15 minutes before and shortly (3 times at approximately 90-

minute intervals each) after a first bortezomib (1 mg/kg, i.p.) or vehicle administration. At day 6, each group of mice received a second treatment identical to that administered at day 1, except for mice treated at day 1 with both HC-030031 and bortezomib, which were subdivided into 2 additional groups. One group was treated a second time with either HC-030031 (300 mg/kg, i.g.) and the second with its vehicle 15 minutes before and shortly after (3 times at approximately 90-minute intervals each) bortezomib administration (Fig. III-6A).

Isolation of primary sensory neurons and calcium imaging experiments. Primary dorsal root ganglia (DRG) from C57/BL6 adult mice were cultured as previously described [250]. Briefly, lumbosacral (L5-S2) ganglia were bilaterally excised under a dissection microscope. Ganglia were digested using 1 mg/mL of collagenase type 1A and 1 mg/mL of papain in Hank's Balanced Salt Solution (25 minutes, 37°C). Neurons were pelleted and resuspended in Ham's-F12 containing 10% FBS, 100 U/mL of penicillin, 0.1 mg/mL of streptomycin, and 2 mmol/L glutamine, dissociated by gentle trituration, and plated on glass coverslips coated with poly-L-lysine (8.3 µmol/L) and laminin (5 µmol/L). Neurons were cultured for 3 to 4 days. Cells were incubated with 5 µmol/L Fura-2AM ester for 30 minutes at 37°C. Intracellular calcium concentration ($[Ca^{2+}]_i$) was measured on a Nikon Eclipse TE2000U microscope. Fluorescence was measured during excitation at 340 and 380 nm, and after correction for the individual background fluorescence signals, the ratio of the fluorescence at both excitation wavelengths ($Ratio_{340/380}$) was monitored. Experiments were conducted using a buffer solution containing (in mmol/L): 150 NaCl, 6 KCl, 1 $MgCl_2$, 1.5 $CaCl_2$, 10 glucose, 10 HEPES and titrated to pH 7.4 with 1 N NaOH. Cells were challenged with bortezomib (10, 50, and 100 µmol/L) or their respective vehicles (0.01 0.5, and 1% DMSO). AITC (30 µmol/L), and capsaicin (0.1 µmol/L) to identify nociceptive neurons. In another series of experiments, DRG neurons were incubated with bortezomib (10 or 100 µmol/L) or its vehicle (0.01 and 0.1% DMSO) for 2 hours and then challenged with AITC (10 or 30 µmol/L). Results are expressed as the increase of $Ratio_{340/380}$ over the baseline normalized to the maximum effect induced by ionomycin (5 µmol/L) added at the end of the experiment.

Protein extraction and Western immunoblot assay. Spinal cord, DRGs, and hindpaw skin were obtained from mice treated with bortezomib or its vehicle at day 7 post treatment. Tissue samples were homogenized in lysis buffer containing (in

mmol/L): 50 Tris, 150 NaCl, 2 EGTA, 100 NaF, 1 Na_3VO_4, 1% NonidetP40, pH7.5, and complete protease inhibitor cocktail (Roche). Lysates were centrifuged at 14,000 g at 4° C for 45 minutes. Protein concentration in supernatants was determined using DC protein assay (BioRad). Samples with equal amounts of proteins (30 µg) were then separated by 10% SDS-PAGE electrophoresis, and there solved proteins were transferred to a polyvinylidenedifluoride membrane (Merck Millipore Billerica). Membranes were incubated with 5% dry milk in Tris buffer containing 0.1% Tween20 (TBST; 20 mmol/L Tris, pH 7.5, 150 mmol/L NaCl) for 1 hour at room temperature, and incubated with rat polyclonal primary antibody for TRPA1 detection (1:200; Novus Biologicals), or mouse monoclonal primary antibody for β-actin (1:6,000; Thermo Scientific), at 4°C overnight. Membranes were then probed with goat anti-mouse or donkey anti-rabbit IgG conjugated with horseradish peroxidase (Bethyl Laboratories Inc.) for 50 minutes at room temperature. Finally, membranes were washed 3 times with TBST, and bound antibodies were detected using chemiluminescence reagents (ECL; Pierce, Thermo Scientific). The density of specific bands was measured using an image processing program (ImageJ 1.32J, Wayne Rasband) and normalized against a loading control (β-actin).

Carboxy-methyl-lysine adducts measurement in plasma. Briefly, blood samples from C57/BL6 mice, taken 1, 3, 6, and 24 hours after the administration of bortezomib (1 mg/kg, i.p.), oxaliplatin (3 mg/kg, i.p.), or their vehicles (1% DMSO and isotonic saline, NaCl 0.9%, respectively), were centrifuged at 3,500 g for 10 minutes, and plasma was used for the carboxy-methyl-lysine (CML) protein adduct ELISA assay. CML protein adducts content in plasma was measured using an ELISA kit (OxiSelect ELISAKit, Cell Biolabs Inc. Valter Occhiena S.R.L.) according to the manufacturer's instructions.

Statistical analysis. Data are presented as mean ± SEM. Statistical analysis was carried out by the unpaired 2-tailed Student *t* test for comparisons between 2 groups, the ANOVA, followed by the *post hoc* Bonferroni test for comparisons of multiple groups. P value less than 0.05 was considered statistically significant (GraphPadPrism version 5.00). To meet ANOVA assumptions, mechanical allodynia data were subjected to log transformation before statistical analysis.

3.2 Results

3.2.1 Bortezomib administration produces persistent mechanical cold and chemical hypersensitivity mediated by TRPA1

Administration of a single dose (0.2, 0.5, and 1 mg/kg, i.p.) of bortezomib induced a dose-dependent mechanical and cold hypersensitivity in C57BL/6 mice (Fig. III-1A and B). Reduced mechanical threshold was observed after bortezomib (1 mg/kg, i.p.) injection as early as 6 hours and lasted until 11 days after treatment (Fig. III-1A). Similar results were obtained for cold allodynia, which was evident at day 1 and persisted until day 11 after bortezomib injection (Fig. III-1B). Bortezomib administration (1 mg/kg, i.p.) did not affect the heat threshold of mice at any time point, from 6 hours to 14 days after treatment. Nociception time to heat stimulus was 19.7 ± 0.8 seconds and 17.2 ± 1.0 seconds at baseline and 7 days after bortezomib treatment, respectively (n=8-10 mice, $P > 0.05$, Student *t* test).

Next, we investigated whether TRPA1 activation is involved in mechanical and cold hypersensitivity induced by bortezomib. Systemic treatment with the TRPA1 selective antagonist HC-030031 (300 mg/kg, i.g.; ref. [214]) at day 7 after bortezomib treatment completely, but transiently, reverted both mechanical hyperalgesia and cold allodynia. Significant inhibition was observed from 30 to 120 minutes after HC-030031 treatment, with maximum reduction (98 ± 12% and 90 ± 6% for mechanical hyperalgesia and cold allodynia, respectively) 60 minutes post dosing (Fig. III-1C and D). Systemic treatment with HC-030031 (300 mg/kg, i.g.) at day 7 after treatment with bortezomib (0.2 or 0.5 mg/kg, i.p.) completely but transiently reverted both mechanical hyperalgesia and cold allodynia (data not shown).

Given that we, as well as others [224, 250], have found that mechanical and cold hypersensitivity evoked by paclitaxel was mediated by both TRPA1- and TRPV4-dependent mechanisms, we tested whether the TRPV4 channel contributes to bortezomib-induced sensory hypersensitivity by using a selective TRPV4 antagonist, HC-067047 (10 mg/kg, i.p.; ref. [235]). HC-067047, at a dose able to reduce mechanical hyperalgesia evoked by paclitaxel [250], failed to affect bortezomib-evoked hypersensitivities (data not shown). Therefore, present pharmacologic evidence indicates an exclusive role for TRPA1 in bortezomib-induced mechanical allodynia and cold hypersensitivity in mice, whereas it rules out a contribution by TRPV4. More

importantly, we found that bortezomib treatment (1 mg/kg, i.p.) produced mechanical hyperalgesia and cold allodynia in *Trpa1*$^{+/+}$ mice with an identical time course to that observed in C57BL/6 mice, an effect that was completely absent in *Trpa1*$^{-/-}$ mice (Fig. III-1E and F).

In addition, we wondered whether bortezomib could cause selective chemical hypersensitivity to TRPA1 agonists. The study of the effects produced by sub-threshold doses of AITC (TRPA1 agonist), capsaicin (TRPV1 agonist), PGE_2 (EP1-4 receptor agonist), or hypotonic saline (which can stimulate TRPV4) showed that bortezomib treatment selectively increased the nociceptive behavior evoked by AITC (Fig. III-2A). In fact, responses to capsaicin, PGE_2, and hypotonic saline were similar in both vehicle- and bortezomib-treated animals (Fig. III-2B-D). As expected, in TRPA1-deficient mice treated with bortezomib or its vehicle, AITC failed to evoke any nociceptive response (data not shown).

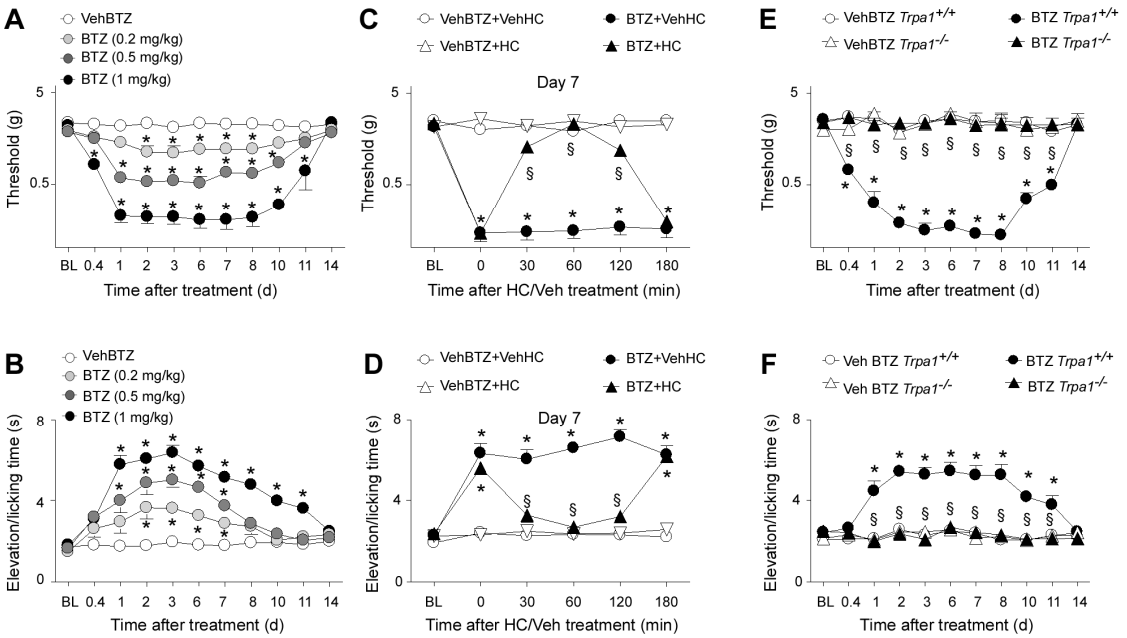

Figure III-1. Bortezomib induces mechanical allodynia and cold hypersensitivity via TRPA1 activation in mice. A single dose of bortezomib (BTZ; 0.2, 0.5, and 1 mg/kg i.p.) induces in C57BL/6 mice a dose- and time-dependent mechanical (A) and cold (B) allodynia, which starts at 6 hours or day 1, respectively, and persists until day 11 after BTZ (1 mg/kg) administration. At day 7 after BTZ administration, the selective TRPA1 receptor antagonist, HC-030031 (HC; 300 mg/kg, i.g.), completely reverses the mechanical (C) and cold (D) allodynia with a maximum effect, 60 minutes after dosing. BTZ treatment produces in *Trpa1*$^{+/+}$ mice mechanical (E) and cold (F) allodynia similar to those observed in C57BL/6. These effects are completely absent in *Trpa*$^{-/-}$ mice (E and F). Veh, vehicle of BTZ or HC. Values are mean ± SEM of 8 to 10 mice. #, P<0.05 versus Veh BTZ, Student t test in A and B; *, P < 0.05 versus VehBTZ-VehHC in C and D and VehBTZ- *Trpa1*$^{+/+}$ in E and F; §, P < 0.05 versus BTZ-VehHC in C and D and BTZ- *Trpa*$^{-/-}$ in E and F;one-way ANOVA and Bonferroni test. BL, baseline withdrawal threshold.

3.2.2 Bortezomib does not affect TRPA1 receptor expression and does not directly activate TRPA1.

TRPA1 expression has been found to vary in different painful conditions, including models of CIPN [258, 259]. Therefore, we evaluated, by Western blotting, the expression of TRPA1receptor in different tissues. At day 7 after administration, when hypersensitivity was at its maximum, TRPA1 immunoreactivity in the spinal cord, DRG, and hind paw skin of mice treated with bortezomib or its vehicle, were similar (Fig. III-2E). To test the hypothesis that bortezomib directly activates the TRPA1 receptor, we studied the ability of bortezomib to evoke calcium responses in cultured mouse DRG neurons. Bortezomib (10, 50, or 100 μmol/L) failed to evoke any calcium response in capsaicin-sensitive DRG neurons (Fig. III-2F and G), which otherwise responded to the TRPA1 agonist AITC (30 μmol/L). *In vitro* pre-exposure to bortezomib (100 μmol/L for 2 hours) did not affect the magnitude or the number of neurons responding to AITC (10 and 30 μmol/L; Fig. III-2H).

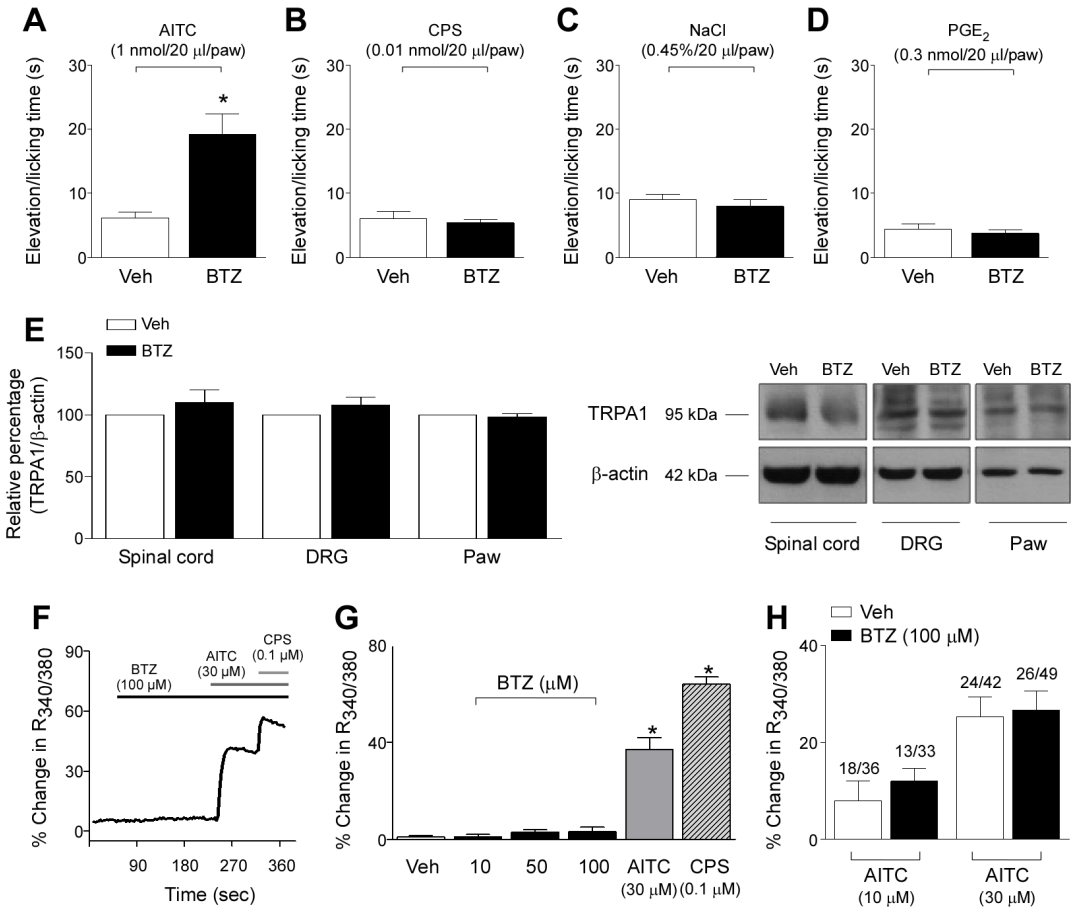

Figure III-2. Bortezomib enhances allyl isothiocyanate-evoked nocifensive behavior but does not increase TRPA1 expression or directly activate TRPA1. Nociceptive behavior produced by a subthreshold dose of intraplantar (i.pl.; 20 µL) injection of allyl isothiocyanate (AITC; 1 nmol/paw; A) in mice is increased 7 days after BTZ (1 mg/kg i.p.). Responses to subthreshold doses of capsaicin (CPS; 0.01 nmol/paw; B), hypotonic saline (NaCl, 0.45%; C), and PGE_2 (0.3 nmol/paw; D) are not affected by BTZ. Values are mean ± SEM of 8 to 10 mice. *, $P < 0.05$ versus VehBTZ-AITC in A; Student *t* test. E, TRPA1 protein content analyzed by Western blotting is not different in tissue homogenates of spinal cord, DRGs, and hindpaw skin obtained from mice on day 7 after treatment with BTZ or its vehicle (Veh). Values are mean ± SEM of 3 samples, Student *t* test. Equally loaded protein was checked by expression of β-actin. A representative blot is shown. BTZ (10, 50, or 100 µmol/L) fails to evoke any visible intracellular calcium $(Ca^{2+})_I$ response in CPS (0.1 µmol/L)-sensitive DRG neurons, which otherwise responded to AITC (F, G). Trace represents an average of 10 neurons. H, *in vitro* preexposure to BTZ (100 µmol/L for 2 hours) does not affect the magnitude of the response, and the number of neurons responding to AITC (10 and 30 µmol/L). Veh is the vehicle of BTZ. Values are mean ± SEM of $n > 30$ neurons. Numbers indicate AITC-responding cells/CPS-responding cells. *, $P < 0.05$ versus Veh; one-way ANOVA and Bonferroni test.

3.2.3 α-Lipoic acid transiently reverts bortezomib-evoked hypersensitivity

As reported for other anticancer drugs, such as oxaliplatin, paclitaxel, and others, there is evidence that bortezomib also produces oxidative stress [55-57, 260]. Therefore, we hypothesized that reactive molecules generated by the oxidative stress burst produced by bortezomib administration could be the underlying mechanism by which the anticancer drug induces TRPA1-dependent mechanical and cold hypersensitivity.

We observed that administration of α-lipoic acid (100 mg/kg, i.g.) completely abated mechanical hyperalgesia and cold allodynia evoked at day 7 after bortezomib treatment. Significant effect of α-lipoic acid was observed from 30 to 120 minutes after treatment, with maximum inhibition (73 ± 9% and 77 ± 6% for mechanical hyperalgesia and cold allodynia, respectively) 60 minutes post dosing (Fig. III-3A and B).

3.2.4 Local treatment with HC-030031 or α-lipoic acid transiently reverts bortezomib- or oxaliplatin-induced hypersensitivity

It has been reported that i.pl. injection of α-lipoic acid reduces oxaliplatin-elicited nociception [257]. In the present study, we observed that i.pl. injection of HC-030031 (100 μg/paw) or α-lipoic acid (10 μg/paw) completely reduced bortezomib-induced mechanical and cold allodynia (Fig. III-3C and D). In addition, we found that mechanical and cold allodynia elicited by oxaliplatin were markedly decreased by i.pl. injection of HC-030031 and α-lipoic acid (Fig. III-3E and F). Contralateral paw thresholds to mechanical or cold stimuli were not affected by the i.pl. injection of HC-030031 or α-lipoic acid (Fig. III-3C-F). Administration of HC-030031 or α-lipoic acid (i.pl.) did not produce any appreciable effect in animals treated with the vehicle of bortezomib or oxaliplatin (data not shown).

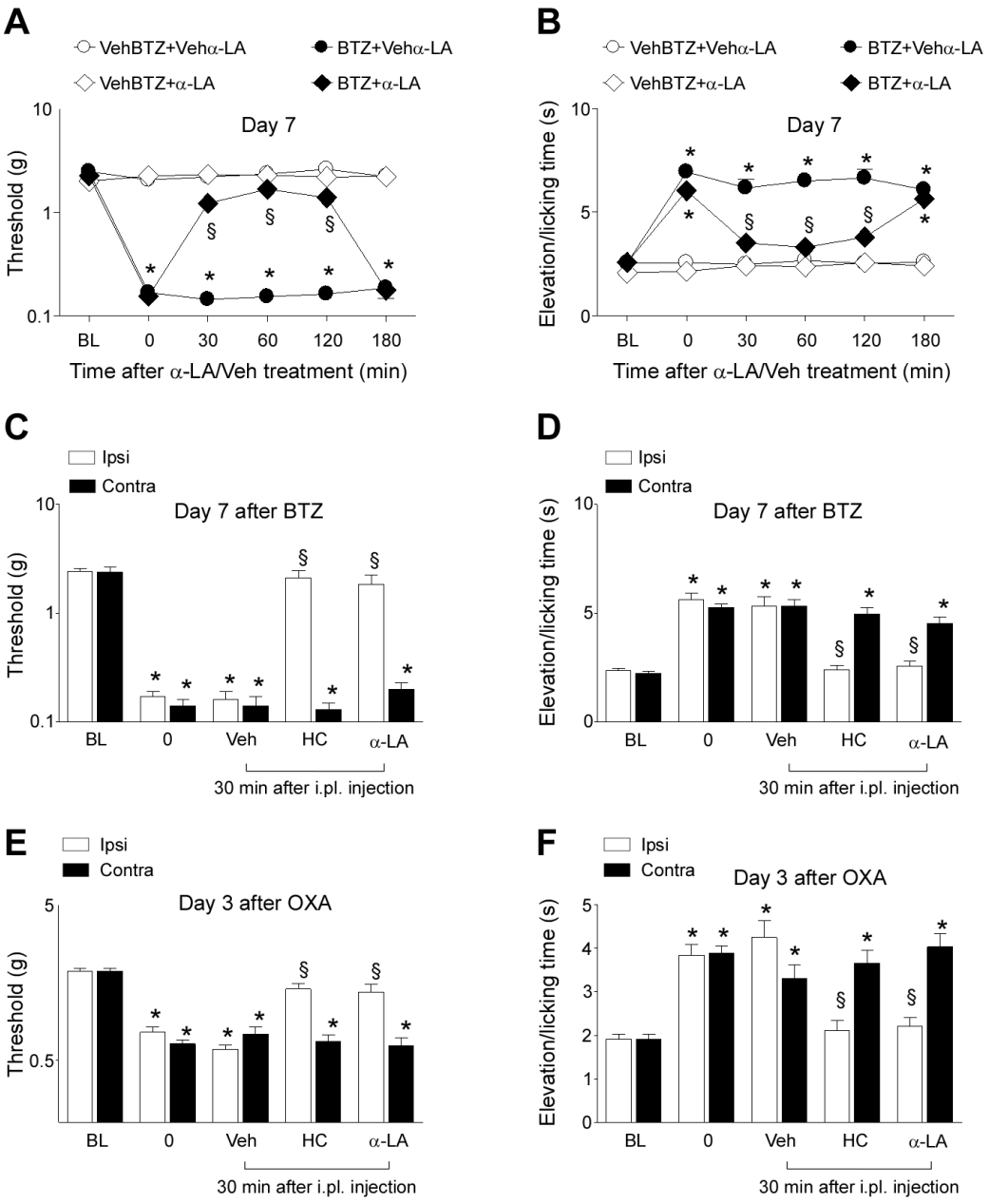

Figure III-3. Systemic or local administration of α-lipoic acid (α-LA) and local administration of HC-030031 (HC) transiently reverse BTZ-evoked mechanical and cold hypersensitivity in mice. At day 7 after BTZ (1 mg/kg i.p.), α-LA (100 mg/kg i.g.) completely reverses the mechanical (A) and cold (B) allodynia with a maximum effect at 60 minutes post dosing. Veh, vehicle of BTZ or α-LA acid. C and E, HC (100 µg/paw, i.pl. 20 µL) or α-LA (10 µg/paw) reduce the mechanical allodynia induced by BTZ or oxaliplatin (OXA; 3 mg/kg, i.p.) in the paw ipsilateral (ipsi) to the injection. D and F, in the contralateral (contra) side, the paw threshold to mechanical stimuli is not affected by local HC or α-LA. Local HC or α-LA acid treatment produces similar findings when cold allodynia is measured. Values are mean ± SEM of 8 to 10 mice. *, $P < 0.05$ versus Vehα-LA acid or VehBTZ or BL values; §, $P < 0.05$ versus BTZ-Vehα-LA or Vehipsi; one-way ANOVA and Bonferroni test. BL, baseline withdrawal threshold.

3.2.5 Bortezomib and oxaliplatin increase plasma level of carboxy-methyl-lysine

Systemic oxidative stress was evaluated by measuring the serum content of Nε-carboxy-methyl-lysine (CML) protein adducts. CML is the reaction product between lysine and glyoxal, an α-ketoaldehyde intermediate formed by ascorbate autoxidation, lipid peroxidation, and oxidative degradation of glucose and degradation of glycated proteins. Due to the fact that CML is formed from either carbohydrates or lipids oxidation, it has been termed as an either advanced glycation or lipoxidation endproducts (EAGLE) modification. CML may be considered as a general marker of oxidative stress and, so far, it is widely used to measure oxidative stress in different pathophysiologic conditions [261]. Bortezomib administration produced a transient increase in plasma CML levels. One hour after bortezomib injection, CML increased by 64% over baseline value, and returned to basal values at 3 hours after treatment (Fig. III-4A). Similar to bortezomib, oxaliplatin administration produced a transient increase in plasma CML levels, which was observed at 1 hour (55% over the baseline) and 3 hours (63% over the baseline), and returned to basal levels 6 hours after treatment (Fig. III-5A).

3.2.6 Early and short-term treatment with HC-030031 or α-lipoic acid completely prevents bortezomib- and oxaliplatin-evoked hypersensitivity

We investigated whether treatment with a TRPA1 antagonist or a ROS scavenger given shortly before and after anticancer drug administration could prevent the development of persistent mechanical, cold, and chemical hypersensitivity. To test this hypothesis HC-030031 (300 mg/kg, i.g.) or α-lipoic acid (100 mg/kg, i.g.), were given respectively, 15 minutes before and 3 times every 90 minutes after bortezomib or oxaliplatin administration. HC-030031 totally prevented the development of chemical hypersensitivity and mechanical and cold allodynia evoked by bortezomib (Fig. III-4B, D, and E) and oxaliplatin (Fig. III-5B, D, and E). Similarly, α-lipoic acid prevented chemical hypersensitivity and mechanical and cold allodynia evoked by bortezomib (Fig. III-4C, F, and G) and oxaliplatin (Fig. III-5C, F, and G). Repeated i.g. administration of TRPA1 antagonist (HC-030031, 300 mg/kg, i.g.) did not affect forced locomotion of animals, as observed by the rotarod test. HC-030031- and vehicle-treated animals did not show any fall during the test (data not shown). Mice, protected by early and short-term treatment with HC-030031, were rechallenged 6 days after a first treatment with bortezomib with a second bortezomib administration (1 mg/kg, i.p.). In

these mice, a second early and short-term treatment with HC-030031 again totally prevented the development of mechanical and cold hypersensitivity (Fig. III-6B and C). In contrast, mice treated with HC-030031 vehicle did not show protection against the hypersensitivity evoked by the second administration of bortezomib. Mice treated with bortezomib and HC-030031 vehicle developed mechanical and cold hypersensitivity, a response that further increased at the second treatment with bortezomib and HC-030031 vehicle (Fig. III-6B and C).

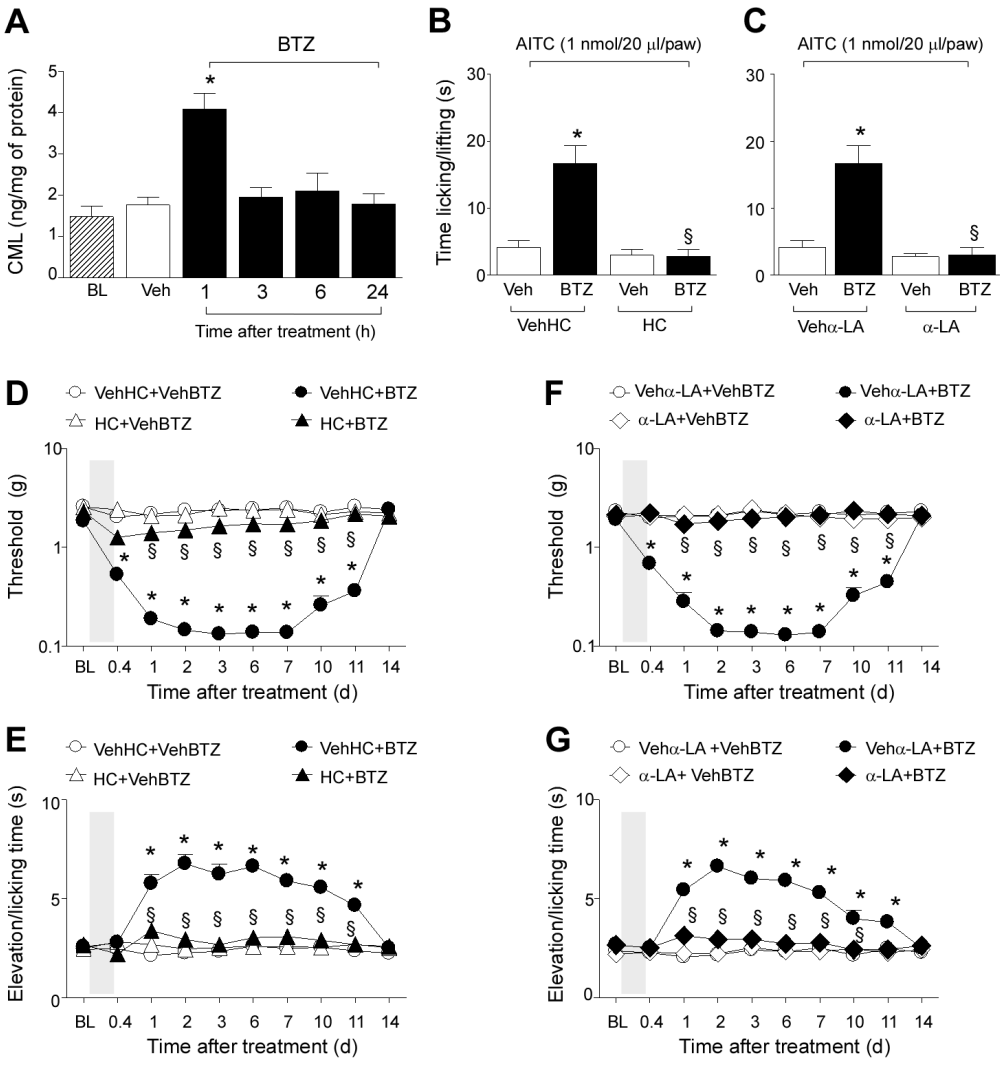

Figure III-4. BTZ increases transiently oxidative stress in plasma and early and short-term treatment with HC and α-LA permanently prevents the development of mechanical, cold, and chemical hypersensitivity evoked by BTZ in mice. A, BTZ (1 mg/kg i.p.) transiently increases carboxy-methyl-lysine (CML) plasma levels in mice. Both HC (300 mg/kg i.g.) and α-LA (100 mg/kg i.g. 15 minutes before and 3 times at 90-minute intervals each after BTZ treatment) prevent the development and maintenance of chemical hyperalgesia (B and C) as well as mechanical (D and F) and cold (E and G) allodynia evoked by BTZ (1 mg/kg i.p.). Veh, of BTZ, HC, or α-LA. Values are mean ± SEM of 8 to 10 mice. *, $P < 0.05$ versus BL in A, VehHC-VehBTZ in B, D, and E, or Veh α-LA-VehBTZ in C, F, and G; §, $P < 0.05$ versus VehHC-BTZ in B, D, and E or Vehα-LA-BTZ in C, F, and G; one-way ANOVA and Bonferroni test. BL, basal level of CML in A and baseline withdrawal threshold in D-G.

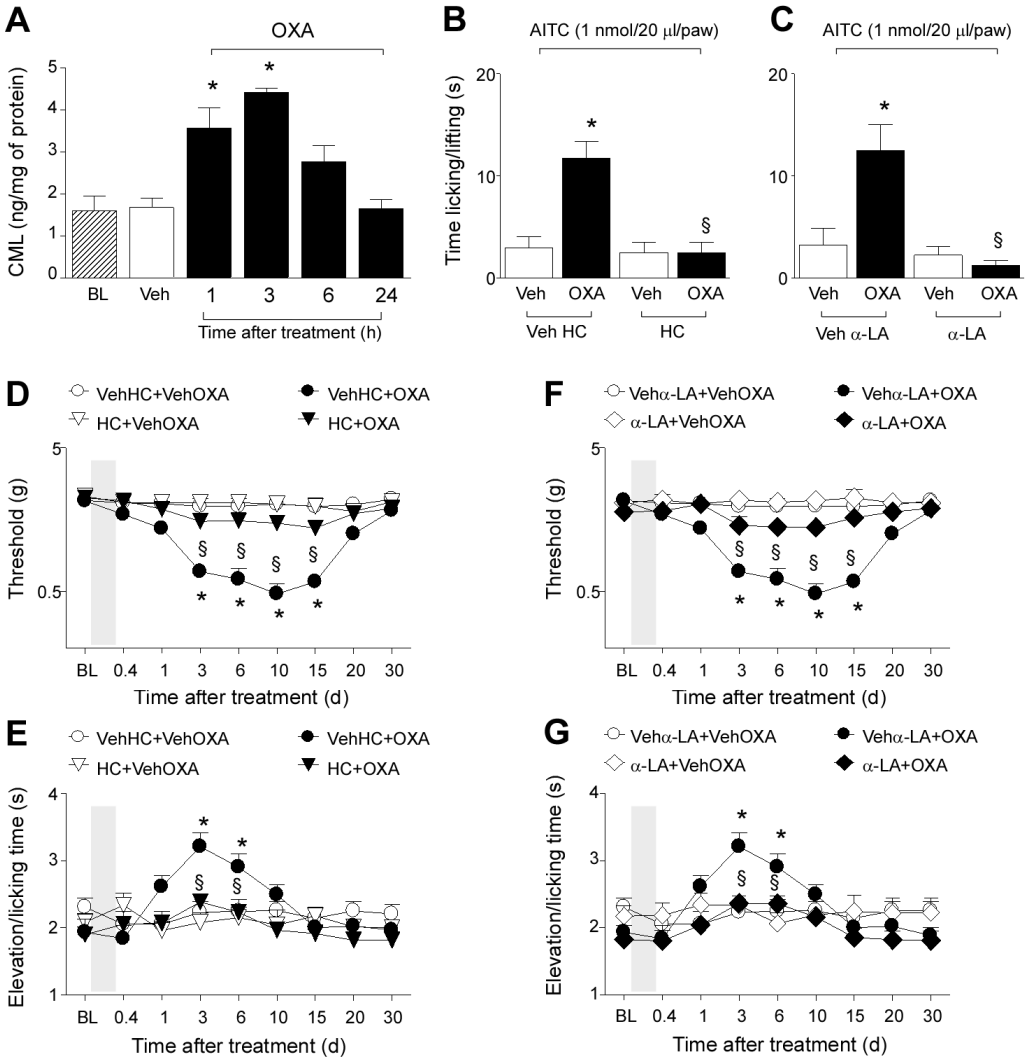

Figure III-5. Oxaliplatin transiently increases oxidative stress in plasma, and early and short-term treatment with HC and α-LA permanently prevents the development of mechanical, cold, and chemical hypersensitivity evoked by BTZ in mice. A, oxaliplatin (OXA; 3 mg/kg i.p.) transiently increases CML plasma levels in mice. Both HC (300 mg/kg i.g.) and α-LA (100 mg/kg i.g. 15 minutes before and 3 times at 90-minute intervals each after BTZ treatment) prevent the development and maintenance of chemical hyperalgesia (B and C) as well as mechanical (D and F) and cold (E and G) allodynia evoked by OXA (3 mg/kg i.p.). Veh, vehicle of OXA, HC, or α-LA. Values are mean ± SEM of 8 to 10 mice. *, $P < 0.05$ versus BL in A, VehHC-VehOXA in B, D, and E or Vehα-LA-VehOXA in C, F, and G; §, $P < 0.05$ versus VehHC-OXA in B, D, and E or Vehα-LA-OXA in C, F, and G; one-way ANOVA and Bonferroni test. BL, basal level of CML in A and baseline withdrawal threshold in D-G.

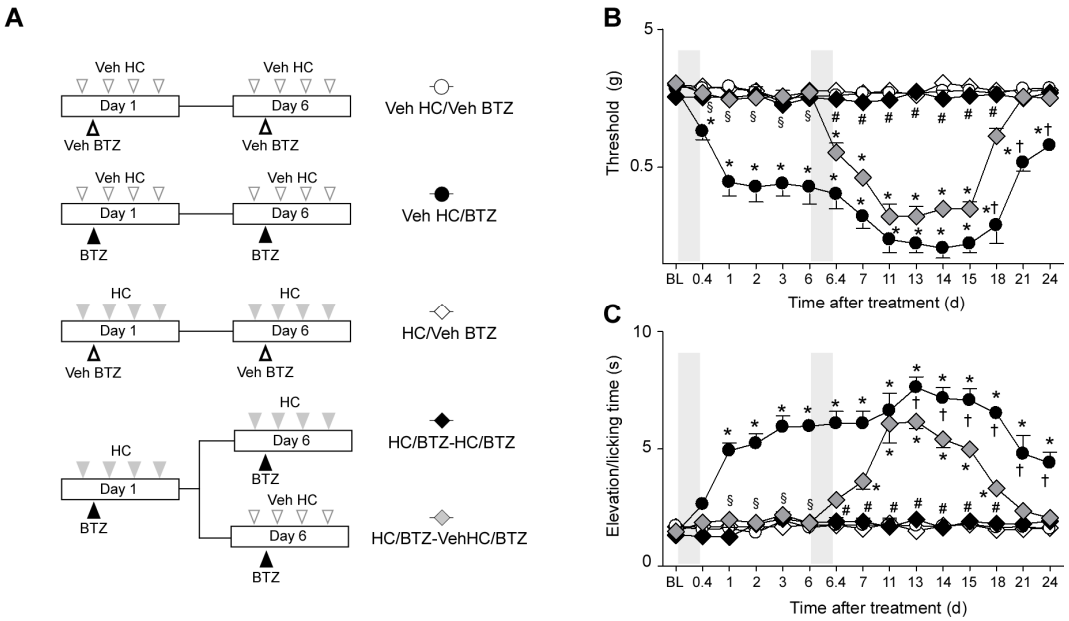

Figure III-6. A repeated early and short-term treatment with HC prevents the development of mechanical and cold hypersensitivity evoked by a second BTZ treatment in mice. A, schematic representation of HC (300 mg/kg, i.g.) and BTZ (1 mg/kg, i.p.) treatment. A group of mice are treated with HC or its vehicle 15 minutes before and shortly after (3 times at 90-minute intervals each) a first BTZ or vehicle administration. At day 6 after the first BTZ administration, all mice receive a second BTZ (1 mg/kg, i.p.) or vehicle administration. Mice pretreated with HC after the first BTZ dose are subdivided into 2 groups. One group is treated a second time with HC (300 mg/kg, i.g.) and a second group with its vehicle 15 minutes before and shortly after (3 times at 90-minute intervals each) BTZ administration. The second early and short-term treatment with HC totally prevents the development of mechanical and cold hypersensitivity (B, C). B and C, mice treated with BTZ and HC vehicle develop mechanical and cold hypersensitivity, a response that is further increased by the second treatment with BTZ and HC vehicle. Values are mean ± SEM of 8 to 10 mice. *, $P < 0.05$ versus VehHC-VehBTZ in B and C; §, $P < 0.05$ versus VehHC-BTZ in B and C; #, $P < 0.05$ versus VehHC-BTZ or HC/BTZ-VehHC/BTZ; †, $P < 0.05$ versus HC/BTZ-VehHC/BTZ one-way ANOVA and Bonferroni test. BL, baseline withdrawal threshold.

3.3 Discussion

In the present study in mice, we found that 1 single administration of bortezomib produced an early and prolonged mechanical and cold hypersensitivity that started 6 hours after and lasted for 11 days after bortezomib administration. With a slight difference in duration, the effect of bortezomib was practically identical to that previously reported for oxaliplatin [60]. A number of preclinical studies and clinical investigations have shown that bortezomib, like oxaliplatin and paclitaxel, increases ROS and their by-products in plasma, cells, and tissues of treated animals or patients, and that ROS scavengers show some degree of protection against CIPN or its rodent counterpart [60, 75, 89, 257, 258, 262]. Two observations suggest that oxidative stress mediates bortezomib-evoked sensory neuropathy. First, the ROS scavenger, α-lipoic acid, completely reversed the established (at day 7 after drug administration) mechanical and cold hypersensitivity evoked by bortezomib. Second, bortezomib and oxaliplatin produced an early and transient (1-3 hours after drug administration) increase in the plasma levels of 1 major by-product of oxidative stress, CML. The finding that oxaliplatin administration also increased plasma oxidative stress by-products is consistent with the previously reported role of oxidative stress in oxaliplatinevoked sensory neuropathy [232].

TRPA1 has been identified as a sensor of oxidative stress, in as much as it is activated by an unprecedented series of ROS, RNS, or RCS [175, 191, 263]. Thus, we hypothesized that oxidative stress by-products, generated by bortezomib, may target the TRPA1 channel in sensory nerve terminals. Indeed, both pharmacologic and genetic findings indicate that TRPA1 plays a key role in bortezomib-evoked mechanical and chemical hyperalgesia and cold allodynia, as these phenomena were completely reverted when they were at their maximum, for example, at day 7 after treatment, by a TRPA1 antagonist and were completely absent in TRPA1-deleted mice. The key contribution of TRPA1 in mechanical, chemical, and cold allodynia does not seem confined to bortezomib model as earlier studies [229, 232, 264] showed a similar role of TRPA1 in oxaliplatin-evoked sensory neuropathy in mice. In addition, the TRPV4-resistant component [224] of the mechanical hyperalgesia evoked by paclitaxel in mice has also been ascribed to the contribution of TRPA1, whereas TRPA1 appears to be the sole channel responsible for paclitaxel-evoked cold allodynia [250]. In addition, we found that an oxidative stress scavenger or a TRPA1 antagonist reversed bortezomib- or

oxaliplatin evoked hypersensitivity selectively on the treated paw, when they were given locally by i.pl. administration. This finding indicates that TRPA1 sensitization/activation occurs at the very terminal region of nociceptive primary afferents, and that channel inhibition at this peripheral level is sufficient to revert the sensory neuropathy.

The protective effect of HC-030031 or α-lipoic acid when administered (either systemically or locally) at day 7 after bortezomib administration, although complete, was transient, lasting no longer than 120 minutes. This is probably due to the pharmacokinetic properties of the 2 drugs, as indicated by previous studies in different models of nociception or hyperalgesia/allodynia [236, 265]. In contrast to the transient reversal produced by pharmacologic treatments when the hypersensitivity is already established, in TRPA1-deficient mice hypersensitivity to bortezomib or oxaliplatin [232] does not develop. These genetic findings and biochemical evidence of the transient increase in plasma CML suggest that early phenotypic changes of TRPA1, presumably associated with the oxidative burst, which are responsible for the development and maintenance of the hypersensitivity, occur a few hours after chemotherapeutic drug administration. To identify the critical role of these early events for the manifestation of the enduring hypersensitivity condition by anticancer drug, we designed an experiment in which HC-030031 or α-lipoic acid were given shortly before and for approximately 6 hours after bortezomib or oxaliplatin treatment. These treatments not only blocked the onset of the hypersensitivity, but, rather surprisingly, completely and stably prevented its development and maintenance. Of interest for translating the present observation to the clinical perspective, the permanent protective effect by early and short-term treatment with the TRPA1 antagonist was also observed when it was repeated after a second bortezomib administration. Although it is not possible to replicate in mice the exact condition experienced by patients, these additional findings suggest a possible treatment schedule to prevent the sensory neuropathy in patients when TRPA1 antagonists are clinically available.

Taken together, these findings indicate that TRPA1, *via* its activation by oxidative stress by-products, is necessary and sufficient to produce a sensory neuropathy paradigm in mice following a single administration of different chemotherapeutics. Oxaliplatin [232], paclitaxel [250], and bortezomib failed to evoke any calcium response in cultured TRPA1-expressing neurons, thus excluding that these drugs may directly target the channel. However, *in vitro* findings support the alternative

explanation, as indicated by *in vivo* results, that chemotherapeutic agents act indirectly by generating oxidative stress by-products [88, 257, 258, 262], which in turn sensitize/activate TRPA1 in sensory neurons.

TRPA1 is apparently required for those early (within 6-8 hours) phenotypic changes that eventually result in the long term hypersensitivity to specific (AITC) and nonspecific (pressure or cold) stimuli caused by exposure to different chemotherapeutic agents in mice. Although some reports have shown changes in TRP expression in different rodent models of CIPN, under the present experimental circumstances, no change in TRPA1 protein expression in nociceptive neurons was found. The molecular mechanism responsible for the TRPA1-mediated hypersensitivity phenotype, produced by chemotherapeutic agents remains unknown. Nevertheless, present experiments with bortezomib and oxaliplatin identify the early phase (a few hours) that follows chemotherapeutic drug administration as the key step when, most likely through oxidative stress by-products, TRPA1 is activated/sensitized. These early events result in a prolonged (several days) condition of hypersensitivity that markedly mimics the long-lasting duration of CIPN in patients treated with bortezomib or oxaliplatin. If ROS scavengers, most likely because of poor pharmacokinetics, could not represent a suitable and effective treatment for CIPN, the present findings suggest a novel therapeutic schedule to prevent CIPN in patients, based on TRPA1 antagonists given before and shortly after each administration of anticancer medicines.

This work has been published in Cancer Research

Trevisan G, Materazzi S, Fusi C, Altomare A, Aldini G, Lodovici M, Patacchini R, Geppetti P, Nassini R. (2013). "Novel therapeutic strategy to prevent chemotherapy-induced persistent sensory neuropathy by TRPA1 blockade." Cancer Res 73(10): 3120-31.

Chapter IV - Steroidal and non-steroidal third-generation aromatase inhibitors induce pain-like symptoms via TRPA1

4.1 Methods

Animals. Animal experiments were carried out in conformity to the European Communities Council (ECC) guidelines for animal care procedures and the Italian legislation (DL 116/92) application of the ECC directive 86/609/EEC. Studies were conducted under the University of Florence research permit number 204/2012-B. Male C57BL/6 (25-30 g) (Harlan Laboratories, Milan, Italy), wild type, *Trpa1*$^{+/+}$, or TRPA1-deficient, *Trpa1*$^{-/-}$, (25-30 g) mice generated by heterozygous on a C57BL/6 background (B6;129P-Trpa1tm1Kykw/J; Jackson Laboratories, Italy) [179], or Sprague-Dawley rats (75-100 g, male, Harlan Laboratories, Milan, Italy) were used. Animals were housed in a temperature- and humidity-controlled *vivarium* (12 hours dark/light cycle, free access to food and water). Behavioral experiments were done in a quiet, temperature-controlled (20 to 22 °C) room between 9 a.m. and 5 p.m., and were performed by an operator blinded to the genotype and the drug treatment. Animals were sacrificed with a high dose of sodium pentobarbital (200 mg/kg, i.p.).

Reagents. Exemestane, letrozole and anastrozole were purchased from Tocris Bioscience (Bristol, UK). The activating peptide (PAR2-AP, SLIGRL-NH_2) and its reverse peptide (PAR2-RP, LRGILS-NH_2) of the murine PAR2 receptor were synthesized from G. Cirino (University of Naples, Naples, Italy) and dissolved in distilled water. If not otherwise indicated, all other reagents were from Sigma-Aldrich (Milan, Italy). HC-030031 was synthesized as previously described [234].

Cell culture and isolation of primary sensory neurons. Human embryonic kidney (HEK293) cells stably transfected with the cDNA for human TRPA1 (hTRPA1-HEK293), kindly donated by A.H. Morice (University of Hull, Hull, UK) or with the cDNA for human TRPV1 (hTRPV1-HEK293), kindly donated by Martin J. Gunthorpe (GlaxoSmithKline, Harlow, UK), and naive untransfected HEK293 cells (American Type Culture Collection, Manassas, VA, USA) were cultured as previously described [199]. HEK293 cells were transiently transfected with the cDNAs (1 µg) codifying for wild-type or mutant 3C/K-Q (C619S, C639S, C663S, K708Q) [184, 186] human TRPA1 using the jetPRIME transfection reagent (Euroclone, Milan, Italy) according to the manufacturer's protocol.

Primary dorsal root ganglion (DRG) neurons were isolated from Sprague-Dawley rats and C57BL/6 or *Trpa1*$^{+/+}$ and *Trpa1*$^{-/-}$ adult mice, and cultured as previously described [250]. Briefly, ganglia were bilaterally excised under a dissection microscope and enzymatically digested using 2 mg/ml of collagenase type 1A and 1 mg/ml of trypsin, for rat DRG neurons, or 1 mg/ml of papain, for mouse DRG neurons, in Hank's Balanced Salt Solution (HBSS) for 25-35 minutes at 37 °C. Rat and mouse DRG neurons were pelleted and resuspended in Dulbecco's Modified Eagle's Medium (DMEM) supplemented with 10% heat inactivated horse serum or Ham's-F12, respectively, containing 10% heat-inactivated fetal bovine serum (FBS), 100 U/ml of penicillin, 0.1 mg/ml of streptomycin, and 2 mM L-glutamine for mechanical digestion. In this step, ganglia were disrupted by several passages through a series of syringe needles (23-25G). Neurons were then pelleted by centrifugation at 1200 g for 5 minutes, suspended in *medium* enriched with 100 ng/ml mouse-NGF and 2.5 mM cytosine-b-D-arabino-furanoside free base, and then plated on 25 mm glass coverslips coated with poly-L-lysine (8.3 µM) and laminin (5 µM). DRG neurons were cultured for 3-4 days before being used for calcium imaging experiments.

Calcium Imaging Assay. Intracellular calcium was measured in transfected and untransfected HEK293 cells or in DRG neurons, as previously reported [266]. Plated cells were loaded with 5 µM Fura-2AM-ester (Alexis Biochemicals, Lausen, Switzerland) added to the buffer solution (37 °C) containing the following (in mM): 2 $CaCl_2$; 5.4 KCl; 0.4 $MgSO_4$; 135 NaCl; 10 D-glucose; 10 HEPES and 0.1% bovine serum albumin at pH 7.4. After 40 minutes, cells were washed and transferred to a chamber on the stage of a Nikon Eclipse TE-2000U microscope for recording. Cells

were excited alternatively at 340 nm and 380 nm to indicate relative intracellular calcium changes by the $Ratio_{340/380}$ recorded with a dynamic image analysis system (Laboratory Automation 2.0, RCSoftware, Florence, Italy). Cells and neurons were exposed to exemestane, letrozole and anastrozole (1-300 μM), AITC (10-30 μM), menthol (100 μM), icilin (30 μM), or their vehicles (1.5-3 % dimetyl sulfoxide, DMSO). The calcium response to capsaicin (0.1 μM) was used to identify nociceptive neurons. The selective TRPA1 antagonist, HC-030031 (30 μM), and TRPV1 antagonist, capsazepine (10 μM) or their vehicles (3% and 0.1% DMSO, respectively), were applied ten minutes before the stimuli. Results are expressed as or the percentage of increase of $Ratio_{340/380}$ over the baseline normalized to the maximum effect induced by ionomycin (5 μM) added at the end of each experiment (% Change in $R_{340/380}$) or $Ratio_{340/380}$.

Electrophysiology. Whole-cell patch-clamp recordings were performed on hTRPA1-HEK293, vector-HEK293 cells or rat DRG neurons grown on a poly-L-lysine-coated 13 mm-diameter glass coverslips. Each coverslip was transferred to a recording chamber (1 ml volume) mounted on the platform of an inverted microscope (Olympus CKX41, Milan, Italy) and superfused at a flow rate of 2 ml/min with a standard extracellular solution containing (in mM): 10 HEPES, 10 D-glucose, 147 NaCl, 4 KCl, 1 $MgCl_2$, and 2 $CaCl_2$ (pH adjusted to 7.4 with NaOH). Borosilicate glass electrodes (Harvard Apparatus, Holliston, MA, USA) were pulled with a Sutter Instruments puller (model P-87) to a final tip resistance of 4-7 MΩ. Pipette solution used for HEK293 cells contained (in mM): 134 K-gluconate, 10 KCl, 11 EGTA, 10 HEPES (pH adjusted to 7.4 with KOH). When recordings were performed on rat DRG neurons, 5 mM $CaCl_2$ was present in the extracellular solution and pipette solution contained (in mM): CsCl 120, Mg_2ATP 3, BAPTA 10, HEPES-Na 10 (pH adjusted to 7.4 with CsOH). Data were acquired with an Axopatch 200B amplifier (Axon Instruments, CA, USA), stored and analyzed with a pClamp 9.2 software (Axon Instruments, CA, USA). All the experiments were carried out at 20-22°C. Cells were voltage-clamped at –60 mV. Cell membrane capacitance was calculated in each cell throughout the experiment by integrating the capacitive currents elicited by a ± 10 mV voltage pulse. In hTRPA1-HEK293 currents were detected as inward currents activated on cell superfusion with AITC (100 μM), exemestane (50-200 μM), letrozole (50-200 μM) or anastrozole (50-200 μM) in the presence of HC-030031 (50 μM) or its vehicle

(0.5% DMSO). TRPV1 currents in rat DRG neurons were detected as inward currents activated by capsaicin (1 μM) in the presence of capsazepine (10 μM) or its vehicle (0.1% DMSO). To evaluate the potentiating effect of H_2O_2 or PAR2-AP on AIs-activated currents, rat DRG neurons were superfused with H_2O_2 or PAR2-AP (both 100 μM) 1 minute before and during the application of exemestane or letrozole (both, 20 μM). Some experiments were performed in the presence of HC-030031 (50 μM) or its vehicle (0.5% DMSO). Peak currents activated by each compound were normalized to cell membrane capacitance and expressed as mean of the current density (pA/pF) in averaged results. Currents were evoked in the voltage-clamp mode at a holding potential of -60 mV; signals were sampled at 1 kHz and low-pass filtered at 10 kHz.

Behavioral experiments. For behavioral experiments, after habituation and baseline of pain sensitivity measurements, mice were randomized into treatment groups. In a first series of experiments, we explored whether the injection (20 μl/paw) of exemestane (1, 5, 10 nmol) or letrozole (10, 20 nmol), or their vehicle (5% DMSO) induced, in C57BL/6 or *Trpa1*$^{+/+}$ and *Trpa1*$^{-/-}$ mice, an acute nociceptive behavior and a delayed mechanical allodynia. In this set of experiments mechanical allodynia was measured just before (30 minutes) and 0.25, 0.5, 1, 2, 4, and 6 hours post injection. Some C57BL/6 mice were pretreated with HC-030031 (100 mg/kg, i.p.) or capsazepine (10 mg/kg, i.p.) or their respective vehicles (4% DMSO and 4% Tween20 in isotonic solution), 60 minutes and 30 minutes, respectively, before exemestane (10 nmol) or letrozole (20 nmol) i.pl. injection. Mechanical allodynia was measured 60 minutes after AIs i.pl. injection.

In a second set of experiments, nociceptive behavior and mechanical allodynia were assayed before and after systemic administration of exemestane (5 mg/kg, i.p. or 10 mg/kg, i.g.) and letrozole (0.5 mg/kg, i.p. or i.g.), or their vehicles (5% DMSO for i.p. or 0.5% carboxymethylcellulose, CMC, for i.g. administration), in C57BL/6 mice or *Trpa1*+/+ and *Trpa1*$^{-/-}$ mice. Mechanical allodynia was measured just before (30 minutes) and 1, 3, 6, 24, 48 hours after injection. Some animals 2 hours after AI administration received HC-030031 (100 mg/kg, i.p.) or its vehicle (4% DMSO and 4% Tween80 in isotonic solution), and mechanical allodynia and the forelimb grip strength were measured 1 and 3 hours after vehicle or HC-030031. In a third series of experiments, *Trpa1*$^{+/+}$ and *Trpa1*$^{-/-}$ mice were treated i.p. once a day for 15 consecutive days with exemestane or letrozole at the dose of 5 mg/kg or 0.5 mg/kg,

respectively, or with their vehicle (5% DMSO) and with i.g. exemestane or letrozole at the dose of 10 mg/kg or 0.5 mg/kg, respectively, or with their vehicle (0.5% CMC). Mechanical allodynia and the forelimb grip strength were measured 10 min before and 1, 3, 6 and 24 hours post administration at day 1, 5, 10 and 15.

To test whether PAR2 activation enhances the nocifensor behavior evoked by exemestane and letrozole, in another experimental setting, the PAR2 activating peptide (PAR2-AP), SLIGRL-NH_2, (10 µg/10 µl i.pl.) or its reversed inactive form (PAR2-RP), LRGILS-NH_2, (10 µg/10 µl i.pl.), were injected in the right hind paw. Ten minutes after i.pl. PAR2-AP or PAR2-RP injection, mice received exemestane (10 nmol/10 µl i.pl.) or letrozole (20 nmol/10 µl, i.pl.), or their vehicle (5% DMSO), in the plantar surface in the same paw injected with PAR2-AP or PAR2-RP, and the acute nociceptive behavior was recorded. In another series of experiments H_2O_2 (0.5 µmol/10 µl, i.pl.) or its vehicle were injected and the acute nocifensor behavior to H_2O_2, which did not last longer than 5 min, was recorded for 10 min. Ten min after vehicle/H_2O_2, exemestane (10 nmol/10 µl i.pl.) or letrozole (20 nmol/10 µl, i.pl.) were injected in the same paw injected with H_2O_2 or vehicle and the acute nociceptive behavior in response to AIs was recorded. Three hours after systemic administration of exemestane (5 mg/kg, i.p.) or letrozole (0.5 mg/kg, i.p.) mice were locally injected with H_2O_2 (0.5 µmol/20 µl, i.pl.) or its vehicle and both acute nocifensor behavior and mechanical allodynia were recorded.

Acute Nocifensive Response. AITC (10 nmol/paw), exemestane (10 nmol/paw), letrozole (20 nmol/paw) or their vehicles (5% DMSO), H_2O_2 (0.5 µmol/paw) or its vehicle (isotonic solution) and PAR2-AP or PAR2-RP (10 µg/paw) (10 or 20 µl) were injected into the paw of C57BL/6, *Trpa1*$^{+/+}$ and *Trpa1*$^{-/-}$ mice, and immediately after injection animals were placed in a plexiglas chamber. The total time spent licking and lifting the injected hind paw was recorded for 5 minutes as previously described [193].

Mechanical Stimulation (Von Frey Hair Test). Mechanical threshold was measured in C57BL/6, *Trpa1*$^{+/+}$ and *Trpa1*$^{-/-}$ mice after both local (i.pl.) administration of AITC (10 nmol/paw), exemestane (10 nmol/paw), letrozole (20 nmol/paw) or their vehicles (5% DMSO), H_2O_2 (0.5 µmol/paw) or its vehicle (isotonic solution), and systemic (i.p.) administration of exemestane (5 mg/kg, i.p.) or letrozole (0.5 mg/kg, i.p.) at different time points by using the up-and-down paradigm [233]. Mechanical nociceptive threshold was determined before (basal level threshold) and after different

treatments. The 50% mechanical paw withdrawal threshold response (in g) was then calculated from these scores, as previously described [233, 251].

Forelimb Grip Strength Test. The grip strength test was performed with a grip strength meter (Ugo Basile, Varese, Italy), as previously reported [267]. Mice were allowed to grasp a triangular ring attached to a force transducer and gently pulled away by the base of the tail until the grip was broken. The test was repeated 4 times and the mean peak force values (g) were calculated for each animal. The grip strength was measured in C57BL/6, *Trpa1*$^{+/+}$ and *Trpa1*$^{-/-}$ mice 10 min before and 1, 3, 6 and 24 hours post AI administration.

Paw Oedema. AITC (10 nmol/paw), exemestane (10 nmol/paw), letrozole (20 nmol/paw) or their vehicles (5% DMSO) (all 20 µl) were injected into the paw of C57BL/6, *Trpa1*$^{+/+}$ and *Trpa1*$^{-/-}$ mice and paw thickness was measured to determine the development and severity of oedema in the hind paws. Some animals received HC-030031 (100 mg/kg, i.p.), a combination of L-733,060 and CGRP8-37 (both, 2 µmol/kg, i.v.), or their vehicles (4% DMSO and 4% Tween20 in isotonic solution for HC-030031, and isotonic solution for L-733,060 and CGRP8-37) prior to stimuli. An engineer's micrometer, with 0.01 mm accuracy (Harvard Apparatus, Kent, UK) was used to measure the paw thickness in millimeters (mm), before and after (60 and 120 minutes) the i.pl. injection with tested agents by an investigator blinded to treatments. Data were expressed as the increase in mm in paw thickness.

CGRP-Like Immunoreactivity (LI) assay. For neuropeptide release experiments, 0.4 mm slices of rat and *Trpa1*$^{+/+}$ or *Trpa1*$^{-/-}$ mouse spinal cords were superfused with an aerated (95% O_2 and 5% CO_2) Krebs solution containing (in mM): 119 NaCl, 25 $NaHCO_3$, 1.2 KH_2PO_4, 1.5 $MgSO_4$, 2.5 $CaCl_2$, 4.7 KCl, 11 D-glucose; the solution was maintained at 37°C, and was added with 0.1% bovine serum albumin, and, to minimize peptide degradation, with the angiotensin converting enzyme inhibitor, captopril (1 µM), and the neutral endopeptidase inhibitor, phosphoramidon (1 µM). Tissues were stimulated with exemestane, letrozole or anastrozole (all 100 µM) or their vehicles (0.05% DMSO) dissolved in the Krebs solution. Some tissues were pre-exposed to capsaicin (10 µM, 20 minutes) or pretreated with HC-030031 (50 µM). Fractions (4 ml) of superfusate were collected at 10-minute intervals before, during, and after administration of the *stimulus* and then freeze-dried, reconstituted with assay

buffer, and analyzed for CGRP-like immunoreactivity (LI) by an ELISA assay kit (Bertin Pharma, Montigny le Bretonneux, France). CGRP-LI was calculated by subtracting the mean *pre-stimulus* value from those obtained during or after stimulation. Detection limits of the assays were 5 pg/ml. Results are expressed as femtomoles of peptide per g of tissue per 10 minutes.

In another set of experiments, exemestane (5 nmol/50 µl) and letrozole (10 nmol/50 µl) or their vehicle (1% DMSO) were i.a. injected in anesthetized (sodium pentobarbital, 50 mg/kg i.p.) rats. Ten minutes after injection, rats were sacrificed and the knee joint was dissected [268]. CGRP-LI was measured in the synovial fluid lavage added with captopril (1 µM) and phosphoramidon (1 µM) by using the ELISA assay kit as previously described [268]. Detection limits of the assays were 5 pg/ml. Results are expressed as femtomoles of peptide per g of tissue per 20 minutes in the spinal cord experiments or pg/ml in the rat synovial fluid.

Assay of Exemestane and Letrozole by Liquid Chromatography-Mass Spectrometry. Blood samples (100 µl) were obtained by venepuncture of the tail vein from each mouse at different time points (0.25, 0.5, 1, 3, 6 and 24 hours) after i.g. administration of exemestane (10 mg/kg) or letrozole (0.5 mg/kg). Blood samples were dropped on a filter paper (903® Whatman GmbH, Dassel, Germany) to obtain dried blood spots (DBS) [269] which were punched, obtaining a 6.0 mm diameter disk, containing approximately 6 µl of blood. DBS, transferred into a 2 ml Eppendorf vial were extracted with 200 µl of methanol:water (95:5, *v/v*) containing 0.1% acetic acid and the appropriate internal standard (for letrozole and exemestane quantification, extracting solutions contained 5 µg/l of anastrozole or 2 µg/l of letrozole, respectively) and after shaking with an orbital shaker for 25 min at 37°C, solutions were dried under a gentle nitrogen stream. Residues were reconstituted with 40 µl water containing 0.1% of acetic acid.

Samples were measured using a 1290 Infinity liquid chromatograph (LC, Agilent Technologies, Waldbronn, Germany) coupled to a QTRAP 5500 (AB SCIEX, Toronto, Canada) equipped with the Turbo Ion Spray source operating in positive ion mode. The capillary voltage was set to 5 kV. Heated turbo gas (400°C, air) at a flow rate of 10.0 l/min was used. The transitions (quantifier and qualifier) recorded in Multiple Reaction Monitoring (MRM) mode were: 286.1>217.1 and 286.1>190.1 for letrozole, 294.1>225.1 and 294.1>210.1 for anastrozole and 297.1>121.0 and

297.1>93.1 for exemestane. The LC column was a Gemini C6-Phenyl (100 x 2 mm, 3 µm) with the corresponding 4x2 mm SecurityGuardTM cartridge (Phenomenex, Torrance, CA), operated at 0.3 ml/min. Eluent A (water + 0.1% acetic acid) and B (acetonitrile) were used. The gradient elution program was as follows: 20% B maintained for 2 min, then to 90% B in 7 min, back to 20% B in 1 min and re-equilibrated for a 20 min total run time. Anastrozole, exemestane and letrozole retention times were 6.12, 6.31 and 7.45 min, respectively. Four µl of the extracted sample were injected for LC-MS/MS assays. System control and data acquisition were done by Analyst 1.5.1 software and calibration curves were calculated using the non-weighted linear least-square regression of Analyst Quantitation program (AB SCIEX, Toronto, Canada).

Calibration curves were constructed for both exemestane and letrozole, using the appropriate internal standard. Whole blood from control mouse was spiked with different concentrations of exemestane (from 2 to 100 µg/l) or letrozole (from 10 to 200 µg/l). A 20 µl volume for each fortified blood sample was spotted on filter paper (DBS) and then treated as described in sample preparation. Each calibration curve was prepared in duplicate. Satisfying linearity was obtained for the two analytes (letrozole, r=0.996; exemestane, r=0.998). Each analytical batch included a double blank sample (without internal standard), a blank sample (with internal standard), five or six standard concentrations for calibration curve, and a set of treated mouse samples (each prepared in duplicate). LC-MS grade acetic acid, methanol, water and acetonitrile were supplied by Sigma Aldrich (Milan, Italy).

Statistical Analysis Data represent mean ± SEM or confidence interval (CI). Statistical analysis was performed by the unpaired two-tailed Student's t-test for comparisons between two groups, the ANOVA, followed by the Bonferroni post-hoc test for comparisons between multiple groups. Agonist potency was expressed as half maximal effective concentration (EC_{50}), that is, the molar concentration of agonist producing 50% of the maximum measured effect, and 95% confidence interval (CI). $P<0.05$ was considered statistically significant (GraphPadPrism version 5.00, San Diego, CA).

4.2 Results

4.2.1 Aromatase inhibitors selectively activate TRPA1 channels

To explore whether AIs gate the human TRPA1 channel, we first used cells stably transfected with human TRPA1 cDNA (hTRPA1-HEK293). In hTRPA1-HEK293 cells, which respond to the selective TRPA1 agonist AITC (30 μM), but not in untransfected HEK293 cells, the three AIs, exemestane, letrozole, and anastrozole evoked concentration-dependent calcium responses that were inhibited by the selective TRPA1 antagonist, HC-030031 (30 μM) [214] (Fig. IV-1a,b,c). EC_{50} of AIs ranged between 58 and 134 μM (Fig. IV-1b). The calcium response was abated in a calcium-free medium, thus supporting the hypothesis that the increase in intracellular calcium originates from extracellular sources (Supplementary Fig. 1a). In HEK293 cells stably transfected with human TRPV1 cDNA (hTRPV1-HEK293) all AIs (100 μM) were ineffective (Supplementary Fig. 1b). Key aminoacid residues are required for channel activation by electrophilic TRPA1 agonists [184-186]. Notably, HEK293 cells expressing a mutated TRPA1 channel (3C/K-Q), which presents substitutions of three cysteine with serine (C619S, C639S, C663S) and one lysine with glutamine (K708Q) residues, were insensitive to both AITC [184, 186] and all three AIs, while maintaining sensitivity to the non-electrophilic agonists, menthol [263] or icilin [185] (Fig. IV-1d and Supplementary Fig 1c). This finding supports the hypothesis that the ability of AIs to target TRPA1 derives from their electrophilic nature. Electrophysiology experiments recapitulated findings obtained by means of the calcium assay. Exemestane, letrozole, and anastrozole selectively activated a concentration-dependent inward current in hTRPA1-HEK293 cells, a response that was abated by HC-030031 (Supplementary Fig. 1d). AIs did not evoke any current in untransfected HEK293 cells (Supplementary Fig. 1d).

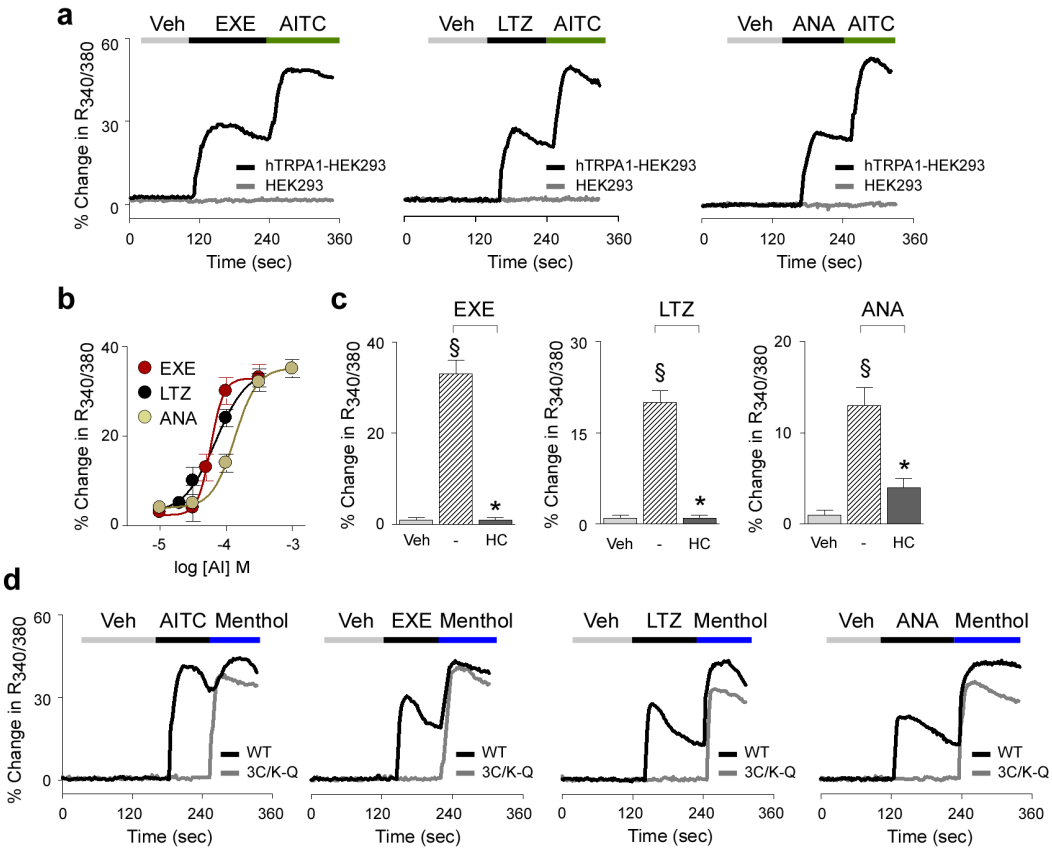

Figure IV-1. Exemestane (EXE), letrozole (LTZ) and anastrozole (ANA) selectively activate the human TRPA1 channel. (**a**) Representative traces of intracellular calcium response evoked by the aromatase inhibitors (AIs), EXE (100 µM), LTZ (100 µM) and ANA (100 µM), in HEK293 cells transfected with the cDNA for human TRPA1 (hTRPA1-HEK293) which respond to the selective TRPA1 agonist, allyl isothiocyanate (AITC; 30 µM). AITC (30 µM), EXE, LTZ, and ANA (all 100 µM) fail to produce any calcium response in untransfected-HEK293 cells (HEK293). (**b**) Concentration-response curves to EXE, LTZ and ANA, yielded EC_{50} (95% confidence interval) of 58 (46-72) µM, 69 (43-109) µM, and 134 (96-186) µM, respectively. (**c**) AI-evoked calcium response in hTRPA1-HEK293 is abolished by the selective TRPA1 antagonist, HC-030031 (HC; 30 µM). (**d**). Representative traces of cells transfected with the cDNA codifying for the mutant hTRPA1 channel (3C/K-Q), which are insensitive to AITC (30 µM) or AIs (100 µM), but respond to the non-electrophilic agonist, menthol (100 µM), whereas HEK293 cells transfected with the cDNA codifying for wild type hTRPA1 (WT) respond to all the drugs. Veh is the vehicle of AIs; dash (-) indicates the vehicle of HC. Each point or column represents the mean ± s.e.m. of at least 25 cells from 3-6 independent experiments. $^{\S}P<0.05$ *vs.* Veh, $^{*}P<0.05$ *vs*. EXE, LTZ or ANA group; ANOVA and Bonferroni *post hoc* test.

Next, to verify whether exemestane, letrozole and anastrozole stimulate nociceptive sensory neurons *via* TRPA1 activation, we used primary culture of both rat and mouse dorsal root ganglion (DRG) neurons. Similar to AITC [186], all AIs produced a concentration-dependent calcium response (Fig. IV-2a,b) in a proportion (about 30%) of cells that responded to the selective TRPV1 agonist, capsaicin (0.1 μM). All cells responding to AIs, but none of the non-responding cells, invariably responded to a subsequent high concentration of AITC (30 μM) (Fig. IV-2a), further documenting TRPA1 as the target of AIs. In rat DRG neurons, EC_{50} ranged between 78 and 135 μM (Fig. IV-2b). Calcium responses evoked by the three AIs were abated by HC-030031 (30 μM), but were unaffected by the selective TRPV1 antagonist, capsazepine (10 μM) (Fig. IV-2c). Notably, AITC and all AIs produced a calcium response in capsaicin-sensitive DRG neurons isolated from wild type (*Trpa1*$^{+/+}$) mice, an effect that was absent in neurons obtained from TRPA1-deficient (*Trpa1*$^{-/-}$) mice (Typical traces Fig. IV-2d and pooled data Fig IV-2e).

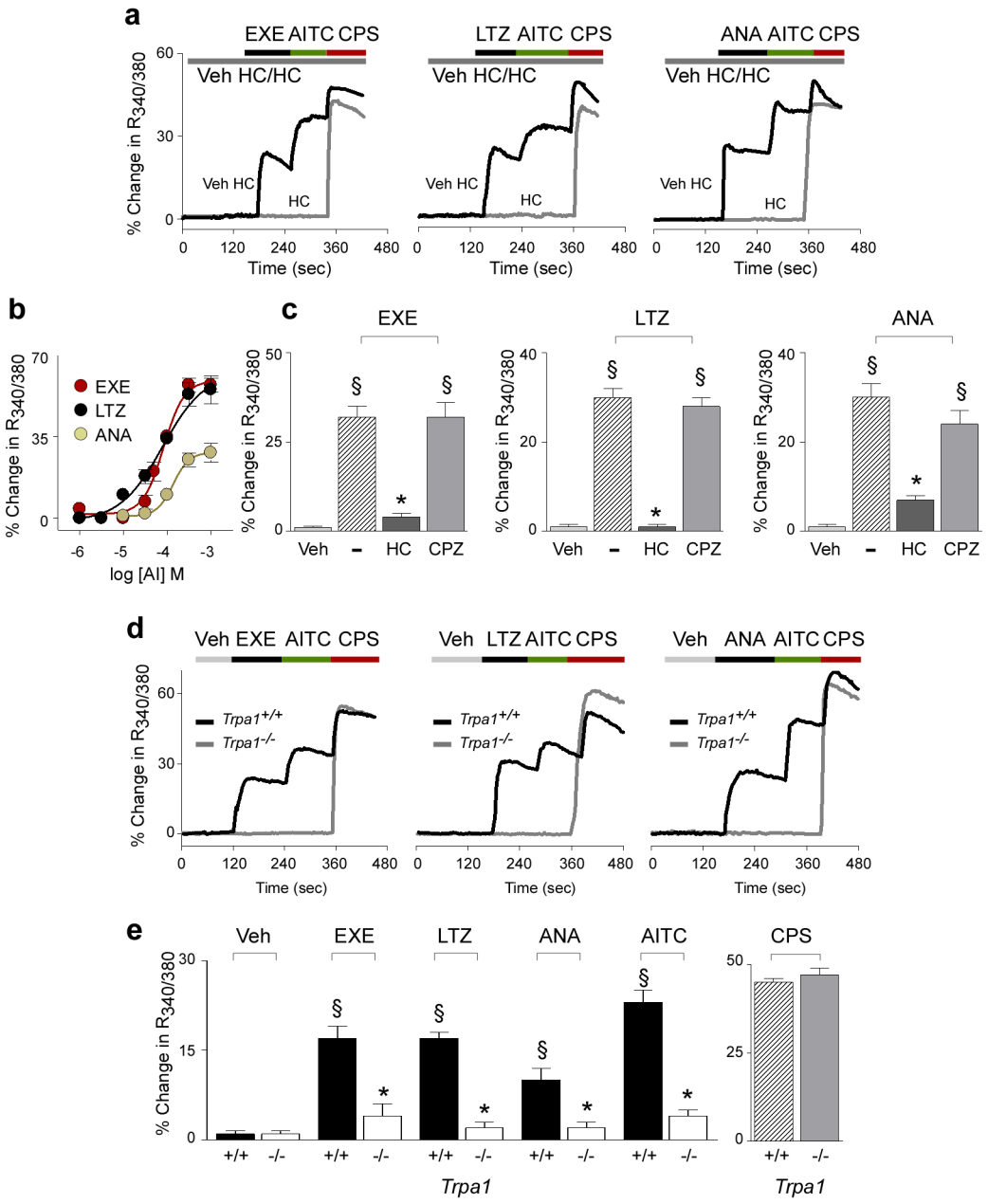

Figure IV-2. Exemestane (EXE), letrozole (LTZ) and anastrozole (ANA) selectively activate the native TRPA1 channel expressed in rodent dorsal root ganglion (DRG) neurons. (**a**) Representative traces of calcium response evoked by EXE (100 µM), LTZ (100 µM), ANA (300 µM) in cultured rat DRG neurons which also respond to allyl isothiocyanate (AITC; 30 µM) and capsaicin (CPS; 0.1 µM). Calcium responses evoked by AIs and AITC are abolished by the selective TRPA1 antagonist, HC-030031 (HC; 30 µM), which does not affect response to CPS. (**b**) Concentration-response curves of EXE, LTZ, and ANA, yielded EC_{50} (95% confidence interval) of 82 (61-108) µM, 78 (39-152) µM, and 135 (78-231) µM, respectively. (**c**) Calcium responses induced by AIs are inhibited by HC and unaffected by the TRPV1 antagonist, capsazepine (CPZ; 10 µM). $^{\S}P<0.05$ *vs.* Veh, $^{*}P<0.05$ *vs.* EXE, LTZ or ANA; ANOVA and Bonferroni *post hoc* test. (**d**) Representative traces and (**e**) pooled data of the calcium response evoked by EXE, LTZ, ANA (all 100 µM) or AITC (30 µM), in neurons isolated from *Trpa1*$^{+/+}$ mice. Neurons isolated from *Trpa1*$^{-/-}$ mice do not respond to AITC, EXE, LTZ and ANA, whereas they do respond normally to CPS (0.1 µM). In DRG neurons isolated from both *Trpa1*$^{+/+}$ and *Trpa1*$^{-/-}$ mice, calcium response is evaluated only in capsaicin responding neurons. $^{\S}P<0.05$ *vs.* Veh, $^{*}P<0.05$ *vs.* EXE, LTZ, ANA or AITC-*Trpa1*$^{+/+}$, ANOVA and Bonferroni *post hoc* test. Veh is the vehicle of AIs; dash (-) indicates the combination of the vehicles of HC and CPZ. Each point or column represents the mean ± s.e.m. of at least 25 neurons obtained from 3-7 independent experiments.

4.2.2 AIs activate nociceptive and hyperalgesic TRPA1-dependent pathways

It has been well documented that local exposure to TRPA1 agonists in experimental animals is associated with an immediate nociceptive response, lasting for a few minutes, and a delayed more prolonged mechanical allodynia [180, 186]. To investigate whether AIs activate such a nociceptive and hyperalgesic TRPA1-dependent pathway, we used one steroidal (exemestane) and one non-steroidal (letrozole) AI. Given the chemical similarity and the hypothesized analogous mechanism of the two non-steroidal AIs, to minimize the number of animals used, anastrozole was not investigated in the following *in vivo* experiments. Intraplantar (i.pl.) injection (20 µl/paw) of exemestane (1, 5, and 10 nmol) (Supplementary Fig. S2a) or letrozole (10, 20 nmol) (Supplementary Fig. 2e) evoked an acute (0-5 min) nociceptive response and a delayed (15-120 min for exemestane and 15-240 min for letrozole) mechanical allodynia in C57BL/6 mice (Supplementary Fig. 2c,g). Both the nociceptive response and mechanical allodynia evoked by AIs were confined to the treated paw (Supplementary Fig. 2c,g) and were almost completely prevented by intraperitoneal (i.p.) pretreatment with HC-030031 (100 mg/kg), but not with capsazepine (4 mg/kg) (Supplementary Fig. 2b,d,f,h). Furthermore, similar to results obtained in C57BL/6 mice, local injection (i.pl.) of exemestane or letrozole in *Trpa1*$^{+/+}$ mice evoked an early nociceptive response and a delayed mechanical allodynia (Supplementary Fig. 2i,j). *Trpa1*$^{-/-}$ mice did not develop such responses (Supplementary Fig. 2i,j). Thus, by using both pharmacological and genetic tools, we demonstrated that local administration of both steroidal and non-steroidal AIs produces a typical TRPA1-dependent behavior, characterized by acute nociception and delayed mechanical allodynia.

4.2.3 AIs produce neurogenic oedema by releasing sensory neuropeptides.

TRPA1 is expressed by peptidergic nociceptors, and its stimulation is associated with proinflammatory neuropeptide release and the ensuing neurogenic inflammatory responses [186, 234]. First, we explored whether AIs are able to directly promote the release of CGRP (one of the proinflammatory neuropeptides, which are usually co-released upon stimulation of peptidergic nociceptors) [6, 270] *via* a TRPA1-dependent pathway. AIs increased CGRP outflow from slices of rat dorsal spinal cord (an anatomical area enriched with central terminals of nociceptors). This effect was

substantially attenuated in rat slices pretreated with a desensitizing concentration of capsaicin (10 µM, 20 min) or in the presence of HC-030031 (Fig. IV-3a). The increase in CGRP outflow observed in slices obtained from *Trpa1*$^{+/+}$ mice was markedly reduced in slices obtained from *Trpa1*$^{-/-}$ mice (Fig. IV-3b).

These neurochemical data were corroborated by functional experiments. Injection (i.pl.) of the TRPA1 agonist, AITC (10 nmol/paw), induced paw edema that peaked at 60 min after injection. The response was abated by treatment with HC-030031 (100 mg/kg, i.p.) or a combination of the SP neurokinin-1 (NK-1) receptor antagonist, L-733,060, and the CGRP receptor antagonist, CGRP8-37 (both, 2 µmol/kg, intravenous, i.v.) (Fig. IV-3c). Similarly, we found that i.pl. administration of exemestane (10 nmol/paw) and letrozole (20 nmol/paw) caused paw edema that peaked at 60 minutes and faded 120 minutes after injection (Fig. IV-3c, insets). Treatment with HC-030031 (100 mg/kg, i.p.) or a combination of L-733,060 and CGRP8-37 (both, 2 µmol/kg, i.v.), markedly reduced the AI-evoked edema (Fig. IV-3c). No edema was found in the paw contralateral to that injected with AIs (Supplementary Fig. 2k). Importantly, the edema produced in *Trpa1*$^{+/+}$ mice by exemestane and letrozole was markedly attenuated in *Trpa1*$^{-/-}$ mice (Fig. IV-3d). Next, to directly evaluate the ability of AIs to release CGRP from peripheral terminals of peptidergic nociceptors, AIs were administered to the rat knee joint. Intraarticular (i.a., 50 µl) injection of exemestane (5 nmol) or letrozole (10 nmol) increased CGRP levels in the synovial fluid, an effect that was markedly attenuated by pretreatment with HC-030031 (100 mg/kg, i.p.) (Fig. IV-3e). Neurochemical and functional data indicate that AIs by TRPA1 activation release sensory neuropeptides from sensory nerve endings, and by this mechanism promote neurogenic inflammatory responses in the innervated peripheral tissue.

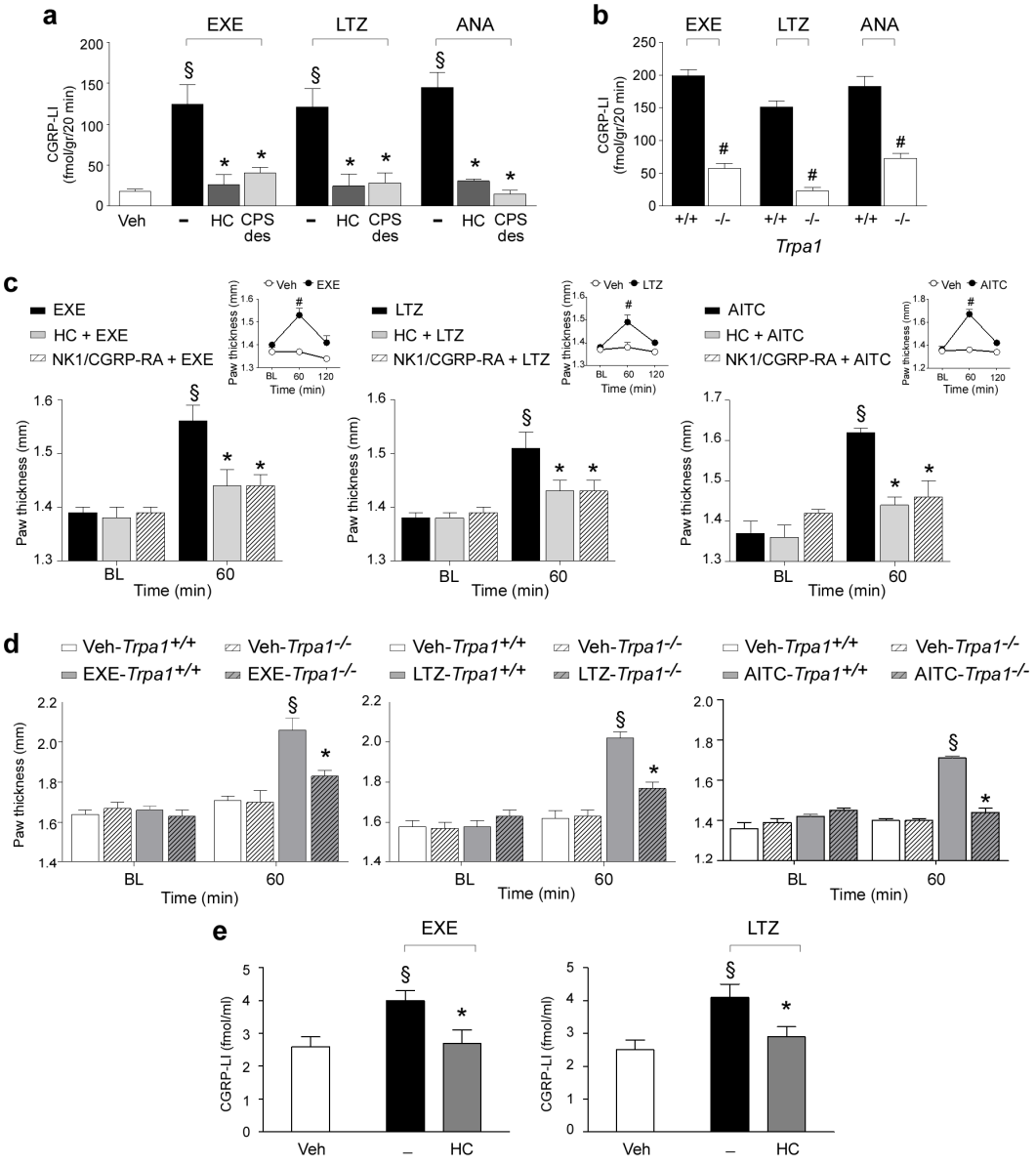

Figure IV-3. Aromatase inhibitors release calcitonin gene-related peptide (CGRP) and produce neurogenic edema. (**a**) Exemestane (EXE), letrozole (LTZ) and anastrozole (ANA) (all 100 µM) increase the CGRP-like immunoreactivity (CGRP-LI) outflow from slices of rat dorsal spinal cord. This effect is prevented by HC-030031 (HC; 30 µM) or after exposure to capsaicin (10 µM, 20 minutes; CPS-des). (**b**) EXE, LTZ and ANA (all 100 µM) increase the CGRP-LI outflow from spinal cord slices obtained from *Trpa1*+/+, but not from *Trpa1*$^{-/-}$ mice. Results are mean ± s.e.m. of at least 4 independent experiments. Veh is the vehicle of EXE, LTZ and ANA, dash (-) indicates the vehicle of HC and CPS. $^{§}P$<0.05 *vs*. Veh, *P<0.05 *vs.* EXE, LTZ or ANA; ANOVA followed by Bonferroni *post hoc* test. $^{\#}P$<0.05 *vs.* EXE-, LTZ-, ANA-*Trpa1*+/+, Student's T test. (**c**) In C57BL/6 mice intraplantar (i.pl.) injection (20 µl) of EXE (10 nmol), LTZ (20 nmol) or allyl isothiocyanate (AITC; 10 nmol) induces paw edema, which peaks at 60 minutes and fades 120 minutes after injection (**c**, upper insets), and is attenuated by pretreatment with HC (100 mg/kg intraperitoneal, i.p.) or the combination of the selective antagonists of the neurokinin-1 receptor, (NK1-RA), L-733,060, and of the CGRP receptor (CGRP-RA), CGRP8-37, (both, 2 µmol/kg, intravenous). (**d**) Paw edema induced by EXE, LTZ and AITC (i.pl.) in *Trpa1*$^{+/+}$ mice is markedly reduced in *Trpa1*$^{-/-}$ mice. BL, baseline level. Results are mean ± s.e.m. of at least 5 mice for each group. Veh is the vehicle of EXE, LTZ and AITC. $^{\#}P$<0.05 *vs*. Veh, Student's T test; $^{§}P$<0.05 *vs.* BL values, *P<0.05 *vs.* EXE, LTZ, AITC or EXE-, LTZ-, AITC-*Trpa1*$^{+/+}$; ANOVA followed by Bonferroni *post hoc* test. (**e**) Injection (50 µl) of EXE (5 nmol) or LTZ (10 nmol) in the rat knee increases CGRP-LI levels in the synovial fluid, an effect that is markedly attenuated by pretreatment with HC (100 mg/kg, i.p.). Results are mean ± s.e.m. of at least 5 mice for each group. Veh is the vehicle of EXE and LTZ, dash (-) indicates the vehicle of HC. $^{§}P$<0.05 *vs.* Veh, *P<0.05 *vs.* EXE, LTZ; ANOVA followed by Bonferroni *post hoc* test.

4.2.4 Systemic AIs induce prolonged pain-like effects by targeting TRPA1

AIs are given to patients by a systemic route of administration. Therefore, we explored in mice whether intraperitoneal (i.p.) or intragastric (i.g.) administration of exemestane and letrozole could produce pain-like effects *via* TRPA1 activation. For i.p. administration experiments, doses, corresponding to those used in humans, were selected according to the mouse to human conversion factor indicated by the National Institute of Health [271]. Exemestane (5 mg/kg, i.p.) or letrozole (0.5 mg/kg, i.p) injection did not produce any visible nociceptive behavior (Supplementary Fig. 3a, and Supplementary Fig. 4a, insets) in mice. However, 3 hours after exemestane or letrozole administration, mice developed a prolonged (3 hours) mechanical allodynia (Supplementary Fig. 3a and Supplementary Fig. 4a) and a reduction in forelimb grip strength (Supplementary Fig. 3c and Supplementary Fig. 4c), a test used in its clinical version for the study of musculoskeletal pain in patients [272]. When mechanical allodynia by exemestane or letrozole was at its maximum, systemic HC-030031 administration (100 mg/kg, i.p.) transiently reverted both responses (Supplementary Fig. 3b,d and Supplementary Fig. 4b,d). Furthermore, mechanical allodynia and the reduction in forelimb grip strength produced by exemestane and letrozole in *Trpa1*$^{+/+}$ mice were markedly reduced in *Trpa1*$^{-/-}$ mice (Supplementary Fig. 3e,f and Supplementary Fig. 4e,f). In experiments where AIs were given by intragastric (i.g.) gavage, doses were adjusted considering the oral bioavailability in humans, which is 99% for letrozole [273], and 40% (with food) for exemestane [274]. First, we found that after i.g. administration of exemestane (10 mg/kg) or letrozole (0.5 mg/kg) their peak plasma levels (13.2 ± 1.7 ng/ml, n=5; and 60.5 ± 12.1 ng/ml, n=5, respectively) (Supplementary Fig. 5) approximated the maximum plasma concentrations found in humans [273, 275]. Second, results similar to those obtained after i.p. administration were reported when AIs were given by i.g. gavage. First, exemestane (10 mg/kg, i.g.) or letrozole (0.5 mg/kg, i.g.) ingestion was not associated with any spontaneous nocifensor behavior (Fig. IV-4a and IV-5a, insets). Second, exemestane or letrozole produced, with a similar time-course, mechanical allodynia and a marked reduction in forelimb grip strength (Fig. IV-4a,c and Fig. IV-5a,c). Pretreatment with HC-030031 or deletion of TRPA1 (*Trpa1*$^{-/-}$ mice) significantly attenuated both responses (Fig. IV-4b,d,e,f and Fig. IV-5b,d,e,f).

Furthermore, since in clinical practice patients are treated with AIs on a daily basis over very long periods of time (up to 5 years), we asked whether exemestane or letrozole maintain the ability to evoke a TRPA1-dependent mechanical hypersensitivity and decreased grip strength upon repeated administration. In *Trpa1*$^{+/+}$ mice, treatment with systemic exemestane (5 mg/kg, i.p.) or letrozole (0.5 mg/kg i.p) (both once a day for 15 consecutive days) produced at day 1, 5, 10 and 15 a transient (from 1 to 6 hours) and reproducible mechanical allodynia (Supplementary Fig. 3e and Supplementary Fig. 4e). Importantly, in *Trpa1*$^{-/-}$ the proalgesic action of AIs was markedly attenuated (Supplementary Fig. S3e and Supplementary Fig. S4e). In addition, the decrease in the grip strength was maintained, without undergoing desensitization, over the entire time period of daily i.p. administration of exemestane or letrozole (Supplementary Fig. 3f and Supplementary Fig. 4f). Both these effects of AIs were significantly reduced in *Trpa1*$^{-/-}$ mice (Supplementary Fig. 3f and Supplementary Fig. 4f). Similar results were obtained after i.g. administration of exemestane or letrozole (once a day for 15 consecutive days at the dose of 10 mg/kg i.g. or 0.5 mg/kg i.g., respectively). Both mechanical allodynia and decreased grip strength were observed, without signs of desensitization, over the 15 days of observation in *Trpa1*$^{+/+}$ mice, but were markedly reduced in *Trpa1*$^{-/-}$ mice (Fig. IV-4e,f and Fig. IV-5e,f). Altogether, the present data demonstrate that both steroidal and non-steroidal third-generation AIs induce a series of pain-like effects predominantly *via* a TRPA1-dependent mechanism, effects that over time do not undergo desensitization, thus mimicking the chronic clinical condition.

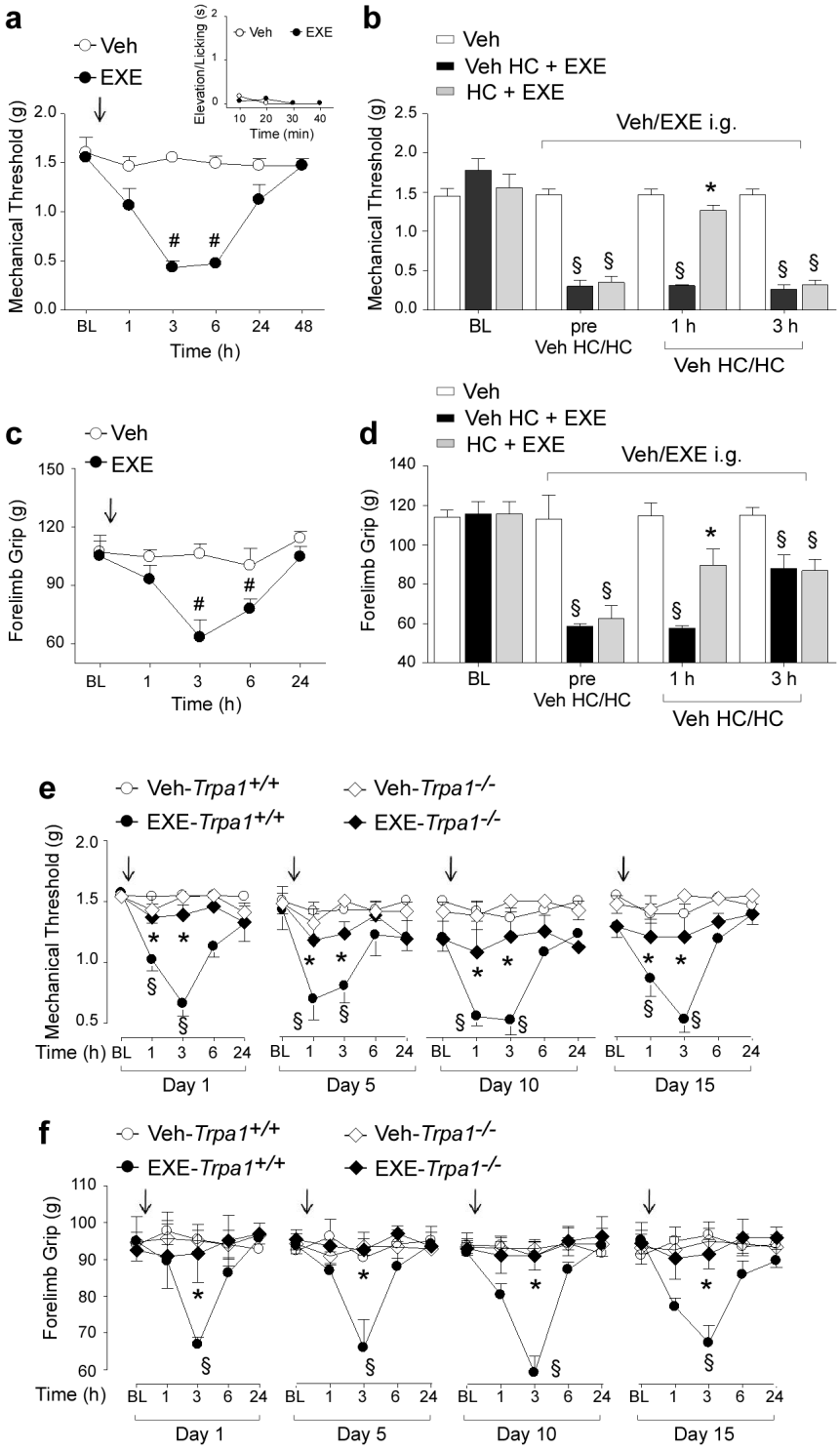

Figure IV-4. Intragastric exemestane (EXE) induces TRPA1-dependent prolonged mechanical allodynia and reduction in forelimb grip strength in mice. In C57BL/6 mice intragastric (i.g.) administration of EXE (10 mg/kg) induces (**a**) mechanical allodynia and (**c**) a reduction in forelimb grip strength that last 3-6 hours after administration. EXE does not produce any acute nocifensor behavior as measured by the indicated test (**a,** inset). (**b,d**) Three hours after EXE administration, HC-030031 (HC; 100 mg/kg i.p.) reverts both mechanical allodynia and the reduction in forelimb grip strength. HC inhibition is no longer visible 3 hours after its administration. Veh is the vehicle of EXE. $^{\#}P<0.05$ *vs.* Veh; Student's T test (**a,c**) and $^{\S}P<0.05$ *vs.* Veh and $^{*}P<0.05$ *vs.* Veh HC-EXE; ANOVA followed by Bonferroni *post hoc* test (**b,d**). (**e,f**) EXE (once a day for 15 consecutive days, 10 mg/kg i.g.) induces reproducible mechanical allodynia and decrease in forelimb grip strength at day 1, 5, 10 and 15 in *Trpa1*$^{+/+}$ mice. Arrows indicate Veh or EXE administration. Both these effects are markedly reduced in *Trpa1*$^{-/-}$ mice. $^{\S}P<0.05$ *vs.* Veh-*Trpa1*$^{+/+}$, $^{*}P<0.05$ *vs.* EXE-*Trpa1*$^{+/+}$; ANOVA followed by Bonferroni *post hoc* test. Results are mean ± s.e.m. of at least 5 mice for each group. In all conditions, baseline (BL) levels were recorded 30 minutes before EXE administration.

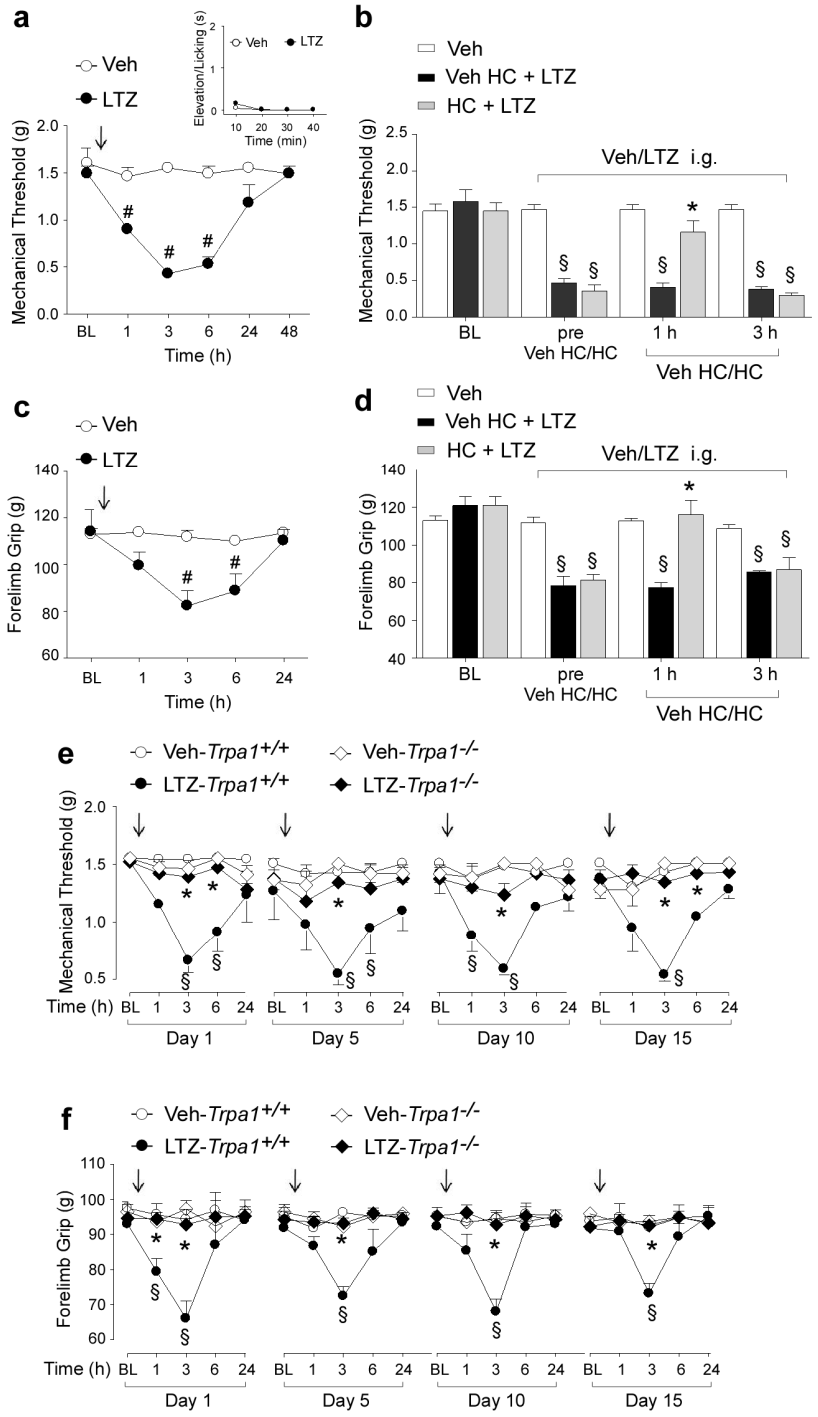

Figure IV-5. Intragastric letrozole (LTZ) induces TRPA1-dependent prolonged mechanical allodynia and reduction in forelimb grip strength in mice. In C57BL/6 mice intragastric (i.g.) administration of LTZ (0.5 mg/kg) induces (a) mechanical allodynia and (c) reduction in forelimb grip strength that last 3-6 hours after administration. LTZ does not produce any acute nocifensor behavior as measured by the indicated test (a, inset). (b,d) Three hours after LTZ administration, HC-030031 (HC; 100 mg/kg i.p.) reverts both mechanical allodynia and the reduction in forelimb grip strength. HC inhibition is no longer visible 3 hours after its administration. Veh is the vehicle of LTZ. #P<0.05 vs. Veh; Student's T test (a,c) and §P<0.05 vs. Veh and *P<0.05 vs. Veh HC-LTZ; ANOVA followed by Bonferroni post hoc test (b,d). (e,f) LTZ (once a day for 15 consecutive days, 0.5 mg/kg i.g.) induces reproducible mechanical allodynia and decrease in forelimb grip strength at day 1, 5, 10 and 15 in *Trpa1*$^{+/+}$ mice. Arrows indicate Veh or LTZ administration. Both effects are markedly reduced in *Trpa1*$^{-/-}$ mice. §P<0.05 vs. Veh-*Trpa1*$^{+/+}$, *P<0.05 vs. LTZ-*Trpa1*$^{+/+}$; ANOVA followed by Bonferroni post hoc test. Results are mean ± s.e.m. of at least 5 mice for each group. In all conditions baseline (BL) levels were recorded 30 minutes before LTZ administration.

4.2.5 AI-evoked TRPA1 activation is enhanced by proinflammatory stimuli

Although it affects a large proportion of subjects, not all patients treated with AIs develop AIMSS. One possible explanation for the peculiar susceptibility to AIMSS of some patients is that, if TRPA1 activation is a necessary prerequisite, *per se* it is not sufficient, and additional proalgesic factors must contribute to the development of pain symptoms. It has been reported that stimulation of proalgesic pathways exaggerates TRPA1-dependent responses *in vitro* and *in vivo* [156, 212]. One example of such potentiating action has been reported for the proteinase-activated receptor-2 (PAR2), whose subthreshold activation results in an exaggerated response to the TRPA1 agonist, AITC [212]. PAR2 undergoes activation upon a unique proteolytic mechanism by cleavage of its tethered ligand domain by trypsin and other proteases, thus mediating inflammation and hyperalgesia [276]. On this basis, and following a previously reported protocol [212], we explored, by *in vivo* functional experiments in C57BL/6 mice, whether PAR2 activation exaggerates TRPA1-dependent hypersensitivity induced by AIs. Prior (10 minutes) injection (i.pl.) of the PAR2 activating peptide (AP) (PAR2-AP, 1 µg/paw), but not the reverse peptide (RP) (PAR2-RP, 1 µg/paw, inactive on PAR2), markedly enhanced the duration of licks and flinches of the hind paw produced by local injection (i.pl.) of exemestane (1 nmol/paw) and letrozole (10 nmol/paw) (Fig. IV-6a). The injected dose of PAR2-AP, as well as PAR2-RP, did not cause *per se* any visible acute nocifensor response (Fig. IV-6a). The exaggerated responses to the combination of PAR2-AP and exemestane or letrozole were inhibited by HC-030031 (100 mg/kg, i.p.) (Fig. IV-6a).

We also tested the ability of a recognized endogenous TRPA1 agonist, H_2O_2 [175, 190] to increase the nocifensor response of exemestane or letrozole. In addition, we explored the ability of AIs to increase either nociception or mechanical allodynia to H_2O_2. H_2O_2 (0.5 µmol/paw) injection produced a transient nocifensor behavior that terminated within 5 min (Fig. IV-6b, inset). We found that 10 min after H_2O_2 injection (when baseline levels of nociception were restored) administration of exemestane (1 nmol/paw) and letrozole (10 nmol/paw) evoked nociceptive responses markedly increased as compared to vehicle-pretreated mice (Fig. IV-6b). The exaggerated responses to AIs were inhibited by HC-030031 (Fig. IV-6b). Thus, both homologous activation of the channel by the TRPA1 agonist H_2O_2, or heterologous stimulation of a classical proinflammatory pathway, such as PAR2, converge in a final common pathway, which results in the potentiation of the AI-evoked and TRPA1-dependent

proalgesic mechanism. In the attempt to understand the mechanism underlying the *in vivo* potentiation between PAR2 or H_2O_2 and AIs, cultured DRG neurons were challenged with combinations of these same agents. First, in *in vitro* electrophysiological experiments, we found that AITC, exemestane and letrozole (all 100 μM) produced inward currents in cultured DRG neurons, effects that were abated in the presence of HC-030031 (50 μM). However, HC-030031 did not affect the inward current produced by capsaicin (Fig. IV-6c). Second, we showed that pre-exposure to subthreshold concentrations of PAR2-AP or H_2O_2 enhanced currents evoked by subthreshold concentrations of either exemestane or letrozole (both 20 μM) (Typical traces Fig. IV-6d and pooled data Fig IV-6e). Third, HC-030031 inhibited the exaggerated responses (Fig IV-6e).

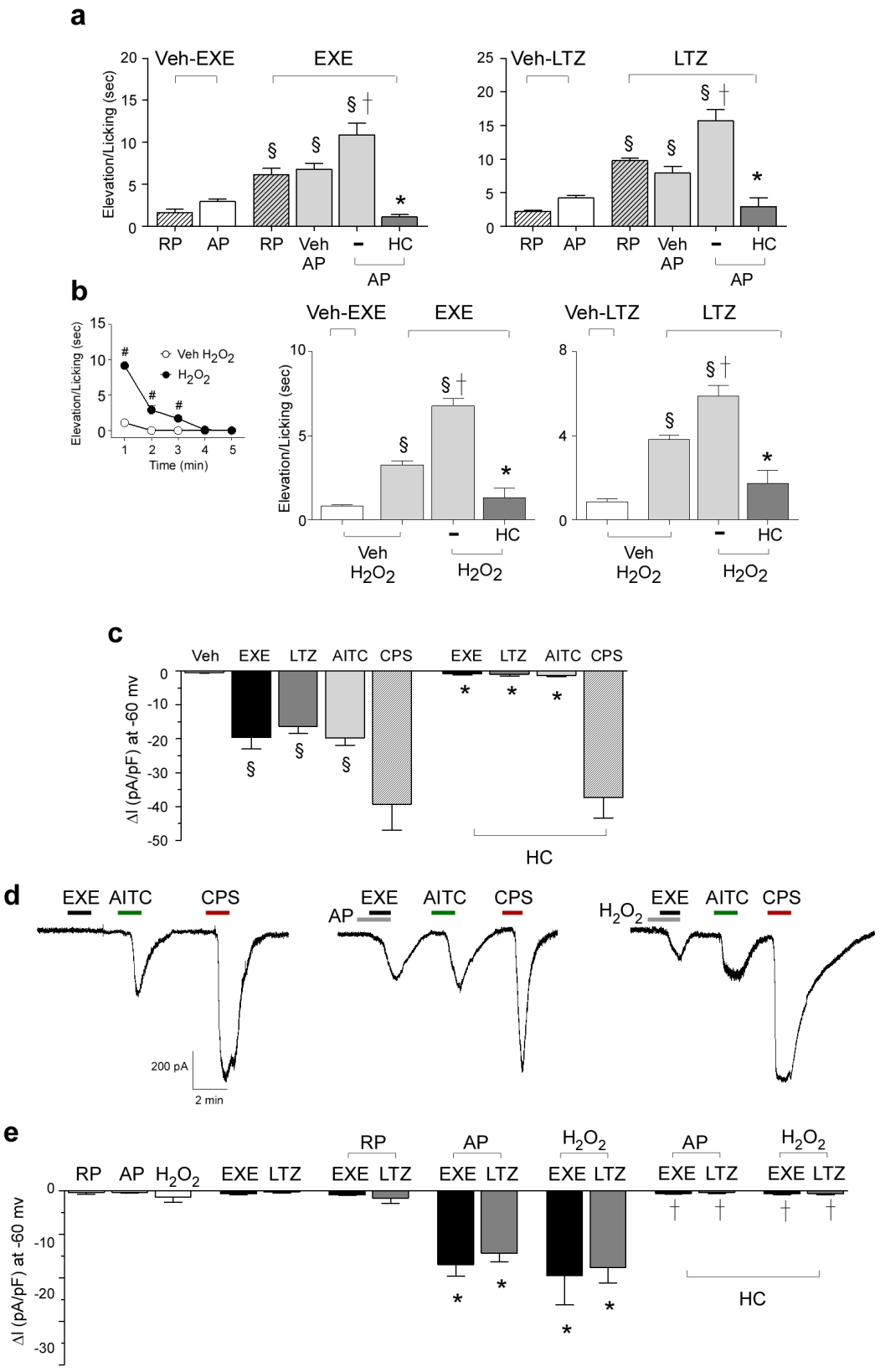
a
Veh-EXE
EXE
Veh-LTZ
LTZ
Elevation/Licking (sec)
RP
AP
Veh
HC
b
Veh H_2O_2
H_2O_2
Time (min)
c
Veh
EXE
LTZ
AITC
CPS
ΔI (pA/pF) at -60 mv
d
200 pA
2 min
e
H_2O_2

◀ **Figure IV-6. TRPA1-activation by exemestane (EXE) and letrozole (LTZ) is enhanced by proinflammatory stimuli.** (**a**) Intraplantar (i.pl.; 10 µl) pretreatment (10 minutes) with the proteinase-activated receptor 2 (PAR2) activating peptide (AP; 1 µg), but not with the inactive PAR2 reverse peptide (RP; 1 µg), enhances nocifensor behavior produced by EXE (1 nmol/10 µl, i.pl.) or LTZ (10 nmol/10 µl, i.pl.). AP and RP alone cause negligible nociception. The potentiated responses to EXE or LTZ are markedly attenuated by HC-030031 (HC; 100 mg/kg, i.p.). (**b**) H_2O_2 (0.5 µmol/10 µl, i.pl.) injection produces a transient nocifensor behavior, lasting only 5 minutes (**b**, inset). Pretreatment (10 minutes before AI administration) with H_2O_2 (0.5 µmol/10 µl, i.pl.) increases nocifensor behavior produced by EXE (1 nmol/10 µl, i.pl.) or LTZ (10 nmol/10 µl, i.pl.). HC (100 mg/kg, i.p.) inhibits the exaggerated responses to both EXE and LTZ. Dash (-) indicates the vehicle of HC. Points or columns are mean ± s.e.m. of at least 5 mice for each group. $^{\S}P<0.05$ *vs.* RP or AP or Veh H_2O_2; $^{\dagger}P<0.05$ *vs.* Veh AP/EXE or Veh AP/LTZ or Veh H_2O_2/EXE or Veh H_2O_2/LTZ; $^{*}P<0.05$ *vs.* AP/EXE or AP/LTZ or H_2O_2/EXE or H_2O_2/LTZ*;* ANOVA followed by Bonferroni *post hoc* test. $^{\#}P<0.05$ *vs.* Veh H_2O_2, Student's T test. (**c**) An active concentration of EXE or LTZ (both 100 µM) evokes inward currents in rat dorsal root ganglion (DRG) neurons, which also respond to allyl isothiocyanate (AITC; 100 µM) and capsaicin (CPS; 1 µM). Inward currents evoked by EXE, LTZ or AITC are inhibited in the presence of HC (50 µM), which does not affect CPS-evoked currents. Typical traces (**d**) and pooled data (**e**) showing that pre-exposure to AP (100 µM) or H_2O_2 (100 µM) exaggerates currents evoked by a subthreshold concentration of EXE and LTZ (both 20 µM). The inactive RP does not affect responses to EXE or LTZ (both 20 µM). The potentiated responses to EXE or LTZ are markedly attenuated by HC (50 µM). Veh is the vehicle of EXE, LTZ and AITC. Results are mean ± s.e.m. of at least 5 independent experiments. $^{\S}P<0.05$ *vs.* Veh, $^{*}P<0.05$ *vs.* EXE, LTZ or AITC and $^{\dagger}P<0.05$ *vs.* EXE- or LTZ-AP and EXE- or LTZ-H_2O_2; ANOVA followed by Bonferroni *post hoc* test.

4.3 Discussion

In the present study, we provide for the first time evidence that third-generation steroidal and non-steroidal AIs, proven to be very effective drugs in the treatment of hormone receptor-positive breast cancer [36, 37], selectively target the TRPA1 channel. This conclusion derives from a series of experiments in cells expressing the recombinant human TRPA1 or in rodent DRG neurons expressing the native channel. Indeed, calcium responses and currents evoked by AIs are confined to TRPA1-expressing cells, and are selectively abolished by HC-030031, or absent in neurons obtained from TRPA1-deficient mice. Exemestane exhibits a chemical structure with a system of highly electrophilic conjugated Michael acceptor groups [277]. A variety of known TRPA1 agonists, including acrolein and other α,β-unsaturated aldehydes, possess an electrophilic carbon or sulfur atom that is subject to nucleophilic attack (Michael addition) by cysteine and lysine residues [278]. Nitriles also exhibit electrophilic properties [279], which may result in TRPA1 gating [280]. Non-steroidal letrozole and anastrozole possess nitrile moieties that underscore their potential ability to activate TRPA1. We show that key cysteine and lysine residues, required for channel activation by electrophilic agonists [111, 184, 186] are also required for TRPA1 activation by AIs. Thus, the three AIs, most likely because of their electrophilic nature, selectively target TRPA1, whereas TRPV1, TRPV2, TRPV3 and TRPV4, all co-expressed with TRPA1 [143, 163], and other channels or receptors in DRG neurons, do not seem to play a relevant role in the direct excitation of nociceptors by AIs.

TRPA1-expressing neurons activated by AIs also responded to capsaicin, a selective TRPV1 agonist. As TRPV1 is considered a specific marker of nociceptors [281], AIs may be assumed to activate pain-like responses. *In vivo* stimulation of the irritant TRPA1 receptor in rodents produces an early nociceptive behavior, followed by a delayed and prolonged mechanical allodynia [180, 186, 214]. Subcutaneous exemestane and letrozole recapitulated the two effects produced by TRPA1 agonists, and produced such responses in a TRPA1-dependent way.

Magnetic resonance imaging of painful wrists in patients treated with AIs has shown signs of inflammatory tenosynovitis poorly reverted by common anti-inflammatory treatments [46]. Systemic increases in plasma cytokines have not been found in patients with AIMSS and, therefore, do not appear to represent the underlying

mechanism for such inflammatory conditions [43, 282]. This implies that pathways different from cytokine-dependent inflammation operate in joints of patients treated with AIs. As TRPA1 is expressed by a subpopulation of peptidergic nociceptors, which mediate neurogenic inflammation [6, 143, 163], we anticipated that AIs, by targeting TRPA1, release proinflammatory neuropeptides, thereby causing neurogenic plasma extravasation. Pharmacological and genetic findings indicate that AIs produce a specific type of edema, which is neurogenic in nature. The conclusion is corroborated by the direct neurochemical observation that exemestane and letrozole evoke TRPA1-dependent CGRP release from peripheral endings of primary sensory neurons. The neurogenic component, mediated by TRPA1-activation and sensory neuropeptide release, may thus represent an important mechanism contributing to the cytokine-independent inflammation observed in AI users.

When AIs were given to mice by systemic (intraperitoneal or intragastric) administration, no acute nocifensive response was observed, but, after ~1 hour delay they produced a prolonged condition (up to 6 hours) of mechanical allodynia and a decrease in forelimb grip strength. Also, in this case, pharmacological and genetic results indicate that AI-evoked pain-like responses are principally TRPA1-dependent. In clinical practice, AIs are used for a 3- or 5-year period, and the pain condition associated to their use is often persistent [283]. Although the present experimental conditions cannot fully mimic the clinical setting in cancer patients, our findings suggest that the TRPA1-dependent ability of AIs to produce mechanical allodynia and to decrease forelimb grip strength is maintained and does not undergo desensitization in mice over a time period of 15 days, which broadly corresponds to a 1-year time in humans. Despite a general good tolerability [45], AIs produce some types of pain, including AIMSS and neuropathic, diffuse and mixed pain in 10-20% of the treated patients [43]. The reason why only some of the patients exposed to AIs develop these severe pain conditions, which may lead to non-adherence or therapy discontinuation, is unknown.

Here, we reveal the key role of TRPA1 as the main mediator of exemestane- and letrozole-evoked nociceptor stimulation. However, it is likely that additional factors contribute to determine the development of AIMSS and related pain symptoms, particularly in those susceptible patients who suffer from the more severe form of this adverse reaction. *In vitro* and *in vivo* experiments with the co-administration of AIs and pro-algesic stimuli, such as PAR2-AP, an agonist of the pro-inflammatory

receptor, PAR2, and the TRPA1 agonist, H_2O_2 [175], indicate that additional factors may cooperate to increase the sensitivity to AIs of TRPA1 expressing nociceptors. Enhancement by PAR2 activation of the proalgesic activity of exemestane and letrozole is fully consistent and closely mimic previous observations that PAR2 activation increases the pro-algesic response evoked by TRPA1 agonists [212]. Findings that a combination of AIs and H_2O_2 exaggerates TRPA1-mediated *in vitro* and *in vivo* responses suggest that increased levels of oxidative stress byproducts, known to be generated under inflammatory conditions [284] may facilitate the development of AIMSS and related pain symptoms. Our present investigation on the cooperation between AIs and proinflammatory mediators has been limited to PAR2 and H_2O_2. However, it is possible that additional pro-inflammatory and pro-algesic mediators can activate similar cooperating pathways. AI concentrations required for TRPA1 activation are higher than those found in the plasma of treated subjects [285, 286]. However, it should be noted that all three AIs have a large volume of distribution, indicating a high tissue distribution [273, 275]. The present findings that in mice plasma levels of both AIs were comparable to those found in humans [273, 275] strengthen the hypothesis that compartmentalization of AIs in mice is similar to that reported in humans [273, 275]. Thus, under standard drug regimens, concentrations sufficient to activate TRPA1 or to potentiate TRPA1-mediated responses evoked in cooperation with inflammatory mediators may be reached in tissues neighboring sensory nerve terminals.

Altogether, the present results indicate that AIs *per se* or, most likely, in cooperation with other proinflammatory mediators, promote TRPA1-dependent neurogenic inflammation, mechanical hypersensitivity, and decreased forelimb grip force in rodents. This novel pathway may represent the main underlying mechanism responsible for pain and inflammatory symptoms associated with AI treatment. The other important proposal deriving from the present findings is that antagonists of the TRPA1 channel may be beneficial in the prevention and treatment of such painful conditions.

This work has been published in Nature Communications

Fusi C, Materazzi M, Benemei S, Coppi E, Trevisan G, Marone IM, Minocci D, De Logu F, Tuccinardi T, Di Tommaso MR, Susini T, Moneti G, Pieraccini G, Geppetti P, Nassini R (2014). "Steroidal and non-steroidal third-generation aromatase inhibitors induce pain-like symptoms via TRPA1." Nat Commun 5(5736): 5736.

Chapter V – Conclusions

CIPN is a common disabling side effect of different cancer treatments characterized by sensory symptoms, including paresthesias and dysesthesias to the extremities, spontaneous pain, and mechanical and thermal hypersensitivity. CIPN leads to a lower quality of life and often causes chemotherapy discontinuation [23]. The mechanisms underlying the acute neuronal hyperexcitability and the onset of the peripheral neuropathy and painful states induced by chemotherapeutic agents remain still to be established. In the recent years remarkable interest has been paid to the different ion channels located to neuronal membrane. In particular, due to their specific and abundant expression on peripheral sensory neurons involved in pain transduction, research on TRP channels represents a promising area of investigation. In this regard, recent evidence has proposed a role for TRPV4 in PXL-evoked mechanical hyperalgesia [218]. Similarly to PXL, treatment with vincristine has been reported to produce mechanical allodynia in rodents through a TRPV4-dependent mechanism [218]. Moreover, treatment with cisplatin has been found to produce up-regulation of TRPV1 mRNA in cultured DRG neurons [221]. In addition, acute exposure to oxaliplatin induces TRPV1 sensitization, which may cause neuronal damage [221]. A recent paper reported a possible contribution of TRPM8 expressing fibers to cold hypersensitivity induced by oxaliplatin [229]. Other recent evidence obtained from our research group demonstrate that TRPA1 acts as a major player in rodent models of CIPN induced by oxaliplatin and cisplatin that target TRPA1mainly *via* oxidative stress generation [232].

Although the mechanism underlying the development of CIPN are still not well understood, oxidative stress seems to contribute to the onset of a prolonged peripheral neuropathy. In fact, it has been well established the ability of chemotherapeutic drugs to produce oxidative stress and its by-products, which strongly contribute to the anticancer action. On the other hand this property seems to be responsible for major adverse reactions, including CIPN. In line with this assumption, it has been reported that

oxaliplatin-induced mechanical hyperalgesia and heat- and cold-evoked allodynia in rats are attenuated by antioxidants, including acetyl-L-carnitine, α-LA, or vitamin C, suggesting the contribution of oxidative stress to these painful conditions [257].

Among the TRP superfamily, the TRPA1 subtype, activated by numerous oxidative stress by-products such as H_2O_2 [190, 175, 191], hypochlorite, and superoxide [191], has been referred to as a major oxidant sensor [191]. Based on this evidence, we supposed that various chemotherapeutic drugs could directly or indirectly target the TRPA1 channels through the generation of oxidative stress inducing painful states.

The results presented in this thesis have been obtained from the study of the painful side effects associated with three chemotherapeutic treatments different in terms of chemical structure and/or mechanism of action, such as PXL, BTZ and AIs.

In the first work we showed that TRPA1 accounts for the remaining TRPV4-resistant component of the mechanical hypersensitivity produced by PXL. This conclusion is derived from both pharmacological study, using selective TRPA1 and TRPV4 antagonists, and genetic study, using TRPA1-deficient mice. In fact, the TRPV4 antagonist, HC-067047, abated completely the component of the PXL-evoked mechanical allodynia that was resistant to TRPA1 pharmacological blockade or genetic deletion. Of interest for the present discussion is the finding that in contrast with the selective TRPA1 agonist, AITC, PXL *per se* does not activate TRPA1 in cultured DRG neurons, as measured by the ability to evoke an early calcium response.

Previous papers [217, 241] reported that PXL releases SP from airway sensory nerves, a neuropeptide co-expressed with CGRP in a subset of primary sensory neurons [242]. Based on this evidence, we tested whether PXL could target sensory nerve terminals by measuring the release of the sensory neuropeptide, CGRP. Here, we confirmed that PXL increases the release of neuropeptides from capsaicin-sensitive peripheral nerve terminals, and for the first time we showed, by using both pharmacological and genetic approach, that the action of PXL is mediated by both TRPA1 and TRPV4 activation. Moreover, the ROS and reactive aldehydes scavenger, GSH, completely abolished the PXL-evoked CGRP release from peripheral tissues of either wild type or TRPA1-deficient mice. These findings indicate that PXL evokes a delayed and prolonged mechanical and thermal hypersensitivity targeting both TRPA1 and TRPV4 channels expressed on nociceptive sensory neurons, through a mechanism which is GSH-sensitive, suggesting the involvement of oxidative stress and/or its by-

products in this phenomenon. This hypothesis is supported by several studies reporting that antioxidants protect against the sensory neuropathy induced by PXL [245, 238].

Similarly to the results obtained with PXL, we found that TRPA1 plays a key role in BTZ-evoked mechanical, chemical and cold prolonged hypersensitivity, as these phenomena were completely, but transiently, reverted by a TRPA1 antagonist and completely absent in TRPA1-deficient mice. As observed with PXL, BTZ failed to evoke any calcium response in cultured TRPA1-expressing neurons, thus excluding that this drug may directly target the channel and suggesting an indirect action. In fact, we found that BTZ increases oxidative stress and its by-products in mice. Behavioural studies demonstrated that the treatment with an oxidative stress scavenger transiently reverted BTZ-evoked mechanical, cold, and chemical hypersensitivity. More importantly, in this paper we demonstrated that an early and short-term treatment with the selective TRPA1 antagonist or an antioxidant permanently prevents the onset of the mechanical, cold, and chemical hypersensitivity evoked by BTZ in mice. This important result suggests a possible treatment schedule to prevent the onset of sensory neuropathy in patients during chemotherapy when TRPA1 antagonists will be clinically available.

Altogether present evidence implies that PXL and BTZ do not directly gate TRPA1, but rather exert this action indirectly *via* the generation of oxidative stress by-products that eventually target the channel in sensory nerve terminals. Whereas endogenous oxidative stress by-products capable of activating TRPA1 are well identified, little information [246] is available regarding activation of TRPV4 by oxidative stress species. Thus, further studies are required to define mechanisms apparently associated to PXL-induced and TRPA1/TRPV4-mediated hypersensitivity.

In the last part, our research focused on uncovering the mechanisms underlying painful states induced by third-generation AIs, the steroidal exemestane and non-steroidal azole derivatives, letrozole and anastrozole. The use of AIs is associated with a series of relevant side effects which are reported in 30-60% of treated patients [39, 40]. Among these, the AI-associated musculoskeletal symptoms (AIMSS) characterized by morning stiffness and pain of the hands, knees, hips, lower back, and shoulders [41, 42]. In addition to musculoskeletal pain, pain symptoms associated with AIs have recently been more accurately described with the inclusion of neuropathic, diffused, and mixed pain [43].

The chemical structure of exemestane includes a system of highly electrophilic conjugated Michael acceptor groups, which might react with the thiol groups of reactive

cysteine residues [277]. Michael addition reaction with specific cysteine residues is a major mechanism that results in TRPA1 activation by a large variety of electrophilic compounds [186, 184, 185]. Aliphatic and aromatic nitriles can react with cysteine to form thiazoline derivatives and accordingly the tear gas 2-chlorobenzylidene malononitrile (CS) has been identified as a TRPA1 agonist [280]. We noticed that both letrozole and anastrozole possess nitrile moieties. Thus, we hypothesized that AIs may produce neurogenic inflammation, nociception and hyperalgesia by targeting TRPA1. In this study, we provide for the first time evidence that AIs, unlike PXL and BTZ, selectively target the TRPA1 channel leading to the onset of painful conditions. However, it is likely that additional factors contribute to determine the development of AIMSS and related pain symptoms, particularly in those susceptible patients who suffer from the more severe form of this adverse reaction. *In vitro* and *in vivo* experiments with the co-administration of AIs and pro-inflammatory stimuli, such as PAR2-AP, and the TRPA1 agonist, H_2O_2 [175], indicate that additional factors may cooperate to increase the sensitivity to AIs of TRPA1 expressing nociceptors. Enhancement by PAR2 activation of the pro-algesic activity of exemestane and letrozole is fully consistent and closely mimic previous observations that PAR2 activation increases the pro-algesic response evoked by TRPA1 agonists [212]. Findings that a combination of AIs and H_2O_2 exaggerates TRPA1-mediated *in vitro* and *in vivo* responses suggest that increased levels of oxidative stress by-products, known to be generated under inflammatory conditions [284] may facilitate the development of AIMSS and related pain symptoms. Our present investigation on the cooperation between AIs and proinflammatory mediators has been limited to PAR2 and H_2O_2 however, it is possible that additional pro-inflammatory and pro-algesic mediators can activate similar cooperating pathways. AI concentrations required for TRPA1 activation are higher than those found in the plasma of treated subjects [285, 286] however, it should be noted that all three AIs have a large volume of distribution, indicating a high tissue distribution [273, 275]. The present findings that in mice plasma levels of both AIs were comparable to those found in humans [273, 275] strengthen the hypothesis that compartmentalization of AIs in mice is similar to that reported in humans [273, 275]. Thus, under standard drug regimens, concentrations sufficient to activate TRPA1 or to potentiate TRPA1-mediated responses evoked in cooperation with inflammatory mediators may be reached in tissues neighboring sensory nerve terminals.

Taken together, these findings indicate that TRPA1, *via* its activation by oxidative stress by-products, is necessary and sufficient to produce a sensory neuropathy paradigm in mice following a single administration of different chemotherapeutics. In addition, the findings obtained in these works suggest a novel therapeutic approach to prevent CIPN and to treat other painful states associated with the chemotherapy, based on the future use of TRPA1 antagonists which may protect patients from neurotoxic effects without affecting the anticancer potential of chemotherapeutic drugs.

References

[1] C.S. Sherrington, The Integrative Action of the Nervous System Scribner, New York, 1906.

[2] D. Julius, A.I. Basbaum, Molecular mechanisms of nociception, Nature 413 (2001) 203-210.

[3] A.I. Basbaum, D.M. Bautista, G. Scherrer, D. Julius, Cellular and molecular mechanisms of pain, Cell 139 (2009) 267-284.

[4] S.P. Hunt, A. Pini, G. Evan, Induction of c-fos-like protein in spinal cord neurons following sensory stimulation, Nature 328 (1987) 632-634.

[5] W.D. Snider, S.B. McMahon, Tackling pain at the source: new ideas about nociceptors, Neuron 20 (1998) 629-632.

[6] P. Geppetti, P. Holzer, Neurogenic inflammation, CRC Press, Boca Raton, 1996.

[7] T. Lewis, The nocifensor system of nerves and its reactions, Br Med J (1937).

[8] J. Szolcsanyi, Capsaicin and nociception, Acta Physiol Hung 69 (1987) 323-332.

[9] S. Amadesi, J. Moreau, M. Tognetto, J. Springer, M. Trevisani, E. Naline, C. Advenier, A. Fisher, D. Vinci, C. Mapp, D. Miotto, G. Cavallesco, P. Geppetti, NK1 receptor stimulation causes contraction and inositol phosphate increase in medium-size human isolated bronchi, Am J Respir Crit Care Med 163 (2001) 1206-1211.

[10] P. Geppetti, C. Bertrand, J. Baker, I. Yamawaki, G. Piedimonte, J.A. Nadel, Ruthenium red, but not capsazepine reduces plasma extravasation by cigarette smoke in rat airways, Br J Pharmacol 108 (1993) 646-650.

[11] A.C. Myers, R.G. Goldie, D.W. Hay, A novel role for tachykinin neurokinin-3 receptors in regulation of human bronchial Ganglia neurons, Am J Respir Crit Care Med 171 (2005) 212-216.

[12] P. Geppetti, E. Del Bianco, R. Cecconi, M. Tramontana, A. Romani, E. Theodorsson, Capsaicin releases calcitonin gene-related peptide from the human iris and ciliary body in vitro, Regul Pept 41 (1992) 83-92.

[13] P.J. Goadsby, L. Edvinsson, R. Ekman, Vasoactive peptide release in the extracerebral circulation of humans during migraine headache, Ann Neurol 28 (1990) 183-187.

[14] H. Doods, G. Hallermayer, D. Wu, M. Entzeroth, K. Rudolf, W. Engel, W. Eberlein, Pharmacological profile of BIBN4096BS, the first selective small molecule CGRP antagonist, Br J Pharmacol 129 (2000) 420-423.

[15] J. Olesen, H.C. Diener, I.W. Husstedt, P.J. Goadsby, D. Hall, U. Meier, S. Pollentier, L.M. Lesko, Calcitonin gene-related peptide receptor antagonist BIBN 4096 BS for the acute treatment of migraine, N Engl J Med 350 (2004) 1104-1110.

[16] C. Miranda, S. Selleri, M.A. Pierotti, A. Greco, The M581V mutation, associated with a mild form of congenital insensitivity to pain with anhidrosis, causes partial inactivation of the NTRK1 receptor, J Invest Dermatol 119 (2002) 978-979.

[17] M. Koltzenburg, J. Scadding, Neuropathic pain, Curr Opin Neurol 14 (2001) 641-647.

[18] R.M. Bennett, The rational management of fibromyalgia patients, Rheum Dis Clin North Am 28 (2002) 181-199, v.

[19] S. Sarkar, Q. Aziz, C.J. Woolf, A.R. Hobson, D.G. Thompson, Contribution of central sensitisation to the development of non-cardiac chest pain, Lancet 356 (2000) 1154-1159.

[20] H. Bolay, U. Reuter, A.K. Dunn, Z. Huang, D.A. Boas, M.A. Moskowitz, Intrinsic brain activity triggers trigeminal meningeal afferents in a migraine model, Nat Med 8 (2002) 136-142.

[21] P. Rainville, G.H. Duncan, D.D. Price, B. Carrier, M.C. Bushnell, Pain affect encoded in human anterior cingulate but not somatosensory cortex, Science 277 (1997) 968-971.

[22] P.W. Mantyh, D.R. Clohisy, M. Koltzenburg, S.P. Hunt, Molecular mechanisms of cancer pain, Nat Rev Cancer 2 (2002) 201-209.

[23] G. Cavaletti, P. Marmiroli, Chemotherapy-induced peripheral neurotoxicity, Nat Rev Neurol 6 (2010) 657-666.

[24] A.J. Windebank, W. Grisold, Chemotherapy-induced neuropathy, J Peripher Nerv Syst 13 (2008) 27-46.

[25] P.M. Dougherty, J.P. Cata, J.V. Cordella, A. Burton, H.R. Weng, Taxol-induced sensory disturbance is characterized by preferential impairment of myelinated fiber function in cancer patients, Pain 109 (2004) 132-142.

[26] E.K. Rowinsky, E.A. Eisenhauer, V. Chaudhry, S.G. Arbuck, R.C. Donehower, Clinical toxicities encountered with paclitaxel (Taxol), Semin Oncol 20 (1993) 1-15.

[27] P.G. Richardson, K.C. Anderson, Bortezomib: a novel therapy approved for multiple myeloma, Clin Adv Hematol Oncol 1 (2003) 596-600.

[28] J.F. San Miguel, R. Schlag, N.K. Khuageva, M.A. Dimopoulos, O. Shpilberg, M. Kropff, I. Spicka, M.T. Petrucci, A. Palumbo, O.S. Samoilova, A. Dmoszynska, K.M. Abdulkadyrov, R. Schots, B. Jiang, M.V. Mateos, K.C. Anderson, D.L. Esseltine, K. Liu, A. Cakana, H. van de Velde, P.G. Richardson, Bortezomib plus melphalan and prednisone for initial treatment of multiple myeloma, N Engl J Med 359 (2008) 906-917.

[29] S. Frankland-Searby, S.R. Bhaumik, The 26S proteasome complex: an attractive target for cancer therapy, Biochim Biophys Acta 1825 (2012) 64-76.

[30] B. Piperdi, Y.H. Ling, L. Liebes, F. Muggia, R. Perez-Soler, Bortezomib: understanding the mechanism of action, Mol Cancer Ther 10 (2011) 2029-2030.

[31] P.G. Richardson, E. Weller, S. Jagannath, D.E. Avigan, M. Alsina, R.L. Schlossman, A. Mazumder, N.C. Munshi, I.M. Ghobrial, D. Doss, D.L. Warren, L.E. Lunde, M. McKenney, C. Delaney, C.S. Mitsiades, T. Hideshima, W. Dalton, R. Knight, D.L. Esseltine, K.C. Anderson, Multicenter, phase I, dose-escalation trial of lenalidomide plus bortezomib for relapsed and relapsed/refractory multiple myeloma, J Clin Oncol 27 (2009) 5713-5719.

[32] M.A. Dimopoulos, E. Kastritis, Bortezomib for AL amyloidosis: moving forward, Blood 118 (2011) 827-828.

[33] P. Richardson, S. Jagannath, K. Colson, Optimizing the efficacy and safety of bortezomib in relapsed multiple myeloma, Clin Adv Hematol Oncol 4 (2006) 1; discussion 8; suppl 13.

[34] U.H. Mellqvist, P. Gimsing, O. Hjertner, S. Lenhoff, E. Laane, K. Remes, H. Steingrimsdottir, N. Abildgaard, L. Ahlberg, C. Blimark, I.M. Dahl, K. Forsberg, T. Gedde-Dahl, H. Gregersen, A. Gruber, N. Guldbrandsen, E. Haukas, K. Carlson, A.K. Kvam, H. Nahi, R. Lindas, N.F. Andersen, I. Turesson, A. Waage, J. Westin, Bortezomib consolidation after autologous stem cell transplantation in multiple myeloma: a Nordic Myeloma Study Group randomized phase 3 trial, Blood 121 (2013) 4647-4654.

[35] A.A. Argyriou, J. Bruna, P. Marmiroli, G. Cavaletti, Chemotherapy-induced peripheral neurotoxicity (CIPN): an update, Crit Rev Oncol Hematol 82 (2012) 51-77.

[36] L. Gibson, D. Lawrence, C. Dawson, J. Bliss, Aromatase inhibitors for treatment of advanced breast cancer in postmenopausal women, Cochrane Database Syst Rev 7 (2009) CD003370.

[37] H.J. Burstein, A.A. Prestrud, J. Seidenfeld, H. Anderson, T.A. Buchholz, N.E. Davidson, K.E. Gelmon, S.H. Giordano, C.A. Hudis, J. Malin, E.P. Mamounas, D. Rowden, A.J. Solky, M.R. Sowers, V. Stearns, E.P. Winer, M.R. Somerfield, J.J. Griggs, American Society of Clinical Oncology clinical practice guideline: update on adjuvant endocrine therapy for women with hormone receptor-positive breast cancer, J Clin Oncol 28 (2010) 3784-3796.

[38] J. Cuzick, I. Sestak, J.F. Forbes, M. Dowsett, J. Knox, S. Cawthorn, C. Saunders, N. Roche, R.E. Mansel, G. von Minckwitz, B. Bonanni, T. Palva, A. Howell, Anastrozole for prevention of breast cancer in high-risk postmenopausal women (IBIS-II): an international, double-blind, randomised placebo-controlled trial, Lancet 383 (2013) 1041-1048.

[39] C. Connor, D. Attai, Adjuvant endocrine therapy for the surgeon: options, side effects, and their management, Ann Surg Oncol 20 (2013) 3188-3193.

[40] H.T. Mouridsen, Incidence and management of side effects associated with aromatase inhibitors in the adjuvant treatment of breast cancer in postmenopausal women, Curr Med Res Opin 22 (2006) 1609-1621.

[41] K.D. Crew, H. Greenlee, J. Capodice, G. Raptis, L. Brafman, D. Fuentes, A. Sierra, D.L. Hershman, Prevalence of joint symptoms in postmenopausal women taking aromatase inhibitors for early-stage breast cancer, J Clin Oncol 25 (2007) 3877-3883.

[42] N.L. Henry, J.T. Giles, V. Stearns, Aromatase inhibitor-associated musculoskeletal symptoms: etiology and strategies for management, Oncology (Williston Park) 22 (2008) 1401-1408.

[43] F. Laroche, J. Coste, T. Medkour, P.H. Cottu, J.Y. Pierga, J.P. Lotz, K. Beerblock, C. Tournigand, X. Decleves, P. de Cremoux, D. Bouhassira, S. Perrot, Classification of and risk factors for estrogen deprivation pain syndromes related to aromatase inhibitor treatments in women with breast cancer: a prospective multicenter cohort study, J Pain 15 (2014) 293-303.

[44] H.J. Burstein, Aromatase inhibitor-associated arthralgia syndrome, Breast 16 (2007) 223-234.

[45] C.A. Presant, L. Bosserman, T. Young, M. Vakil, R. Horns, G. Upadhyaya, B. Ebrahimi, C. Yeon, F. Howard, Aromatase inhibitor-associated arthralgia and/ or bone pain: frequency and characterization in non-clinical trial patients, Clin Breast Cancer 7 (2007) 775-778.

[46] L. Morales, S. Pans, R. Paridaens, R. Westhovens, D. Timmerman, J. Verhaeghe, H. Wildiers, K. Leunen, F. Amant, P. Berteloot, A. Smeets, E. Van Limbergen, C. Weltens, W. Van den Bogaert, L. De Smet, I. Vergote, M.R. Christiaens, P. Neven, Debilitating musculoskeletal pain and stiffness with letrozole and exemestane: associated tenosynovial changes on magnetic resonance imaging, Breast Cancer Res Treat 104 (2007) 87-91.

[47] I. Sestak, J. Cuzick, F. Sapunar, R. Eastell, J.F. Forbes, A.R. Bianco, A.U. Buzdar, Risk factors for joint symptoms in patients enrolled in the ATAC trial: a retrospective, exploratory analysis, Lancet Oncol 9 (2008) 866-872.

[48] V. Shishkin, E. Potapenko, E. Kostyuk, O. Girnyk, N. Voitenko, P. Kostyuk, Role of mitochondria in intracellular calcium signaling in primary and secondary sensory neurones of rats, Cell Calcium 32 (2002) 121-130.

[49] J.M. Chung, The role of reactive oxygen species (ROS) in persistent pain, Mol Interv 4 (2004) 248-250.

[50] E.K. Joseph, J.D. Levine, Caspase signalling in neuropathic and inflammatory pain in the rat, Eur J Neurosci 20 (2004) 2896-2902.

[51] S.J. Flatters, G.J. Bennett, Studies of peripheral sensory nerves in paclitaxel-induced painful peripheral neuropathy: evidence for mitochondrial dysfunction, Pain 122 (2006) 245-257.

[52] C. Siau, G.J. Bennett, Dysregulation of cellular calcium homeostasis in chemotherapy-evoked painful peripheral neuropathy, Anesth Analg 102 (2006) 1485-1490.

[53] J.G. Pastorino, J.W. Snyder, A. Serroni, J.B. Hoek, J.L. Farber, Cyclosporin and carnitine prevent the anoxic death of cultured hepatocytes by inhibiting the mitochondrial permeability transition, J Biol Chem 268 (1993) 13791-13798.

[54] H.W. Jin, S.J. Flatters, W.H. Xiao, H.L. Mulhern, G.J. Bennett, Prevention of paclitaxel-evoked painful peripheral neuropathy by acetyl-L-carnitine: effects on axonal mitochondria, sensory nerve fiber terminal arbors, and cutaneous Langerhans cells, Exp Neurol 210 (2008) 229-237.

[55] G. Cavaletti, A. Gilardini, A. Canta, L. Rigamonti, V. Rodriguez-Menendez, C. Ceresa, P. Marmiroli, M. Bossi, N. Oggioni, M. D'Incalci, R. De Coster, Bortezomib-induced peripheral neurotoxicity: a neurophysiological and pathological study in the rat, Exp Neurol 204 (2007) 317-325.

[56] A. Broyl, S.L. Corthals, J.L. Jongen, B. van der Holt, R. Kuiper, Y. de Knegt, M. van Duin, L. el Jarari, U. Bertsch, H.M. Lokhorst, B.G. Durie, H. Goldschmidt, P. Sonneveld, Mechanisms of peripheral neuropathy associated with bortezomib and vincristine in patients with newly diagnosed multiple myeloma: a prospective analysis of data from the HOVON-65/GMMG-HD4 trial, Lancet Oncol 11 (2010) 1057-1065.

[57] T.H. Landowski, C.J. Megli, K.D. Nullmeyer, R.M. Lynch, R.T. Dorr, Mitochondrial-mediated disregulation of Ca2+ is a critical determinant of Velcade (PS-341/bortezomib) cytotoxicity in myeloma cell lines, Cancer Res 65 (2005) 3828-3836.

[58] G. Melli, M. Taiana, F. Camozzi, D. Triolo, P. Podini, A. Quattrini, F. Taroni, G. Lauria, Alpha-lipoic acid prevents mitochondrial damage and neurotoxicity in experimental chemotherapy neuropathy, Exp Neurol 214 (2008) 276-284.

[59] J.F. Kidd, M.F. Pilkington, M.J. Schell, K.E. Fogarty, J.N. Skepper, C.W. Taylor, P. Thorn, Paclitaxel affects cytosolic calcium signals by opening the mitochondrial permeability transition pore, J Biol Chem 277 (2002) 6504-6510.

[60] W. Xiao, A. Boroujerdi, G.J. Bennett, Z.D. Luo, Chemotherapy-evoked painful peripheral neuropathy: analgesic effects of gabapentin and effects on expression of the alpha-2-delta type-1 calcium channel subunit, Neuroscience 144 (2007) 714-720.

[61] S.J. Flatters, G.J. Bennett, Ethosuximide reverses paclitaxel- and vincristine-induced painful peripheral neuropathy, Pain 109 (2004) 150-161.

[62] P. Gauchan, T. Andoh, K. Ikeda, M. Fujita, A. Sasaki, A. Kato, Y. Kuraishi, Mechanical allodynia induced by paclitaxel, oxaliplatin and vincristine: different effectiveness of gabapentin and different expression of voltage-dependent calcium channel alpha(2)delta-1 subunit, Biol Pharm Bull 32 (2009) 732-734.

[63] M. Matsumoto, M. Inoue, A. Hald, W. Xie, H. Ueda, Inhibition of paclitaxel-induced A-fiber hypersensitization by gabapentin, J Pharmacol Exp Ther 318 (2006) 735-740.

[64] H. Adelsberger, S. Quasthoff, J. Grosskreutz, A. Lepier, F. Eckel, C. Lersch, The chemotherapeutic oxaliplatin alters voltage-gated Na(+) channel kinetics on rat sensory neurons, Eur J Pharmacol 406 (2000) 25-32.

[65] F. Grolleau, L. Gamelin, M. Boisdron-Celle, B. Lapied, M. Pelhate, E. Gamelin, A possible explanation for a neurotoxic effect of the anticancer agent oxaliplatin on neuronal voltage-gated sodium channels, J Neurophysiol 85 (2001) 2293-2297.

[66] S.L. Wolf, New data question treatment for oxaliplatin neurotoxicity, Clin J Oncol Nurs 12 (2008) 14; author reply 14.

[67] R.G. Webster, K.L. Brain, R.H. Wilson, J.L. Grem, A. Vincent, Oxaliplatin induces hyperexcitability at motor and autonomic neuromuscular junctions through effects on voltage-gated sodium channels, Br J Pharmacol 146 (2005) 1027-1039.

[68] S.B. Rutkove, M.A. Geffroy, S.H. Lichtenstein, Heat-sensitive conduction block in ulnar neuropathy at the elbow, Clin Neurophysiol 112 (2001) 280-285.

[69] M. Bouhours, D. Sternberg, C.S. Davoine, X. Ferrer, J.C. Willer, B. Fontaine, N. Tabti, Functional characterization and cold sensitivity of T1313A, a new mutation of the skeletal muscle sodium channel causing paramyotonia congenita in humans, J Physiol 554 (2004) 635-647.

[70] A.V. Krishnan, D. Goldstein, M. Friedlander, M.C. Kiernan, Oxaliplatin and axonal Na+ channel function in vivo, Clin Cancer Res 12 (2006) 4481-4484.

[71] S.B. Park, C.S. Lin, A.V. Krishnan, D. Goldstein, M.L. Friedlander, M.C. Kiernan, Oxaliplatin-induced lhermitte's phenomenon as a manifestation of severe generalized neurotoxicity, Oncology 77 (2009) 342-348.

[72] F.R. Nieto, J.M. Entrena, C.M. Cendan, E.D. Pozo, J.M. Vela, J.M. Baeyens, Tetrodotoxin inhibits the development and expression of neuropathic pain induced by paclitaxel in mice, Pain 137 (2008) 520-531.

[73] S.K. Joshi, J.P. Mikusa, G. Hernandez, S. Baker, C.C. Shieh, T. Neelands, X.F. Zhang, W. Niforatos, K. Kage, P. Han, D. Krafte, C. Faltynek, J.P. Sullivan, M.F. Jarvis, P. Honore, Involvement of the TTX-resistant sodium channel Nav 1.8 in inflammatory and neuropathic, but not post-operative, pain states, Pain 123 (2006) 75-82.

[74] G. Kaur, A.S. Jaggi, N. Singh, Exploring the potential effect of Ocimum sanctum in vincristine-induced neuropathic pain in rats, J Brachial Plex Peripher Nerve Inj 5 (2010) 3.

[75] A. Muthuraman, N. Singh, Attenuating effect of hydroalcoholic extract of Acorus calamus in vincristine-induced painful neuropathy in rats, J Nat Med 65 (2011) 480-487.

[76] S. Mangiacavalli, A. Corso, M. De Amici, M. Varettoni, E. Alfonsi, A. Lozza, M. Lazzarino, Emergent T-helper 2 profile with high interleukin-6 levels correlates with the appearance of bortezomib-induced neuropathic pain, Br J Haematol 149 (2011) 916-918.

[77] A.A. Qureshi, J. Hosoi, S. Xu, A. Takashima, R.D. Granstein, E.A. Lerner, Langerhans cells express inducible nitric oxide synthase and produce nitric oxide, J Invest Dermatol 107 (1996) 815-821.

[78] H. Torii, Z. Yan, J. Hosoi, R.D. Granstein, Expression of neurotrophic factors and neuropeptide receptors by Langerhans cells and the Langerhans cell-like cell line XS52: further support for a functional relationship between Langerhans cells and epidermal nerves, J Invest Dermatol 109 (1997) 586-591.

[79] A. Ledeboer, B.M. Jekich, E.M. Sloane, J.H. Mahoney, S.J. Langer, E.D. Milligan, D. Martin, S.F. Maier, K.W. Johnson, L.A. Leinwand, R.A. Chavez, L.R. Watkins, Intrathecal interleukin-10 gene therapy attenuates paclitaxel-induced mechanical allodynia and proinflammatory cytokine expression in dorsal root ganglia in rats, Brain Behav Immun 21 (2007) 686-698.

[80] J.P. Cata, H.R. Weng, J.H. Chen, P.M. Dougherty, Altered discharges of spinal wide dynamic range neurons and down-regulation of glutamate transporter expression in rats with paclitaxel-induced hyperalgesia, Neuroscience 138 (2006) 329-338.

[81] S.M. Sweitzer, J.L. Pahl, J.A. DeLeo, Propentofylline attenuates vincristine-induced peripheral neuropathy in the rat, Neurosci Lett 400 (2006) 258-261.

[82] J. Boyette-Davis, P.M. Dougherty, Protection against oxaliplatin-induced mechanical hyperalgesia and intraepidermal nerve fiber loss by minocycline, Exp Neurol 229 (2011) 353-357.

[83] B.G. McCarthy, S.T. Hsieh, A. Stocks, P. Hauer, C. Macko, D.R. Cornblath, J.W. Griffin, J.C. McArthur, Cutaneous innervation in sensory neuropathies: evaluation by skin biopsy, Neurology 45 (1995) 1848-1855.

[84] J.L. Ochoa, D. Yarnitsky, The triple cold syndrome. Cold hyperalgesia, cold hypoaesthesia and cold skin in peripheral nerve disease, Brain 117 (Pt 1) (1994) 185-197.

[85] C. Gedlicka, W. Scheithauer, B. Schull, G.V. Kornek, Effective treatment of oxaliplatin-induced cumulative polyneuropathy with alpha-lipoic acid, J Clin Oncol 20 (2002) 3359-3361.

[86] E.K. Joseph, J.D. Levine, Comparison of oxaliplatin- and cisplatin-induced painful peripheral neuropathy in the rat, J Pain 10 (2009) 534-541.

[87] H.T. Wang, Z.G. Liu, W. Yang, A.J. Liao, R. Zhang, B. Wu, H.H. Wang, K. Yao, Y.C. Li, [Study on mechanism of bortezomib inducing peripheral neuropathy and the reversing effect of reduced glutathione], Zhonghua Xue Ye Xue Za Zhi 32 (2011) 107-111.

[88] A. Nakano, M. Abe, A. Oda, H. Amou, M. Hiasa, S. Nakamura, H. Miki, T. Harada, S. Fujii, K. Kagawa, K. Takeuchi, T. Watanabe, S. Ozaki, T. Matsumoto, Delayed treatment with vitamin C and N-acetyl-L-cysteine protects Schwann cells without compromising the anti-myeloma activity of bortezomib, Int J Hematol 93 (2011) 727-735.

[89] A.S. Jaggi, N. Singh, Mechanisms in cancer-chemotherapeutic drugs-induced peripheral neuropathy, Toxicology 291 (2011) 1-9.

[90] B. Minke, Drosophila mutant with a transducer defect, Biophys Struct Mech 3 (1977) 59-64.

[91] C. Montell, G.M. Rubin, Molecular characterization of the Drosophila trp locus: a putative integral membrane protein required for phototransduction, Neuron 2 (1989) 1313-1323.
[92] J. Vriens, H. Watanabe, A. Janssens, G. Droogmans, T. Voets, B. Nilius, Cell swelling, heat, and chemical agonists use distinct pathways for the activation of the cation channel TRPV4, Proc Natl Acad Sci U S A 101 (2004) 396-401.
[93] B. Nilius, Transient receptor potential (TRP) cation channels: rewarding unique proteins, Bull Mem Acad R Med Belg 162 (2007) 244-253.
[94] V. Denis, M.S. Cyert, Internal Ca(2+) release in yeast is triggered by hypertonic shock and mediated by a TRP channel homologue, J Cell Biol 156 (2002) 29-34.
[95] M. de Bono, D.M. Tobin, M.W. Davis, L. Avery, C.I. Bargmann, Social feeding in Caenorhabditis elegans is induced by neurons that detect aversive stimuli, Nature 419 (2002) 899-903.
[96] K. Kiselyov, D.B. van Rossum, R.L. Patterson, TRPC channels in pheromone sensing, Vitam Horm 83 (2010) 197-213.
[97] Y. Zhang, M.A. Hoon, J. Chandrashekar, K.L. Mueller, B. Cook, D. Wu, C.S. Zuker, N.J. Ryba, Coding of sweet, bitter, and umami tastes: different receptor cells sharing similar signaling pathways, Cell 112 (2003) 293-301.
[98] D.E. Clapham, TRP channels as cellular sensors, Nature 426 (2003) 517-524.
[99] C. Montell, L. Birnbaumer, V. Flockerzi, R.J. Bindels, E.A. Bruford, M.J. Caterina, D.E. Clapham, C. Harteneck, S. Heller, D. Julius, I. Kojima, Y. Mori, R. Penner, D. Prawitt, A.M. Scharenberg, G. Schultz, N. Shimizu, M.X. Zhu, A unified nomenclature for the superfamily of TRP cation channels, Mol Cell 9 (2002) 229-231.
[100] D.E. Clapham, L.W. Runnels, C. Strubing, The TRP ion channel family, Nat Rev Neurosci 2 (2001) 387-396.
[101] S.G. Sedgwick, S.J. Smerdon, The ankyrin repeat: a diversity of interactions on a common structural framework, Trends Biochem Sci 24 (1999) 311-316.
[102] D.E. Clapham, C. Montell, G. Schultz, D. Julius, International Union of Pharmacology. XLIII. Compendium of voltage-gated ion channels: transient receptor potential channels, Pharmacol Rev 55 (2005) 591-596.
[103] R. Maroto, A. Raso, T.G. Wood, A. Kurosky, B. Martinac, O.P. Hamill, TRPC1 forms the stretch-activated cation channel in vertebrate cells, Nat Cell Biol 7 (2005) 179-185.
[104] J. Vriens, G. Owsianik, B. Fisslthaler, M. Suzuki, A. Janssens, T. Voets, C. Morisseau, B.D. Hammock, I. Fleming, R. Busse, B. Nilius, Modulation of the Ca2 permeable cation channel TRPV4 by cytochrome P450 epoxygenases in vascular endothelium, Circ Res 97 (2005) 908-915.
[105] R. Vennekens, J.G. Hoenderop, J. Prenen, M. Stuiver, P.H. Willems, G. Droogmans, B. Nilius, R.J. Bindels, Permeation and gating properties of the novel epithelial Ca(2+) channel, J Biol Chem 275 (2000) 3963-3969.
[106] E. den Dekker, J.G. Hoenderop, B. Nilius, R.J. Bindels, The epithelial calcium channels, TRPV5 & TRPV6: from identification towards regulation, Cell Calcium 33 (2003) 497-507.
[107] M.J. Caterina, M.A. Schumacher, M. Tominaga, T.A. Rosen, J.D. Levine, D. Julius, The capsaicin receptor: a heat-activated ion channel in the pain pathway, Nature 389 (1997) 816-824.
[108] M. Tominaga, M.J. Caterina, A.B. Malmberg, T.A. Rosen, H. Gilbert, K. Skinner, B.E. Raumann, A.I. Basbaum, D. Julius, The cloned capsaicin receptor integrates multiple pain-producing stimuli, Neuron 21 (1998) 531-543.
[109] H. Xu, N.T. Blair, D.E. Clapham, Camphor activates and strongly desensitizes the transient receptor potential vanilloid subtype 1 channel in a vanilloid-independent mechanism, J Neurosci 25 (2005) 8924-8937.
[110] L.J. Macpherson, B.H. Geierstanger, V. Viswanath, M. Bandell, S.R. Eid, S. Hwang, A. Patapoutian, The pungency of garlic: activation of TRPA1 and TRPV1 in response to allicin, Curr Biol 15 (2005) 929-934.
[111] L.J. Macpherson, B. Xiao, K.Y. Kwan, M.J. Petrus, A.E. Dubin, S. Hwang, B. Cravatt, D.P. Corey, A. Patapoutian, An ion channel essential for sensing chemical damage, J Neurosci 27 (2007) 11412-11415.
[112] T. Yoshida, R. Inoue, T. Morii, N. Takahashi, S. Yamamoto, Y. Hara, M. Tominaga, S. Shimizu, Y. Sato, Y. Mori, Nitric oxide activates TRP channels by cysteine S-nitrosylation, Nat Chem Biol 2 (2006) 596-607.
[113] J. Siemens, S. Zhou, R. Piskorowski, T. Nikai, E.A. Lumpkin, A.I. Basbaum, D. King, D. Julius, Spider toxins activate the capsaicin receptor to produce inflammatory pain, Nature 444 (2006) 208-212.
[114] M. Trevisani, D. Smart, M.J. Gunthorpe, M. Tognetto, M. Barbieri, B. Campi, S. Amadesi, J. Gray, J.C. Jerman, S.J. Brough, D. Owen, G.D. Smith, A.D. Randall, S. Harrison, A. Bianchi,

J.B. Davis, P. Geppetti, Ethanol elicits and potentiates nociceptor responses via the vanilloid receptor-1, Nat Neurosci 5 (2002) 546-551.
[115] G.P. Ahern, I.M. Brooks, R.L. Miyares, X.B. Wang, Extracellular cations sensitize and gate capsaicin receptor TRPV1 modulating pain signaling, J Neurosci 25 (2005) 5109-5116.
[116] S. Doly, J. Fischer, C. Salio, M. Conrath, The vanilloid receptor-1 is expressed in rat spinal dorsal horn astrocytes, Neurosci Lett 357 (2004) 123-126.
[117] M. Tominaga, T. Tominaga, Structure and function of TRPV1, Pflugers Arch 451 (2005) 143-150.
[118] R.R. Ji, T.A. Samad, S.X. Jin, R. Schmoll, C.J. Woolf, p38 MAPK activation by NGF in primary sensory neurons after inflammation increases TRPV1 levels and maintains heat hyperalgesia, Neuron 36 (2002) 57-68.
[119] X. Zhang, J. Huang, P.A. McNaughton, NGF rapidly increases membrane expression of TRPV1 heat-gated ion channels, Embo J 24 (2005) 4211-4223.
[120] D.P. Mohapatra, C. Nau, Desensitization of capsaicin-activated currents in the vanilloid receptor TRPV1 is decreased by the cyclic AMP-dependent protein kinase pathway, J Biol Chem 278 (2003) 50080-50090.
[121] H.H. Chuang, E.D. Prescott, H. Kong, S. Shields, S.E. Jordt, A.I. Basbaum, M.V. Chao, D. Julius, Bradykinin and nerve growth factor release the capsaicin receptor from PtdIns(4,5)P2-mediated inhibition, Nature 411 (2001) 957-962.
[122] S.W. Hwang, H. Cho, J. Kwak, S.Y. Lee, C.J. Kang, J. Jung, S. Cho, K.H. Min, Y.G. Suh, D. Kim, U. Oh, Direct activation of capsaicin receptors by products of lipoxygenases: endogenous capsaicin-like substances, Proc Natl Acad Sci U S A 97 (2000) 6155-6160.
[123] S. Amadesi, J. Nie, N. Vergnolle, G.S. Cottrell, E.F. Grady, M. Trevisani, C. Manni, P. Geppetti, J.A. McRoberts, H. Ennes, J.B. Davis, E.A. Mayer, N.W. Bunnett, Protease-activated receptor 2 sensitizes the capsaicin receptor transient receptor potential vanilloid receptor 1 to induce hyperalgesia, J Neurosci 24 (2004) 4300-4312.
[124] S. Amadesi, G.S. Cottrell, L. Divino, K. Chapman, E.F. Grady, F. Bautista, R. Karanjia, C. Barajas-Lopez, S. Vanner, N. Vergnolle, N.W. Bunnett, Protease-activated receptor 2 sensitizes TRPV1 by protein kinase Cepsilon- and A-dependent mechanisms in rats and mice, J Physiol 575 (2006) 555-571.
[125] W. Liedtke, Y. Choe, M.A. Marti-Renom, A.M. Bell, C.S. Denis, A. Sali, A.J. Hudspeth, J.M. Friedman, S. Heller, Vanilloid receptor-related osmotically activated channel (VR-OAC), a candidate vertebrate osmoreceptor, Cell 103 (2000) 525-535.
[126] N.S. Delany, M. Hurle, P. Facer, T. Alnadaf, C. Plumpton, I. Kinghorn, C.G. See, M. Costigan, P. Anand, C.J. Woolf, D. Crowther, P. Sanseau, S.N. Tate, Identification and characterization of a novel human vanilloid receptor-like protein, VRL-2, Physiol Genomics 4 (2001) 165-174.
[127] U. Wissenbach, M. Bodding, M. Freichel, V. Flockerzi, Trp12, a novel Trp related protein from kidney, FEBS Lett 485 (2000) 127-134.
[128] M. Suzuki, A. Mizuno, K. Kodaira, M. Imai, Impaired pressure sensation in mice lacking TRPV4, J Biol Chem 278 (2003) 22664-22668.
[129] A.D. Guler, H. Lee, T. Iida, I. Shimizu, M. Tominaga, M. Caterina, Heat-evoked activation of the ion channel, TRPV4, J Neurosci 22 (2002) 6408-6414.
[130] A. Grant, S. Amadesi, N.W. Bunnett, Protease-Activated Receptors: Mechanisms by Which Proteases Sensitize TRPV Channels to Induce Neurogenic Inflammation and Pain, (2007).
[131] R. Strotmann, C. Harteneck, K. Nunnenmacher, G. Schultz, T.D. Plant, OTRPC4, a nonselective cation channel that confers sensitivity to extracellular osmolarity, Nat Cell Biol 2 (2000) 695-702.
[132] X. Gao, L. Wu, R.G. O'Neil, Temperature-modulated diversity of TRPV4 channel gating: activation by physical stresses and phorbol ester derivatives through protein kinase C-dependent and -independent pathways, J Biol Chem 278 (2003) 27129-27137.
[133] H. Watanabe, J. Vriens, S.H. Suh, C.D. Benham, G. Droogmans, B. Nilius, Heat-evoked activation of TRPV4 channels in a HEK293 cell expression system and in native mouse aorta endothelial cells, J Biol Chem 277 (2002) 47044-47051.
[134] H. Watanabe, J. Vriens, J. Prenen, G. Droogmans, T. Voets, B. Nilius, Anandamide and arachidonic acid use epoxyeicosatrienoic acids to activate TRPV4 channels, Nature 424 (2003) 434-438.
[135] R.G. O'Neil, L. Leng, Osmo-mechanically sensitive phosphatidylinositol signaling regulates a Ca2+ influx channel in renal epithelial cells, Am J Physiol 273 (1997) F120-128.
[136] S. Pedersen, I.H. Lambert, S.M. Thoroed, E.K. Hoffmann, Hypotonic cell swelling induces translocation of the alpha isoform of cytosolic phospholipase A2 but not the gamma isoform in Ehrlich ascites tumor cells, Eur J Biochem 267 (2000) 5531-5539.

[137] H. Xu, H. Zhao, W. Tian, K. Yoshida, J.B. Roullet, D.M. Cohen, Regulation of a transient receptor potential (TRP) channel by tyrosine phosphorylation. SRC family kinase-dependent tyrosine phosphorylation of TRPV4 on TYR-253 mediates its response to hypotonic stress, J Biol Chem 278 (2003) 11520-11527.

[138] N. Alessandri-Haber, O.A. Dina, E.K. Joseph, D. Reichling, J.D. Levine, A transient receptor potential vanilloid 4-dependent mechanism of hyperalgesia is engaged by concerted action of inflammatory mediators, J Neurosci 26 (2006) 3864-3874.

[139] Y. Chen, C. Yang, Z.J. Wang, Proteinase-activated receptor 2 sensitizes transient receptor potential vanilloid 1, transient receptor potential vanilloid 4, and transient receptor potential ankyrin 1 in paclitaxel-induced neuropathic pain, Neuroscience 193 (2011) 440-451.

[140] A.A. Soyombo, S. Tjon-Kon-Sang, Y. Rbaibi, E. Bashllari, J. Bisceglia, S. Muallem, K. Kiselyov, TRP-ML1 regulates lysosomal pH and acidic lysosomal lipid hydrolytic activity, J Biol Chem 281 (2006) 7294-7301.

[141] K. Hanaoka, F. Qian, A. Boletta, A.K. Bhunia, K. Piontek, L. Tsiokas, V.P. Sukhatme, W.B. Guggino, G.G. Germino, Co-assembly of polycystin-1 and -2 produces unique cation-permeable currents, Nature 408 (2000) 990-994.

[142] K. Nagata, A. Duggan, G. Kumar, J. Garcia-Anoveros, Nociceptor and hair cell transducer properties of TRPA1, a channel for pain and hearing, J Neurosci 25 (2005) 4052-4061.

[143] G.M. Story, A.M. Peier, A.J. Reeve, S.R. Eid, J. Mosbacher, T.R. Hricik, T.J. Earley, A.C. Hergarden, D.A. Andersson, S.W. Hwang, P. McIntyre, T. Jegla, S. Bevan, A. Patapoutian, ANKTM1, a TRP-like channel expressed in nociceptive neurons, is activated by cold temperatures, Cell 112 (2003) 819-829.

[144] D. Jaquemar, T. Schenker, B. Trueb, An ankyrin-like protein with transmembrane domains is specifically lost after oncogenic transformation of human fibroblasts, J Biol Chem 274 (1999) 7325-7333.

[145] S.E. Jordt, D.M. Bautista, H.H. Chuang, D.D. McKemy, P.M. Zygmunt, E.D. Hogestatt, I.D. Meng, D. Julius, Mustard oils and cannabinoids excite sensory nerve fibres through the TRP channel ANKTM1, Nature 427 (2004) 260-265.

[146] B. Nilius, G. Owsianik, The transient receptor potential family of ion channels, Genome Biol 12 (2011) 218.

[147] B. Nilius, G. Appendino, G. Owsianik, The transient receptor potential channel TRPA1: from gene to pathophysiology, Pflugers Arch 464 (2012) 425-458.

[148] J. Chen, D. Kim, B.R. Bianchi, E.J. Cavanaugh, C.R. Faltynek, P.R. Kym, R.M. Reilly, Pore dilation occurs in TRPA1 but not in TRPM8 channels, Mol Pain 5 (2009) 3.

[149] T.G. Banke, S.R. Chaplan, A.D. Wickenden, Dynamic changes in the TRPA1 selectivity filter lead to progressive but reversible pore dilation, Am J Physiol Cell Physiol 298 (2010) C1457-1468.

[150] T. Voets, G. Droogmans, U. Wissenbach, A. Janssens, V. Flockerzi, B. Nilius, The principle of temperature-dependent gating in cold- and heat-sensitive TRP channels, Nature 430 (2004) 748-754.

[151] Y. Karashima, J. Prenen, V. Meseguer, G. Owsianik, T. Voets, B. Nilius, Modulation of the transient receptor potential channel TRPA1 by phosphatidylinositol 4,5-biphosphate manipulators, Pflugers Arch 457 (2008) 77-89.

[152] R. Gaudet, A primer on ankyrin repeat function in TRP channels and beyond, Mol Biosyst 4 (2008) 372-379.

[153] L. Wang, T.L. Cvetkov, M.R. Chance, V.Y. Moiseenkova-Bell, Identification of in vivo disulfide conformation of TRPA1 ion channel, J Biol Chem 287 (2012) 6169-6176.

[154] D.A. Andersson, C. Gentry, S. Moss, S. Bevan, Clioquinol and pyrithione activate TRPA1 by increasing intracellular Zn2+, Proc Natl Acad Sci U S A 106 (2009) 8374-8379.

[155] H. Hu, M. Bandell, M.J. Petrus, M.X. Zhu, A. Patapoutian, Zinc activates damage-sensing TRPA1 ion channels, Nat Chem Biol 5 (2009) 183-190.

[156] Y.Y. Wang, R.B. Chang, H.N. Waters, D.D. McKemy, E.R. Liman, The nociceptor ion channel TRPA1 is potentiated and inactivated by permeating calcium ions, J Biol Chem 283 (2008) 32691-32703.

[157] L. Sura, V. Zima, L. Marsakova, A. Hynkova, I. Barvik, V. Vlachova, C-terminal acidic cluster is involved in Ca2+-induced regulation of human transient receptor potential ankyrin 1 channel, J Biol Chem 287 (2012) 18067-18077.

[158] J.F. Doerner, G. Gisselmann, H. Hatt, C.H. Wetzel, Transient receptor potential channel A1 is directly gated by calcium ions, J Biol Chem 282 (2007) 13180-13189.

[159] S. Zurborg, B. Yurgionas, J.A. Jira, O. Caspani, P.A. Heppenstall, Direct activation of the ion channel TRPA1 by Ca2+, Nat Neurosci. 10 (2007) 277-279. Epub 2007 Jan 2028. Write to the

Help Desk NCBI | NLM | NIH Department of Health & Human Services Privacy Statement | Freedom of Information Act | Disclaimer Apr 2030 2007 2004:2056:2027.

[160] T.L. Cvetkov, K.W. Huynh, M.R. Cohen, V.Y. Moiseenkova-Bell, Molecular architecture and subunit organization of TRPA1 ion channel revealed by electron microscopy, J Biol Chem 286 (2011) 38168-38176.

[161] J. Hjerling-Leffler, M. Alqatari, P. Ernfors, M. Koltzenburg, Emergence of functional sensory subtypes as defined by transient receptor potential channel expression, J Neurosci 27 (2007) 2435-2443.

[162] J.H. La, E.S. Schwartz, G.F. Gebhart, Differences in the expression of transient receptor potential channel V1, transient receptor potential channel A1 and mechanosensitive two pore-domain K+ channels between the lumbar splanchnic and pelvic nerve innervations of mouse urinary bladder and colon, Neuroscience 186 (2011) 179-187.

[163] M.R. Bhattacharya, D.M. Bautista, K. Wu, H. Haeberle, E.A. Lumpkin, D. Julius, Radial stretch reveals distinct populations of mechanosensitive mammalian somatosensory neurons, Proc Natl Acad Sci U S A 105 (2008) 20015-20020.

[164] S. Hayashi, E. Nakamura, T. Endo, Y. Kubo, K. Takeuchi, Impairment by activation of TRPA1 of gastric epithelial restitution in a wound model using RGM1 cell monolayer, Inflammopharmacology 15 (2007) 218-222.

[165] S. Du, I. Araki, H. Kobayashi, H. Zakoji, N. Sawada, M. Takeda, Differential expression profile of cold (TRPA1) and cool (TRPM8) receptors in human urogenital organs, Urology 72 (2008) 450-455.

[166] C. Gratzke, P. Weinhold, O. Reich, M. Seitz, B. Schlenker, C.G. Stief, K.E. Andersson, P. Hedlund, Transient Receptor Potential A1 and Cannabinoid Receptor Activity in Human Normal and Hyperplastic Prostate: Relation to Nerves and Interstitial Cells, Eur Urol 28 (2009) 28.

[167] K. Nozawa, E. Kawabata-Shoda, H. Doihara, R. Kojima, H. Okada, S. Mochizuki, Y. Sano, K. Inamura, H. Matsushime, T. Koizumi, T. Yokoyama, H. Ito, TRPA1 regulates gastrointestinal motility through serotonin release from enterochromaffin cells, Proc Natl Acad Sci U S A 106 (2009) 3408-3413.

[168] S. Earley, A.L. Gonzales, R. Crnich, Endothelium-dependent cerebral artery dilation mediated by TRPA1 and Ca2+-Activated K+ channels, Circ Res 104 (2009) 987-994.

[169] N.W. Bellono, L.G. Kammel, A.L. Zimmerman, E. Oancea, UV light phototransduction activates transient receptor potential A1 ion channels in human melanocytes, Proc Natl Acad Sci U S A 110 (2013) 2383-2388.

[170] S. Yu, G. Gao, B.Z. Peterson, A. Ouyang, TRPA1 in mast cell activation-induced long-lasting mechanical hypersensitivity of vagal afferent C-fibers in guinea pig esophagus, Am J Physiol Gastrointest Liver Physiol 297 (2009) G34-42.

[171] V. Hox, J.A. Vanoirbeek, Y.A. Alpizar, S. Voedisch, I. Callebaut, S. Bobic, A. Sharify, V. De Vooght, L. Van Gerven, F. Devos, A. Liston, T. Voets, R. Vennekens, D.M. Bullens, A. De Vries, P. Hoet, A. Braun, J.L. Ceuppens, K. Talavera, B. Nemery, P.W. Hellings, Crucial role of transient receptor potential ankyrin 1 and mast cells in induction of nonallergic airway hyperreactivity in mice, Am J Respir Crit Care Med 187 (2013) 486-493.

[172] A.R. Son, Y.M. Yang, J.H. Hong, S.I. Lee, Y. Shibukawa, D.M. Shin, Odontoblast TRP channels and thermo/mechanical transmission, J Dent Res 88 (2009) 1014-1019.

[173] M.J. Caterina, Transient receptor potential ion channels as participants in thermosensation and thermoregulation, Am J Physiol Regul Integr Comp Physiol 292 (2007) R64-76.

[174] M. Bandell, G.M. Story, S.W. Hwang, V. Viswanath, S.R. Eid, M.J. Petrus, T.J. Earley, A. Patapoutian, Noxious cold ion channel TRPA1 is activated by pungent compounds and bradykinin, Neuron 41 (2004) 849-857.

[175] Y. Sawada, H. Hosokawa, K. Matsumura, S. Kobayashi, Activation of transient receptor potential ankyrin 1 by hydrogen peroxide, Eur J Neurosci 27 (2008) 1131-1142.

[176] D.M. Bautista, J. Siemens, J.M. Glazer, P.R. Tsuruda, A.I. Basbaum, C.L. Stucky, S.E. Jordt, D. Julius, The menthol receptor TRPM8 is the principal detector of environmental cold, Nature 448 (2007) 204-208.

[177] Y. Karashima, K. Talavera, W. Everaerts, A. Janssens, K.Y. Kwan, R. Vennekens, B. Nilius, T. Voets, TRPA1 acts as a cold sensor in vitro and in vivo, Proc Natl Acad Sci U S A 106 (2009) 1273-1278.

[178] B. Abrahamsen, J. Zhao, C.O. Asante, C.M. Cendan, S. Marsh, J.P. Martinez-Barbera, M.A. Nassar, A.H. Dickenson, J.N. Wood, The cell and molecular basis of mechanical, cold, and inflammatory pain, Science 321 (2008) 702-705.

[179] K.Y. Kwan, A.J. Allchorne, M.A. Vollrath, A.P. Christensen, D.S. Zhang, C.J. Woolf, D.P. Corey, TRPA1 contributes to cold, mechanical, and chemical nociception but is not essential for hair-cell transduction, Neuron 50 (2006) 277-289.

[180] D.M. Bautista, S.E. Jordt, T. Nikai, P.R. Tsuruda, A.J. Read, J. Poblete, E.N. Yamoah, A.I. Basbaum, D. Julius, TRPA1 mediates the inflammatory actions of environmental irritants and proalgesic agents, Cell 124 (2006) 1269-1282.

[181] M. Petrus, A.M. Peier, M. Bandell, S.W. Hwang, T. Huynh, N. Olney, T. Jegla, A. Patapoutian, A role of TRPA1 in mechanical hyperalgesia is revealed by pharmacological inhibition, Mol Pain 3 (2007) 40.

[182] X.F. Zhang, J. Chen, C.R. Faltynek, R.B. Moreland, T.R. Neelands, Transient receptor potential A1 mediates an osmotically activated ion channel, Eur J Neurosci 27 (2008) 605-611.

[183] S. Bang, S.W. Hwang, Polymodal ligand sensitivity of TRPA1 and its modes of interactions, J Gen Physiol 133 (2009) 257-262.

[184] A. Hinman, H.H. Chuang, D.M. Bautista, D. Julius, TRP channel activation by reversible covalent modification, Proc Natl Acad Sci U S A 103 (2006) 19564-19568.

[185] L.J. Macpherson, A.E. Dubin, M.J. Evans, F. Marr, P.G. Schultz, B.F. Cravatt, A. Patapoutian, Noxious compounds activate TRPA1 ion channels through covalent modification of cysteines, Nature 445 (2007) 541-545.

[186] M. Trevisani, J. Siemens, S. Materazzi, D.M. Bautista, R. Nassini, B. Campi, N. Imamachi, E. Andre, R. Patacchini, G.S. Cottrell, R. Gatti, A.I. Basbaum, N.W. Bunnett, D. Julius, P. Geppetti, 4-Hydroxynonenal, an endogenous aldehyde, causes pain and neurogenic inflammation through activation of the irritant receptor TRPA1, Proc Natl Acad Sci U S A 104 (2007) 13519-13524.

[187] A. Benedetti, M. Comporti, H. Esterbauer, Identification of 4-hydroxynonenal as a cytotoxic product originating from the peroxidation of liver microsomal lipids, Biochim Biophys Acta 620 (1980) 281-296.

[188] H. Esterbauer, R.J. Schaur, H. Zollner, Chemistry and biochemistry of 4-hydroxynonenal, malonaldehyde and related aldehydes, Free Radic Biol Med 11 (1991) 81-128.

[189] T.E. Taylor-Clark, M.A. McAlexander, C. Nassenstein, S.A. Sheardown, S. Wilson, J. Thornton, M.J. Carr, B.J. Undem, Relative contributions of TRPA1 and TRPV1 channels in the activation of vagal bronchopulmonary C-fibres by the endogenous autacoid 4-oxononenal, J Physiol 586 (2008) 3447-3459.

[190] D.A. Andersson, C. Gentry, S. Moss, S. Bevan, Transient receptor potential A1 is a sensory receptor for multiple products of oxidative stress, J Neurosci 28 (2008) 2485-2494.

[191] B.F. Bessac, M. Sivula, C.A. von Hehn, J. Escalera, L. Cohn, S.E. Jordt, TRPA1 is a major oxidant sensor in murine airway sensory neurons, J Clin Invest 118 (2008) 1899-1910.

[192] T.E. Taylor-Clark, S. Ghatta, W. Bettner, B.J. Undem, Nitrooleic acid, an endogenous product of nitrative stress, activates nociceptive sensory nerves via the direct activation of TRPA1, Mol Pharmacol 75 (2009) 820-829.

[193] S. Materazzi, R. Nassini, E. Andre, B. Campi, S. Amadesi, M. Trevisani, N.W. Bunnett, R. Patacchini, P. Geppetti, Cox-dependent fatty acid metabolites cause pain through activation of the irritant receptor TRPA1, Proc Natl Acad Sci U S A 105 (2008) 12045-12050.

[194] T.E. Taylor-Clark, B.J. Undem, D.W. Macglashan, Jr., S. Ghatta, M.J. Carr, M.A. McAlexander, Prostaglandin-induced activation of nociceptive neurons via direct interaction with transient receptor potential A1 (TRPA1), Mol Pharmacol 73 (2008) 274-281.

[195] R. Miyamoto, K. Otsuguro, S. Ito, Time- and concentration-dependent activation of TRPA1 by hydrogen sulfide in rat DRG neurons, Neurosci Lett 499 (2011) 137-142.

[196] Y.Y. Wang, R.B. Chang, E.R. Liman, TRPA1 is a component of the nociceptive response to CO2, J Neurosci 30 (2010) 12958-12963.

[197] F. Fujita, K. Uchida, T. Moriyama, A. Shima, K. Shibasaki, H. Inada, T. Sokabe, M. Tominaga, Intracellular alkalization causes pain sensation through activation of TRPA1 in mice, J Clin Invest 118 (2008) 4049-4057.

[198] R. Nassini, S. Materazzi, E. Andre, L. Sartiani, G. Aldini, M. Trevisani, C. Carnini, D. Massi, P. Pedretti, M. Carini, E. Cerbai, D. Preti, G. Villetti, M. Civelli, G. Trevisan, C. Azzari, S. Stokesberry, L. Sadofsky, L. McGarvey, R. Patacchini, P. Geppetti, Acetaminophen, via its reactive metabolite N-acetyl-p-benzo-quinoneimine and transient receptor potential ankyrin-1 stimulation, causes neurogenic inflammation in the airways and other tissues in rodents, Faseb J 24 (2010) 4904-4916.

[199] R. Nassini, S. Materazzi, J. Vriens, J. Prenen, S. Benemei, G. De Siena, G. la Marca, E. Andre, D. Preti, C. Avonto, L. Sadofsky, V. Di Marzo, L. De Petrocellis, G. Dussor, F. Porreca, O. Taglialatela-Scafati, G. Appendino, B. Nilius, P. Geppetti, The 'headache tree' via umbellulone and TRPA1 activates the trigeminovascular system, Brain 135 (2012) 376-390.

[200] J. Zhong, A. Minassi, J. Prenen, O. Taglialatela-Scafati, G. Appendino, B. Nilius, Umbellulone modulates TRP channels, Pflugers Arch 462 (2011) 861-870.

[201] L.R. Sadofsky, A.N. Boa, S.A. Maher, M.A. Birrell, M.G. Belvisi, A.H. Morice, TRPA1 is activated by direct addition of cysteine residues to the N-hydroxysuccinyl esters of acrylic and cinnamic acids, Pharmacol Res 63 (2011) 30-36.
[202] I. Dalle-Donne, G. Aldini, M. Carini, R. Colombo, R. Rossi, A. Milzani, Protein carbonylation, cellular dysfunction, and disease progression, J Cell Mol Med 10 (2006) 389-406.
[203] M.J. Fischer, A. Leffler, F. Niedermirtl, K. Kistner, M. Eberhardt, P.W. Reeh, C. Nau, The general anesthetic propofol excites nociceptors by activating TRPV1 and TRPA1 rather than GABAA receptors, J Biol Chem 285 (2010) 34781-34792.
[204] A. Leffler, A. Lattrell, S. Kronewald, F. Niedermirtl, C. Nau, Activation of TRPA1 by membrane permeable local anesthetics, Mol Pain 7 (2011) 62.
[205] A.L. Motter, G.P. Ahern, TRPA1 is a polyunsaturated fatty acid sensor in mammals, PLoS One 7 (2012) e38439.
[206] Y. Karashima, N. Damann, J. Prenen, K. Talavera, A. Segal, T. Voets, B. Nilius, Bimodal action of menthol on the transient receptor potential channel TRPA1, J Neurosci 27 (2007) 9874-9884.
[207] D.D. McKemy, W.M. Neuhausser, D. Julius, Identification of a cold receptor reveals a general role for TRP channels in thermosensation, Nature 416 (2002) 52-58.
[208] A.M. Peier, A. Moqrich, A.C. Hergarden, A.J. Reeve, D.A. Andersson, G.M. Story, T.J. Earley, I. Dragoni, P. McIntyre, S. Bevan, A. Patapoutian, A TRP channel that senses cold stimuli and menthol, Cell 108 (2002) 705-715.
[209] H. Hu, J. Tian, Y. Zhu, C. Wang, R. Xiao, J.M. Herz, J.D. Wood, M.X. Zhu, Activation of TRPA1 channels by fenamate nonsteroidal anti-inflammatory drugs, Pflugers Arch 4 (2009) 4.
[210] S.B. McMahon, W.B. Cafferty, F. Marchand, Immune and glial cell factors as pain mediators and modulators, Exp Neurol 192 (2005) 444-462.
[211] A. Dray, M. Perkins, Bradykinin and inflammatory pain, Trends Neurosci 16 (1993) 99-104.
[212] Y. Dai, S. Wang, M. Tominaga, S. Yamamoto, T. Fukuoka, T. Higashi, K. Kobayashi, K. Obata, H. Yamanaka, K. Noguchi, Sensitization of TRPA1 by PAR2 contributes to the sensation of inflammatory pain, J Clin Invest 117 (2007) 1979-1987.
[213] A. Diogenes, A.N. Akopian, K.M. Hargreaves, NGF up-regulates TRPA1: implications for orofacial pain, J Dent Res 86 (2007) 550-555.
[214] C.R. McNamara, J. Mandel-Brehm, D.M. Bautista, J. Siemens, K.L. Deranian, M. Zhao, N.J. Hayward, J.A. Chong, D. Julius, M.M. Moran, C.M. Fanger, TRPA1 mediates formalin-induced pain, Proc Natl Acad Sci U S A 104 (2007) 13525-13530.
[215] P.C. Kerstein, D. del Camino, M.M. Moran, C.L. Stucky, Pharmacological blockade of TRPA1 inhibits mechanical firing in nociceptors, Mol Pain 5 (2009) 19.
[216] H. Wei, M.M. Hamalainen, M. Saarnilehto, A. Koivisto, A. Pertovaara, Attenuation of mechanical hypersensitivity by an antagonist of the TRPA1 ion channel in diabetic animals, Anesthesiology 111 (2009) 147-154.
[217] Y. Tatsushima, N. Egashira, T. Kawashiri, Y. Mihara, T. Yano, K. Mishima, R. Oishi, Involvement of substance P in peripheral neuropathy induced by paclitaxel but not oxaliplatin, J Pharmacol Exp Ther 337 (2011) 226-235.
[218] N. Alessandri-Haber, O.A. Dina, E.K. Joseph, D.B. Reichling, J.D. Levine, Interaction of transient receptor potential vanilloid 4, integrin, and SRC tyrosine kinase in mechanical hyperalgesia, J Neurosci 28 (2008) 1046-1057.
[219] K. Miyano, H.B. Tang, Y. Nakamura, N. Morioka, A. Inoue, Y. Nakata, Paclitaxel and vinorelbine, evoked the release of substance P from cultured rat dorsal root ganglion cells through different PKC isoform-sensitive ion channels, Neuropharmacology 57 (2009) 25-32.
[220] N. Attal, D. Bouhassira, M. Gautron, J.N. Vaillant, E. Mitry, C. Lepere, P. Rougier, F. Guirimand, Thermal hyperalgesia as a marker of oxaliplatin neurotoxicity: a prospective quantified sensory assessment study, Pain 144 (2009) 245-252.
[221] U. Anand, W.R. Otto, P. Anand, Sensitization of capsaicin and icilin responses in oxaliplatin treated adult rat DRG neurons, Mol Pain 6 (2010) 82.
[222] L.E. Ta, A.J. Bieber, S.M. Carlton, C.L. Loprinzi, P.A. Low, A.J. Windebank, Transient Receptor Potential Vanilloid 1 is essential for cisplatin-induced heat hyperalgesia in mice, Mol Pain 6 (2010) 15.
[223] A. Patapoutian, S. Tate, C.J. Woolf, Transient receptor potential channels: targeting pain at the source, Nat Rev Drug Discov 8 (2009) 55-68.
[224] N. Alessandri-Haber, O.A. Dina, J.J. Yeh, C.A. Parada, D.B. Reichling, J.D. Levine, Transient receptor potential vanilloid 4 is essential in chemotherapy-induced neuropathic pain in the rat, J Neurosci 24 (2004) 4444-4452.
[225] A.F. Odell, J.L. Scott, D.F. Van Helden, Epidermal growth factor induces tyrosine phosphorylation, membrane insertion, and activation of transient receptor potential channel 4, J Biol Chem 280 (2005) 37974-37987.

[226] L. Sternfeld, I. Anderie, A. Schmid, H. Al-Shaldi, E. Krause, T. Magg, D. Schreiner, H.W. Hofer, I. Schulz, Identification of tyrosines in the putative regulatory site of the Ca2+ channel TRPV6, Cell Calcium 42 (2007) 91-102.

[227] J. Chen, S.K. Joshi, S. DiDomenico, R.J. Perner, J.P. Mikusa, D.M. Gauvin, J.A. Segreti, P. Han, X.F. Zhang, W. Niforatos, B.R. Bianchi, S.J. Baker, C. Zhong, G.H. Simler, H.A. McDonald, R.G. Schmidt, S.P. McGaraughty, K.L. Chu, C.R. Faltynek, M.E. Kort, R.M. Reilly, P.R. Kym, Selective blockade of TRPA1 channel attenuates pathological pain without altering noxious cold sensation or body temperature regulation, Pain 152 (2011) 1165-1172.

[228] J. Frederick, M.E. Buck, D.J. Matson, D.N. Cortright, Increased TRPA1, TRPM8, and TRPV2 expression in dorsal root ganglia by nerve injury, Biochem Biophys Res Commun 358 (2007) 1058-1064.

[229] J. Descoeur, V. Pereira, A. Pizzoccaro, A. Francois, B. Ling, V. Maffre, B. Couette, J. Busserolles, C. Courteix, J. Noel, M. Lazdunski, A. Eschalier, N. Authier, E. Bourinet, Oxaliplatin-induced cold hypersensitivity is due to remodelling of ion channel expression in nociceptors, EMBO Mol Med 3 (2011) 266-278.

[230] L.A. Colvin, P.R. Johnson, R. Mitchell, S.M. Fleetwood-Walker, M. Fallon, From bench to bedside: a case of rapid reversal of bortezomib-induced neuropathic pain by the TRPM8 activator, menthol, J Clin Oncol 26 (2008) 4519-4520.

[231] D.J. Storey, L.A. Colvin, M.J. Mackean, R. Mitchell, S.M. Fleetwood-Walker, M.T. Fallon, Reversal of dose-limiting carboplatin-induced peripheral neuropathy with TRPM8 activator, menthol, enables further effective chemotherapy delivery, J Pain Symptom Manage 39 (2010) e2-4.

[232] R. Nassini, M. Gees, S. Harrison, G. De Siena, S. Materazzi, N. Moretto, P. Failli, D. Preti, N. Marchetti, A. Cavazzini, F. Mancini, P. Pedretti, B. Nilius, R. Patacchini, P. Geppetti, Oxaliplatin elicits mechanical and cold allodynia in rodents via TRPA1 receptor stimulation, Pain 152 (2011) 1621-1631.

[233] S.R. Chaplan, F.W. Bach, J.W. Pogrel, J.M. Chung, T.L. Yaksh, Quantitative assessment of tactile allodynia in the rat paw, J Neurosci Methods 53 (1994) 55-63.

[234] E. Andre, B. Campi, S. Materazzi, M. Trevisani, S. Amadesi, D. Massi, C. Creminon, N. Vaksman, R. Nassini, M. Civelli, P.G. Baraldi, D.P. Poole, N.W. Bunnett, P. Geppetti, R. Patacchini, Cigarette smoke-induced neurogenic inflammation is mediated by alpha,beta-unsaturated aldehydes and the TRPA1 receptor in rodents, J Clin Invest 118 (2008) 2574-2582.

[235] W. Everaerts, X. Zhen, D. Ghosh, J. Vriens, T. Gevaert, J.P. Gilbert, N.J. Hayward, C.R. McNamara, F. Xue, M.M. Moran, T. Strassmaier, E. Uykal, G. Owsianik, R. Vennekens, D. De Ridder, B. Nilius, C.M. Fanger, T. Voets, Inhibition of the cation channel TRPV4 improves bladder function in mice and rats with cyclophosphamide-induced cystitis, Proc Natl Acad Sci U S A 107 (2010) 19084-19089.

[236] S.R. Eid, E.D. Crown, E.L. Moore, H.A. Liang, K.C. Choong, S. Dima, D.A. Henze, S.A. Kane, M.O. Urban, HC-030031, a TRPA1 selective antagonist, attenuates inflammatory- and neuropathy-induced mechanical hypersensitivity, Mol Pain 4 (2008) 48.

[237] J. Alexandre, F. Batteux, C. Nicco, C. Chereau, A. Laurent, L. Guillevin, B. Weill, F. Goldwasser, Accumulation of hydrogen peroxide is an early and crucial step for paclitaxel-induced cancer cell death both in vitro and in vivo, Int J Cancer 119 (2006) 41-48.

[238] B. Ramanathan, K.Y. Jan, C.H. Chen, T.C. Hour, H.J. Yu, Y.S. Pu, Resistance to paclitaxel is proportional to cellular total antioxidant capacity, Cancer Res 65 (2005) 8455-8460.

[239] B. Rigas, Y. Sun, Induction of oxidative stress as a mechanism of action of chemopreventive agents against cancer, Br J Cancer 98 (2008) 1157-1160.

[240] P.A. Lyle, P. Mitsopoulos, Z.E. Suntres, N-acetylcysteine modulates the cytotoxic effects of Paclitaxel, Chemotherapy 57 (2011) 298-304.

[241] Y. Itoh, T. Sendo, T. Hirakawa, T. Goromaru, S. Takasaki, H. Yahata, H. Nakano, R. Oishi, Role of sensory nerve peptides rather than mast cell histamine in paclitaxel hypersensitivity, Am J Respir Crit Care Med 169 (2004) 113-119.

[242] S. Harrison, P. Geppetti, Substance p, Int J Biochem Cell Biol 33 (2001) 555-576.

[243] B.F. Bessac, S.E. Jordt, Sensory detection and responses to toxic gases: mechanisms, health effects, and countermeasures, Proc Am Thorac Soc 7 (2010) 269-277.

[244] N. Vergnolle, N. Cenac, C. Altier, L. Cellars, K. Chapman, G.W. Zamponi, S. Materazzi, R. Nassini, W. Liedtke, F. Cattaruzza, E.F. Grady, P. Geppetti, N.W. Bunnett, A role for transient receptor potential vanilloid 4 in tonicity-induced neurogenic inflammation, Br J Pharmacol 159 (2010) 1161-1173.

[245] M. Fukui, N. Yamabe, B.T. Zhu, Resveratrol attenuates the anticancer efficacy of paclitaxel in human breast cancer cells in vitro and in vivo, Eur J Cancer 46 (2010) 1882-1891.

[246] J.Z. Bai, J. Lipski, Differential expression of TRPM2 and TRPV4 channels and their potential role in oxidative stress-induced cell death in organotypic hippocampal culture, Neurotoxicology 31 (2010) 204-214.
[247] C. Meregalli, A. Canta, V.A. Carozzi, A. Chiorazzi, N. Oggioni, A. Gilardini, C. Ceresa, F. Avezza, L. Crippa, P. Marmiroli, G. Cavaletti, Bortezomib-induced painful neuropathy in rats: a behavioral, neurophysiological and pathological study in rats, Eur J Pain 14 (2009) 343-350.
[248] J. Bruna, E. Udina, A. Ale, J.J. Vilches, A. Vynckier, J. Monbaliu, L. Silverman, X. Navarro, Neurophysiological, histological and immunohistochemical characterization of bortezomib-induced neuropathy in mice, Exp Neurol 223 (2010) 599-608.
[249] V.A. Carozzi, A. Canta, N. Oggioni, B. Sala, A. Chiorazzi, C. Meregalli, M. Bossi, P. Marmiroli, G. Cavaletti, Neurophysiological and neuropathological characterization of new murine models of chemotherapy-induced chronic peripheral neuropathies, Exp Neurol 226 (2010) 301-309.
[250] S. Materazzi, C. Fusi, S. Benemei, P. Pedretti, R. Patacchini, B. Nilius, J. Prenen, C. Creminon, P. Geppetti, R. Nassini, TRPA1 and TRPV4 mediate paclitaxel-induced peripheral neuropathy in mice via a glutathione-sensitive mechanism, Pflugers Arch 463 (2012) 561-569.
[251] W.J. Dixon, Efficient analysis of experimental observations, Annu Rev Pharmacol Toxicol 20 (1980) 441-462.
[252] J. Ferreira, M.M. Campos, R. Araujo, M. Bader, J.B. Pesquero, J.B. Calixto, The use of kinin B1 and B2 receptor knockout mice and selective antagonists to characterize the nociceptive responses caused by kinins at the spinal level, Neuropharmacology 43 (2002) 1188-1197.
[253] N. Alessandri-Haber, E. Joseph, O.A. Dina, W. Liedtke, J.D. Levine, TRPV4 mediates pain-related behavior induced by mild hypertonic stimuli in the presence of inflammatory mediator, Pain 118 (2005) 70-79.
[254] C.A. Kassuya, J. Ferreira, R.F. Claudino, J.B. Calixto, Intraplantar PGE2 causes nociceptive behaviour and mechanical allodynia: the role of prostanoid E receptors and protein kinases, Br J Pharmacol 150 (2007) 727-737.
[255] G. Trevisan, M.F. Rossato, C.I. Walker, J.Z. Klafke, F. Rosa, S.M. Oliveira, R. Tonello, G.P. Guerra, A.A. Boligon, R.B. Zanon, M.L. Athayde, J. Ferreira, Identification of the plant steroid alpha-spinasterol as a novel transient receptor potential vanilloid 1 antagonist with antinociceptive properties, J Pharmacol Exp Ther 343 (2012) 258-269.
[256] D.S. da Costa, F.C. Meotti, E.L. Andrade, P.C. Leal, E.M. Motta, J.B. Calixto, The involvement of the transient receptor potential A1 (TRPA1) in the maintenance of mechanical and cold hyperalgesia in persistent inflammation, Pain 148 (2009) 431-437.
[257] E.K. Joseph, X. Chen, O. Bogen, J.D. Levine, Oxaliplatin acts on IB4-positive nociceptors to induce an oxidative stress-dependent acute painful peripheral neuropathy, J Pain 9 (2008) 463-472.
[258] D.A. Barriere, J. Rieusset, D. Chanteranne, J. Busserolles, M.A. Chauvin, L. Chapuis, J. Salles, C. Dubray, B. Morio, Paclitaxel therapy potentiates cold hyperalgesia in streptozotocin-induced diabetic rats through enhanced mitochondrial reactive oxygen species production and TRPA1 sensitization, Pain 153 (2012) 553-561.
[259] K. Obata, H. Katsura, T. Mizushima, H. Yamanaka, K. Kobayashi, Y. Dai, T. Fukuoka, A. Tokunaga, M. Tominaga, K. Noguchi, TRPA1 induced in sensory neurons contributes to cold hyperalgesia after inflammation and nerve injury, J Clin Invest 115 (2005) 2393-2401.
[260] D.R. Premkumar, E.P. Jane, N.R. Agostino, J.D. DiDomenico, I.F. Pollack, Bortezomib-induced sensitization of malignant human glioma cells to vorinostat-induced apoptosis depends on reactive oxygen species production, mitochondrial dysfunction, Noxa upregulation, Mcl-1 cleavage, and DNA damage, Mol Carcinog 52 (2011) 118-133.
[261] G. Aldini, I. Dalle-Donne, R.M. Facino, A. Milzani, M. Carini, Intervention strategies to inhibit protein carbonylation by lipoxidation-derived reactive carbonyls, Med Res Rev 27 (2007) 817-868.
[262] D.R. Pachman, D.L. Barton, J.C. Watson, C.L. Loprinzi, Chemotherapy-induced peripheral neuropathy: prevention and treatment, Clin Pharmacol Ther 90 (2011) 377-387.
[263] T.E. Taylor-Clark, B.J. Undem, Ozone activates airway nerves via the selective stimulation of TRPA1 ion channels, J Physiol 14 (2009) 14.
[264] M. Zhao, K. Isami, S. Nakamura, H. Shirakawa, T. Nakagawa, S. Kaneko, Acute cold hypersensitivity characteristically induced by oxaliplatin is caused by the enhanced responsiveness of TRPA1 in mice, Mol Pain 8 (2012) 55.
[265] C. Morgado, P. Pereira-Terra, I. Tavares, alpha-Lipoic acid normalizes nociceptive neuronal activity at the spinal cord of diabetic rats, Diabetes Obes Metab 13 (2011) 736-741.
[266] S. Materazzi, S. Benemei, C. Fusi, R. Gualdani, G. De Siena, N. Vastani, D.A. Andersson, G. Trevisan, M.R. Moncelli, X. Wei, G. Dussor, F. Pollastro, R. Patacchini, G. Appendino, P.

Geppetti, R. Nassini, Parthenolide inhibits nociception and neurogenic vasodilatation in the trigeminovascular system by targeting the TRPA1 channel, Pain 154 (2013) 2750-2758.

[267] J. Doig, L.A. Griffiths, D. Peberdy, P. Dharmasaroja, M. Vera, F.J. Davies, H.J. Newbery, D. Brownstein, C.M. Abbott, In vivo characterization of the role of tissue-specific translation elongation factor 1A2 in protein synthesis reveals insights into muscle atrophy, Febs J 280 (2013) 6528-6540.

[268] G. Trevisan, C. Hoffmeister, M.F. Rossato, S.M. Oliveira, M.A. Silva, C.R. Silva, C. Fusi, R. Tonello, D. Minocci, G.P. Guerra, S. Materazzi, R. Nassini, P. Geppetti, J. Ferreira, TRPA1 receptor stimulation by hydrogen peroxide is critical to trigger hyperalgesia and inflammation in a model of acute gout, Free Radic Biol Med 72 (2014) 200-209.

[269] G. la Marca, S. Malvagia, L. Filippi, P. Fiorini, M. Innocenti, F. Luceri, G. Pieraccini, G. Moneti, S. Francese, F.R. Dani, R. Guerrini, Rapid assay of topiramate in dried blood spots by a new liquid chromatography-tandem mass spectrometric method, J Pharm Biomed Anal 48 (2008) 1392-1396.

[270] M.S. Steinhoff, B. von Mentzer, P. Geppetti, C. Pothoulakis, N.W. Bunnett, Tachykinins and their receptors: contributions to physiological control and the mechanisms of disease, Physiol Rev 94 (2014) 265-301.

[271] S. Reagan-Shaw, M. Nihal, N. Ahmad, Dose translation from animal to human studies revisited, Faseb J 22 (2008) 659-661.

[272] A. Lintermans, B. Van Calster, M. Van Hoydonck, S. Pans, J. Verhaeghe, R. Westhovens, N.L. Henry, H. Wildiers, R. Paridaens, A.S. Dieudonne, K. Leunen, L. Morales, K. Verschueren, D. Timmerman, L. De Smet, I. Vergote, M.R. Christiaens, P. Neven, Aromatase inhibitor-induced loss of grip strength is body mass index dependent: hypothesis-generating findings for its pathogenesis, Ann Oncol 22 (2011) 1763-1769.

[273] S.J. Jin, J.A. Jung, S.H. Cho, U.J. Kim, S. Choe, J.L. Ghim, Y.H. Noh, H.J. Park, J.C. Kim, J.A. Jung, H.S. Lim, K.S. Bae, The pharmacokinetics of letrozole: association with key body mass metrics, Int J Clin Pharmacol Ther 50 (2012) 557-565.

[274] R. Jukanti, S. Sheela, S. Bandari, P.R. Veerareddy, Enhanced bioavailability of exemestane via proliposomes based transdermal delivery, J Pharm Sci 100 (2011) 3208-3222.

[275] M. Valle, E. Di Salle, M.G. Jannuzzo, I. Poggesi, M. Rocchetti, R. Spinelli, D. Verotta, A predictive model for exemestane pharmacokinetics/pharmacodynamics incorporating the effect of food and formulation, Br J Clin Pharmacol 59 (2005) 355-364.

[276] N. Vergnolle, N.W. Bunnett, K.A. Sharkey, V. Brussee, S.J. Compton, E.F. Grady, G. Cirino, N. Gerard, A.I. Basbaum, P. Andrade-Gordon, M.D. Hollenberg, J.L. Wallace, Proteinase-activated receptor-2 and hyperalgesia: A novel pain pathway, Nat Med 7 (2001) 821-826.

[277] H. Liu, P. Talalay, Relevance of anti-inflammatory and antioxidant activities of exemestane and synergism with sulforaphane for disease prevention, Proc Natl Acad Sci U S A 110 (2013) 19065-19070.

[278] I. Dalle-Donne, M. Carini, G. Vistoli, L. Gamberoni, D. Giustarini, R. Colombo, R. Maffei Facino, R. Rossi, A. Milzani, G. Aldini, Actin Cys374 as a nucleophilic target of alpha,beta-unsaturated aldehydes, Free Radic Biol Med 42 (2007) 583-598.

[279] R.M. Oballa, J.F. Truchon, C.I. Bayly, N. Chauret, S. Day, S. Crane, C. Berthelette, A generally applicable method for assessing the electrophilicity and reactivity of diverse nitrile-containing compounds, Bioorg Med Chem Lett 17 (2007) 998-1002.

[280] B. Brone, P.J. Peeters, R. Marrannes, M. Mercken, R. Nuydens, T. Meert, H.J. Gijsen, Tear gasses CN, CR, and CS are potent activators of the human TRPA1 receptor, Toxicol Appl Pharmacol 231 (2008) 150-156.

[281] M.M. Moran, M.A. McAlexander, T. Biro, A. Szallasi, Transient receptor potential channels as therapeutic targets, Nat Rev Drug Discov 10 (2011) 601-620.

[282] N.L. Henry, D. Pchejetski, R. A'Hern, A.T. Nguyen, P. Charles, J. Waxman, L. Li, A.M. Storniolo, D.F. Hayes, D.A. Flockhart, V. Stearns, J. Stebbing, Inflammatory cytokines and aromatase inhibitor-associated musculoskeletal syndrome: a case-control study, Br J Cancer 103 (2010) 291-296.

[283] H.F. Kennecke, I.A. Olivotto, C. Speers, B. Norris, S.K. Chia, C. Bryce, K.A. Gelmon, Late risk of relapse and mortality among postmenopausal women with estrogen responsive early breast cancer after 5 years of tamoxifen, Ann Oncol 18 (2007) 45-51.

[284] H. Sies, Role of metabolic H2O2 generation: redox signaling and oxidative stress, J Biol Chem 289 (2014) 8735-8741.

[285] Z. Desta, Y. Kreutz, A.T. Nguyen, L. Li, T. Skaar, L.K. Kamdem, N.L. Henry, D.F. Hayes, A.M. Storniolo, V. Stearns, E. Hoffmann, R.F. Tyndale, D.A. Flockhart, Plasma letrozole concentrations in postmenopausal women with breast cancer are associated with CYP2A6 genetic variants, body mass index, and age, Clin Pharmacol Ther 90 (2011) 693-700.

[286] M. Dowsett, J. Cuzick, A. Howell, I. Jackson, Pharmacokinetics of anastrozole and tamoxifen alone, and in combination, during adjuvant endocrine therapy for early breast cancer in postmenopausal women: a sub-protocol of the 'Arimidex and tamoxifen alone or in combination' (ATAC) trial, Br J Cancer 85 (2001) 317-324.
[287] Burstein, R., M. F. Cutrer, The development of cutaneous allodynia during a migraine attack clinical evidence for the sequential recruitment of spinal and supraspinal nociceptive neurons in migraine. Brain 123 (2000) 1703-9.
[288] Horvath, P., J. Szilvassy, Decreased sensory neuropeptide release in isolated bronchi of rats with cisplatin-induced neuropathy. Eur J Pharmacol 507 (2005) 247-52.
[289] Tatsushima, Y., N. Egashira, Involvement of substance P in peripheral neuropathy induced by paclitaxel but not oxaliplatin. J Pharmacol Exp Ther 337 (2011) 226-35.
[290] Kim, Y. S., J. Y. Son, Expression of transient receptor potential ankyrin 1 (TRPA1) in the rat trigeminal sensory afferents and spinal dorsal horn. J Comp Neurol 518 (2010) 687-98.
[291] Tominaga, M., M. Numazaki, Regulation mechanisms of vanilloid receptors. Novartis Found Symp 261 (2004) 4-12.
[292] Braz, J., C. Solorzano, Transmitting pain and itch messages: a contemporary view of the spinal cord circuits that generate gate control. Neuron 82 (2014) 522-36.
[293] Cata, J. P., H. R. Weng, Quantitative sensory findings in patients with bortezomib-induced pain. J Pain 8 (2007) 296-306.
[294] Takahashi, N., D. Kozai, TRP channels: sensors and transducers of gasotransmitter signals. Front Physiol 3 (2012) 324.
[295] Julius, D. TRP channels and pain. Annu Rev Cell Dev Biol 29 (2013) 355-84.
[296] Ramsey, I. S., M. Delling, An introduction to TRP channels. Annu Rev Physiol 68 (2006) 619-47.

Pflugers Arch - Eur J Physiol (2012) 463:561–569
DOI 10.1007/s00424-011-1071-x

ION CHANNELS, RECEPTORS AND TRANSPORTERS

TRPA1 and TRPV4 mediate paclitaxel-induced peripheral neuropathy in mice via a glutathione-sensitive mechanism

Serena Materazzi · Camilla Fusi · Silvia Benemei · Pamela Pedretti · Riccardo Patacchini · Bernd Nilius · Jean Prenen · Christophe Creminon · Pierangelo Geppetti · Romina Nassini

Received: 20 December 2011 / Accepted: 28 December 2011 / Published online: 19 January 2012

Abstract Paclitaxel produces a sensory neuropathy, characterized by mechanical and cold hypersensitivity, which are abated by antioxidants. The transient receptor potential vanilloid 4 (TRPV4) channel has been reported to contribute to paclitaxel-evoked allodynia in rodents. We recently showed that TRP ankyrin 1 (TRPA1) channel mediates oxaliplatin-evoked cold and mechanical allodynia, and the drug targets TRPA1 via generation of oxidative stress. Here, we have explored whether TRPA1 activation contributes to paclitaxel-induced mechanical and cold hypersensitivity and whether this activation is mediated by oxidative stress generation. Paclitaxel-evoked mechanical allodynia was reduced partially by the TRPA1 antagonist, HC-030031, and the TRPV4 antagonist, HC-067047, and was completely abated by the combination of the two antagonists. The reduced paclitaxel-evoked mechanical allodynia, observed in TRPA1-deficient mice, was completely abolished when mice were treated with HC-067047. Cold allodynia was abated completely by HC-030031 and in TRPA1-deficient mice. Exposure to paclitaxel of slices of mouse esophagus released the sensory neuropeptide, calcitonin gene-related peptide (CGRP). This effect was abolished by capsaicin desensitization and in calcium-free medium (indicating neurosecretion from sensory nerve terminals), partially reduced by either HC-030031 or HC-067047, and completely abated in the presence of glutathione (GSH). Finally, the reduced CGRP release, observed in esophageal slices of TRPA1-deficient mice, was further inhibited by GSH. Paclitaxel via oxygen radical formation targets TRPA1 and TRPV4, and both channels are key for the delayed development of mechanical allodynia. Cold allodynia is, however, entirely dependent on TRPA1.

Keywords Paclitaxel · TRPA1 · Cold and mechanical hyperalgesia · Primary sensory neurons · Oxidative stress

S. Materazzi · C. Fusi · S. Benemei · P. Pedretti · P. Geppetti (✉) · R. Nassini
Department of Preclinical and Clinical Pharmacology, University of Florence, Viale Pieraccini 6, 50139 Florence, Italy
e-mail: pierangelo.geppetti@unifi.it

R. Patacchini
Department of Pharmacology, Chiesi Farmaceutici, Parma, Italy

B. Nilius · J. Prenen
Department of Molecular Cell Biology, Katholieke Universiteit, Leuven, Belgium

C. Creminon
CEA, Institut de Biologie et Technologies de Saclay (iBiTec-S), Service de pharmacologie et d'immuno analyse (SPI), Gif sur Yvette, France

Introduction

Paclitaxel (Taxol) is a microtubule-targeting agent labeled for the treatment of a wide variety of solid neoplasms, including ovarian, breast and prostate cancer, currently under investigation to assess its efficacy to treat additional malignant tumors. Peripheral neuropathy (PN) represents a dose-limiting adverse reaction, which negatively affects the quality of life of a relevant portion of patients and, importantly, results in therapy interruption or discontinuation [16]. As described by treated patients, PN by paclitaxel is characterized by various sensory symptoms including mechanical allodynia, spontaneous pain, cold allodynia, ongoing burning pain, tingling, and numbness in a "stocking and glove" distribution [16]. Not infrequently, these symptoms do not resolve with the cessation of paclitaxel therapy and become chronic

for months or years [12, 43]. The mechanism underlying paclitaxel-evoked PN is poorly understood, although a series of studies have focused on a subpopulation of peptidergic primary sensory neurons expressing specific ion channels as the primary target [1, 2, 33, 40].

A subset of primary sensory neurons expresses several members of the transient receptor potential (TRP) family of ion channels, which convey different sensory modalities, including thermo-, mechano-/osmo-, and chemical sensations [8]. These include the vanilloid 1 (TRPV1, the so called "capsaicin receptor"), 2 (TRPV2), 3 (TRPV3), and 4 (TRPV4) channels, the TRPM8 (the "menthol receptor"), and TRPA1 (the ankyrin 1) channels. There is evidence that TRPV4, which has been implicated in the process of osmo-mechanical transduction, mediates part of the mechanical hyperalgesia produced by treatment of rats or mice with paclitaxel [1, 2]. We have recently reported that, in mice and rats, platinum-derived drugs produce a long-lasting mechanical and cold hypersensitivity, by a mechanism that is entirely mediated by TRPA1 [34]. We also showed that both cisplatin and oxaliplatin cause acute TRPA1 activation, an effect that is not mediated by direct channel targeting, but rather is due to the generation of reactive oxygen species (ROS) that eventually gate TRPA1 [34]. Indeed, TRPA1 is activated not only by exogenous irritants, such as allyl isothiocyanate (mustard oil) or cinnamaldehyde (cinnamon) [28, 36], but also by a structurally diverse series of oxidative stress byproducts, including hydrogen peroxide, nitrooleic acid [5, 11], and the unsaturated aldehydes, 4-hydroxy-trans-2-nonenal (4-HNE) [41], 4-oxononenal [5], and acrolein [9].

In vitro studies have shown that paclitaxel-evoked oxidative stress, and the resultant production of hydrogen peroxide and formation of DNA oxidative adducts [38], are associated with the drug cytotoxicity in breast cancer cells [4, 25]. In agreement with this observation, susceptibility to paclitaxel by breast cancer cells was found to be reduced by antioxidant treatments [21], and resistance to paclitaxel has been associated with the total antioxidant cell capacity in a large series of different cancer cell lines [38], suggesting that oxidative stress contributes to the antineoplastic mechanism of action of this drug. Patients subjected to chemotherapy with paclitaxel present immediate systemic oxidative stress and red blood cell oxidative injury associated with the development of anemia [37]. Thus, we have hypothesized that, in addition to TRPV4, TRPA1 also contributes to paclitaxel-induced mechanical and thermal (cold) hypersensitivity and targets these TRP channels via generation of oxidative stress byproducts. Data show that in mice both TRPV4 and TRPA1 contribute to the delayed mechanical allodynia, whereas only TRPA1 mediates the delayed cold hypersensitivity evoked by paclitaxel. In addition, paclitaxel acutely induces neuropeptide release from sensory nerve terminals by activation of TRPA1 and TRPV4, apparently via ROS generation.

Materials and methods

Animals

All animal experiments were carried out in accordance with the European Union Community Council guidelines and approved by the local ethics committee. C57BL/6 mice (male, 25 g) (Harlan Laboratories, Milan, Italy) wild-type (*Trpa1*$^{+/+}$), or TRPA1-deficient mice (*Trpa1*$^{-/-}$), generated by heterozygous mice on a C57BL/6 background [9] were used. Animals were housed in a temperature- and humidity-controlled vivarium (12-h dark/light cycle, free access to food and water). Behavioral experiments were done in a quiet, temperature-controlled room (20°C to 22°C) between 10 a.m. and 4 p.m. and were performed by an operator blinded to the genotype and the status of drug treatment. Animals were sacrificed with a high dose of intraperitoneal (i.p.) sodium pentobarbital (200 mg/kg).

Paclitaxel-induced painful neuropathy models and drugs administration

After habituation and baseline measurements of pain sensitivity, animals were randomized into treatment groups. C57BL/6, *Trpa1*$^{+/+}$, or *Trpa1*$^{-/-}$ mice were treated with a single i.p. administration of paclitaxel (6 mg/kg) or its vehicle (ethanol and Cremophore EL, 50:50, *v*/*v*) [1]. No weight loss was observed in mice throughout the duration of the experiments after paclitaxel treatment. Paclitaxel was formulated at a concentration of 1 mg/ml and was first dissolved in a vehicle containing absolute ethanol and Cremophore EL (50:50, *v*/*v*) because of its poor aqueous solubility. Final solution (10% of this stock solution) was made in sterile saline (NaCl 0.9%) at the time of injection, and the volume was adjusted to 10 ml/kg for the i.p. administration [2]. Intragastric (i.g.) HC-030031 (300 mg/kg) or its vehicle (0.5% carboxymethyl cellulose, CMC), and HC-067047 (10 mg/kg, i.p.) or its vehicle (2.5% DMSO), were administered at day 8 after the administration of paclitaxel or its vehicle. In another experimental setting, HC-030031 (300 mg/kg, i.g.) or its vehicle (0.5% CMC), and HC-067047 (10 mg/kg, i.p.) or its vehicle (2.5% DMSO), were coadministered at day 8 after the administration of paclitaxel or its vehicle.

Tactile allodynia (Von Frey hair test)

Paclitaxel-induced mechanical allodynia was measured in C57BL/6, *Trpa1*$^{+/+}$, or *Trpa1*$^{-/-}$ mice by using the up-and-

down paradigm [13]. Mechanical nociceptive threshold was determined before (basal level threshold) and after drug administration. The effect of paclitaxel was tested for 20 days after treatment. Data are expressed as the mean threshold values (in grams).

Cold stimulation

Cold allodynia was assessed in C57BL/6, *Trpa1*$^{+/+}$, or *Trpa1*$^{-/-}$ by measuring the acute nocifensive responses to the acetone-evoked evaporative cooling as previously described [22]. Briefly, the animal was held in the hand and a droplet (50 μl) of acetone, formed on the flat-tip needle of a syringe, was gently touched to the plantar surface of the hind paw. The mouse was immediately put in a cage with a transparent floor, and the time spent in elevation and licking of the plantar region over a 60-s period was measured. Acetone was applied three times at a 10–15-min interval, and the average of elevation/licking time was calculated. Cold allodynia was measured in mice before (baseline) and for 20 days after drug treatment.

Isolation of primary sensory neurons

Primary dorsal root ganglia (DRG) from *Trpa1*$^{+/+}$ or *Trpa1*$^{-/-}$ adult mice were cultured as previously described [31]. Briefly, lumbosacral (L5–S2) ganglia were bilaterally excised under a dissection microscope. Ganglia were digested using 2 mg/ml of collagenase type 1A and 1 mg/ml of papain in HBSS (25 min, 37°C). Neurons were pelleted and resuspended in Ham's-F12 containing 10% FBS, 100 U/ml of penicillin, 0.1 mg/ml of streptomycin, and 2 mM glutamine, dissociated by gentle trituration, and plated on glass coverslips coated with poly-L-lysine (8.3 μM) and laminin (5 μM). Neurons were cultured for 3–4 days.

Calcium imaging experiments

Cells were incubated with 5 μM Fura-2 AM ester for 30 min at 37°C. Intracellular calcium concentration ($[Ca^{2+}]_i$) was measured on Nikon Eclipse TE2000U microscope. Fluorescence was measured during excitation at 340 and 380 nm for 5 min before and 10 min after stimulus administration, and after correction for the individual background fluorescence signals, the ratio of the fluorescence at both excitation wavelengths (F_{340}/F_{380}) was monitored. Experiments were performed using a buffer solution containing (in millimolars): 150 NaCl, 6 KCl, 1 $MgCl_2$, 1.5 $CaCl_2$, 10 glucose, and 10 HEPES and titrated to pH 7.4 with 1 N NaOH. Cells were exposed to paclitaxel (10 and 50 μM), allyl isothiocyanate (AITC, 30 μM), or their respective vehicles (0.1%, 0.5%, and 0.03% DMSO). DRGs were challenged with capsaicin (0.1 μM) and by KCl (50 mM) to identify nociceptive neurons and at the end of each experiment with ionomycin (5 μM).

Calcitonin gene-related peptide release

Slices (0.4 mm) of esophagus taken from C57/BL6, *Trpa1*$^{+/+}$, or *Trpa1*$^{-/-}$ were superfused with paclitaxel (10-30-50 μM), or the vehicle (2.5% DMSO), dissolved in a modified Krebs solution at 37°C, and oxygenated with 95% O_2 and 5% CO_2, containing (in millimolars): 119 NaCl, 25 $NaHCO_3$, 1.2 KH_2PO_4, 1.5 $MgSO_4$, 2.5 $CaCl_2$, 4.7 KCl, 11 D-glucose, 0.1% BSA, phosphoramidon (1 μM), and captopril (1 μM). Some tissues were preexposed to capsaicin (10 μM) for 20 min to desensitize TRPV1-expressing sensory nerve terminals. Some experiments were performed in a calcium-free medium, containing EDTA (1 mM). Other experiments were performed in the presence of HC-030031 (30 μM) and HC-067047 (3 μM) or in the presence of the unsaturated aldehyde and ROS scavenger, glutathione monoethylester (GSH, 1 mM). Calcitonin gene-related peptide (CGRP) immunoreactivity (CGRP-IR) was assayed in 10-min fractions (two before, one during, and one after exposure to the stimulus) according to the methods previously reported [41]. The detection limit was 5 pg/ml. CGRP-IR release was calculated by subtracting the mean pre-stimulus value from those obtained during or after stimulation. Stimuli did not cross react with CGRP antiserum.

Reagents

If not otherwise indicated, all reagents were from Sigma-Aldrich (Milan, Italy). HC-030031 was synthesized as previously described [6]. HC-067047 was from Tocris Bioscience (Bristol, United Kingdom), and paclitaxel was from Ascent Scientific Ltd (Bristol, UK).

Statistical analysis

Data are presented as mean±SEM. Statistical analyses were performed by the unpaired two-tailed Student's *t* test for comparisons between two groups, the one-way analysis of variance, followed by the post-hoc Bonferroni's test for comparisons of multiple groups. $p<0.05$ was considered statistically significant.

Results

TRPA1 and TRPV4 receptors activation contributes to the mechanical allodynia evoked by paclitaxel in mice

We first investigated the involvement of TRPA1 in the mechanical allodynia induced by paclitaxel in mice. As

previously reported [1], administration of a single dose of paclitaxel (6 mg/kg, i.p.) produced a delayed reduction in mechanical nociceptive threshold as assayed by the Von Frey hair test in C57BL/6 mice. Reduction from baseline value was significant at day 2, peaked at day 8, and returned to baseline about 20 days after paclitaxel administration (Fig. 1a). A role for the TRPV4 channel in paclitaxel-induced sensory hypersensitivity has been previously reported by using TRPV4 knockout mice and antisense-mediated TRPV4 knockdown [1, 14]. Here we confirm that administration of the selective TRPV4 antagonist, HC-067047 (10 mg/kg, i.p.) [18], 8 days after paclitaxel injection partially reverted paclitaxel-evoked mechanical allodynia. In agreement with previous reports in a different pain model [18], maximum inhibition by HC-067047 was evident 30 min post dosing. HC-067047 did not affect the baseline threshold for mechanical stimulation in naïve animals (Fig. 1c). In the present study, we also investigated TRPA1 contribution to mechanical allodynia induced by paclitaxel. Eight days after paclitaxel administration, systemic administration of the TRPA1 selective antagonist, HC-030031 (300 mg/kg, i.g.) [32], reverted partially mechanical allodynia. In keeping with previous data obtained in different models of hyperalgesia [17], the effect of HC-030031 was evident 60 min post dosing. HC-030031 did not affect the threshold in mechanical allodynia in naïve animals (Fig. 1b). Finally, we found that treatment with a combination of the TRPA1 antagonist, HC-030031 (300 mg/kg, i.g.) and the TRPV4 antagonist, HC-067047 (10 mg/kg, i.p.), 8 days after paclitaxel injection completely reverted paclitaxel-evoked mechanical allodynia (Fig. 1d).

In another series of experiments, we treated *Trpa1*$^{+/+}$ and *Trpa1*$^{-/-}$ mice following the same protocol used in C57BL/6 mice (one single dose of paclitaxel, 6 mg/kg, i.p.). In *Trpa1*$^{+/+}$ mice, the reduction in mechanical nociceptive threshold from baseline value was already significant at day 2, peaked at day 8, and returned to baseline about 20 days after paclitaxel administration. *Trpa1*$^{-/-}$ mice treated with paclitaxel developed a similar, although less pronounced, mechanical allodynia than that observed in *Trpa1*$^{+/+}$ mice. In particular, at days 7, 8, and 9 after paclitaxel administration, the threshold in the mechanical nociceptive response was significantly reduced in *Trpa1*$^{+/+}$ compared to *Trpa1*$^{-/-}$ mice (Fig. 1e). To further investigate the relative contribution of TRPV4 and TRPA1 in mechanical allodynia induced by paclitaxel, the effect of HC-067047 was studied in *Trpa1*$^{-/-}$ mice at day 8 after drug injection. Thirty minutes after treatment with HC-067047 (10 mg/kg, i.p.), mechanical allodynia induced by paclitaxel was completely reverted (Fig. 1f). Thus, present pharmacological and genetics data indicate that, in addition to TRPV4 [1], TRPA1 contributes to paclitaxel-evoked mechanical allodynia.

TRPA1 activation mediates the paclitaxel-induced cold hypersensitivity in mice

Next, by using the same treatment protocol, we addressed whether paclitaxel produced cold hypersensitivity by assaying the time spent licking the hind paw following acetone application for cooling stimulation, and the relative contribution of TRPA1 and TRPV4 activation in this response. A single dose of paclitaxel (6 mg/kg, i.p.) significantly increased the behavioral responses evoked following acetone application for cooling stimulation in C57BL/6 mice from day 4 to day 12 after paclitaxel administration (Fig. 2a). Peak increase was seen at day 8 (Fig. 2a). This effect of paclitaxel was completely reverted by treatment with HC-030031 (300 mg/kg, i.g.), 60 min post dosing. It should be underlined that time course of inhibition by HC-030031 of either mechanical or cold hypersensitivity was similar. HC-030031 did not affect cold sensitivity in naïve animals (Fig. 2b). Treatment with HC-067047 (10 mg/kg, i.p.) 8 days after paclitaxel injection did not affect the cold allodynia induced by the drug (Fig. 2c). Like C57BL/6 mice, *Trpa1*$^{+/+}$ mice treated with paclitaxel developed a cold hypersensitivity that started at day 2, peaked at day 8, and returned to baseline 18 days after paclitaxel administration (Fig. 2d). The increased response to the cold stimulus observed in *Trpa1*$^{+/+}$ mice was completely absent in *Trpa1*$^{-/-}$ mice, which responded to the stimulus in a manner superimposable to vehicle-treated animals. Pharmacological and genetic findings indicate that TRPA1, but not TRPV4, contributes to paclitaxel-evoked cold allodynia.

Paclitaxel does not directly activate TRPA1 or TRPV4 in dorsal root ganglion neurons but releases CGRP from peripheral nerve endings via glutathione-sensitive mechanism

Exposure to AITC (30 μM) of mouse DRG evoked a calcium response in neurons obtained from *Trpa1*$^{+/+}$ mice (24 cells of the 48 capsaicin (0.1 μM) sensitive neurons responded to AITC), an effect that was completely absent in DRG neurons taken from *Trpa1*$^{-/-}$ mice (0 cells of the 52 responding to capsaicin). Exposure to paclitaxel (50 μM) failed to evoke any significant calcium response in the 68 neurons tested, taken from *Trpa1*$^{+/+}$.

TRPA1 activation of peripheral terminals of capsaicin-sensitive primary sensory neurons is associated with the release of sensory neuropeptides, including CGRP [23]. Several peripheral tissues, including the esophagus [42], have been previously used to study the release of sensory neuropeptides. Paclitaxel increased the basal outflow of CGRP from slices of C57BL/6 mouse esophagus in a concentration-dependent manner (Fig. 3a), a response that was markedly reduced (>80% inhibition) by preexposure of

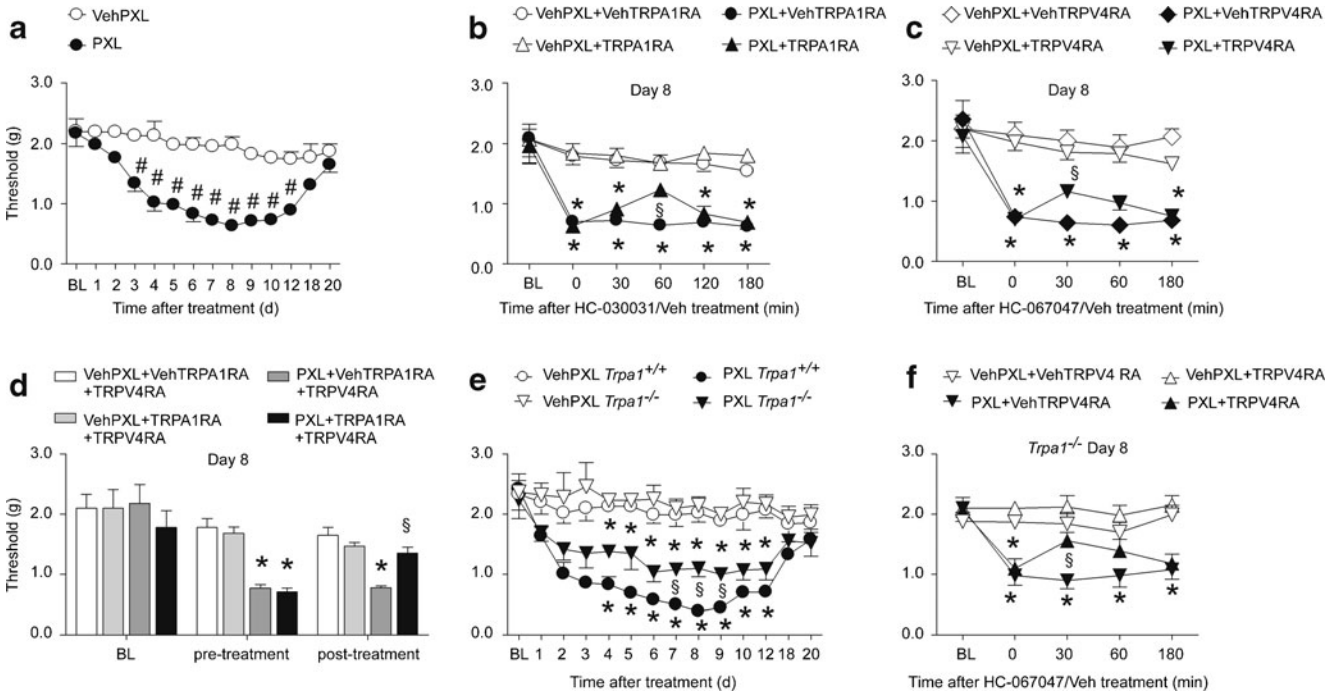

Fig. 1 Paclitaxel induces mechanical allodynia via TRPA1 and TRPV4 activation in mice. **a** The administration of a single dose of paclitaxel (*PXL*; 6 mg/kg, i.p.) in C57BL/6 mice induces a time-dependent reduction in mechanical nociceptive threshold (Von Frey test), with a maximum effect at day (*d*) 8 after PXL administration. At day 8 after PXL administration, treatment with TRPA1 receptor antagonist, HC-030031 (TRPA1RA; 300 mg/kg i.g), significantly reduces mechanical allodynia 60 min post dosing (**b**). A similar significant reduction in mechanical allodynia is visible after treatment with the TRPV4 receptor antagonist, HC-067047 (TRPV4RA; 10 mg/kg, i.p.), 30 min post dosing (**c**). At day 8 after PXL, treatment with a combination of TRPA1 and TRPV4 receptor antagonists HC-030031 and HC-067047 (TRPA1RA+ TRPV4RA) completely reverses the mechanical allodynia at the time of the maximum effect of inhibition for each antagonist (post-treatment; 60 and 30 min post HC-030031 and HC-067047 administration, respectively) (**d**). The administration of the same dose of PXL (6 mg/kg, i.p.) induces a time-dependent reduction in mechanical nociceptive threshold *Trpa1*$^{+/+}$ mice (**e**). The development of mechanical allodynia observed in *Trpa1*$^{+/+}$ mice after PXL treatment is not completely absent in *Trpa1*$^{-/-}$ mice. A significant difference in the reduction of mechanical nociceptive threshold between *Trpa1*$^{+/+}$ and T*rpa1*$^{-/-}$ mice is visible at days 7, 8, and 9 after PXL treatment. At day 8 after PXL administration, treatment with the TRPV4 antagonist HC-067047 (TRPV4RA; 10 mg/kg, i.p.) significantly reduces mechanical allodynia developed by *Trpa1*$^{-/-}$ mice after PXL treatment (**f**). Values are mean ± SEM of $n=8$–10 mice. #$p<0.05$ vs. VehPXL in **a**; Student's *t* test; *$p<0.05$ vs. VehPXL-VehTRPA1RA and VehPXL-TRPA1RA in **b**, or VehPXL-VehTRPV4RA and VehPXL-TRPV4RA in **c** or VehPXL-VehTRPA1 + TRPV4RA and VehPXL-TRPA1RA + TRPV4RA in **d** or VehPXL-*Trpa1*$^{+/+}$ and Veh PXL-*Trpa1*$^{-/-}$ in **e** or VehPXL-Veh TRPV4RA and VehPXL-TRPV4RA in **f**; $^{§}p<0.05$ vs. PXL-Veh TRPA1RA in **b**, or PXL-VehTRPV4RA in **c** and **f**, or PXL-Veh TRPA1RA + TRPV4RA in **d** or PXL *Trpa1*$^{-/-}$ in **e**; one-way ANOVA and Bonferroni's test. *BL* baseline withdrawal threshold

the tissue to a high capsaicin concentration (a procedure known to cause desensitization of sensory nerve terminals) or by removal of extracellular calcium ions from the bath solution (Fig. 3a). Thus, paclitaxel evokes a calcium-dependent neurosecretory process of CGRP from capsaicin-sensitive sensory neurons. Paclitaxel-evoked CGRP-IR release was reduced, but not abolished, in the presence of each individual antagonist of TRPA1 (HC-030031) or TRPV4 (HC-067047) channel (Fig. 3b). However, pretreatment of the tissue with GSH (1 mM) abated completely the paclitaxel-evoked increase in CGRP-IR outflow (Fig. 3b).

Exposure to paclitaxel increased the CGRP-IR outflow from slices of esophagus obtained from *Trpa1*$^{+/+}$ mice. This response was significantly, but not completely, reduced in preparations obtained from *Trpa1*$^{-/-}$ mice (Fig. 3c). To further investigate the contribution of the oxidative stress byproducts that eventually target TRPV4 receptor, esophageal slices from *Trpa1*$^{-/-}$ mice were exposed to paclitaxel in the presence of GSH. Under these circumstances, GSH further decreased paclitaxel-evoked CGRP-IR release (Fig. 3c). Thus, paclitaxel evokes a calcium-dependent neurosecretory process from capsaicin-sensitive neurons by a dual TRPA1 and TRPV4 dependent mechanism and in a manner entirely sensitive to GSH.

Discussion

Sensory PN affects a proportion of patients treated with the anticancer drug, paclitaxel, and this adverse reaction is often the cause for drug discontinuation [16]. The experimental counterpart of this clinical condition has been described in a large series of studies in rodents showing that paclitaxel causes mechanical and cold allodynia. Among the various

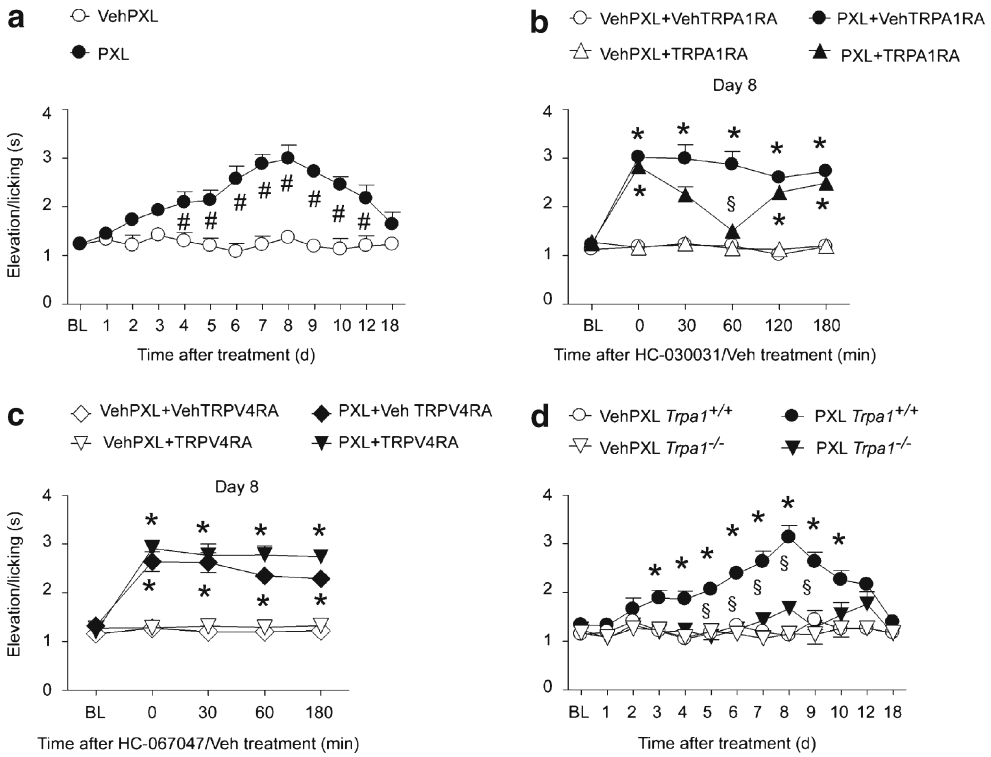

Fig. 2 Paclitaxel-induced cold hypersensitivity is mediated by TRPA1 activation in mice. **a** The administration of paclitaxel (PXL; 6 mg/kg, i.p.) induces in C57BL/6 mice a time-dependent increase in cold hypersensitivity (acetone test) with maximum effect at day (*d*) 8 after PXL administration. At day 8 after PXL treatment, TRPA1 receptor antagonist HC-030031 (TRPA1 RA; 300 mg/kg, i.g.) completely reverses the cold allodynia 60 min post dosing (**b**). Treatment with the TRPV4 receptor antagonist HC-067047 (TRPV4 RA; 10 mg/kg, i.p.) does not affect the cold allodynia induced by PXL (**c**). The development of cold allodynia observed in *Trpa1*$^{+/+}$ mice after PXL (6 mg/kg, i.p.) treatment is completely absent in *Trpa1*$^{-/-}$ mice (**d**). Values are mean ± SEM of n=8–10 mice. #p<0.05 vs. Veh PXL in **a**; Student's *t* test; *p<0.05 vs. VehPXL-VehTRPA1RA and VehPXL-TRPA1RA in **b**, or VehPXL-Veh TRPV4RA and VehPXL-TRPV4RA in **c** or VehPXL-*Trpa1*$^{+/+}$ in **d**; $^{§}p$<0.05 vs. PXL-VehTRPA1RA in **b** or PXL-*Trpa1*$^{-/-}$ in **e**; one-way ANOVA and Bonferroni's test. *BL* baseline withdrawal threshold

mechanisms proposed as causing the paclitaxel sensory neuropathy, recent evidence proposed a role for the TRPV4 channel in mechanical allodynia in mouse and rat models [1, 2]. Here, we confirm in a mouse model that TRPV4 contributes to mechanical allodynia induced by paclitaxel. We also show that TRPA1 accounts for the remaining TRPV4-

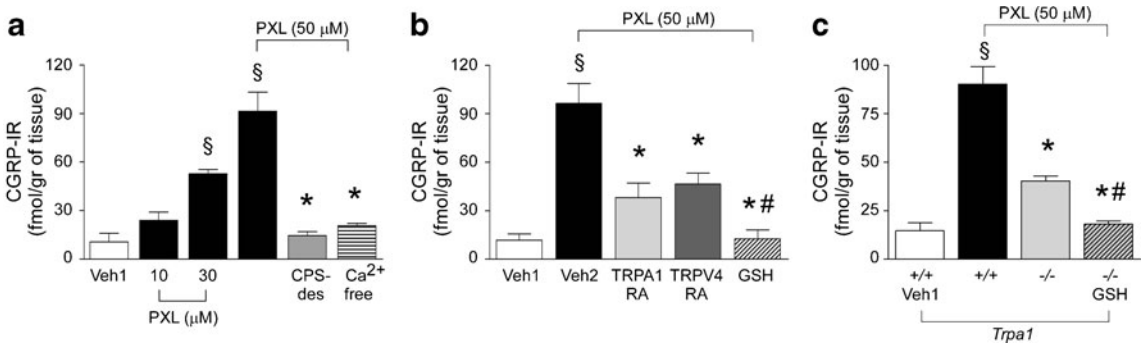

Fig. 3 Paclitaxel releases calcitonin gene-related peptide (CGRP) from mouse esophagus peripheral nerve endings. **a** Paclitaxel (*PXL*) increases the outflow of CGRP immunoreactivity (*CGRP-IR*) from slices of C57BL/6 mice esophagus in a concentration-dependent manner. CGRP-IR release evoked by PXL is abolished by capsaicin desensitization (*CPS-des*) or calcium removal (*Ca^{2+}-free*). **b** CGRP-IR evoked by PXL in peripheral tissues is significantly reduced by pretreatment with TRPA1, HC-030031 (*TRPA1 RA*, 30 μM), or TRPV4, HC-067047 (*TRPV4 RA*, 3 μM) selective antagonists and by glutathione (*GSH*, 1 mM). **c** Paclitaxel increases the release of CGRP-IR from esophageal slices obtained from *Trpa1*$^{+/+}$ mice, an effect significantly reduced in preparations taken from *Trpa1*$^{-/-}$ mice. Pretreatment of the esophageal slices taken from *Trpa1*$^{-/-}$ mice with GSH (1 mM) abated the CGRP-IR release induced by paclitaxel. Veh1 is the vehicle of PXL and Veh2 is a combination of vehicles of the various treatments. Values are mean ± SEM of n=5 experiments. $^{§}p$<0.05 vs. Veh1; *p<0.05 vs. Veh2 or PXL-*Trpa1*$^{+/+}$, $^{\#}p$<0.05 vs. TRPA1 RA and TRPV4 RA or PXL-*Trpa1*$^{-/-}$

resistant component of the mechanical hypersensitivity produced by the anticancer drug. This conclusion is derived from either pharmacological study, using selective TRPA1 and TRPV4 antagonists, or genetic study, using TRPA1-deficient mice. The TRPV4 antagonist, HC-067047, abated completely the component of the paclitaxel-evoked mechanical allodynia that was resistant to TRPA1 pharmacological blockade or genetic deletion.

Paclitaxel administration to rodents evokes a typical cold hypersensitivity, reminiscent of the clinical condition caused by the drug in treated patients [19]. In contrast, with mechanical allodynia, either pharmacological or genetic studies indicate a primary and unique role of TRPA1 in the present mouse model of cold hypersensitivity evoked by paclitaxel. This conclusion is derived from the observation that, either after treatment with HC-030031, or in TRPA1-deficient mice, paclitaxel-induced cold allodynia was completely abated, and that HC-067047 failed to affect the increased response to acetone after paclitaxel treatment. Thus, under the present circumstances, cold hypersensitivity is completely mediated by TRPA1, whereas both TRPA1 and TRPV4 contribute to mechanical allodynia.

There is compelling evidence obtained both in vitro or in vivo, both in experimental animals and in humans, that paclitaxel treatment is associated with production of oxidative stress [3, 38]. Indeed, accumulation of hydrogen peroxide is an early and crucial step for paclitaxel-induced cancer cell death [3]. In general, induction of oxidative stress as a mechanism that may contribute to the antineoplastic effect of several chemotherapeutic agents has been gaining acceptance [39]. Antioxidants, such as *N*-acetylcysteine, have been shown to inhibit both paclitaxel-evoked decreases in cell viability and increases in intracellular levels of ROS and apoptosis, [30]. *N*-acetylcysteine has been reported to prevent completely paclitaxel-evoked mechanical hypersensitivity [20]. Thus, the proapototic effects on one side, and the establishment of the sensory PN on the other side, seem to be dependent on one single mechanism, e.g., the ability of paclitaxel to generate oxidative stress. We have recently identified the primary role of TRPA1 in mediating mechanical and cold hypersensitivity to oxaliplatin and its ability to target TRPA1, not directly, but rather via oxidative stress generation [34]. In fact, we showed that, in contrast with the selective TRPA1 agonist, AITC, oxaliplatin per se does not activate TRPA1 in cultured DRG neurons, as measured by the ability to evoke an early calcium response [34]. However, in a more complex preparation, such as the isolated guinea pig pulmonary artery, oxaliplatin caused a TRPA1- and CGRP-dependent relaxation that mechanistically was indistinguishable from the relaxation evoked by AITC [34]. This finding suggested that oxaliplatin, like AITC, targets TRPA1 on sensory nerve endings, thereby releasing the sensory neuropeptide CGRP, which eventually relaxes the artery [34]. Of interest for the present discussion is the finding that oxaliplatin-evoked, but not AITC-evoked, arterial relaxation was completely abated by GSH. These findings imply that oxaliplatin does not directly gate TRPA1, but rather probably exerts this action indirectly via the generation by neighboring cells of oxidative stress byproducts that eventually target the channel in sensory nerve terminals, through direct formation of disulfide bridges.

Following this hypothesis, we tested whether paclitaxel could target sensory nerve terminals in a manner similar to that of oxaliplatin by measuring the release of the sensory neuropeptide, CGRP. Previous papers [27, 40] reported that paclitaxel releases substance P (SP) from airway sensory nerves, another neuropeptide co-expressed with CGRP in a subset of primary sensory neurons [26]. The mechanism of action of paclitaxel on sensory neurons remained unknown, although inhibition of paclitaxel-evoked SP release from DRG neurons by ruthenium red [33], a nonspecific TRP channels inhibitor [35], suggests the involvement of this type of channels. Here, we confirm that paclitaxel releases neuropeptides from terminals of capsaicin-sensitive primary sensory neurons, and for the first time we show, by using both pharmacological and genetic data, that the action of paclitaxel is mediated in part by TRPA1 activation and in part by TRPV4 activation. In addition, the ROS and reactive aldehydes, scavenger, GSH, completely abolished paclitaxel-evoked CGRP release from esophageal slices of either wild type or TRPA1-deficient mice. These findings indicate that GSH-sensitive compounds are generated by paclitaxel and finally target TRPA1 and TRPV4.

Additional issues remain to be determined. Although release experiments indicate that paclitaxel is apparently able to acutely stimulate both TRPA1 and TRPV4, it is only after a significant time delays (days) that mechanical allodynia (mediated by both TRPA1 and TRPV4) and cold hypersensitivity (mediated by TRPA1) develop. The time-dependent mechanism(s), which from early stimulation leads to the delayed and enduring hypersensitivity, is unknown. Pathophysiological functions of TRPV4 and TRPA1 are not completely understood; although TRPV4 is considered to mediate osmomechanical stimuli [29], TRPA1 has been proposed as a sensor of chemical irritants [10], and both may play a role in hyperalgesia [17]. Our present data are in agreement with recent findings reporting a contribution of TRPA1 and TRPV4 in paclitaxel-evoked hypersensitivity [14]. However, in our study, pharmacological inhibition and, more importantly, TRPA1 genetic deletion, reduced mechanical allodynia only partially, and it was only after TRPV4 inhibition that paclitaxel-evoked response was completely abated. The difference may be due to the diverse protocols of paclitaxel administration used in the present study (one single administration) as compared to the other study (repeated administrations) [14]. In the latter paper,

antagonism in the central nervous system of the proteinase-activated receptor 2 (PAR2) completely inhibited heat, cold, and mechanical hypersensitivity, three sensory modalities that, at different degrees, were mediated by TRPV1, TRPV4, and TRPA1, respectively. TRPV4 has been reported to induce thermal and mechanical hyperalgesia [44]. There is evidence that TRPA1 and TRPV4 can be sensitized by PAR2 [15, 24]. Thus, it is possible that PAR2 orchestrates the mechanism that eventually results in TRP channel-mediated hypersensitivity. However, the mechanism of the interaction between PAR2 and TRP channels, and the anatomo-functional site where the interaction occurs, remain to be determined.

A number of studies reported that antioxidants protect against the sensory neuropathy induced by paclitaxel [21, 38]. Present evidence shows that GSH inhibits TRPA1 and TRPV4 targeting on sensory nerves induced by paclitaxel. However, whereas endogenous oxidative stress byproducts capable of activating TRPA1 are well identified, little information [7] is available regarding activation of TRPV4 by oxidative stress byproducts, and no evidence exists that oxidative stress may activate PAR2. Thus, further studies are required to define upstream (oxidative stress) or downstream (PAR2) mechanisms apparently associated to paclitaxel-induced and TRPA1/TRPV4-mediated hypersensitivity. Irrespective of the underlying mechanism, previous [1, 2, 14, 34] and present findings support the hypothesis of using TRPA1 and TRPV4 antagonists to treat patients with PN evoked by anticancer medicines, such as paclitaxel or oxaliplatin.

Acknowledgments This work was supported by grants from Istituto Italiano di Tecnologia (Grant SEED, P.G.), Regione Toscana (Regional Health Research Program 2009, P.G.), and Ente Cassa Risparmio di Firenze.

References

1. Alessandri-Haber N, Dina OA, Joseph EK, Reichling DB, Levine JD (2008) Interaction of transient receptor potential vanilloid 4, integrin, and SRC tyrosine kinase in mechanical hyperalgesia. J Neurosci 28:1046–1057
2. Alessandri-Haber N, Dina OA, Yeh JJ, Parada CA, Reichling DB, Levine JD (2004) Transient receptor potential vanilloid 4 is essential in chemotherapy-induced neuropathic pain in the rat. J Neurosci 24:4444–4452
3. Alexandre J, Batteux F, Nicco C, Chereau C, Laurent A, Guillevin L, Weill B, Goldwasser F (2006) Accumulation of hydrogen peroxide is an early and crucial step for paclitaxel-induced cancer cell death both in vitro and in vivo. Int J Cancer 119:41–48
4. Alexandre J, Hu Y, Lu W, Pelicano H, Huang P (2007) Novel action of paclitaxel against cancer cells: bystander effect mediated by reactive oxygen species. Cancer Res 67:3512–3517
5. Andersson DA, Gentry C, Moss S, Bevan S (2008) Transient receptor potential A1 is a sensory receptor for multiple products of oxidative stress. J Neurosci 28:2485–2494
6. Andre E, Campi B, Materazzi S, Trevisani M, Amadesi S, Massi D, Creminon C, Vaksman N, Nassini R, Civelli M, Baraldi PG, Poole DP, Bunnett NW, Geppetti P, Patacchini R (2008) Cigarette smoke-induced neurogenic inflammation is mediated by alpha, beta-unsaturated aldehydes and the TRPA1 receptor in rodents. J Clin Invest 118:2574–2582
7. Bai J-Z, Lipski J (2010) Differential expression of TRPM2 and TRPV4 channels and their potential role in oxidative stress-induced cell death in organotypic hippocampal culture. Neurotoxicology 31:204–214
8. Basbaum AI, Bautista DM, Scherrer G, Julius D (2009) Cellular and molecular mechanisms of pain. Cell 139:267–284
9. Bautista DM, Jordt SE, Nikai T, Tsuruda PR, Read AJ, Poblete J, Yamoah EN, Basbaum AI, Julius D (2006) TRPA1 mediates the inflammatory actions of environmental irritants and proalgesic agents. Cell 124:1269–1282
10. Bessac BF, Jordt SE (2010) Sensory detection and responses to toxic gases: mechanisms, health effects, and countermeasures. Proc Am Thorac Soc 7:269–277
11. Bessac BF, Sivula M, von Hehn CA, Escalera J, Cohn L, Jordt SE (2008) TRPA1 is a major oxidant sensor in murine airway sensory neurons. J Clin Invest 118:1899–1910
12. Cella D, Peterman A, Hudgens S, Webster K, Socinski MA (2003) Measuring the side effects of taxane therapy in oncology: the functional assessment of cancer therapy-taxane (FACT-taxane). Cancer 98:822–831
13. Chaplan SR, Bach FW, Pogrel JW, Chung JM, Yaksh TL (1994) Quantitative assessment of tactile allodynia in the rat paw. J Neurosci Methods 53:55–63
14. Chen Y, Yang C, Wang ZJ (2011) Proteinase-activated receptor 2 sensitizes transient receptor potential vanilloid 1, transient receptor potential vanilloid 4, and transient receptor potential ankyrin 1 in paclitaxel-induced neuropathic pain. Neuroscience 193:440–451
15. Dai Y, Wang S, Tominaga M, Yamamoto S, Fukuoka T, Higashi T, Kobayashi K, Obata K, Yamanaka H, Noguchi K (2007) Sensitization of TRPA1 by PAR2 contributes to the sensation of inflammatory pain. J Clin Invest 117:1979–1987
16. Dougherty PM, Cata JP, Cordella JV, Burton A, Weng HR (2004) Taxol-induced sensory disturbance is characterized by preferential impairment of myelinated fiber function in cancer patients. Pain 109:132–142
17. Eid SR, Crown ED, Moore EL, Liang HA, Choong KC, Dima S, Henze DA, Kane SA, Urban MO (2008) HC-030031, a TRPA1 selective antagonist, attenuates inflammatory- and neuropathy-induced mechanical hypersensitivity. Mol Pain 4:48–58
18. Everaerts W, Zhen X, Ghosh D, Vriens J, Gevaert T, Gilbert JP, Hayward NJ, McNamara CR, Xue F, Moran MM, Strassmaier T, Uykal E, Owsianik G, Vennekens R, De Ridder D, Nilius B, Fanger CM, Voets T (2010) Inhibition of the cation channel TRPV4 improves bladder function in mice and rats with cyclophosphamide-induced cystitis. Proc Natl Acad Sci USA 107:19084–19089
19. Flatters SJ, Bennett GJ (2004) Ethosuximide reverses paclitaxel- and vincristine-induced painful peripheral neuropathy. Pain 109:150–161
20. Flatters SJ, Xiao WH, Bennett GJ (2006) Acetyl-L-carnitine prevents and reduces paclitaxel-induced painful peripheral neuropathy. Neurosci Lett 397:219–223
21. Fukui M, Yamabe N, Zhu BT (2010) Resveratrol attenuates the anticancer efficacy of paclitaxel in human breast cancer cells in vitro and in vivo. Eur J Cancer 46:1882–1891
22. Gauchan P, Andoh T, Kato A, Kuraishi Y (2009) Involvement of increased expression of transient receptor potential melastatin 8 in oxaliplatin-induced cold allodynia in mice. Neurosci Lett 458:93–95
23. Geppetti P, Holzer P (1996) Neurogenic inflammation. CRC, Boca Raton

24. Grant AD, Cottrell GS, Amadesi S, Trevisani M, Nicoletti P, Materazzi S, Altier C, Cenac N, Zamponi GW, Bautista-Cruz F, Lopez CB, Joseph EK, Levine JD, Liedtke W, Vanner S, Vergnolle N, Geppetti P, Bunnett NW (2007) Protease-activated receptor 2 sensitizes the transient receptor potential vanilloid 4 ion channel to cause mechanical hyperalgesia in mice. J Physiol 578:715–733
25. Hadzic T, Aykin-Burns N, Zhu Y, Coleman MC, Leick K, Jacobson GM, Spitz DR (2010) Paclitaxel combined with inhibitors of glucose and hydroperoxide metabolism enhances breast cancer cell killing via H2O2-mediated oxidative stress. Free Radic Biol Med 48:1024–1033
26. Harrison S, Geppetti P (2001) Substance p. Int J Biochem Cell Biol 33:555–576
27. Itoh Y, Sendo T, Hirakawa T, Goromaru T, Takasaki S, Yahata H, Nakano H, Oishi R (2004) Role of sensory nerve peptides rather than mast cell histamine in paclitaxel hypersensitivity. Am J Respir Crit Care Med 169:113–119
28. Jordt SE, Bautista DM, Chuang HH, McKemy DD, Zygmunt PM, Hogestatt ED, Meng ID, Julius D (2004) Mustard oils and cannabinoids excite sensory nerve fibres through the TRP channel ANKTM1. Nature 427:260–265
29. Liedtke W, Choe Y, Marti-Renom MA, Bell AM, Denis CS, Sali A, Hudspeth AJ, Friedman JM, Heller S (2000) Vanilloid receptor-related osmotically activated channel (VR-OAC), a candidate vertebrate osmoreceptor. Cell 103:525–535
30. Lyle PA, Mitsopoulos P, Suntres ZE (2011) N-acetylcysteine modulates the cytotoxic effects of paclitaxel. Chemotherapy 57:298–304
31. Materazzi S, Nassini R, Andre E, Campi B, Amadesi S, Trevisani M, Bunnett NW, Patacchini R, Geppetti P (2008) Cox-dependent fatty acid metabolites cause pain through activation of the irritant receptor TRPA1. Proc Natl Acad Sci USA 105:12045–12050
32. McNamara CR, Mandel-Brehm J, Bautista DM, Siemens J, Deranian KL, Zhao M, Hayward NJ, Chong JA, Julius D, Moran MM, Fanger CM (2007) TRPA1 mediates formalin-induced pain. Proc Natl Acad Sci USA 104:13525–13530
33. Miyano K, Tang HB, Nakamura Y, Morioka N, Inoue A, Nakata Y (2009) Paclitaxel and vinorelbine, evoked the release of substance P from cultured rat dorsal root ganglion cells through different PKC isoform-sensitive ion channels. Neuropharmacology 57:25–32
34. Nassini R, Gees M, Harrison S, De Siena G, Materazzi S, Moretto N, Failli P, Preti D, Marchetti N, Cavazzini A, Mancini F, Pedretti P, Nilius B, Patacchini R, Geppetti P (2011) Oxaliplatin elicits mechanical and cold allodynia in rodents via TRPA1 receptor. Pain 152:1621–1631
35. Nilius B, Owsianik G, Voets T, Peters JA (2007) Transient receptor potential cation channels in disease. Physiol Rev 87:165–217
36. Nilius B, Voets T (2007) Neurophysiology: channelling cold reception. Nature 448:147–148
37. Panis C, Herrera AC, Victorino VJ, Campos FC, Freitas LF, De Rossi T, Colado Simao AN, Cecchini AL, Cecchini R (2011) Oxidative stress and hematological profiles of advanced breast cancer patients subjected to paclitaxel or doxorubicin chemotherapy. Breast Cancer Res Treat. doi:10.1007/s10549-011-1693-x
38. Ramanathan B, Jan KY, Chen CH, Hour TC, Yu HJ, Pu YS (2005) Resistance to paclitaxel is proportional to cellular total antioxidant capacity. Cancer Res 65:8455–8460
39. Rigas B, Sun Y (2008) Induction of oxidative stress as a mechanism of action of chemopreventive agents against cancer. Br J Cancer 98:1157–1160
40. Tatsushima Y, Egashira N, Kawashiri T, Mihara Y, Yano T, Mishima K, Oishi R (2011) Involvement of substance P in peripheral neuropathy induced by paclitaxel but not oxaliplatin. J Pharmacol Exp Ther 337:226–235
41. Trevisani M, Siemens J, Materazzi S, Bautista DM, Nassini R, Campi B, Imamachi N, Andre E, Patacchini R, Cottrell GS, Gatti R, Basbaum AI, Bunnett NW, Julius D, Geppetti P (2007) 4-Hydroxynonenal, an endogenous aldehyde, causes pain and neurogenic inflammation through activation of the irritant receptor TRPA1. Proc Natl Acad Sci USA 104:13519–13524
42. Trevisani M, Smart D, Gunthorpe MJ, Tognetto M, Barbieri M, Campi B, Amadesi S, Gray J, Jerman JC, Brough SJ, Owen D, Smith GD, Randall AD, Harrison S, Bianchi A, Davis JB, Geppetti P (2002) Ethanol elicits and potentiates nociceptor responses via the vanilloid receptor-1. Nat Neurosci 5:546–551
43. van den Bent MJ, van Raaij-van den, Aarssen VJ, Verweij J, Doorn PA, Sillevis Smitt PA (1997) Progression of paclitaxel-induced neuropathy following discontinuation of treatment. Muscle Nerve 20:750–752
44. Vergnolle N, Cenac N, Altier C, Cellars L, Chapman K, Zamponi GW, Materazzi S, Nassini R, Liedtke W, Cattaruzza F, Grady EF, Geppetti P, Bunnett NW (2010) A role for transient receptor potential vanilloid 4 in tonicity-induced neurogenic inflammation. Br J Pharmacol 159:1161–1173

Published OnlineFirst March 11, 2013; DOI: 10.1158/0008-5472.CAN-12-4370

Novel Therapeutic Strategy to Prevent Chemotherapy-Induced Persistent Sensory Neuropathy By TRPA1 Blockade

Gabriela Trevisan[1,2], Serena Materazzi[2], Camilla Fusi[2], Alessandra Altomare[4], Giancarlo Aldini[4], Maura Lodovici[3], Riccardo Patacchini[5], Pierangelo Geppetti[2], and Romina Nassini[2]

Abstract

Chemotherapy-induced peripheral neuropathy (CIPN) is a severe and painful adverse reaction of cancer treatment in patients that is little understood or treated. Cytotoxic drugs that cause CIPN exert their effects by increasing oxidative stress, which activates the ion channel TRPA1 expressed by nociceptors. In this study, we evaluated whether TRPA1 acted as a critical mediator of CIPN by bortezomib or oxaliplatin in a mouse model system. Bortezomib evoked a prolonged mechanical, cold, and selective chemical hypersensitivity (the latter against the TRPA1 agonist allyl isothiocyanate). This CIPN hypersensitivity phenotype that was stably established by bortezomib could be transiently reverted by systemic or local treatment with the TRPA1 antagonist HC-030031. A similar effect was produced by the oxidative stress scavenger α-lipoic acid. Notably, the CIPN phenotype was abolished completely in mice that were genetically deficient in TRPA1, highlighting its essential role. Administration of bortezomib or oxaliplatin, which also elicits TRPA1-dependent hypersensitivity, produced a rapid, transient increase in plasma of carboxy-methyl-lysine, a by-product of oxidative stress. Short-term systemic treatment with either HC-030031 or α-lipoic acid could completely prevent hypersensitivity if administered before the cytotoxic drug. Our findings highlight a key role for early activation/sensitization of TRPA1 by oxidative stress by-products in producing CIPN. Furthermore, they suggest prevention strategies for CIPN in patients through the use of early, short-term treatments with TRPA1 antagonists. *Cancer Res; 73(10); 3120–31.* ©*2013 AACR.*

Introduction

Several anticancer medicines evoke sensory adverse events, collectively referred to as chemotherapy-induced peripheral neuropathy (CIPN), which are represented by sensory symptoms (from paresthesias, allodynia, and hyperalgesia to severe pain). In addition to impairing patient quality of life, CIPN may lead to dose-limitation or even discontinuation of anticancer treatment (1). No effective therapy is currently available to treat or prevent CIPN, most likely because the underlying mechanisms are poorly understood. A host of hypotheses has been proposed to explain CIPN, including mitochondrial dysfunction, increased content of oxidative substances, and altered function of different ion channels (2–7). Nonetheless, no unified mechanism that may reconcile results of clinical investigation and findings obtained in experimental animals has been advanced so far.

Chemotherapeutic drugs, which produce CIPN, are known to increase oxidative stress and reactive oxygen, nitrogen, or carbonyl species (ROS, RNS, and RCS, respectively) and treatment with antioxidant substances has been shown to reduce sensory hypersensitivity in experimental animals and to exhibit some degree of protection in patients with CIPN (3, 7–10). The transient potential receptor ankyrin 1 (TRPA1) is a nonselective cation channel, coexpressed with TRP vanilloid 1 (TRPV1) in a subset of C-fiber nociceptors, where it functions as a multimodal sensor to noxious stimuli (11, 12). TRPA1 shows a unique sensitivity for an unprecedented number of endogenous reactive molecules produced at sites of tissue injury or inflammation, which include ROS, RNS, and RCS (13–16).

Bortezomib is a proteasome inhibitor used in different types of cancer (17). CIPN has emerged as a major complication of bortezomib therapy, which usually appears in the first courses of therapy with a number of sensory and painful symptoms, including reduced threshold to mechanical and cold stimuli (18, 19). No satisfactory explanation or effective treatment

Authors' Affiliations: [1]Graduate Program in Biological Sciences: Toxicological Biochemistry, Department of Chemistry, Center of Natural and Exact Sciences, Federal University of Santa Maria (UFSM), Santa Maria, Brazil; [2]Department of Health Sciences, Clinical Pharmacology and Oncology Unit; [3]NEUROFARBA, Section of Pharmacology and Toxicology, University of Florence, Florence, Italy; [4]Department of Pharmaceutical Sciences, University of Milan, Milan; and [5]Pharmacology Department, Chiesi Farmaceutici SpA, Parma, Italy

Note: Supplementary data for this article are available at Cancer Research Online (http://cancerres.aacrjournals.org/).

Corresponding Author: Pierangelo Geppetti, Department of Health Sciences, Clinical Pharmacology and Oncology Unit, University of Florence, Viale Pieraccini 6, 50139 Florence, Italy. Phone: 39-055-427-1329; Fax: 39-055-427-1280; Email: geppetti@unifi.it

doi: 10.1158/0008-5472.CAN-12-4370

Published OnlineFirst March 11, 2013; DOI: 10.1158/0008-5472.CAN-12-4370

exists for bortezomib-evoked CIPN (20, 21). As described for other chemotherapeutics, bortezomib has been reported to increase oxidative stress (22, 23).

In the present study, first, we investigated the role of oxidative stress and TRPA1 in a mouse model of CIPN evoked by bortezomib. Biochemical, pharmacologic, and genetic findings show that TRPA1 is necessary and sufficient to develop and maintain bortezomib-evoked mechanical, cold, and chemical hypersensitivity in mice. Second, we showed that early and short-term pharmacologic TRPA1 blockade totally prevented the sensory neuropathy evoked by bortezomib and oxaliplatin (previously shown to produce a TRPA1-dependent hypersensitivity in mice; refs. 5, 6, 24), thus opening new perspectives for CIPN prevention and treatment.

Materials and Methods

Animals

Animal experiments were carried out according to Italian legislation (DL 116/92) and European Communities Council Directive (86/609/EEC). Studies were conducted under the permit (number 143/2008-B and 204/2012-B, University of Florence, Florence, Italy) approved by the Italian National Committee for Animal Research. C57BL/6 mice (male, 25–30 g; Harlan Laboratories), wild-type (*Trpa1*$^{+/+}$), or TRPA1-deficient mice (*Trpa1*$^{-/-}$; 25–30 g; Jackson Laboratories) were used. Animals were housed in a temperature- and humidity-controlled vivarium (12-hour dark/light cycle, free access to food and water). Behavioral experiments were done in a quiet, temperature-controlled room (20–22°C) between 9 a.m. and 5 p.m., and were conducted by an operator blinded to the genotype and the status of drug treatment. Animals were sacrificed with a high dose of intraperitoneal (i.p.) sodium pentobarbital (200 mg/kg).

Reagents

If not otherwise indicated, all reagents were from Sigma-Aldrich. HC-030031 [2-(1,3-Dimethyl-2,6-dioxo-1,2,3,6-tetrahydro-7H-purin-7-yl)-N-(4-isopropylphenyl)acetamide; Supplementary Fig. S1A] was synthesized as previously described (15). HC-067047 (2-Methyl-1-[3-(4-morpholinyl)propyl]-5-phenyl-N-[3-(trifluoromethyl)phenyl]-1H-pyrrole-3-carboxamide; Supplementary Fig. S1B) was obtained from Tocris Bioscience, and bortezomib was purchased from LC Laboratories.

Chemotherapy-induced painful neuropathy models

Previous studies have described rat and mouse models of peripheral neuropathy induced by repeated and prolonged administration of bortezomib (25–28). On the basis of these findings, in the first series of experiments, we explored whether a single administration of bortezomib produced mechanical and cold hypersensitivity in mice, as observed for different chemotherapeutic agents including oxaliplatin, paclitaxel, and vincristine (4, 6, 29). After habituation and baseline measurements of pain sensitivity, animals were randomized into treatment groups. C57BL/6, *Trpa1*$^{+/+}$, or *Trpa1*$^{-/-}$ mice were treated with a single intraperitoneal administration of different doses of bortezomib (0.2, 0.5, and 1 mg/kg), or vehicle (dimethyl sulfoxide, DMSO 1%; ref. 27). Bortezomib, formulated at a concentration of 1 mg/mL, was first dissolved in a vehicle containing DMSO, and the volume was adjusted to 10 mL/kg to a final concentration of 1% DMSO, then diluted in isotonic saline (NaCl 0.9%) to obtain lower doses. A different group of C57BL/6 mice was treated with a single administration of oxaliplatin (3 mg/kg, i.p.) or its vehicle (isotonic saline, NaCl 0.9%; ref. 6). No weight loss was observed in mice after bortezomib or oxaliplatin treatment throughout the duration of the experiments. Effects induced by bortezomib and oxaliplatin were tested for 14 and 30 days (starting 6 hours after drug administration), respectively. Baseline values for nociceptive tests were observed before chemotherapy treatment.

Nociceptive tests

Von frey hair test. Mechanical threshold was measured in C57/BL6, *Trpa1*$^{+/+}$, or *Trpa1*$^{-/-}$ mice after a single administration of bortezomib or oxaliplatin by using the up-and-down paradigm (30). Mechanical nociceptive threshold was determined before (basal level threshold) and after different treatments. The 50% mechanical paw withdrawal threshold (in g) response was then calculated from these scores, as previously described (30, 31).

Hot plate test. The paw thermal hyperalgesia was assessed in C57/BL6, *Trpa1*$^{+/+}$, or *Trpa1*$^{-/-}$ by placing animals on a hot plate (UgoBasile) with the temperature adjusted to 50 ± 0.1°C (32). The latency to the first hind paw licking or withdrawal was taken as an index of nociceptive threshold. The cut-off time was set at 30 seconds, to avoid damage to the paw. The paw-withdrawal latency to the first response was reported as mean of 2 different trials.

Cold stimulation. Cold allodynia was assessed in C57/BL6, *Trpa1*$^{+/+}$, or *Trpa1*$^{-/-}$ by measuring the acute nocifensive response to the acetone-evoked evaporative cooling as previously described (29). Briefly, a droplet (50 μL) of acetone, formed on the flat-tip needle of a syringe, was gently touched to the plantar surface of the mouse hind paw, and the time spent in elevation and licking of the plantar region over a 60-second period was measured. Acetone was applied 3 times at a 10- to 15-minute intervals, and the average of elevation/licking time was calculated.

Chemical hyperalgesia. Nociceptive behavior was assessed by measuring spontaneous nociceptive response induced by intraplantar (i.pl.) injection (20 μL) of sub-threshold doses of allyl isothiocyanate (AITC; 1 nmol/paw), capsaicin (0.01 nmol/paw), hypotonic saline (NaCl, 0.45%), or prostaglandin E_2 (PGE_2, 0.3 nmol/paw) at day 7 after the administration of bortezomib or its vehicle. Immediately after the injection, mice were placed inside a Plexiglas chamber and the total time spent licking and lifting the injected hind paw was recorded for 5 minutes (AITC, capsaicin, and hypotonic saline), or 20 minutes (PGE_2). Previous experiments conducted in our laboratory and previous findings (33, 34) suggested subthreshold doses that do not cause nociception in naïve mice.

Rotarod test

Locomotor function, coordination, and sedation of animals were tested by using a rotarod apparatus (UgoBasile). The test was done as previously described (35). Briefly, 24 hours before

Published OnlineFirst March 11, 2013; DOI: 10.1158/0008-5472.CAN-12-4370

the experiments, the animals were trained on the rotarod apparatus, programmed at 8 rpm, until they remained without falling for 60 seconds. The day of the experiment, the latency (seconds) to the first fall and the number of falls were recorded. Cut-off time was 240 seconds.

Treatment protocols

In a first set of experiments, intragastric (i.g.) HC-030031 (300 mg/kg) or its vehicle (0.5% carboxymethyl cellulose, CMC), HC-067047 (10 mg/kg, i.p.) or its vehicle (2.5% DMSO), or α-lipoic acid (100 mg/kg, i.g.) or its vehicle (0.5% CMC), were administered at day 7 after the administration of bortezomib (1 mg/kg, i.p.) or its vehicle. In a second set of experiments, i.pl. HC-030031 (100 μg/paw, 20 μL; ref. 36), α-lipoic acid (10 μg/paw, 20 μL; ref. 3), or vehicle (20 μL/paw, 1% DMSO in isotonic saline, NaCl 0.9%) were injected at day 3 or day 7 after the administration of oxaliplatin or bortezomib (see earlier section for dosing), respectively. In a third set of experiments, HC-030031 (300 mg/kg, i.g.), α-lipoic acid (100 mg/kg, i.g.), or their respective vehicles, were administered 15 minutes before the administration of bortezomib, oxaliplatin, or their vehicles and treatment was repeated 3 times at approximately 90-minute intervals each after the administration of bortezomib or oxaliplatin. In a fourth and final set of experiments, a group of mice was treated with HC-030031 or its vehicle 15 minutes before and shortly (3 times at approximately 90-minute intervals each) after a first bortezomib (1 mg/kg, i.p.) or vehicle administration. At day 6, each group of mice received a second treatment identical to that administered at day 1, except for mice treated at day 1 with both HC-030031 and bortezomib, which were subdivided into 2 additional groups. One group was treated a second time with either HC-030031 (300 mg/kg, i.g.) and the second with its vehicle 15 minutes before and shortly after (3 times at approximately 90-minute intervals each) bortezomib administration (Fig. 6A).

Isolation of primary sensory neurons and calcium imaging experiments

Primary dorsal root ganglia (DRG) from C57/BL6 adult mice were cultured as previously described (29). Briefly, lumbosacral (L5–S2) ganglia were bilaterally excised under a dissection microscope. Ganglia were digested using 1 mg/mL of collagenase type 1A and 1 mg/mL of papain in Hank's Balanced Salt Solution (25 minutes, 37°C). Neurons were pelleted and resuspended in Ham's-F12 containing 10% FBS, 100 U/mL of penicillin, 0.1 mg/mL of streptomycin, and 2 mmol/L glutamine, dissociated by gentle trituration, and plated on glass coverslips coated with poly-L-lysine (8.3 μmol/L) and laminin (5 μmol/L). Neurons were cultured for 3 to 4 days.

Cells were incubated with 5 μmol/L Fura-2AM ester for 30 minutes at 37°C. Intracellular calcium concentration ($[Ca^{2+}]_i$) was measured on a Nikon Eclipse TE2000U microscope. Fluorescence was measured during excitation at 340 and 380 nm, and after correction for the individual background fluorescence signals, the ratio of the fluorescence at both excitation wavelengths ($Ratio_{340/380}$) was monitored. Experiments were conducted using a buffer solution containing (in mmol/L): 150 NaCl, 6 KCl, 1 $MgCl_2$, 1.5 $CaCl_2$, 10 glucose, 10 HEPES and titrated to pH 7.4 with 1N NaOH. Cells were challenged with bortezomib (10, 50, and 100 μmol/L) or their respective vehicles (0.01, 0.5, and 1% DMSO), AITC (30 μmol/L), and capsaicin (0.1 μmol/L) to identify nociceptive neurons. In another series of experiments, DRG neurons were incubated with bortezomib (10 or 100 μmol/L) or its vehicle (0.01 and 0.1% DMSO) for 2 hours and then challenged with AITC (10 or 30 μmol/L). Results are expressed as the increase of $Ratio_{340/380}$ over the baseline normalized to the maximum effect induced by ionomycin (5 μmol/L) added at the end of the experiment.

Protein extraction and Western immunoblotassay

Spinal cord, DRGs, and hind paw skin were obtained from mice treated with bortezomib or its vehicle at day 7 post treatment. Tissue samples were homogenized in lysis buffer containing (in mmol/L): 50 Tris, 150 NaCl, 2 EGTA, 100 NaF, 1 Na_3VO_4, 1% Nonidet P40, pH 7.5, and complete protease inhibitor cocktail (Roche). Lysates were centrifuged at 14,000*g* at 4°C for 45 minutes. Protein concentration in supernatants was determined using DC protein assay (Bio-Rad). Samples with equal amounts of proteins (30 μg) were then separated by 10% SDS-PAGE electrophoresis, and the resolved proteins were transferred to a polyvinylidenedifluoride membrane (Merck Millipore Billerica). Membranes were incubated with 5% dry milk in Tris buffer containing 0.1% Tween 20 (TBST; 20 mmol/L Tris, pH 7.5, 150 mmol/L NaCl) for 1 hour at room temperature, and incubated with rat polyclonal primary antibody for TRPA1 detection (1:200; Novus Biologicals), or mouse monoclonal primary antibody for β-actin (1:6,000; Thermo Scientific), at 4°C overnight. Membranes were then probed with goat anti-mouse or donkey anti-rabbit IgG conjugated with horseradish peroxidase (Bethyl Laboratories Inc.) for 50 minutes at room temperature. Finally, membranes were washed 3 times with TBST, and bound antibodies were detected using chemiluminescence reagents (ECL; Pierce, Thermo Scientific). The density of specific bands was measured using an image-processing program (ImageJ 1.32J, Wayne Rasband) and normalized against a loading control (β-actin).

Carboxy-methyl-lysine adducts measurement in plasma

Briefly, blood samples from C57/BL6 mice, taken 1, 3, 6, and 24 hours after the administration of bortezomib (1 mg/kg, i.p.), oxaliplatin (3 mg/kg, i.p.), or their vehicles (1% DMSO and isotonic saline, NaCl 0.9%, respectively), were centrifuged at 3,500*g* for 10 minutes, and plasma was used for the carboxymethyl-lysine (CML) protein adduct ELISA assay. CML protein adducts content in plasma was measured using as ELISA kit (OxiSelect ELISA Kit, Cell Biolabs Inc. Valter Occhiena S.R.L.) according to the manufacturer's instructions.

Statistical analysis

Data are presented as mean ± SEM. Statistical analysis was carried out by the unpaired 2-tailed Student *t* test for comparisons between 2 groups, the ANOVA, followed by the *post hoc* Bonferroni test for comparisons of multiple groups. *P* value less than 0.05 was considered statistically significant (GraphPadPrism version 5.00). To meet ANOVA assumptions, mechanical

Published OnlineFirst March 11, 2013; DOI: 10.1158/0008-5472.CAN-12-4370

allodynia data were subjected to log transformation before statistical analysis.

Results

Bortezomib administration produces persistent mechanical cold and chemical hypersensitivity mediated by TRPA1

Administration of a single dose (0.2, 0.5, and 1 mg/kg, i.p.) of bortezomib induced a dose-dependent mechanical and cold hypersensitivity in C57BL/6 mice (Fig. 1A and B). Reduced mechanical threshold was observed after bortezomib (1 mg/kg, i.p.) injection as early as 6 hours and lasted until 11 days after treatment (Fig. 1A). Similar results were obtained for cold allodynia, which was evident at day 1 and persisted until day 11 after bortezomib injection (Fig. 1B). Bortezomib administration (1 mg/kg, i.p.) did not affect the heat threshold of mice at any time point, from 6 hours to 14 days after treatment. Nociception time to heat stimulus was 19.7 $\pm$ 0.8 seconds and 17.2 $\pm$ 1.0 seconds at baseline and 7 days after bortezomib treatment, respectively ($n = 8$–10 mice, $P > 0.05$, Student t test).

Next, we investigated whether TRPA1 activation is involved in mechanical and cold hypersensitivity induced by bortezomib. Systemic treatment with the TRPA1 selective antagonist HC-030031 (300 mg/kg, i.g.; ref. 37) at day 7 after bortezomib treatment completely, but transiently, reverted both mechanical hyperalgesia and cold allodynia. Significant inhibition was observed from 30 to 120 minutes after HC-030031 treatment, with maximum reduction (98 $\pm$ 12% and 90 $\pm$ 6% for mechanical hyperalgesia and cold allodynia, respectively) 60 minutes post dosing (Fig. 1C and D). Systemic treatment with HC-030031 (300 mg/kg, i.g.) at day 7 after treatment with bortezomib (0.2 or 0.5 mg/kg, i.p.) completely but transiently reverted both mechanical hyperalgesia and cold allodynia (data not shown).

Given that we, as well as others (29, 38), have found that mechanical and cold hypersensitivity evoked by paclitaxel was mediated by both TRPA1- and TRPV4-dependent mechanisms, we tested whether the TRPV4 channel contributes to bortezomib-induced sensory hypersensitivity by using a selective TRPV4 antagonist, HC-067047 (10 mg/kg, i.p.; ref. 39). HC-067047, at a dose able to reduce mechanical hyperalgesia evoked by paclitaxel (29), failed to affect bortezomib-evoked hypersensitivities (data not shown). Therefore, present pharmacologic evidence indicates an exclusive role for TRPA1 in bortezomib-induced mechanical allodynia and cold hypersensitivity in mice, whereas it rules out a contribution by TRPV4.

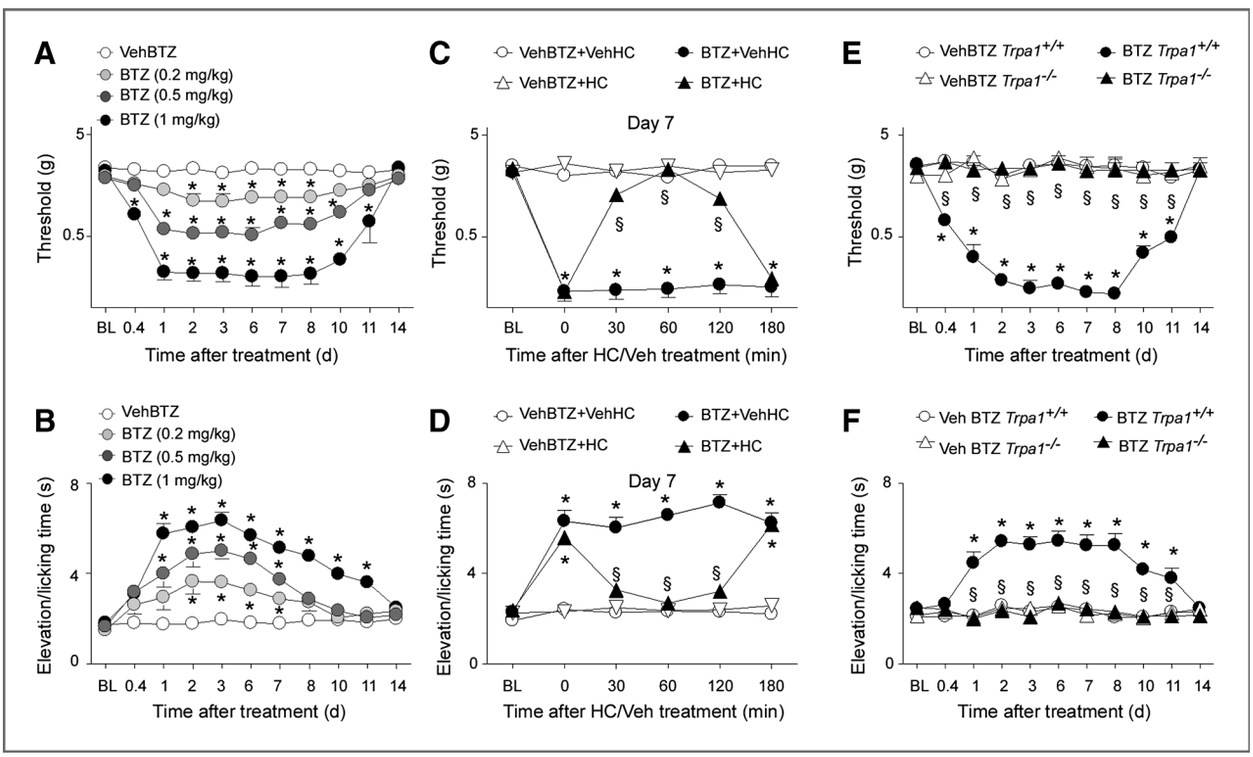

Figure 1. Bortezomib induces mechanical allodynia and cold hypersensitivity via TRPA1 activation in mice. A single dose of bortezomib (BTZ; 0.2, 0.5, and 1 mg/kg i.p.) induces in C57BL/6 mice a dose- and time-dependent mechanical (A) and cold (B) allodynia, which starts at 6 hours or day 1, respectively, and persists until day 11 after BTZ (1 mg/kg) administration. At day 7 after BTZ administration, the selective TRPA1 receptor antagonist, HC-030031 (HC; 300 mg/kg i.g.), completely reverses the mechanical (C) and cold (D) allodynia with a maximum effect, 60 minutes after dosing. BTZ treatment produces in *Trpa1*$^{+/+}$ mice mechanical (E) and cold (F) allodynia similar to those observed in C57BL/6. These effects are completely absent in *Trpa1*$^{-/-}$ mice (E and F). Veh, vehicle of BTZ or HC. Values are mean $\pm$ SEM of 8 to 10 mice. $^{\#}$, $P < 0.05$ versus VehBTZ, Student t test in A and B; *, $P < 0.05$ versus VehBTZ-VehHC in C and D and VehBTZ-*Trpa1*$^{+/+}$ in E and F; §, $P < 0.05$ versus BTZ-VehHC in C and D and BTZ-*Trpa1*$^{-/-}$ in E and F; one-way ANOVA and Bonferroni test. BL, baseline withdrawal threshold.

Published OnlineFirst March 11, 2013; DOI: 10.1158/0008-5472.CAN-12-4370

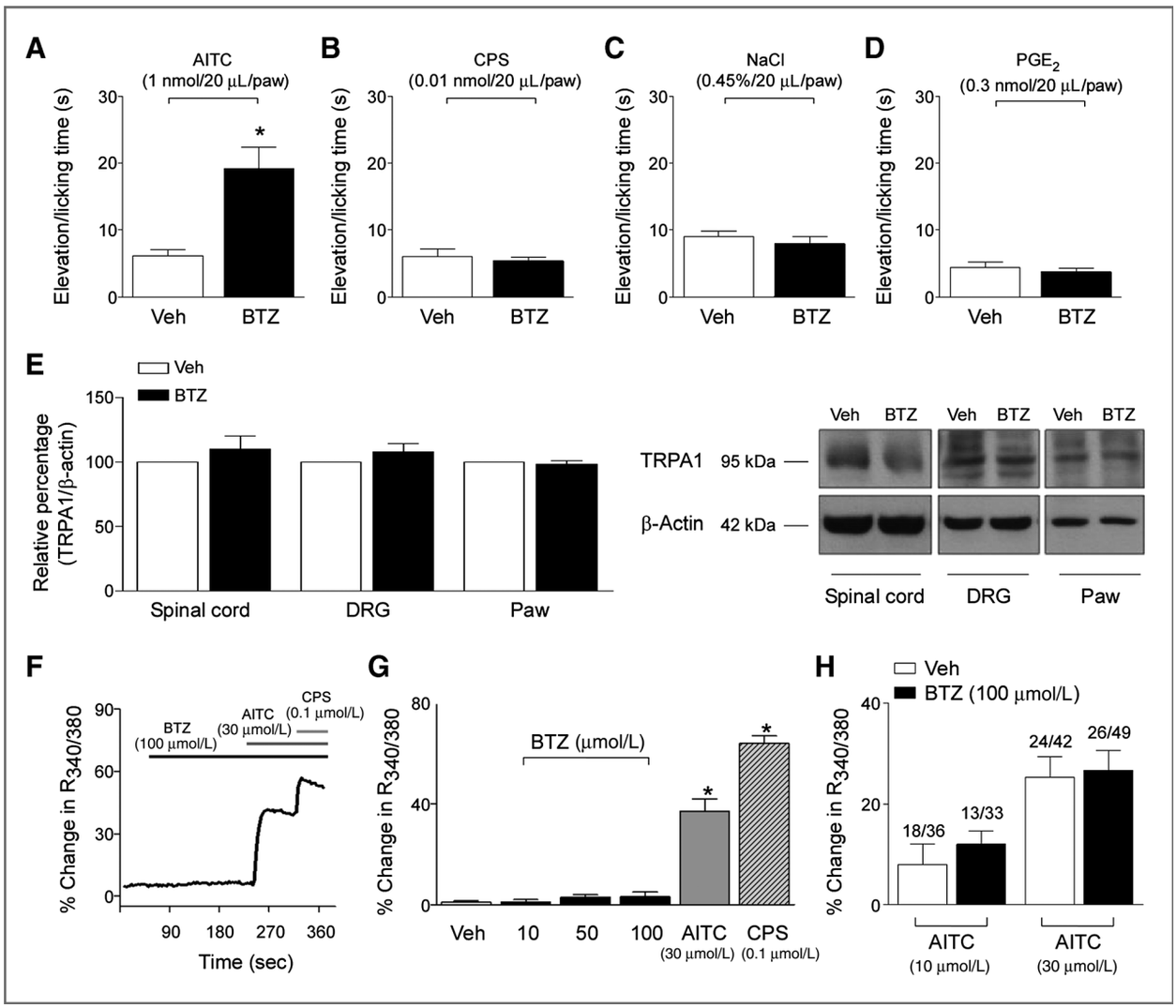

Figure 2. Bortezomib enhances allyl isothiocyanate-evoked nocifensive behavior but does not increase TRPA1 expression or directly activate TRPA1. Nociceptive behavior produced by a sub-threshold dose of intraplantar (i.pl.; 20 μL) injection of allyl isothiocyanate (AITC; 1 nmol/paw; A) in mice is increased 7 days after BTZ (1 mg/kg i.p.). Responses to subthreshold doses of capsaicin (CPS; 0.01 nmol/paw; B), hypotonic saline (NaCl, 0.45%; C), and PGE_2 (0.3 nmol/paw; D) are not affected by BTZ. Values are mean ± SEM of 8 to 10 mice. *, $P < 0.05$ versus VehBTZ-AITC in A; Student *t* test. E, TRPA1 protein content analyzed by Western blotting is not different in tissue homogenates of spinal cord, DRGs, and hind paw skin obtained from mice on day 7 after treatment with BTZ or its vehicle (Veh). Values are mean ± SEM of 3 samples, Student *t* test. Equally loaded protein was checked by expression of β-actin. A representative blot is shown. BTZ (10, 50, or 100 μmol/L) fails to evoke any visible intracellular calcium $(Ca^{2+})_i$ response in CPS (0.1 μmol/L)-sensitive DRG neurons, which otherwise responded to AITC (F, G). Trace represents an average of 10 neurons. H, *in vitro* preexposure to BTZ (100 μmol/L for 2 hours) does not affect the magnitude of the response, and the number of neurons responding to AITC (10 and 30 μmol/L). Veh is the vehicle of BTZ. Values are mean ± SEM of $n > 30$ neurons. Numbers indicate AITC-responding cells/CPS-responding cells. *, $P < 0.05$ versus Veh; one-way ANOVA and Bonferroni test.

More importantly, we found that bortezomib treatment (1 mg/kg, i.p.) produced mechanical hyperalgesia and cold allodynia in *Trpa1*$^{+/+}$ mice with an identical time course to that observed in C57BL/6 mice, an effect that was completely absent in *Trpa1*$^{-/-}$ mice (Fig. 1E and F).

In addition, we wondered whether bortezomib could cause selective chemical hypersensitivity to TRPA1 agonists. The study of the effects produced by sub-threshold doses of AITC (TRPA1 agonist), capsaicin (TRPV1 agonist), PGE_2 ($EP_{1\text{-}4}$ receptor agonist), or hypotonic saline (which can stimulate TRPV4) showed that bortezomib treatment selectively increased the nociceptive behavior evoked by AITC (Fig. 2A). In fact, responses to capsaicin, PGE_2, and hypotonic saline were similar in both vehicle- and bortezomib-treated animals (Fig. 2B–D). As expected, in TRPA1-deficient mice treated with bortezomib or its vehicle, AITC failed to evoke any nociceptive response (data not shown).

Bortezomib does not affect TRPA1 receptor expression and does not directly activate TRPA1

TRPA1 expression has been found to vary in different painful conditions, including models of CIPN (9, 40). Therefore, we

Published OnlineFirst March 11, 2013; DOI: 10.1158/0008-5472.CAN-12-4370

evaluated, by Western blotting, the expression of TRPA1 receptor in different tissues. At day 7 after administration, when hypersensitivity was at its maximum, TRPA1 immunoreactivity in the spinal cord, DRG, and hind paw skin of mice treated with bortezomib or its vehicle, were similar (Fig. 2E).

To test the hypothesis that bortezomib directly activates the TRPA1 receptor, we studied the ability of bortezomib to evoke calcium responses in cultured mouse DRG neurons. Bortezomib (10, 50, or 100 μmol/L) failed to evoke any calcium response in capsaicin-sensitive DRG neurons (Fig. 2F and G), which otherwise responded to the TRPA1 agonist AITC (30 μmol/L). *In vitro* pre-exposure to bortezomib (100 μmol/L for 2 hours) did not affect the magnitude or the number of neurons responding to AITC (10 and 30 μmol/L; Fig. 2H).

α-Lipoic acid transiently reverts bortezomib-evoked hypersensitivity

As reported for other anticancer drugs, such as oxaliplatin, paclitaxel, and others, there is evidence that bortezomib also produces oxidative stress (20, 21, 25, 41, 42). Therefore, we hypothesized that reactive molecules generated by the oxidative stress burst produced by bortezomib administration could be the underlying mechanism by which the anticancer drug induces TRPA1-dependent mechanical and cold hypersensitivity.

We observed that administration of α-lipoic acid (100 mg/kg, i.g.) completely abated mechanical hyperalgesia and cold allodynia evoked at day 7 after bortezomib treatment. Significant effect of α-lipoic acid was observed from 30 to 120 minutes after treatment, with maximum inhibition (73 ± 9% and 77 ± 6% for mechanical hyperalgesia and cold allodynia, respectively) 60 minutes post dosing (Fig. 3A and B).

Local treatment with HC-030031 or α-lipoic acid transiently reverts bortezomib- or oxaliplatin-induced hypersensitivity

It has been reported that i.pl. injection of α-lipoic acid reduces oxaliplatin-elicited nociception (3). In the present study, we observed that i.pl. injection of HC-030031 (100 μg/paw) or α-lipoic acid (10 μg/paw) completely reduced bortezomib-induced mechanical and cold allodynia (Fig. 3C and D). In addition, we found that mechanical and cold allodynia elicited by oxaliplatin were markedly decreased by i.pl. injection of HC-030031 and α-lipoic acid (Fig. 3E and F). Contralateral paw thresholds to mechanical or cold stimuli were not affected by the i.pl. injection of HC-030031 or α-lipoic acid (Fig. 3C–F). Administration of HC-030031 or α-lipoic acid (i.pl.) did not produce any appreciable effect in animals treated with the vehicle of bortezomib or oxaliplatin (data not shown).

Bortezomib and oxaliplatin increase plasma level of carboxy-methyl-lysine

Systemic oxidative stress was evaluated by measuring the serum content of Nε-carboxy-methyl-lysine (CML) protein adducts. CML is the reaction product between lysine and glyoxal, an α-ketoaldehyde intermediate formed by ascorbate autoxidation, lipid peroxidation, and oxidative degradation of glucose and degradation of glycated proteins. Due to the fact that CML is formed from either carbohydrates or lipids oxidation, it has been termed as an either advanced glycation or lipoxidation endproducts (EAGLE) modification. CML may be considered as a general marker of oxidative stress and, so far, it is widely used to measure oxidative stress in different pathophysiologic conditions (43). Bortezomib administration produced a transient increase in plasma CML levels. One hour after bortezomib injection, CML increased by 64% over baseline value, and returned to basal values at 3 hours after treatment (Fig. 4A). Similar to bortezomib, oxaliplatin administration produced a transient increase in plasma CML levels, which was observed at 1 hour (55% over the baseline) and 3 hours (63% over the baseline), and returned to basal levels 6 hours after treatment (Fig. 5A).

Early and short-term treatment with HC-030031 or α-lipoic acid completely prevents bortezomib- and oxaliplatin-evoked hypersensitivity

We investigated whether treatment with a TRPA1 antagonist or a ROS scavenger given shortly before and after anticancer drug administration could prevent the development of persistent mechanical, cold, and chemical hypersensitivity. To test this hypothesis HC-030031 (300 mg/kg, i.g.) or α-lipoic acid (100 mg/kg, i.g.), were given respectively, 15 minutes before and 3 times every 90 minutes after bortezomib or oxaliplatin administration. HC-030031 totally prevented the development of chemical hypersensitivity and mechanical and cold allodynia evoked by bortezomib (Fig. 4B, D, and E) and oxaliplatin (Fig. 5B, D, and E). Similarly, α-lipoic acid prevented chemical hypersensitivity and mechanical and cold allodynia evoked by bortezomib (Fig. 4C, F, and G) and oxaliplatin (Fig. 5C, F, and G). Repeated i.g. administration of TRPA1 antagonist (HC-030031, 300 mg/kg, i.g.) did not affect forced locomotion of animals, as observed by the rotarod test. HC-030031- and vehicle-treated animals did not show any fall during the test (data not shown).

Mice, protected by early and short-term treatment with HC-030031, were rechallenged 6 days after a first treatment with bortezomib with a second bortezomib administration (1 mg/kg, i.p.). In these mice, a second early and short-term treatment with HC-030031 again totally prevented the development of mechanical and cold hypersensitivity (Fig. 6B and C). In contrast, mice treated with HC-030031 vehicle did not show protection against the hypersensitivity evoked by the second administration of bortezomib. Mice treated with bortezomib and HC-030031 vehicle developed mechanical and cold hypersensitivity, a response that further increased at the second treatment with bortezomib and HC-030031 vehicle (Fig. 6B and C).

Discussion

In the present study in mice, we found that 1 single administration of bortezomib produced an early and prolonged mechanical and cold hypersensitivity that started 6 hours after and lasted for 11 days after bortezomib administration. With a slight difference in duration, the effect of bortezomib was practically identical to that previously reported for oxaliplatin (6). A number of preclinical studies and clinical investigations

Published OnlineFirst March 11, 2013; DOI: 10.1158/0008-5472.CAN-12-4370

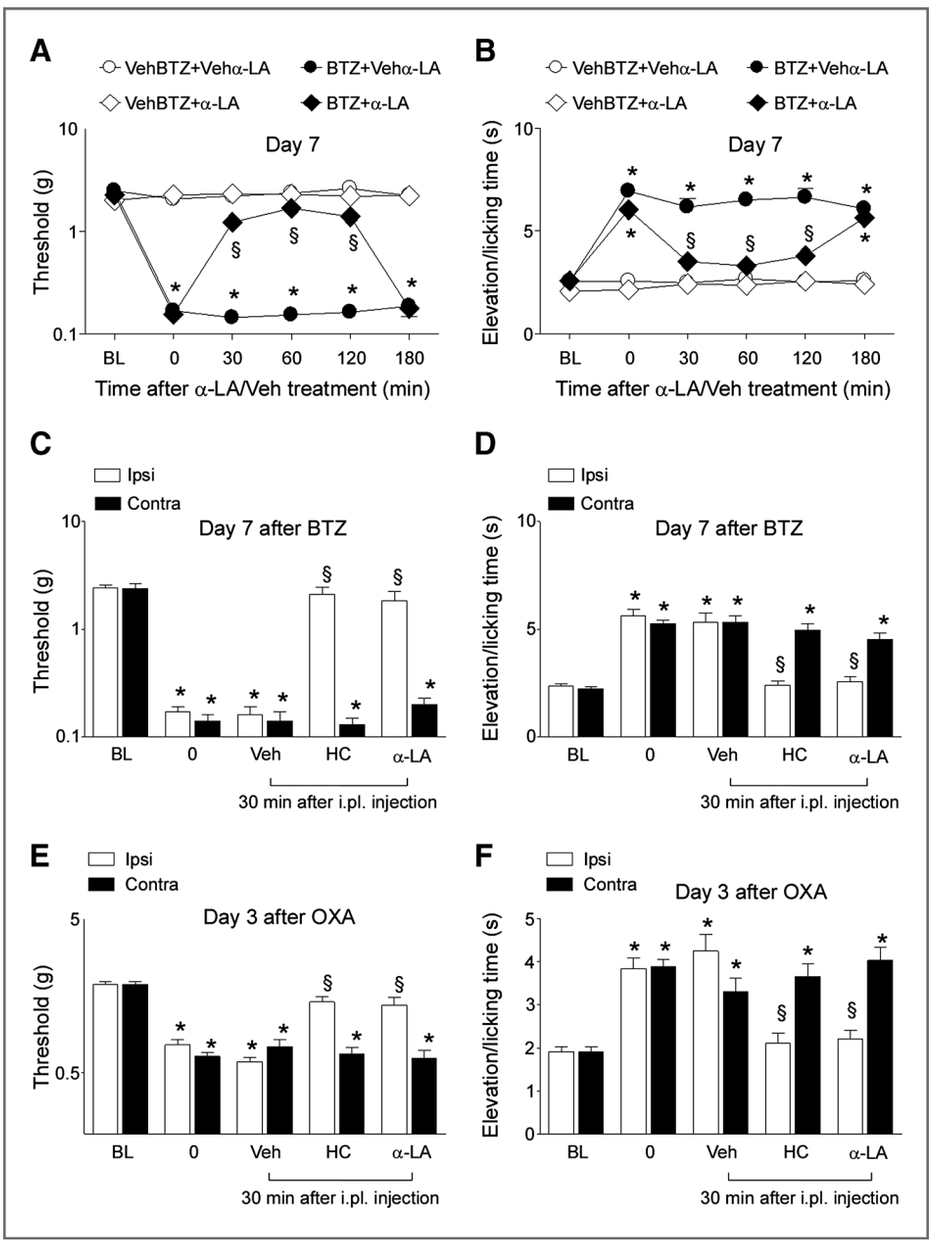

Figure 3. Systemic or local administration of α-lipoic acid (α-LA) and local administration of HC-030031 (HC) transiently reverse BTZ-evoked mechanical and cold hypersensitivity in mice. At day 7 after BTZ (1 mg/kg i.p.), α-LA (100 mg/kg i.g.) completely reverses the mechanical (A) and cold (B) allodynia with a maximum effect at 60 minutes post dosing. Veh, vehicle of BTZ or α-LA acid. C and E, HC (100 μg/paw, i.pl. 20 μL) or α-LA (10 μg/paw) reduce the mechanical allodynia induced by BTZ or oxaliplatin (OXA; 3 mg/kg, i.p.) in the paw ipsilateral (ipsi) to the injection. D and F, in the contralateral (contra) side, the paw threshold to mechanical stimuli is not affected by local HC or α-LA. Local HC or α-LA acid treatment produces similar findings when cold allodynia is measured. Values are mean ± SEM of 8 to 10 mice. *, $P < 0.05$ versus Vehα-LA acid or VehBTZ or BL values; §, $P < 0.05$ versus BTZ-Vehα-LA or Vehipsi; one-way ANOVA and Bonferroni test. BL, baseline withdrawal threshold.

have shown that bortezomib, like oxaliplatin and paclitaxel, increases ROS and their by-products in plasma, cells, and tissues of treated animals or patients, and that ROS scavengers show some degree of protection against CIPN or its rodent counterpart (3, 7–10, 44). Two observations suggest that oxidative stress mediates bortezomib-evoked sensory neuropathy. First, the ROS scavenger, α-lipoic acid, completely reversed the established (at day 7 after drug administration) mechanical and cold hypersensitivity evoked by bortezomib. Second, bortezomib and oxaliplatin produced an early and transient (1–3 hours after drug administration) increase in the plasma levels of 1 major by-product of oxidative stress, CML. The finding that oxaliplatin administration also increased plasma oxidative stress by-products is consistent with the previously reported role of oxidative stress in oxaliplatin-evoked sensory neuropathy (6).

TRPA1 has been identified as a sensor of oxidative stress, in as much as it is activated by an unprecedented series of ROS, RNS, or RCS (16, 45, 46). Thus, we hypothesized that oxidative stress by-products, generated by bortezomib, may target the TRPA1 channel in sensory nerve terminals. Indeed, both pharmacologic and genetic findings indicate that TRPA1 plays a key role in bortezomib-evoked mechanical and chemical hyperalgesia and cold allodynia, as these phenomena were completely reverted when they were at their maximum, for example, at day 7 after treatment, by a TRPA1 antagonist and were completely absent in TRPA1-deleted mice. The key contribution of TRPA1 in mechanical, chemical, and cold

Published OnlineFirst March 11, 2013; DOI: 10.1158/0008-5472.CAN-12-4370

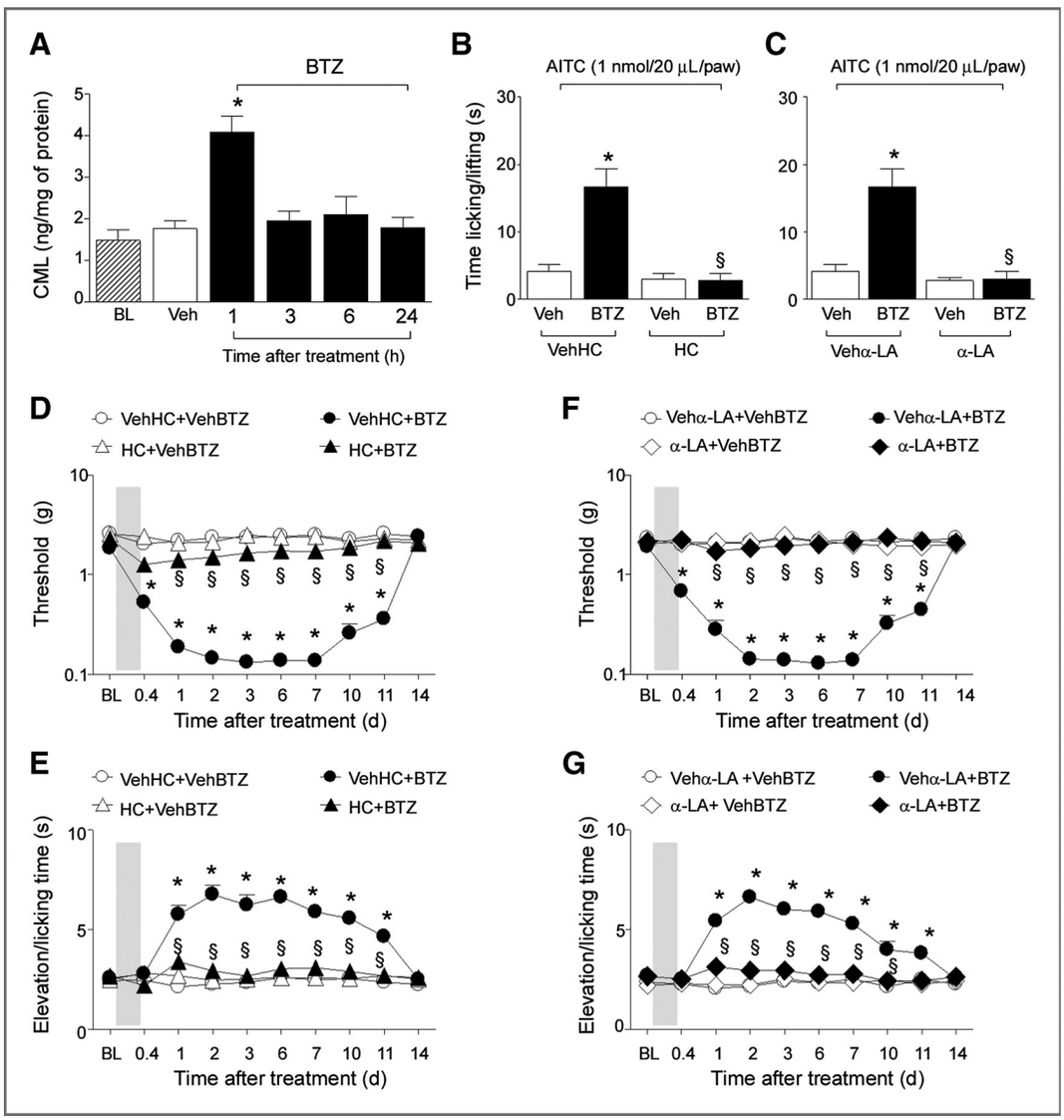

Figure 4. BTZ increases transiently oxidative stress in plasma and early and short-term treatment with HC and α-LA permanently prevents the development of mechanical, cold, and chemical hypersensitivity evoked by BTZ in mice. A, BTZ (1 mg/kg i.p.) transiently increases carboxy-methyl-lysine (CML) plasma levels in mice. Both HC (300 mg/kg i.g.) and α-LA (100 mg/kg i.g. 15 minutes before and 3 times at 90-minute intervals each after BTZ treatment) prevent the development and maintenance of chemical hyperalgesia (B and C) as well as mechanical (D and F) and cold (E and G) allodynia evoked by BTZ (1 mg/kg i.p.). Veh, of BTZ, HC, or α-LA. Values are mean ± SEM of 8 to 10 mice. *, $P < 0.05$ versus BL in A, VehHC-VehBTZ in B, D, and E, or Vehα-LA-VehBTZ in C, F, and G; §, $P < 0.05$ versus VehHC-BTZ in B, D, and E or Vehα-LA-BTZ- in C, F, and G; one-way ANOVA and Bonferroni test. BL, basal level of CML in A and baseline withdrawal threshold in D–G.

allodynia does not seem confined to bortezomib model as earlier studies (5, 6, 24) showed a similar role of TRPA1 in oxaliplatin-evoked sensory neuropathy in mice. In addition, the TRPV4-resistant component (38) of the mechanical hyperalgesia evoked by paclitaxel in mice has also been ascribed to the contribution of TRPA1, whereas TRPA1 appears to be the sole channel responsible for paclitaxel-evoked cold allodynia (29). In addition, we found that an oxidative stress scavenger or a TRPA1 antagonist reversed bortezomib- or oxaliplatin-evoked hypersensitivity selectively on the treated paw, when they were given locally by i.pl. administration. This finding indicates that TRPA1 sensitization/activation occurs at the very terminal region of nociceptive primary afferents, and that channel inhibition at this peripheral level is sufficient to revert the sensory neuropathy.

The protective effect of HC-030031 or α-lipoic acid when administered (either systemically or locally) at day 7 after bortezomib administration, although complete, was transient, lasting no longer than 120 minutes. This is probably due to the pharmacokinetic properties of the 2 drugs, as indicated by previous studies in different models of nociception or hyperalgesia/allodynia (47, 48). In contrast to the transient reversal produced by pharmacologic treatments when the hypersensitivity is already established, in TRPA1-deficient

Published OnlineFirst March 11, 2013; DOI: 10.1158/0008-5472.CAN-12-4370

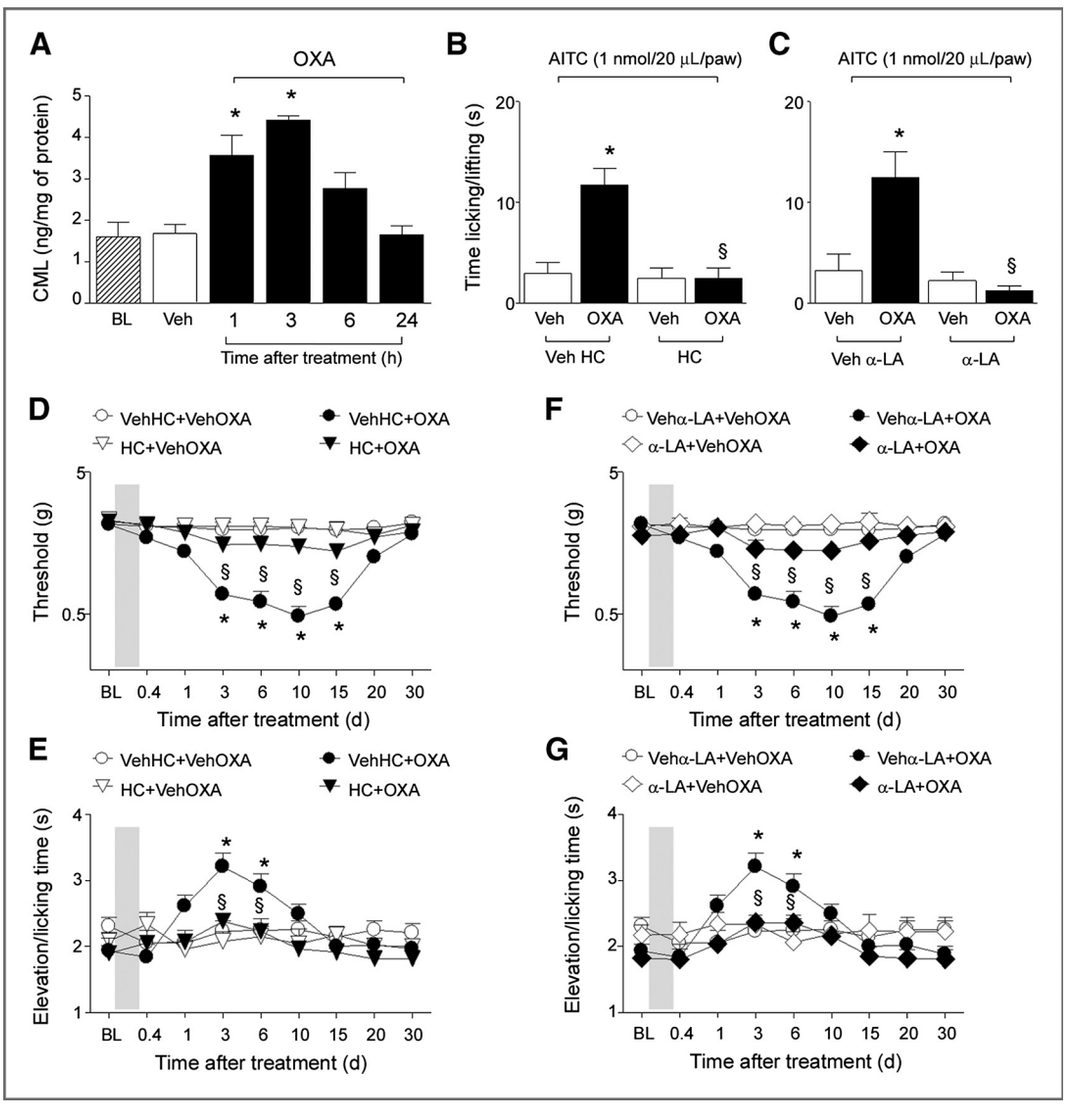

Figure 5. Oxaliplatin transiently increases oxidative stress in plasma, and early and short-term treatment with HC and α-LA permanently prevents the development of mechanical, cold, and chemical hypersensitivity evoked by BTZ in mice. A, oxaliplatin (OXA; 3 mg/kg i.p.) transiently increases CML plasma levels in mice. Both HC (300 mg/kg i.g.) and α-LA (100 mg/kg i.g. 15 minutes before and 3 times at 90-minute intervals each after BTZ treatment) prevent the development and maintenance of chemical hyperalgesia (B and C) as well as mechanical (D and F) and cold (E and G) allodynia evoked by OXA (3 mg/kg i.p.). Veh, vehicle of OXA, HC, or α-LA. Values are mean ± SEM of 8 to 10 mice. *, $P < 0.05$ versus BL in A, VehHC-VehOXA in B, D, and E or Vehα-LA-VehOXA in C, F, and G; §, $P < 0.05$ versus VehHC-OXA in B, D, and E or Vehα-LA-OXA in C, F, and G; one-way ANOVA and Bonferroni test. BL, basal level of CML in A and baseline withdrawal threshold in D–G.

mice hypersensitivity to bortezomib or oxaliplatin (6) does not develop. These genetic findings and biochemical evidence of the transient increase in plasma CML suggest that early phenotypic changes of TRPA1, presumably associated with the oxidative burst, which are responsible for the development and maintenance of the hypersensitivity, occur a few hours after chemotherapeutic drug administration. To identify the critical role of these early events for the manifestation of the enduring hypersensitivity condition by anticancer drug, we designed an experiment in which HC-030031 or α-lipoic acid were given shortly before and for approximately 6 hours after bortezomib or oxaliplatin treatment. These treatments not only blocked the onset of the hypersensitivity, but, rather surprisingly, completely and stably prevented its development and maintenance. Of interest for translating the present observation to the clinical perspective, the permanent protective effect by early and short-term treatment with the TRPA1 antagonist was also observed when it was repeated after a second bortezomib administration. Although it is not possible to replicate in mice the exact condition experienced by patients, these additional findings suggest a possible treatment schedule to prevent the sensory neuropathy in patients when TRPA1 antagonists are clinically available.

Published OnlineFirst March 11, 2013; DOI: 10.1158/0008-5472.CAN-12-4370

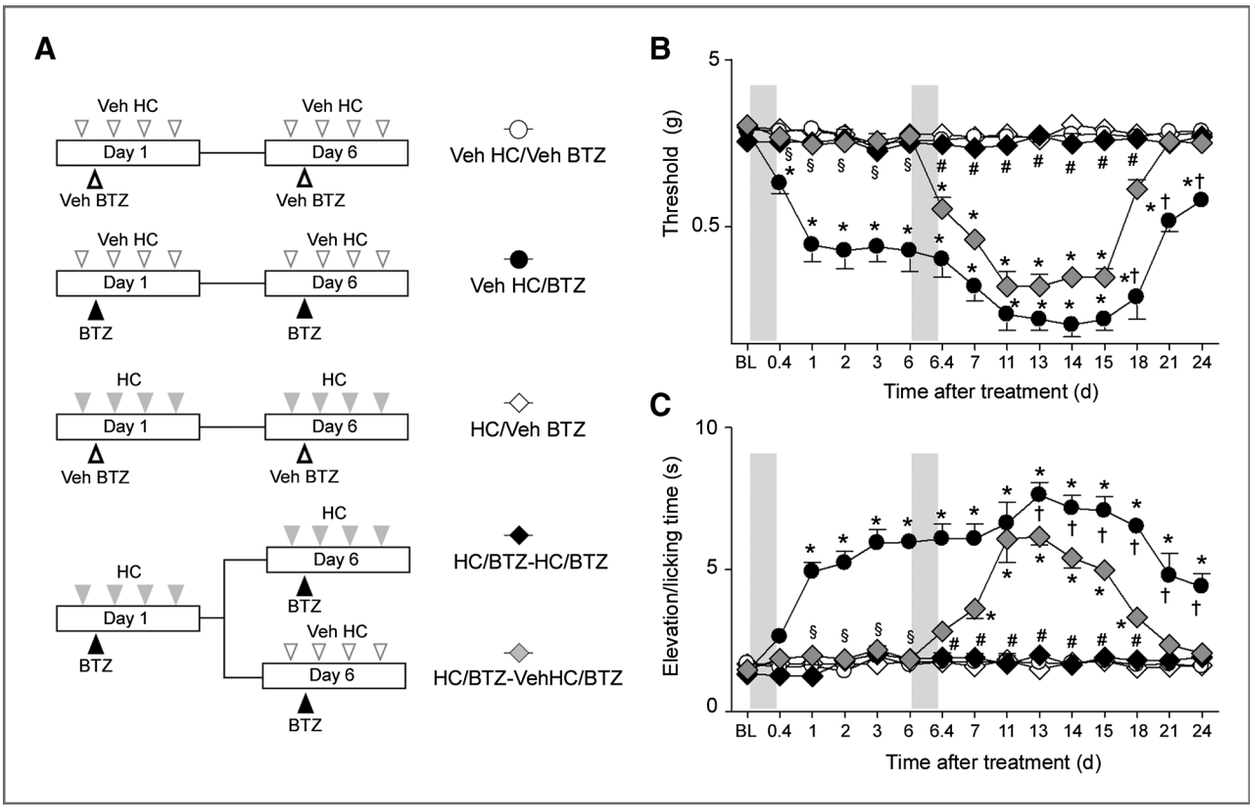

Figure 6. A repeated early and short-term treatment with HC prevents the development of mechanical and cold hypersensitivity evoked by a second BTZ treatment in mice. A, schematic representation of HC (300 mg/kg, i.g.) and BTZ (1 mg/kg, i.p.) treatment. A group of mice are treated with HC or its vehicle 15 minutes before and shortly after (3 times at ~90-minute intervals each) a first BTZ or vehicle administration. At day 6 after the first BTZ administration, all mice receive a second BTZ (1 mg/kg, i.p.) or vehicle administration. Mice pretreated with HC after the first BTZ dose are subdivided into 2 groups. One group is treated a second time with HC (300 mg/kg, i.g.) and a second group with its vehicle 15 minutes before and shortly after (3 times at ~90-minute intervals each) BTZ administration. The second early and short-term treatment with HC totally prevents the development of mechanical and cold hypersensitivity (B, C). B and C, mice treated with BTZ and HC vehicle develop mechanical and cold hypersensitivity, a response that is further increased by the second treatment with BTZ and HC vehicle. Values are mean ± SEM of 8 to 10 mice. *, $P < 0.05$ versus VehHC-VehBTZ in B and C; §, $P < 0.05$ versus VehHC-BTZ in B and C; #, $P < 0.05$ versus VehHC-BTZ or HC/BTZ-VehHC/BTZ; †, $P < 0.05$ versus HC/BTZ-VehHC/BTZ one-way ANOVA and Bonferroni test. BL, baseline withdrawal threshold.

Taken together, these findings indicate that TRPA1, via its activation by oxidative stress by-products, is necessary and sufficient to produce a sensory neuropathy paradigm in mice following a single administration of different chemotherapeutics. Oxaliplatin (6), paclitaxel (29), and bortezomib failed to evoke any calcium response in cultured TRPA1-expressing neurons, thus excluding that these drugs may directly target the channel. However, *in vitro* findings support the alternative explanation, as indicated by *in vivo* results, that chemotherapeutic agents act indirectly by generating oxidative stress by-products (3, 8, 9, 23), which in turn sensitize/activate TRPA1 in sensory neurons.

TRPA1 is apparently required for those early (within 6–8 hours) phenotypic changes that eventually result in the long-term hypersensitivity to specific (AITC) and nonspecific (pressure or cold) stimuli caused by exposure to different chemotherapeutic agents in mice. Although some reports have shown changes in TRP expression in different rodent models of CIPN, under the present experimental circumstances, no change in TRPA1 protein expression in nociceptive neurons was found. The molecular mechanism responsible for the TRPA1-mediated hypersensitivity phenotype, produced by chemotherapeutic agents remains unknown. Nevertheless, present experiments with bortezomib and oxaliplatin identify the early phase (a few hours) that follows chemotherapeutic drug administration as the key step when, most likely through oxidative stress by-products, TRPA1 is activated/sensitized. These early events result in a prolonged (several days) condition of hypersensitivity that markedly mimics the long-lasting duration of CIPN in patients treated with bortezomib or oxaliplatin. If ROS scavengers, most likely because of poor pharmacokinetics, could not represent a suitable and effective treatment for CIPN, the present findings suggest a novel therapeutic schedule to prevent CIPN in patients, based on TRPA1 antagonists given before and shortly after each administration of anticancer medicines.

Disclosure of Potential Conflicts of Interest

No potential conflicts of interest were disclosed.

Authors' Contributions

Conception and design: G. Trevisan, R. Patacchini, P. Geppetti, R. Nassini
Development of methodology: G. Trevisan, C. Fusi, M. Lodovici, R. Nassini
Acquisition of data (provided animals, acquired and managed patients, provided facilities, etc.): G. Trevisan, S. Materazzi, C. Fusi, A. Altomare, R. Nassini
Analysis and interpretation of data (e.g., statistical analysis, biostatistics, computational analysis): G. Trevisan, S. Materazzi, C. Fusi, G. Aldini, R. Nassini
Writing, review, and/or revision of the manuscript: G. Trevisan, S. Materazzi, M. Lodovici, R. Patacchini, P. Geppetti, R. Nassini
Study supervision: G. Trevisan, P. Geppetti, R. Nassini

Grant Support

This work was supported by grants from the Istituto Italiano di Tecnologia (Grant SEED, P. Geppetti), the Regione Toscana (Regional Health Research Program 2009 to P. Geppetti), the Fondazione Attilia Pofferi, Pistoia (P. Geppetti) and Associazione Italiana per la Ricerca sul Cancro (AIRC MFAG, 13336 to R. Nassini).

The costs of publication of this article were defrayed in part by the payment of page charges. This article must therefore be hereby marked *advertisement* in accordance with 18 U.S.C. Section 1734 solely to indicate this fact.

Received November 28, 2012; revised February 4, 2013; accepted February 25, 2013; published OnlineFirst March 11, 2013.

References

1. Cavaletti G, Marmiroli P. Chemotherapy-induced peripheral neurotoxicity. Nat Rev Neurol 2010;6:657–66.
2. Alessandri-Haber N, Dina OA, Joseph EK, Reichling DB, Levine JD. Interaction of transient receptor potential vanilloid 4, integrin, and SRC tyrosine kinase in mechanical hyperalgesia. J Neurosci 2008;28:1046–57.
3. Joseph EK, Chen X, Bogen O, Levine JD. Oxaliplatin acts on IB4-positive nociceptors to induce an oxidative stress-dependent acute painful peripheral neuropathy. J Pain 2008;9:463–72.
4. Gauchan P, Andoh T, Kato A, Sasaki A, Kuraishi Y. Effects of the prostaglandin E1 analog limaprost on mechanical allodynia caused by chemotherapeutic agents in mice. J Pharmacol Sci 2009;109:469–72.
5. Descoeur J, Pereira V, Pizzoccaro A, Francois A, Ling B, Maffre V, et al. Oxaliplatin-induced cold hypersensitivity is due to remodelling of ion channel expression in nociceptors. EMBO Mol Med 2011;3:266–78.
6. Nassini R, Gees M, Harrison S, De Siena G, Materazzi S, Moretto N, et al. Oxaliplatin elicits mechanical and cold allodynia in rodents via TRPA1 receptor stimulation. Pain 2011;152:1621–31.
7. Xiao WH, Bennett GJ. Effects of mitochondrial poisons on the neuropathic pain produced by the chemotherapeutic agents, paclitaxel and oxaliplatin. Pain 2012;153:704–9.
8. Pachman DR, Barton DL, Watson JC, Loprinzi CL. Chemotherapy-induced peripheral neuropathy: prevention and treatment. Clin Pharmacol Ther 2011;90:377–87.
9. Barriere DA, Rieusset J, Chanteranne D, Busserolles J, Chauvin MA, Chapuis L, et al. Paclitaxel therapy potentiates cold hyperalgesia in streptozotocin-induced diabetic rats through enhanced mitochondrial reactive oxygen species production and TRPA1 sensitization. Pain 2012;153:553–61.
10. Jaggi AS, Singh N. Mechanisms in cancer-chemotherapeutic drugs-induced peripheral neuropathy. Toxicology 2012;291:1–9.
11. Story GM, Peier AM, Reeve AJ, Eid SR, Mosbacher J, Hricik TR, et al. ANKTM1, a TRP-like channel expressed in nociceptive neurons, is activated by cold temperatures. Cell 2003;112:819–29.
12. Nilius B, Owsianik G, Voets T, Peters JA. Transient receptor potential cation channels in disease. Physiol Rev 2007;87:165–217.
13. Trevisani M, Siemens J, Materazzi S, Bautista DM, Nassini R, Campi B, et al. 4-Hydroxynonenal, an endogenous aldehyde, causes pain and neurogenic inflammation through activation of the irritant receptor TRPA1. Proc Natl Acad Sci U S A 2007;104:13519–24.
14. Andersson DA, Gentry C, Moss S, Bevan S. Transient receptor potential A1 is a sensory receptor for multiple products of oxidative stress. J Neurosci 2008;28:2485–94.
15. Materazzi S, Nassini R, Andre E, Campi B, Amadesi S, Trevisani M, et al. Cox-dependent fatty acid metabolites cause pain through activation of the irritant receptor TRPA1. Proc Natl Acad Sci U S A 2008;105:12045–50.
16. Sawada Y, Hosokawa H, Matsumura K, Kobayashi S. Activation of transient receptor potential ankyrin 1 by hydrogen peroxide. Eur J Neurosci 2008;27:1131–42.
17. Paramore A, Frantz S. Bortezomib. Nat Rev Drug Discov 2003;2:611–2.
18. Cata JP, Weng HR, Burton AW, Villareal H, Giralt S, Dougherty PM. Quantitative sensory findings in patients with bortezomib-induced pain. J Pain 2007;8:296–306.
19. Mohty B, El-Cheikh J, Yakoub-Agha I, Moreau P, Harousseau JL, Mohty M. Peripheral neuropathy and new treatments for multiple myeloma: background and practical recommendations. Haematologica 2010;95:311–9.
20. Broyl A, Corthals SL, Jongen JL, van der Holt B, Kuiper R, de Knegt Y, et al. Mechanisms of peripheral neuropathy associated with bortezomib and vincristine in patients with newly diagnosed multiple myeloma: a prospective analysis of data from the HOVON-65/GMMG-HD4 trial. Lancet Oncol 2010;11:1057–65.
21. Premkumar DR, Jane EP, Agostino NR, Didomenico JD, Pollack IF. Bortezomib-induced sensitization of malignant human glioma cells to vorinostat-induced apoptosis depends on reactive oxygen species production, mitochondrial dysfunction, Noxa upregulation, Mcl-1 cleavage, and DNA damage. Mol Carcinog 2011;2011:21835.
22. Shin YK, Jang SY, Lee HK, Jung J, Suh DJ, Seo SY, et al. Pathological adaptive responses of Schwann cells to endoplasmic reticulum stress in bortezomib-induced peripheral neuropathy. Glia 2010;58:1961–76.
23. Nakano A, Abe M, Oda A, Amou H, Hiasa M, Nakamura S, et al. Delayed treatment with vitamin C and *N*-acetyl-L-cysteine protects Schwann cells without compromising the anti-myeloma activity of bortezomib. Int J Hematol 2011;93:727–35.
24. Zhao M, Isami K, Nakamura S, Shirakawa H, Nakagawa T, Kaneko S. Acute cold hypersensitivity characteristically induced by oxaliplatin is caused by the enhanced responsiveness of TRPA1 in mice. Mol Pain 2012;8:55.
25. Cavaletti G, Gilardini A, Canta A, Rigamonti L, Rodriguez-Menendez V, Ceresa C, et al. Bortezomib-induced peripheral neurotoxicity: a neurophysiological and pathological study in the rat. Exp Neurol 2007;204:317–25.
26. Meregalli C, Canta A, Carozzi VA, Chiorazzi A, Oggioni N, Gilardini A, et al. Bortezomib-induced painful neuropathy in rats: a behavioral, neurophysiological and pathological study in rats. Eur J Pain 2009;14:343–50.
27. Bruna J, Udina E, Ale A, Vilches JJ, Vynckier A, Monbaliu J, et al. Neurophysiological, histological and immunohistochemical characterization of bortezomib-induced neuropathy in mice. Exp Neurol 2010;223:599–608.
28. Carozzi VA, Canta A, Oggioni N, Sala B, Chiorazzi A, Meregalli C, et al. Neurophysiological and neuropathological characterization of new murine models of chemotherapy-induced chronic peripheral neuropathies. Exp Neurol 2010;226:301–9.
29. Materazzi S, Fusi C, Benemei S, Pedretti P, Patacchini R, Nilius B, et al. TRPA1 and TRPV4 mediate paclitaxel-induced peripheral neuropathy in mice via a glutathione-sensitive mechanism. Pflugers Arch 2012;463:561–9.
30. Chaplan SR, Bach FW, Pogrel JW, Chung JM, Yaksh TL. Quantitative assessment of tactile allodynia in the rat paw. J Neurosci Methods 1994;53:55–63.
31. Dixon WJ. Efficient analysis of experimental observations. Annu Rev Pharmacol Toxicol 1980;20:441–62.
32. Ferreira J, Campos MM, Araujo R, Bader M, Pesquero JB, Calixto JB. The use of kinin B1 and B2 receptor knockout mice and selective antagonists to characterize the nociceptive responses caused by kinins at the spinal level. Neuropharmacology 2002;43:1188–97.

Published OnlineFirst March 11, 2013; DOI: 10.1158/0008-5472.CAN-12-4370

33. Alessandri-Haber N, Joseph E, Dina OA, Liedtke W, Levine JD. TRPV4 mediates pain-related behavior induced by mild hypertonic stimuli in the presence of inflammatory mediator. Pain 2005;118:70–9.
34. Kassuya CA, Ferreira J, Claudino RF, Calixto JB. Intraplantar PGE2 causes nociceptive behaviour and mechanical allodynia: the role of prostanoid E receptors and protein kinases. Br J Pharmacol 2007;150: 727–37.
35. Trevisan G, Rossato MF, Walker CI, Klafke JZ, Rosa F, Oliveira SM, et al. Identification of the plant steroid alpha-spinasterol as a novel transient receptor potential vanilloid 1 antagonist with antinociceptive properties. J Pharmacol Exp Ther 2012;343:258–69.
36. da Costa DS, Meotti FC, Andrade EL, Leal PC, Motta EM, Calixto JB. The involvement of the transient receptor potential A1 (TRPA1) in the maintenance of mechanical and cold hyperalgesia in persistent inflammation. Pain 2009;148:431–7.
37. McNamara CR, Mandel-Brehm J, Bautista DM, Siemens J, Deranian KL, Zhao M, et al. TRPA1 mediates formalin-induced pain. Proc Natl Acad Sci U S A 2007;104:13525–30.
38. Alessandri-Haber N, Dina OA, Yeh JJ, Parada CA, Reichling DB, Levine JD. Transient receptor potential vanilloid 4 is essential in chemotherapy-induced neuropathic pain in the rat. J Neurosci 2004;24:4444–52.
39. Everaerts W, Zhen X, Ghosh D, Vriens J, Gevaert T, Gilbert JP, et al. Inhibition of the cation channel TRPV4 improves bladder function in mice and rats with cyclophosphamide-induced cystitis. Proc Natl Acad Sci U S A 2010;107:19084–9.
40. Obata K, Katsura H, Mizushima T, Yamanaka H, Kobayashi K, Dai Y, et al. TRPA1 induced in sensory neurons contributes to cold hyperalgesia after inflammation and nerve injury. J Clin Invest 2005;115:2393–401.
41. Landowski TH, Megli CJ, Nullmeyer KD, Lynch RM, Dorr RT. Mitochondrial-mediated disregulation of Ca2+ is a critical determinant of Velcade (PS-341/bortezomib) cytotoxicity in myeloma cell lines. Cancer Res 2005;65:3828–36.
42. Wang HT, Liu ZG, Yang W, Liao AJ, Zhang R, Wu B, et al. [Study on mechanism of bortezomib inducing peripheral neuropathy and the reversing effect of reduced glutathione]. Zhonghua Xue Ye Xue Za Zhi 2011;32:107–11.
43. Aldini G, Dalle-Donne I, Facino RM, Milzani A, Carini M. Intervention strategies to inhibit protein carbonylation by lipoxidation-derived reactive carbonyls. Med Res Rev 2007;27:817–68.
44. Muthuraman A, Jaggi AS, Singh N, Singh D. Ameliorative effects of amiloride and pralidoxime in chronic constriction injury and vincristine induced painful neuropathy in rats. Eur J Pharmacol 2008; 587:104–11.
45. Bessac BF, Sivula M, von Hehn CA, Escalera J, Cohn L, Jordt SE. TRPA1 is a major oxidant sensor in murine airway sensory neurons. J Clin Invest 2008;118:1899–910.
46. Taylor-Clark TE, Ghatta S, Bettner W, Undem BJ. Nitrooleic acid, an endogenous product of nitrative stress, activates nociceptive sensory nerves via the direct activation of TRPA1. Mol Pharmacol 2009;75: 820–29.
47. Eid SR, Crown ED, Moore EL, Liang HA, Choong KC, Dima S, et al. HC-030031, a TRPA1 selective antagonist, attenuates inflammatory- and neuropathy-induced mechanical hypersensitivity. Mol Pain 2008;4: 48–58.
48. Morgado C, Pereira-Terra P, Tavares I. alpha-Lipoic acid normalizes nociceptive neuronal activity at the spinal cord of diabetic rats. Diabetes Obes Metab 2011;13:736–41.

nature COMMUNICATIONS

ARTICLE

Received 18 Apr 2014 | Accepted 3 Nov 2014 | Published 8 Dec 2014

DOI: 10.1038/ncomms6736 OPEN

Steroidal and non-steroidal third-generation aromatase inhibitors induce pain-like symptoms via TRPA1

Camilla Fusi[1,*], Serena Materazzi[1,*], Silvia Benemei[1,*], Elisabetta Coppi[1], Gabriela Trevisan[2], Ilaria M. Marone[1], Daiana Minocci[1], Francesco De Logu[1], Tiziano Tuccinardi[3], Maria Rosaria Di Tommaso[4], Tommaso Susini[4], Gloriano Moneti[1,5], Giuseppe Pieraccini[1,5], Pierangelo Geppetti[1] & Romina Nassini[1]

Use of aromatase inhibitors (AIs), exemestane, letrozole and anastrozole, for breast cancer therapy is associated with severe pain symptoms, the underlying mechanism of which is unknown. The electrophilic nature of AIs suggests that they may target the transient receptor potential ankyrin 1 (TRPA1) channel, a major pathway in pain transmission and neurogenic inflammation. AIs evoke TRPA1-mediated calcium response and current in rodent nociceptors and human cells expressing the recombinant channel. In mice, AIs produce acute nociception, which is exaggerated by pre-exposure to proalgesic stimuli, and, by releasing sensory neuropeptides, neurogenic inflammation in peripheral tissues. AIs also evoke mechanical allodynia and decreased grip strength, which do not undergo desensitization on prolonged AI administration. These effects are markedly attenuated by TRPA1 pharmacological blockade or in TRPA1-deficient mice. TRPA1 is a major mediator of the proinflammatory/proalgesic actions of AIs, thus suggesting TRPA1 antagonists for the treatment of pain symptoms associated with AI use.

[1] Department of Health Sciences, Section of Clinical Pharmacology and Oncology, University of Florence, Florence 50139, Italy. [2] Laboratory of Biological and Molecular Biology, Graduate Program in Health Sciences, University of the Extreme South of Santa Catarina (UNESC), Santa Catarina 88806-000, Brazil. [3] Department of Pharmacy, University of Pisa, Pisa 56126, Italy. [4] Department of Health Sciences, Section of Pediatrics, Obstetrics and Gynecology and Nursing, Florence 50139, Italy. [5] Mass Spectrometry Center, University of Florence, Florence 50139, Italy. * These authors contributed equally to this work. Correspondence and requests for materials should be addressed to P.G. (email: geppetti@unifi.it).

Third-generation aromatase inhibitors (AIs) are currently recommended for adjuvant endocrine treatment as primary, sequential or extended therapy with tamoxifen, for postmenopausal women diagnosed with oestrogen receptor-positive breast cancer[1–3]. AIs include the steroidal exemestane and non-steroidal azole derivatives, letrozole and anastrozole, which, via a covalent (exemestane) and non-covalent (azoles) binding, inactivate aromatase, the enzyme that catalyzes the conversion of androgens to oestrogens in peripheral tissue[4]. The use of AIs is, however, associated with a series of relevant side effects that are reported in 30–60% of treated patients[5,6]. Among these, the AI-associated musculoskeletal symptoms (AIMSS) are characterized by morning stiffness and pain of the hands, knees, hips, lower back and shoulders[7,8]. In addition to musculoskeletal pain, pain symptoms associated with AIs have recently been more accurately described with the inclusion of neuropathic, diffused and mixed pain[9]. The whole spectrum of painful conditions has been reported to affect up to 40% of patients, and to lead 10–20% of patients to non-adherence or discontinuation of treatment[7–14]. Although it has been proposed that oestrogen deprivation and several other factors, including a higher level of anxiety, may contribute to the development of AIMSS and related pain symptoms, none of these hypotheses has been confirmed[9,15]. Thus, the exact mechanism of such conditions is still unclear and, consequently, patients are undertreated.

The transient receptor potential ankyrin 1 (TRPA1) channel, belonging to the larger family of the TRP channels[16,17], is a polymodal sensor activated by chemical, mechanical and thermal stimuli[18–23]. TRPA1 is principally expressed by a subpopulation of primary sensory neurons[24,25], which express additional TRPs, including the TRP vanilloid 1 (TRPV1) channel, which is selectively targeted by capsaicin, the hot ingredient of red peppers[16]. TRPA1 and TRPV1 expressing pseudounipolar nociceptors produce and release from central and peripheral terminals the sensory neuropeptides, substance P (SP), neurokinin A (NKA) and calcitonin gene-related peptide (CGRP), which mediate neurogenic inflammation[26]. In particular, TRPA1 is the main target of many different irritant stimuli, such as allyl isothiocyanate (AITC, contained in mustard or wasabi) or cinnamaldehyde (contained in cinnamon), and of an unprecedented series of endogenous reactive molecules produced at sites of inflammation and tissue injury, including reactive oxygen (ROS), nitrative (RNS) or carbonyl (RCS) species[19,27–30]. TRPA1 is emerging as a major nociceptive and hyperalgesic mechanism in a variety of inflammatory pain models such as those induced by formalin, carrageenan and complete Freund adjuvant[31–34]. Also, in models of neuropathic pain, such as those evoked by spinal nerve ligation[35], streptozotocin[36] and chemotherapeutic-induced peripheral neuropathy[37–39], a key role of TRPA1 has been identified.

The chemical structure of exemestane includes a system of highly electrophilic conjugated Michael acceptor groups, which might react with the thiol groups of reactive cysteine residues[40]. Michael addition reaction with specific cysteine residues is a major mechanism that results in TRPA1 activation by a large variety of electrophilic compounds[19,41,42]. Aliphatic and aromatic nitriles can react with cysteine to form thiazoline derivatives and accordingly the tear gas 2-chlorobenzylidene malononitrile (CS) has been identified as a TRPA1 agonist[43]. We noticed that both letrozole and anastrozole possess nitrile moieties. Thus, we hypothesized that exemestane, letrozole and anastrozole may produce neurogenic inflammation, nociception and hyperalgesia by targeting TRPA1. Our present findings show that AIs directly stimulate TRPA1, and via this pathway provoke neurogenic inflammatory oedema, acute nociception, mechanical allodynia and reduced grip strength, indicating a new mechanism through which AIs induce cytokine-independent inflammation and pain, and suggesting TRPA1 antagonists as possible innovative therapies for pain-like symptoms associated with the use of AIs.

Results

Aromatase inhibitors selectively activate TRPA1 channels. To explore whether AIs gate the human TRPA1 channel, we first used cells stably transfected with human TRPA1 cDNA (hTRPA1-HEK293). In hTRPA1-HEK293 cells, which respond to the selective TRPA1 agonist AITC (30 μM), but not in untransfected HEK293 cells, the three AIs, exemestane, letrozole and anastrozole, evoked concentration-dependent calcium responses that were inhibited by the selective TRPA1 antagonist, HC-030031 (30 μM)[44] (Fig. 1a–c). EC_{50} of AIs ranged between 58 and 134 μM (Fig. 1b). The calcium response was abated in a calcium-free medium, thus supporting the hypothesis that the increase in intracellular calcium originates from extracellular sources (Supplementary Fig. 1a). In HEK293 cells stably transfected with human TRPV1 cDNA (hTRPV1-HEK293) all AIs (100 μM) were ineffective (Supplementary Fig. 1b). Key amino-acid residues are required for channel activation by electrophilic TRPA1 agonists[19,41,42]. Notably, HEK293 cells expressing a mutated TRPA1 channel (3C/K-Q), which presents substitutions of three cysteine with serine (C619S, C639S, C663S) and one lysine with glutamine (K708Q) residues, were insensitive to both AITC[19,41] and all three AIs, while maintaining sensitivity to the non-electrophilic agonists, menthol[29] or icilin[42] (Fig. 1d and Supplementary Fig. 1c). This finding supports the hypothesis that the ability of AIs to target TRPA1 derives from their electrophilic nature. Electrophysiology experiments recapitulated findings obtained by means of the calcium assay. Exemestane, letrozole and anastrozole selectively activated a concentration-dependent inward current in hTRPA1-HEK293 cells, a response that was abated by HC-030031 (Supplementary Fig. 1d). AIs did not evoke any current in untransfected HEK293 cells (Supplementary Fig. 1d).

Next, to verify whether exemestane, letrozole and anastrozole stimulate nociceptive sensory neurons via TRPA1 activation, we used primary culture of both rat and mouse dorsal root ganglion (DRG) neurons. Similar to AITC[19], all AIs produced a concentration-dependent calcium response (Fig. 2a,b) in a proportion (about 30%) of cells that responded to the selective TRPV1 agonist, capsaicin (0.1 μM). All cells responding to AIs, but none of the non-responding cells, invariably responded to a subsequent high concentration of AITC (30 μM) (Fig. 2a), further documenting TRPA1 as the target of AIs. In rat DRG neurons, EC_{50} ranged between 78 and 135 μM (Fig. 2b). Calcium responses evoked by the three AIs were abated by HC-030031 (30 μM), but were unaffected by the selective TRPV1 antagonist, capsazepine (10 μM) (Fig. 2c). Notably, AITC and all AIs produced a calcium response in capsaicin-sensitive DRG neurons isolated from wild-type ($Trpa1^{+/+}$) mice, an effect that was absent in neurons obtained from TRPA1-deficient ($Trpa1^{-/-}$) mice (Typical traces Fig. 2d and pooled data Fig. 2e).

AIs activate nociceptive and hyperalgesic TRPA1-dependent pathways. It has been well documented that local exposure to TRPA1 agonists in experimental animals is associated with an immediate nociceptive response, lasting for a few minutes, and a delayed more prolonged mechanical allodynia[18,19]. To investigate whether AIs activate such a nociceptive and hyperalgesic TRPA1-dependent pathway, we used one steroidal (exemestane) and one non-steroidal (letrozole) AI. Given the chemical similarity and the hypothesized analogous mechanism of the two non-steroidal AIs, to minimize the number of animals used, anastrozole was not

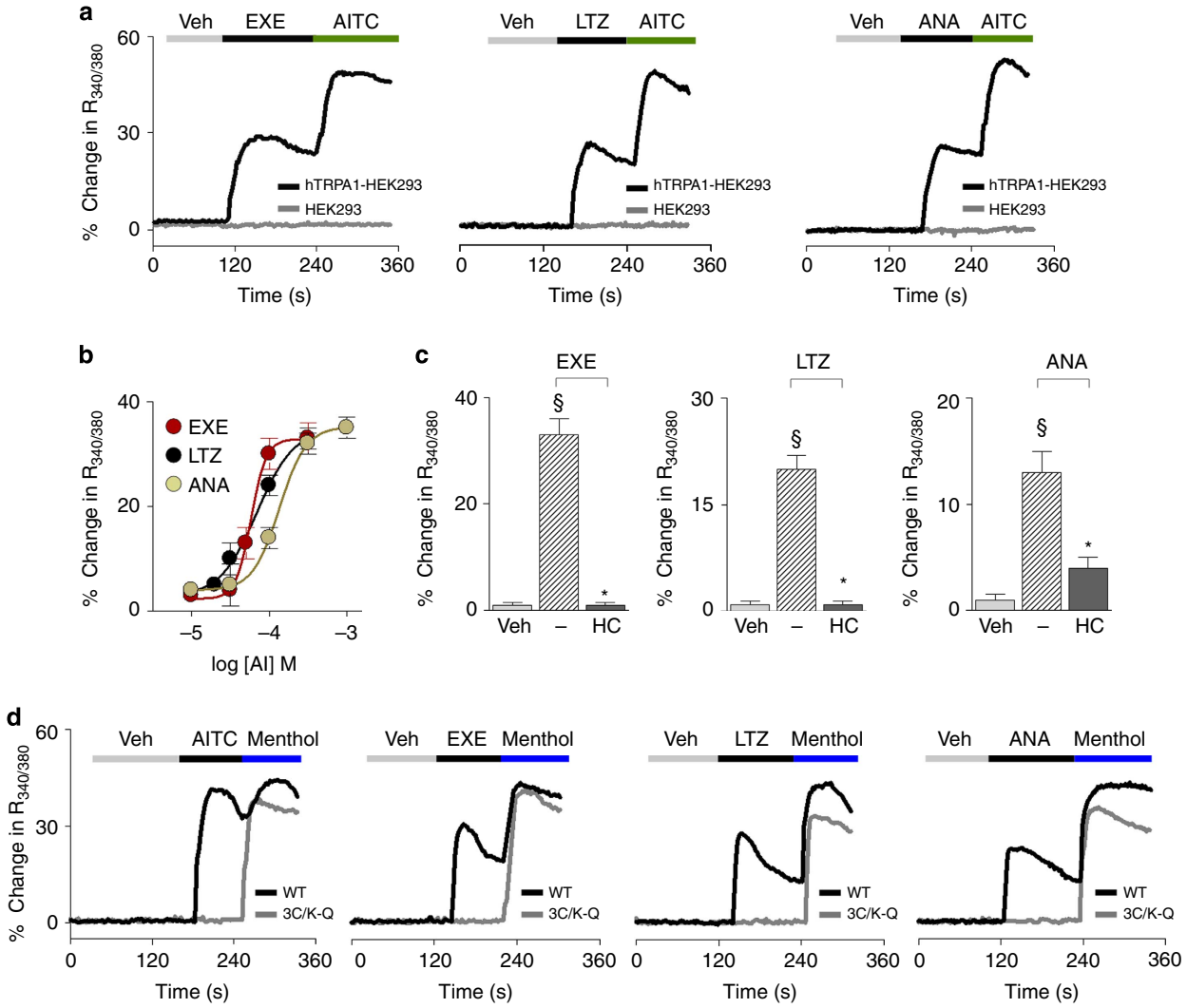

Figure 1 | Exemestane (EXE), letrozole (LTZ) and anastrozole (ANA) selectively activate the human TRPA1 channel. (**a**) Representative traces of intracellular calcium response evoked by the aromatase inhibitors (AIs), EXE (100 μM), LTZ (100 μM) and ANA (100 μM), in HEK293 cells transfected with the cDNA for human TRPA1 (hTRPA1-HEK293), which respond to the selective TRPA1 agonist, allyl isothiocyanate (AITC; 30 μM). AITC (30 μM), EXE, LTZ and ANA (all 100 μM) fail to produce any calcium response in untransfected-HEK293 cells (HEK293). (**b**) Concentration-response curves to EXE, LTZ and ANA, yielded EC_{50} (95% confidence interval) of 58 (46–72) μM, 69 (43–109) μM, and 134 (96–186) μM, respectively. (**c**) AI-evoked calcium response in hTRPA1-HEK293 is abolished by the selective TRPA1 antagonist, HC-030031 (HC; 30 μM). (**d**) Representative traces of cells transfected with the cDNA codifying for the mutant hTRPA1 channel (3C/K-Q), which are insensitive to AITC (30 μM) or AIs (100 μM), but respond to the non-electrophilic agonist, menthol (100 μM), whereas HEK293 cells transfected with the cDNA codifying for wild-type hTRPA1 (WT) respond to all the drugs. Veh is the vehicle of AIs; dash (–) indicates the vehicle of HC. Each point or column represents the mean ± s.e.m. of at least 25 cells from 3–6 independent experiments. $^{§}P<0.05$ versus Veh, $^{*}P<0.05$ versus EXE, LTZ or ANA group; ANOVA and Bonferroni *post hoc* test.

investigated in the following *in vivo* experiments. Intraplantar (i.pl.) injection (20 μl per paw) of exemestane (1, 5 and 10 nmol) (Supplementary Fig. 2a) or letrozole (10, 20 nmol) (Supplementary Fig. 2e) evoked an acute (0–5 min) nociceptive response and a delayed (15–120 min for exemestane and 15–240 min for letrozole) mechanical allodynia in C57BL/6 mice (Supplementary Fig. 2c,g). Both the nociceptive response and mechanical allodynia evoked by AIs were confined to the treated paw (Supplementary Fig. 2c,g) and were almost completely prevented by intraperitoneal (i.p.) pretreatment with HC-030031 ($100\,mg\,kg^{-1}$), but not with capsazepine ($4\,mg\,kg^{-1}$) (Supplementary Fig. 2b,d,f,h). Furthermore, similar to results obtained in C57BL/6 mice, local injection (i.pl.) of exemestane or letrozole in *Trpa1*$^{+/+}$ mice evoked an early nociceptive response and a delayed mechanical allodynia (Supplementary Fig. 2i,j). *Trpa1*$^{-/-}$ mice did not develop such responses (Supplementary Fig. 2i,j). Thus, by using both pharmacological and genetic tools, we demonstrated that local administration of both steroidal and non-steroidal AIs produces a typical TRPA1-dependent behaviour, characterized by acute nociception and delayed mechanical allodynia.

AIs produce neurogenic oedema by releasing sensory neuropeptides. TRPA1 is expressed by peptidergic nociceptors, and its stimulation is associated with proinflammatory neuropeptide release and the ensuing neurogenic inflammatory responses[19,45]. First, we explored whether AIs are able to directly promote the release of CGRP (one of the proinflammatory neuropeptides, which are usually co-released on stimulation of peptidergic nociceptors)[26,46] via a TRPA1-dependent pathway. AIs increased CGRP outflow from slices of rat dorsal spinal cord (an anatomical

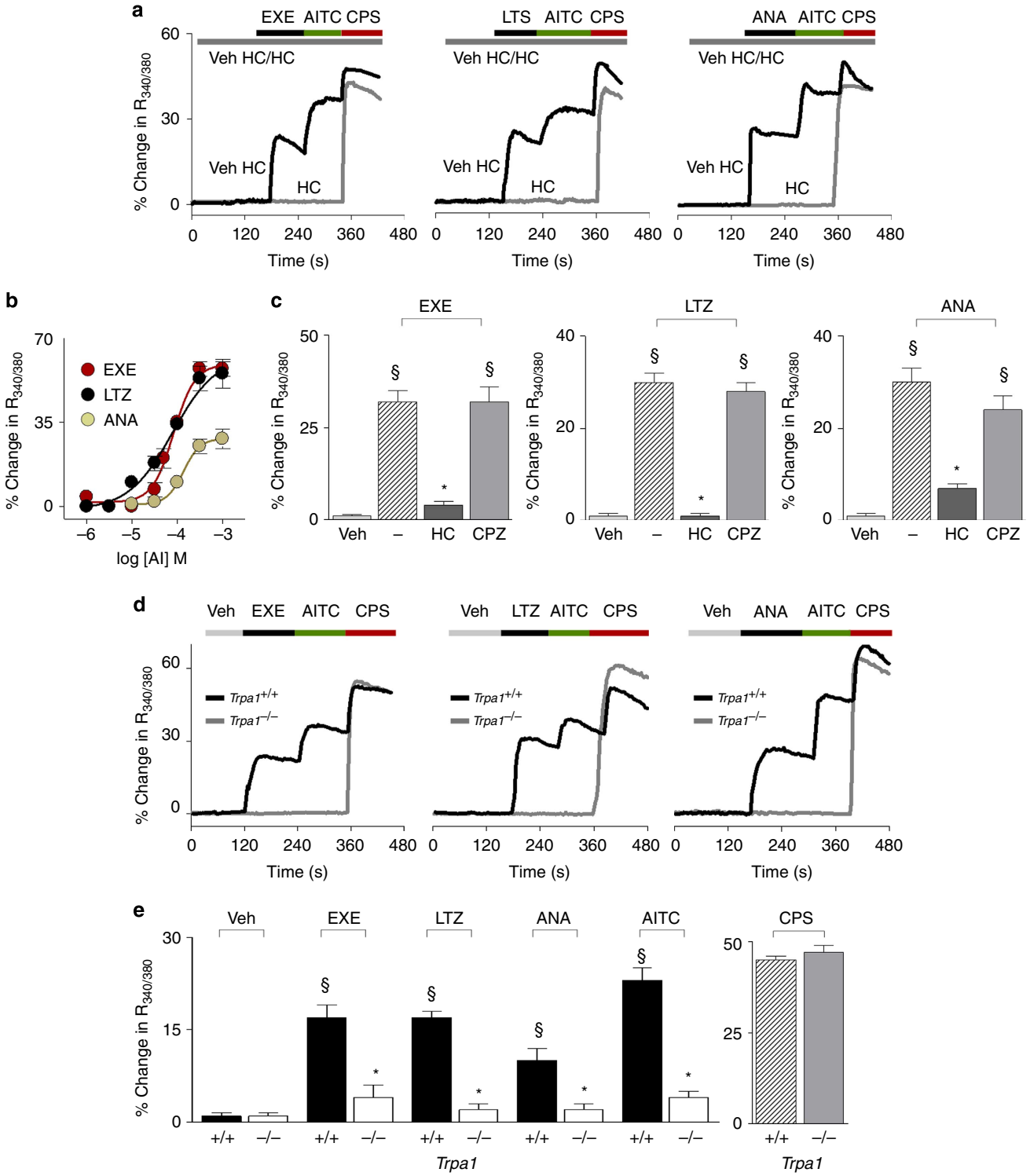

Figure 2 | Exemestane (EXE), letrozole (LTZ) and anastrozole (ANA) selectively activate the native TRPA1 channel expressed in rodent dorsal root ganglion (DRG) neurons. (**a**) Representative traces of calcium response evoked by EXE (100 μM), LTZ (100 μM), ANA (300 μM) in cultured rat DRG neurons, which also respond to allyl isothiocyanate (AITC; 30 μM) and capsaicin (CPS; 0.1 μM). Calcium responses evoked by AIs and AITC are abolished by the selective TRPA1 antagonist, HC-030031 (HC; 30 μM), which does not affect response to CPS. (**b**) Concentration-response curves of EXE, LTZ and ANA, yielded EC_{50} (95% confidence interval) of 82 (61–108) μM, 78 (39–152) μM, and 135 (78–231) μM, respectively. (**c**) Calcium responses induced by AIs are inhibited by HC and unaffected by the TRPV1 antagonist, capsazepine (CPZ; 10 μM). $^{§}P<0.05$ versus Veh, $^{*}P<0.05$ versus EXE, LTZ or ANA; ANOVA and Bonferroni *post hoc* test. (**d**) Representative traces and (**e**) pooled data of the calcium response evoked by EXE, LTZ, ANA (all 100 μM) or AITC (30 μM), in neurons isolated from *Trpa1*$^{+/+}$ mice. Neurons isolated from *Trpa1*$^{-/-}$ mice do not respond to AITC, EXE, LTZ and ANA, whereas they do respond normally to CPS (0.1 μM). In DRG neurons isolated from both *Trpa1*$^{+/+}$ and *Trpa1*$^{-/-}$ mice, calcium response is evaluated only in capsaicin responding neurons. $^{§}P<0.05$ versus Veh, $^{*}P<0.05$ versus EXE, LTZ, ANA or AITC-*Trpa1*$^{+/+}$, ANOVA and Bonferroni *post hoc* test. Veh is the vehicle of AIs; dash (-) indicates the combination of the vehicles of HC and CPZ. Each point or column represents the mean ± s.e.m. of at least 25 neurons obtained from 3 to 7 independent experiments.

area enriched with central terminals of nociceptors). This effect was substantially attenuated in rat slices pretreated with a desensitizing concentration of capsaicin (10 μM, 20 min) or in the presence of HC-030031 (Fig. 3a). The increase in CGRP outflow observed in slices obtained from *Trpa1*$^{+/+}$ mice was markedly reduced in slices obtained from *Trpa1*$^{-/-}$ mice (Fig. 3b).

These neurochemical data were corroborated by functional experiments. Injection (i.pl.) of the TRPA1 agonist, AITC (10 nmol per paw), induced paw oedema that peaked at 60 min after injection. The response was abated by treatment with HC-030031 (100 mg kg^{-1}, i.p.) or a combination of the SP neurokinin-1 (NK-1) receptor antagonist, L-733,060, and the CGRP receptor antagonist, CGRP8-37 (both, 2 μmol kg^{-1}, intravenous, i.v.) (Fig. 3c). Similarly, we found that i.pl. administration of exemestane (10 nmol per paw) and letrozole (20 nmol per paw) caused paw oedema that peaked at 60 min and faded 120 min after injection (Fig. 3c, insets). Treatment with HC-030031 (100 mg kg^{-1}, i.p.) or a combination of L-733,060 and CGRP8-37 (both, 2 μmol kg^{-1}, i.v.), markedly reduced the AI-evoked oedema (Fig. 3c). No oedema was found in the paw contralateral to that injected with AIs (Supplementary Fig. 2k). Importantly, the oedema produced in *Trpa1*$^{+/+}$ mice by exemestane and letrozole was markedly attenuated in *Trpa1*$^{-/-}$ mice (Fig. 3d). Next, to directly evaluate the ability of AIs to release CGRP from peripheral terminals of peptidergic nociceptors, AIs were administered to the rat knee joint. Intra-articular (i.a., 50 μl) injection of exemestane (5 nmol) or letrozole (10 nmol) increased CGRP levels in the synovial fluid, an effect that was markedly attenuated by pretreatment with HC-030031 (100 mg kg^{-1}, i.p.) (Fig. 3e). Neurochemical and functional data indicate that AIs by TRPA1 activation release sensory neuropeptides from sensory nerve endings, and by this mechanism promote neurogenic inflammatory responses in the innervated peripheral tissue.

Systemic AIs induce prolonged pain-like effects by targeting TRPA1. AIs are given to patients by a systemic route of administration. Therefore, we explored in mice whether intraperitoneal (i.p.) or intragastric (i.g.) administration of exemestane and letrozole could produce pain-like effects via TRPA1 activation. For i.p. administration experiments, doses, corresponding to those used in humans, were selected according to the mouse to human conversion factor indicated by the National Institute of Health[47]. Exemestane (5 mg kg^{-1}, i.p.) or letrozole (0.5 mg kg^{-1}, i.p) injection did not produce any visible nociceptive behaviour (Supplementary Figs 3a,4a, insets) in mice. However, 3 h after exemestane or letrozole administration, mice developed a prolonged (3 h) mechanical allodynia (Supplementary Figs 3a,4a) and a reduction in forelimb grip strength (Supplementary Figs 3c,4c), a test used in its clinical version for the study of musculoskeletal pain in patients[48]. When mechanical allodynia by exemestane or letrozole was at its maximum, systemic HC-030031 administration (100 mg kg^{-1}, i.p.) transiently reverted both responses (Supplementary Figs 3b,d and 4b,d). Furthermore, mechanical allodynia and the reduction in forelimb grip strength produced by exemestane and letrozole in *Trpa1*$^{+/+}$ mice were markedly reduced in *Trpa1*$^{-/-}$ mice (Supplementary Figs 3e,f and 4e,f). In experiments where AIs were given by intragastric (i.g.) gavage, doses were adjusted considering the oral bioavailability in humans, which is 99% for letrozole[49], and 40% (with food) for exemestane[50]. First, we found that after i.g. administration of exemestane (10 mg kg^{-1}) or letrozole (0.5 mg kg^{-1}) their peak plasma levels (13.2 ± 1.7 ng ml^{-1}, $n = 5$; and 60.5 ± 12.1 ng ml^{-1}, $n = 5$, respectively, Supplementary Fig. 5) approximated the maximum plasma concentrations found in humans[49,51]. Second, results similar to those obtained after i.p. administration were reported when AIs were given by i.g. gavage. First, exemestane (10 mg kg^{-1}, i.g.) or letrozole (0.5 mg kg^{-1}, i.g.) ingestion was not associated with any spontaneous nocifensor behaviour (Figs 4a, 5a, insets). Second, exemestane or letrozole produced, with a similar time-course, mechanical allodynia and a marked reduction in forelimb grip strength (Figs 4a,c and 5a,c). Pretreatment with HC-030031 or deletion of TRPA1 (*Trpa1*$^{-/-}$ mice) significantly attenuated both responses (Figs 4b,d,e,f and 5b,d,e,f).

Furthermore, since in clinical practice patients are treated with AIs on a daily basis over very long periods of time (up to 5 years), we asked whether exemestane or letrozole maintains the ability to evoke a TRPA1-dependent mechanical hypersensitivity and decreased grip strength on repeated administration. In *Trpa1*$^{+/+}$ mice, treatment with systemic exemestane (5 mg kg^{-1}, i.p.) or letrozole (0.5 mg kg^{-1} i.p) (both once a day for 15 consecutive days) produced at day 1, 5, 10 and 15 a transient (from 1 to 6 h) and reproducible mechanical allodynia (Supplementary Figs 3e, 4e). Importantly, in *Trpa1*$^{-/-}$ the proalgesic action of AIs was markedly attenuated (Supplementary Figs 3e, 4e). In addition, the decrease in the grip strength was maintained, without undergoing desensitization, over the entire time period of daily i.p. administration of exemestane or letrozole (Supplementary Figs 3f,4f). Both these effects of AIs were significantly reduced in *Trpa1*$^{-/-}$ mice (Supplementary Figs 3f, 4f). Similar results were obtained after i.g. administration of exemestane or letrozole (once a day for 15 consecutive days at the dose of 10 mg kg^{-1} i.g. or 0.5 mg kg^{-1} i.g., respectively). Both mechanical allodynia and decreased grip strength were observed, without signs of desensitization, over the 15 days of observation in *Trpa1*$^{+/+}$ mice, but were markedly reduced in *Trpa1*$^{-/-}$ mice (Figs 4e,f and 5e,f). Altogether, the present data demonstrate that both steroidal and non-steroidal third-generation AIs induce a series of pain-like effects predominantly via a TRPA1-dependent mechanism, effects that over time do not undergo desensitization, thus mimicking the chronic clinical condition.

AI-evoked TRPA1 activation is enhanced by proinflammatory stimuli. Although it affects a large proportion of subjects, not all patients treated with AIs develop AIMSS. One possible explanation for the peculiar susceptibility to AIMSS of some patients is that, if TRPA1 activation is a necessary prerequisite, *per se* it is not sufficient, and additional proalgesic factors must contribute to the development of pain symptoms. It has been reported that stimulation of proalgesic pathways exaggerates TRPA1-dependent responses *in vitro* and *in vivo*[52,53]. One example of such potentiating action has been reported for the proteinase-activated receptor-2 (PAR2), whose subthreshold activation results in an exaggerated response to the TRPA1 agonist, AITC[52]. PAR2 undergoes activation on a unique proteolytic mechanism by cleavage of its tethered ligand domain by trypsin and other proteases, thus mediating inflammation and hyperalgesia[54]. On this basis, and following a previously reported protocol[52], we explored, by *in vivo* functional experiments in C57BL/6 mice, whether PAR2 activation exaggerates TRPA1-dependent hypersensitivity induced by AIs. Before (10 min) injection (i.pl.) of the PAR2-activating peptide (AP) (PAR2-AP, 1 μg per paw), but not the reverse peptide (RP) (PAR2-RP, 1 μg per paw, inactive on PAR2), markedly enhanced the duration of licks and flinches of the hind paw produced by local injection (i.pl.) of exemestane (1 nmol per paw) and letrozole (10 nmol per paw) (Fig. 6a). The injected dose of PAR2-AP, as well as PAR2-RP, did not cause *per se* any visible acute nocifensor response (Fig. 6a). The exaggerated responses to the combination of PAR2-AP and

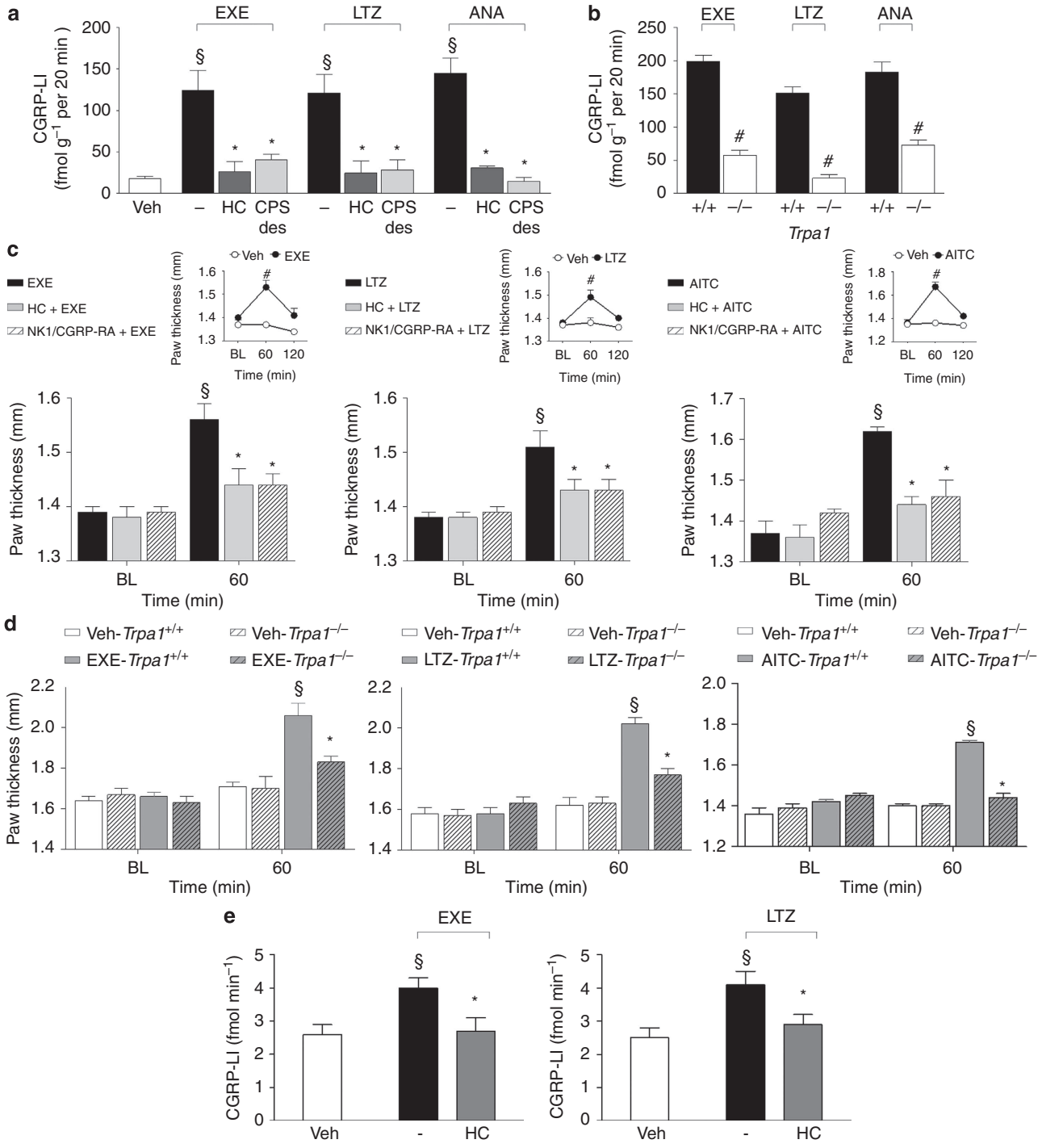

Figure 3 | Aromatase inhibitors release calcitonin gene-related peptide (CGRP) and produce neurogenic edema. (**a**) Exemestane (EXE), letrozole (LTZ) and anastrozole (ANA) (all 100 μM) increase the CGRP-like immunoreactivity (CGRP-LI) outflow from slices of rat dorsal spinal cord. This effect is prevented by HC-030031 (HC; 30 μM) or after exposure to capsaicin (10 μM, 20 min; CPS-des). (**b**) EXE, LTZ and ANA (all 100 μM) increase the CGRP-LI outflow from spinal cord slices obtained from *Trpa1*$^{+/+}$, but not from *Trpa1*$^{-/-}$ mice. Results are mean ± s.e.m. of at least four independent experiments. Veh is the vehicle of EXE, LTZ and ANA, dash (-) indicates the vehicle of HC and CPS. $^{\S}P<0.05$ versus Veh, $^{*}P<0.05$ versus EXE, LTZ or ANA; ANOVA followed by Bonferroni *post hoc* test. $^{\#}P<0.05$ versus EXE-, LTZ-, ANA-*Trpa1*$^{+/+}$, Student's *t*-test. (**c**) In C57BL/6 mice intraplantar (i.pl.) injection (20 μl) of EXE (10 nmol), LTZ (20 nmol) or allyl isothiocyanate (AITC; 10 nmol) induces paw oedema, which peaks at 60 min and fades 120 min after injection (**c**, upper insets), and is attenuated by pretreatment with HC (100 mg kg^{-1} intraperitoneal, i.p.) or the combination of the selective antagonists of the neurokinin-1 receptor, (NK1-RA), L-733,060, and of the CGRP receptor (CGRP-RA), CGRP8-37, (both, 2 μmol kg^{-1}, intravenous). (**d**) Paw oedema induced by EXE, LTZ and AITC (i.pl.) in *Trpa1*$^{+/+}$ mice is markedly reduced in *Trpa1*$^{-/-}$ mice. BL = baseline level. Results are mean ± s.e.m. of at least five mice for each group. Veh is the vehicle of EXE, LTZ and AITC. $^{\#}P<0.05$ versus Veh, Student's *t*-test; $^{\S}P<0.05$ versus BL values, $^{*}P<0.05$ versus EXE, LTZ, AITC or EXE-, LTZ-, AITC-*Trpa1*$^{+/+}$; ANOVA followed by Bonferroni *post hoc* test. (**e**) Injection (50 μl) of EXE (5 nmol) or LTZ (10 nmol) in the rat knee increases CGRP-LI levels in the synovial fluid, an effect that is markedly attenuated by pretreatment with HC (100 mg kg^{-1}, i.p.). Results are mean ± s.e.m. of at least five mice for each group. Veh is the vehicle of EXE and LTZ, dash (-) indicates the vehicle of HC. $^{\S}P<0.05$ versus Veh, $^{*}P<0.05$ versus EXE, LTZ; ANOVA followed by Bonferroni *post hoc* test.

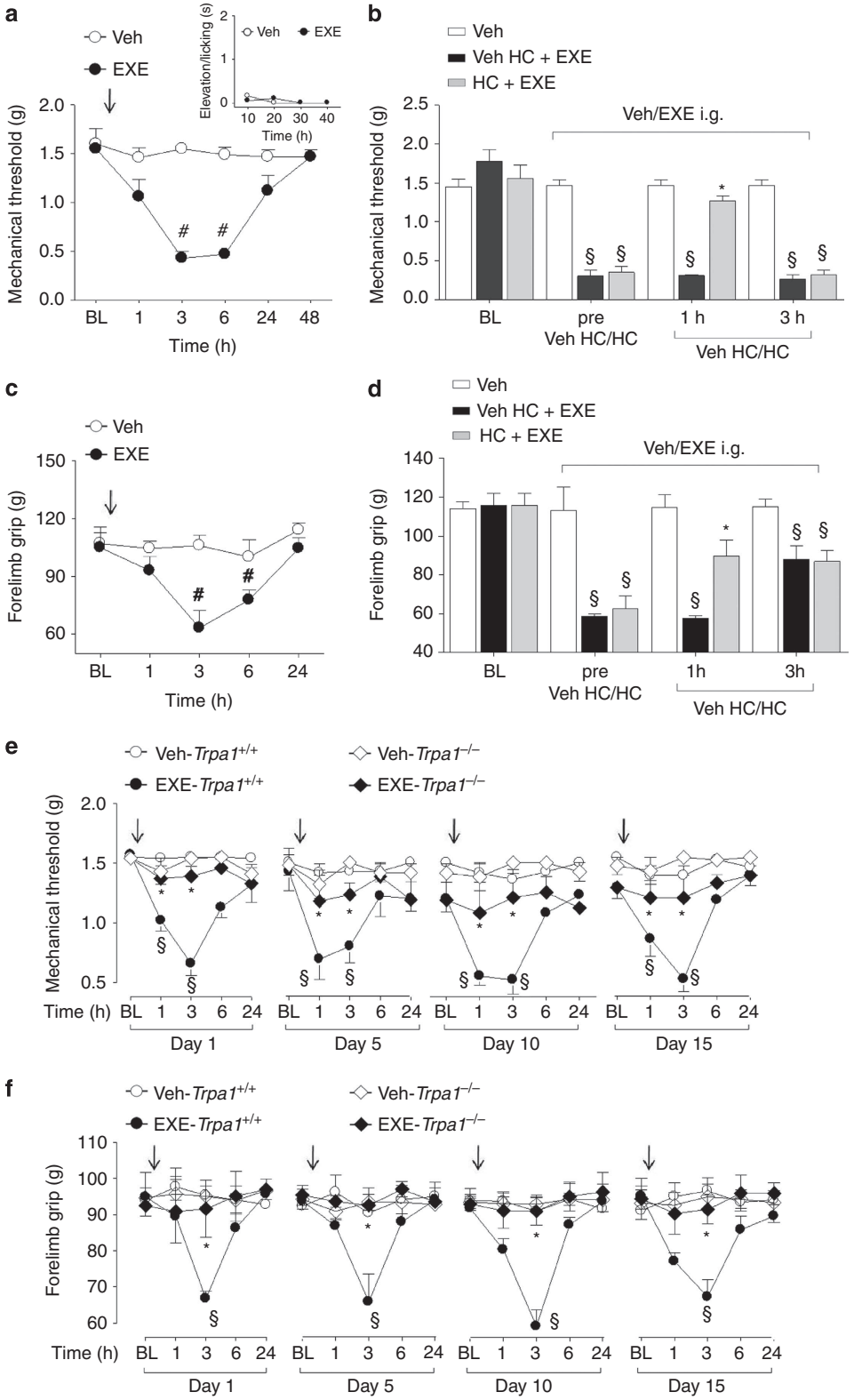

Figure 4 | Intragastric exemestane (EXE) induces TRPA1-dependent prolonged mechanical allodynia and reduction in forelimb grip strength in mice. In C57BL/6 mice intragastric (i.g.) administration of EXE (10 mg kg^{-1}) induces (**a**) mechanical allodynia and (**c**) a reduction in forelimb grip strength that last 3–6 h after administration. EXE does not produce any acute nocifensor behaviour as measured by the indicated test (**a**, inset). (**b**,**d**) Three hours after EXE administration, HC-030031 (HC; 100 mg kg^{-1} i.p.) reverts both mechanical allodynia and the reduction in forelimb grip strength. HC inhibition is no longer visible 3 h after its administration. Veh is the vehicle of EXE. $^{\#}P<0.05$ versus Veh; Student's *t*-test (**a**,**c**) and $^{\S}P<0.05$ versus Veh and $^{*}P<0.05$ versus Veh HC-EXE; ANOVA followed by Bonferroni *post hoc* test (**b**,**d**). (**e**,**f**) EXE (once a day for 15 consecutive days, 10 mg kg^{-1} i.g.) induces reproducible mechanical allodynia and decrease in forelimb grip strength at day 1, 5, 10 and 15 in *Trpa1*$^{+/+}$ mice. Arrows indicate Veh or EXE administration. Both these effects are markedly reduced in *Trpa1*$^{-/-}$ mice. $^{\S}P<0.05$ versus Veh-*Trpa1*$^{+/+}$, $^{*}P<0.05$ versus EXE-*Trpa1*$^{+/+}$; ANOVA followed by Bonferroni *post hoc* test. Results are mean ± s.e.m. of at least five mice for each group. In all conditions, baseline (BL) levels were recorded 30 min before EXE administration.

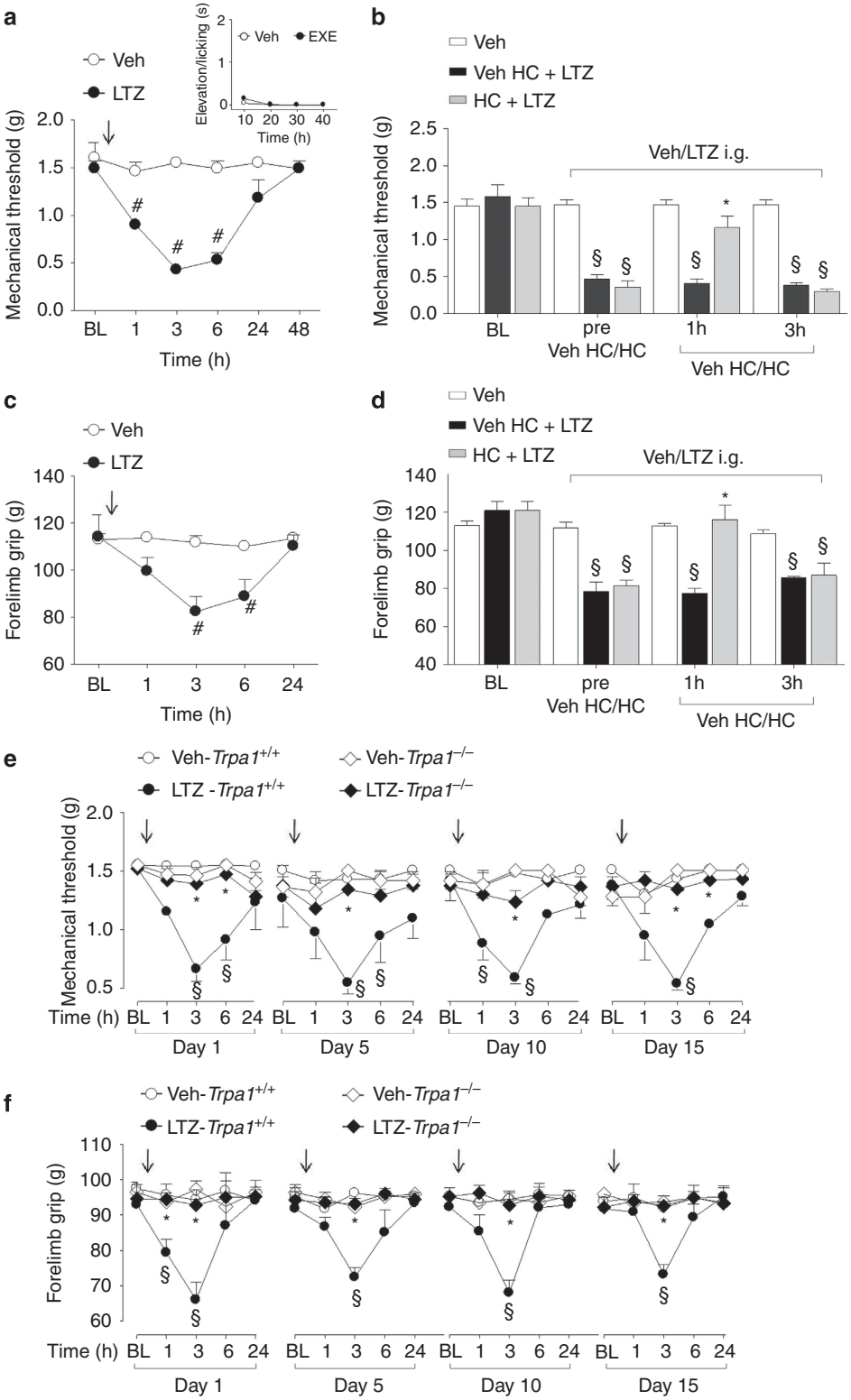

Figure 5 | Intragastric letrozole (LTZ) induces TRPA1-dependent prolonged mechanical allodynia and reduction in forelimb grip strength in mice. In C57BL/6 mice intragastric (i.g.) administration of LTZ (0.5 mg kg^{-1}) induces (**a**) mechanical allodynia and (**c**) reduction in forelimb grip strength that last 3–6 h after administration. LTZ does not produce any acute nocifensor behaviour as measured by the indicated test (**a**, inset). (**b**,**d**) Three hours after LTZ administration, HC-030031 (HC; 100 mg kg^{-1} i.p.) reverts both mechanical allodynia and the reduction in forelimb grip strength. HC inhibition is no longer visible 3 h after its administration. Veh is the vehicle of LTZ. $^{\#}P<0.05$ versus Veh; Student's *t*-test (**a**,**c**) and $^{\S}P<0.05$ versus Veh and $^{*}P<0.05$ versus Veh HC-LTZ; ANOVA followed by Bonferroni *post hoc* test (**b**,**d**). (**e**,**f**) LTZ (once a day for 15 consecutive days, 0.5 mg kg^{-1} i.g.) induces reproducible mechanical allodynia and decrease in forelimb grip strength at day 1, 5, 10 and 15 in *Trpa1*$^{+/+}$ mice. Arrows indicate Veh or LTZ administration. Both effects are markedly reduced in *Trpa1*$^{-/-}$ mice. $^{\S}P<0.05$ versus Veh-*Trpa1*$^{+/+}$, $^{*}P<0.05$ versus LTZ-*Trpa1*$^{+/+}$; ANOVA followed by Bonferroni *post hoc* test. Results are mean ± s.e.m. of at least five mice for each group. In all conditions baseline (BL) levels were recorded 30 min before LTZ administration.

exemestane or letrozole were inhibited by HC-030031 (100 mg kg^{-1}, i.p.) (Fig. 6a).

We also tested the ability of a recognized endogenous TRPA1 agonist, H_2O_2 (refs 27,28) to increase the nocifensor response of exemestane or letrozole. In addition, we explored the ability of AIs to increase either nociception or mechanical allodynia to H_2O_2. H_2O_2 (0.5 µmol per paw) injection produced a transient nocifensor behaviour that terminated within 5 min (Fig. 6b, inset). We found that 10 min after H_2O_2 injection (when baseline levels of nociception were restored) administration of exemestane (1 nmol per paw) and letrozole (10 nmol per paw) evoked nociceptive responses markedly increased as compared with vehicle-pretreated mice (Fig. 6b). The exaggerated responses to AIs were inhibited by HC-030031 (Fig. 6b). Thus, both homologous activation of the channel by the TRPA1 agonist H_2O_2, or heterologous stimulation of a classical proinflammatory pathway, such as PAR2, converge in a final common pathway, which results in the potentiation of the AI-evoked and TRPA1-dependent proalgesic mechanism. In the attempt to understand the mechanism underlying the *in vivo* potentiation between PAR2 or H_2O_2 and AIs, cultured DRG neurons were challenged with combinations of these same agents. First, in *in vitro* electrophysiological experiments, we found that AITC, exemestane and letrozole (all 100 µM) produced inward currents in cultured DRG neurons, effects that were abated in the presence of HC-030031 (50 µM). However, HC-030031 did not affect the inward current produced by capsaicin (Fig. 6c). Second, we showed that pre-exposure to subthreshold concentrations of PAR2-AP or H_2O_2 enhanced currents evoked by subthreshold concentrations of either exemestane or letrozole (both 20 µM) (Typical traces Fig. 6d and pooled data Fig. 6e). Third, HC-030031 inhibited the exaggerated responses (Fig. 6e).

Discussion

In the present study, we provide for the first time evidence that third-generation steroidal and non-steroidal AIs, proven to be very effective drugs in the treatment of hormone receptor-positive breast cancer[1,2], selectively target the TRPA1 channel. This conclusion derives from a series of experiments in cells expressing the recombinant human TRPA1 or in rodent DRG neurons expressing the native channel. Indeed, calcium responses and currents evoked by AIs are confined to TRPA1-expressing cells, and are selectively abolished by HC-030031, or absent in neurons obtained from TRPA1-deficient mice. Exemestane exhibits a chemical structure with a system of highly electrophilic conjugated Michael acceptor groups[40]. A variety of known TRPA1 agonists, including acrolein and other α,β-unsaturated aldehydes, possesses an electrophilic carbon or sulfur atom that is subject to nucleophilic attack (Michael addition) by cysteine and lysine residues[55]. Nitriles also exhibit electrophilic properties[56], which may result in TRPA1 gating[43]. Non-steroidal letrozole and anastrozole possess nitrile moieties that underscore their potential ability to activate TRPA1. We show that key cysteine and lysine residues, required for channel activation by electrophilic agonists[19,41,42], are also required for TRPA1 activation by AIs. Thus, the three AIs, most likely because of their electrophilic nature, selectively target TRPA1, whereas TRPV1, TRPV2, TRPV3 and TRPV4 all co-expressed with TRPA1 (refs 24,25), and other channels or receptors in DRG neurons do not seem to play a relevant role in the direct excitation of nociceptors by AIs.

TRPA1-expressing neurons activated by AIs also responded to capsaicin, a selective TRPV1 agonist. As TRPV1 is considered a specific marker of nociceptors[57], AIs may be assumed to activate pain-like responses. *In vivo* stimulation of the irritant TRPA1 receptor in rodents produces an early nociceptive behaviour, followed by a delayed and prolonged mechanical allodynia[18,19,44]. Subcutaneous exemestane and letrozole recapitulated the two effects produced by TRPA1 agonists and produced such responses in a TRPA1-dependent way.

Magnetic resonance imaging of painful wrists in patients treated with AIs has shown signs of inflammatory tenosynovitis poorly reverted by common anti-inflammatory treatments[12]. Systemic increases in plasma cytokines have not been found in patients with AIMSS and, therefore, do not appear to represent the underlying mechanism for such inflammatory conditions[9,13]. This implies that pathways different from cytokine-dependent inflammation operate in joints of patients treated with AIs. As TRPA1 is expressed by a subpopulation of peptidergic nociceptors, which mediate neurogenic inflammation[24–26], we anticipated that AIs, by targeting TRPA1, release proinflammatory neuropeptides, thereby causing neurogenic plasma extravasation. Pharmacological and genetic findings indicate that AIs produce a specific type of edema, which is neurogenic in nature. The conclusion is corroborated by the direct neurochemical observation that exemestane and letrozole evoke TRPA1-dependent CGRP release from peripheral endings of primary sensory neurons. The neurogenic component, mediated by TRPA1-activation and sensory neuropeptide release, may thus represent an important mechanism contributing to the cytokine-independent inflammation observed in AI users.

When AIs were given to mice by systemic (intraperitoneal or intragastric) administration, no acute nocifensive response was observed, but, after ~1 h delay they produced a prolonged condition (up to 6 h) of mechanical allodynia and a decrease in forelimb grip strength. Also, in this case, pharmacological and genetic results indicate that AI-evoked pain-like responses are principally TRPA1-dependent. In clinical practice, AIs are used for a 3- or 5-year period, and the pain condition associated with their use is often persistent[58]. Although the present experimental conditions can not fully mimic the clinical setting in cancer patients, our findings suggest that the TRPA1-dependent ability of AIs to produce mechanical allodynia and to decrease forelimb grip strength is maintained and does not undergo desensitization in mice over a time period of 15 days, which broadly corresponds to a 1-year time in humans. Despite a general good tolerability[11], AIs produce some types of pain, including AIMSS and neuropathic, diffuse and mixed pain in 10–20% of the treated patients[9]. The reason why only some of the patients exposed to AIs develop these severe pain conditions, which may lead to non-adherence or therapy discontinuation, is unknown.

Here, we reveal the key role of TRPA1 as the main mediator of exemestane- and letrozole-evoked nociceptor stimulation. However, it is likely that additional factors contribute to determine the development of AIMSS and related pain symptoms, particularly in those susceptible patients who suffer from the more severe form of this adverse reaction. *In vitro* and *in vivo* experiments with the co-administration of AIs and pro-algesic stimuli, such as PAR2-AP, an agonist of the pro-inflammatory receptor, PAR2, and the TRPA1 agonist, H_2O_2 (ref. 28), indicate that additional factors may cooperate to increase the sensitivity to AIs of TRPA1 expressing nociceptors. Enhancement by PAR2 activation of the proalgesic activity of exemestane and letrozole is fully consistent and closely mimic previous observations that PAR2 activation increases the pro-algesic response evoked by TRPA1 agonists[52]. Findings that a combination of AIs and H_2O_2 exaggerates TRPA1-mediated *in vitro* and *in vivo* responses suggest that increased levels of oxidative stress byproducts, known to be generated under inflammatory conditions[59], may facilitate the development of AIMSS and related pain symptoms. Our present investigation on the cooperation between AIs and

proinflammatory mediators has been limited to PAR2 and H_2O_2. However, it is possible that additional pro-inflammatory and pro-algesic mediators can activate similar cooperating pathways. AI concentrations required for TRPA1 activation are higher than those found in the plasma of treated subjects[60–62]. However, it should be noted that all three AIs have a large volume of distribution, indicating a high tissue distribution[49,51]. The present findings that in mice plasma levels of both AIs were comparable to those found in humans[49,51] strengthen the hypothesis that compartmentalization of AIs in mice is similar to that reported in humans[49,51]. Thus, under standard drug regimens, concentrations sufficient to activate TRPA1 or to potentiate TRPA1-mediated responses evoked in cooperation with inflammatory mediators may be reached in tissues neighbouring sensory nerve terminals.

Altogether, the present results indicate that AIs *per se* or, most likely, in cooperation with other proinflammatory mediators promote TRPA1-dependent neurogenic inflammation, mechanical hypersensitivity and decreased forelimb grip force in rodents. This novel pathway may represent the main underlying mechanism responsible for pain and inflammatory symptoms associated with AI treatment. The other important proposal deriving from the present findings is that antagonists of the TRPA1 channel may be beneficial in the prevention and treatment of such painful conditions.

Methods

Animals. Animal experiments were carried out in conformity to the European Communities Council (ECC) guidelines for animal care procedures and the Italian legislation (DL 116/92) application of the ECC directive 86/609/EEC. Studies were conducted under the University of Florence research permit number 204/2012-B. Male C57BL/6 (25–30 g) (Harlan Laboratories, Milan, Italy), wild type, *Trpa1*$^{+/+}$, or TRPA1-deficient, *Trpa1*$^{-/-}$, (25–30 g) mice generated by heterozygous on a C57BL/6 background (B6;129P-Trpa1tm1Kykw/J; Jackson Laboratories, Italy)[63], or Sprague–Dawley rats (75–100 g, male, Harlan Laboratories, Milan, Italy) were used. Animals were housed in a temperature- and humidity-controlled *vivarium* (12 h dark/light cycle, free access to food and water). Behavioural experiments were done in a quiet, temperature-controlled (20 to 22 °C) room between 0900 and 1700 hours and were performed by an operator blinded to the genotype and the drug treatment. Animals were killed with a high dose of sodium pentobarbital (200 mg kg^{-1}, i.p.).

Reagents. Exemestane, letrozole and anastrozole were purchased from Tocris Bioscience (Bristol, UK). The activating peptide (PAR2-AP, SLIGRL-NH_2) and its reverse peptide (PAR2-RP, LRGILS-NH_2) of the murine PAR2 receptor were synthesized from G. Cirino (University of Naples, Naples, Italy) and dissolved in distilled water. If not otherwise indicated, all other reagents were from Sigma-Aldrich (Milan, Italy). HC-030031 was synthesized as previously described[45].

Cell culture and isolation of primary sensory neurons. Human embryonic kidney (HEK293) cells stably transfected with the cDNA for human TRPA1 (hTRPA1-HEK293), kindly donated by A.H. Morice (University of Hull, Hull, UK) or with the cDNA for human TRPV1 (hTRPV1-HEK293), kindly donated by Martin J. Gunthorpe (GlaxoSmithKline, Harlow, UK) and naive untransfected HEK293 cells (American Type Culture Collection, Manassas, VA, USA) were cultured as previously described[64]. HEK293 cells were transiently transfected with the cDNAs (1 μg) codifying for wild-type or mutant 3C/K-Q (C619S, C639S, C663S, K708Q)[19,41] human TRPA1 using the jetPRIME transfection reagent (Euroclone, Milan, Italy) according to the manufacturer's protocol.

Primary DRG neurons were isolated from Sprague–Dawley rats and C57BL/6 or *Trpa1*$^{+/+}$ and *Trpa1*$^{-/-}$ adult mice, and cultured as previously described[38]. In brief, ganglia were bilaterally excised under a dissection microscope and enzymatically digested using 2 mg ml^{-1} of collagenase type 1A and 1 mg ml^{-1} of trypsin, for rat DRG neurons, or 1 mg ml^{-1} of papain, for mouse DRG neurons, in Hank's Balanced Salt Solution (HBSS) for 25–35 min at 37 °C. Rat and mouse DRG neurons were pelleted and resuspended in Dulbecco's Modified Eagle's Medium (DMEM) supplemented with 10% heat inactivated horse serum or Ham's-F12, respectively, containing 10% heat-inactivated fetal bovine serum (FBS), 100 U ml^{-1} of penicillin, 0.1 mg ml^{-1} of streptomycin and 2 mM L-glutamine for mechanical digestion. In this step, ganglia were disrupted by several passages through a series of syringe needles (23–25G). Neurons were then pelleted by centrifugation at 1,200 *g* for 5 min, suspended in *medium* enriched with 100 ng ml^{-1} mouse-NGF and 2.5 mM cytosine-b-D-arabino-furanoside free base, and then plated on 25 mm glass coverslips coated with poly-L-lysine (8.3 μM) and laminin (5 μM). DRG neurons were cultured for 3–4 days before being used for calcium imaging experiments.

Calcium imaging assay. Intracellular calcium was measured in transfected and untransfected HEK293 cells or in DRG neurons, as previously reported[65]. Plated cells were loaded with 5 μM Fura-2AM-ester (Alexis Biochemicals, Lausen, Switzerland) added to the buffer solution (37 °C) containing the following (in mM): 2 $CaCl_2$; 5.4 KCl; 0.4 $MgSO_4$; 135 NaCl; 10 D-glucose; 10 HEPES and 0.1% bovine serum albumin at pH 7.4. After 40 min, cells were washed and transferred to a chamber on the stage of a Nikon Eclipse TE-2000U microscope for recording. Cells were excited alternatively at 340 and 380 nm to indicate relative intracellular calcium changes by the $Ratio_{340/380}$ recorded with a dynamic image analysis system (Laboratory Automation 2.0, RCSoftware, Florence, Italy). Cells and neurons were exposed to exemestane, letrozole and anastrozole (1–300 μM), AITC (10–30 μM), menthol (100 μM), icilin (30 μM) or their vehicles (1.5–3% dimethyl sulfoxide, DMSO). The calcium response to capsaicin (0.1 μM) was used to identify nociceptive neurons. The selective TRPA1 antagonist, HC-030031 (30 μM), and TRPV1 antagonist, capsazepine (10 μM) or their vehicles (3% and 0.1% DMSO, respectively), were applied 10 min before the stimuli. Results are expressed as or the percentage of increase of $Ratio_{340/380}$ over the baseline normalized to the maximum effect induced by ionomycin (5 μM) added at the end of each experiment (% change in $R_{340/380}$) or $Ratio_{340/380}$.

Electrophysiology. Whole-cell patch-clamp recordings were performed on hTRPA1-HEK293, vector-HEK293 cells or rat DRG neurons grown on a poly-L-lysine-coated 13 mm-diameter glass coverslips. Each coverslip was transferred to a recording chamber (1 ml volume) mounted on the platform of an inverted microscope (Olympus CKX41, Milan, Italy) and superfused at a flow rate of 2 ml min^{-1} with a standard extracellular solution containing (in mM): 10 HEPES, 10 D-glucose, 147 NaCl, 4 KCl, 1 $MgCl_2$ and 2 $CaCl_2$ (pH adjusted to 7.4 with NaOH). Borosilicate glass electrodes (Harvard Apparatus, Holliston, MA, USA) were pulled with a Sutter Instruments puller (model P-87) to a final tip resistance of 4–7 MΩ. Pipette solution used for HEK293 cells contained (in mM): 134 K-gluconate, 10 KCl, 11 EGTA, 10 HEPES (pH adjusted to 7.4 with KOH). When recordings were performed on rat DRG neurons, 5 mM $CaCl_2$ was present in the extracellular solution and pipette solution contained (in mM): CsCl 120, Mg_2ATP 3, BAPTA 10, HEPES-Na 10 (pH adjusted to 7.4 with CsOH). Data were acquired with an Axopatch 200B amplifier (Axon Instruments, CA, USA), stored and analysed with a pClamp 9.2 software (Axon Instruments, CA, USA). All the

Figure 6 | TRPA1 activation by exemestane (EXE) and letrozole (LTZ) is enhanced by proinflammatory stimuli. (**a**) Intraplantar (i.pl.; 10 μl) pretreatment (10 min) with the proteinase-activated receptor 2 (PAR2) activating peptide (AP; 1 μg), but not with the inactive PAR2 reverse peptide (RP; 1 μg), enhances nocifensor behaviour produced by EXE (1 nmol per 10 μl, i.pl.) or LTZ (10 nmol per 10 μl, i.pl.). AP and RP alone causes negligible nociception. The potentiated responses to EXE or LTZ are markedly attenuated by HC-030031 (HC; 100 mg kg^{-1}, i.p.). (**b**) H_2O_2 (0.5 μmol per 10 μl, i.pl.) injection produces a transient nocifensor behaviour, lasting only 5 min (**b**, inset). Pretreatment (10 min before AI administration) with H_2O_2 (0.5 μmol per 10 μl, i.pl.) increases nocifensor behaviour produced by EXE (1 nmol per 10 μl, i.pl.) or LTZ (10 nmol per 10 μl, i.pl.). HC (100 mg kg^{-1}, i.p.) inhibits the exaggerated responses to both EXE and LTZ. Dash (-) indicates the vehicle of HC. Points or columns are mean ± s.e.m. of at least fiv mice for each group. $^{§}P<0.05$ versus RP or AP or Veh H_2O_2; $^{†}P<0.05$ versus Veh AP/EXE or Veh AP/LTZ or Veh H_2O_2/EXE or Veh H_2O_2/LTZ; $^{*}P<0.05$ versus AP/EXE or AP/LTZ or H_2O_2/EXE or H_2O_2/LTZ; ANOVA followed by Bonferroni *post hoc* test. $^{\#}P<0.05$ versus Veh H_2O_2, Student's *t*-test. (**c**) An active concentration of EXE or LTZ (both 100 μM) evokes inward currents in rat dorsal root ganglion (DRG) neurons, which also respond to allyl isothiocyanate (AITC; 100 μM) and capsaicin (CPS; 1 μM). Inward currents evoked by EXE, LTZ or AITC are inhibited in the presence of HC (50 μM), which does not affect CPS-evoked currents. Typical traces (**d**) and pooled data (**e**) showing that pre-exposure to AP (100 μM) or H_2O_2 (100 μM) exaggerates currents evoked by a subthreshold concentration of EXE and LTZ (both 20 μM). The inactive RP does not affect responses to EXE or LTZ (both 20 μM). The potentiated responses to EXE or LTZ are markedly attenuated by HC (50 μM). Veh is the vehicle of EXE, LTZ and AITC. Results are mean ± s.e.m. of at least five independent experiments. $^{§}P<0.05$ versus Veh, $^{*}P<0.05$ versus EXE, LTZ or AITC and $^{†}P<0.05$ versus EXE- or LTZ-AP and EXE- or LTZ-H_2O_2; ANOVA followed by Bonferroni *post hoc* test.

experiments were carried out at 20–22 °C. Cells were voltage-clamped at −60 mV. Cell membrane capacitance was calculated in each cell throughout the experiment by integrating the capacitive currents elicited by a ±10 mV voltage pulse. In hTRPA1-HEK293 currents were detected as inward currents activated on cell superfusion with AITC (100 μM), exemestane (50–200 μM), letrozole (50–200 μM) or anastrozole (50–200 μM) in the presence of HC-030031 (50 μM) or its vehicle (0.5% DMSO). TRPV1 currents in rat DRG neurons were detected as inward currents activated by capsaicin (1 μM) in the presence of capsazepine (10 μM) or its vehicle (0.1% DMSO). To evaluate the potentiating effect of H_2O_2 or PAR2-AP on AI-activated currents, rat DRG neurons were superfused with H_2O_2 or PAR2-AP (both 100 μM) 1 min before and during the application of exemestane or letrozole (both, 20 μM). Some experiments were performed in the presence of HC-030031

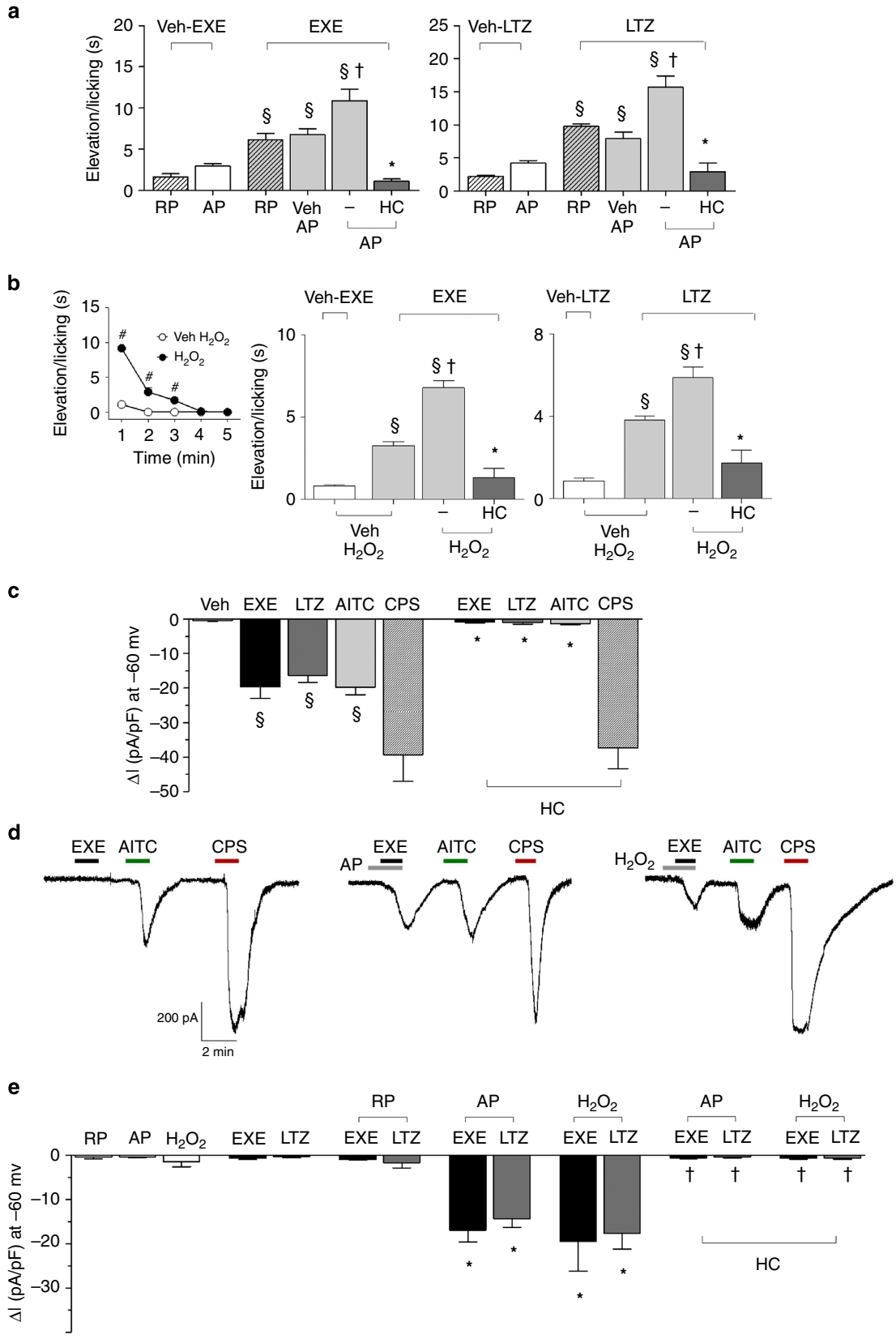

(50 μM) or its vehicle (0.5% DMSO). Peak currents activated by each compound were normalized to cell membrane capacitance and expressed as mean of the current density (pA/pF) in averaged results. Currents were evoked in the voltage-clamp mode at a holding potential of −60 mV; signals were sampled at 1 kHz and low-pass filtered at 10 kHz.

Behavioural experiments. For behavioural experiments, after habituation and baseline of pain sensitivity measurements, mice were randomized into treatment groups. In a first series of experiments, we explored whether the injection (20 μl per paw) of exemestane (1, 5, 10 nmol) or letrozole (10, 20 nmol), or their vehicle (5% DMSO) induced, in C57BL/6 or *Trpa1*$^{+/+}$ and *Trpa1*$^{-/-}$ mice, an acute nociceptive behaviour and a delayed mechanical allodynia. In this set of experiments mechanical allodynia was measured just before (30 min) and 0.25, 0.5, 1, 2, 4 and 6 h post injection. Some C57BL/6 mice were pretreated with HC-030031 (100 mg kg^{-1}, i.p.) or capsazepine (10 mg kg^{-1}, i.p.) or their respective vehicles (4% DMSO and 4% Tween20 in isotonic solution), 60 min and 30 min, respectively, before exemestane (10 nmol) or letrozole (20 nmol) i.pl. injection. Mechanical allodynia was measured 60 min after AIs i.pl. injection.

In a second set of experiments, nociceptive behaviour and mechanical allodynia were assayed before and after systemic administration of exemestane (5 mg kg^{-1}, i.p. or 10 mg kg^{-1}, i.g.) and letrozole (0.5 mg kg^{-1}, i.p. or i.g.), or their vehicles (5% DMSO for i.p. or 0.5% carboxymethylcellulose, CMC, for i.g. administration), in C57BL/6 mice or *Trpa1*$^{+/+}$ and *Trpa1*$^{-/-}$ mice. Mechanical allodynia was measured just before (30 min) and 1, 3, 6, 24, 48 h after injection. Some animals 2 h after AI administration received HC-030031 (100 mg kg^{-1}, i.p.) or its vehicle (4% DMSO and 4% Tween80 in isotonic solution), and mechanical allodynia and the forelimb grip strength were measured 1 and 3 h after vehicle or HC-030031. In a third series of experiments, *Trpa1*$^{+/+}$ and *Trpa1*$^{-/-}$ mice were treated i.p. once a day for 15 consecutive days with exemestane or letrozole at the dose of 5 or 0.5 mg kg^{-1}, respectively, or with their vehicle (5% DMSO) and with i.g. exemestane or letrozole at the dose of 10 or 0.5 mg kg^{-1}, respectively, or with their vehicle (0.5% CMC). Mechanical allodynia and the forelimb grip strength were measured 10 min before and 1, 3, 6 and 24 h post administration at day 1, 5, 10 and 15.

To test whether PAR2 activation enhances the nocifensor behaviour evoked by exemestane and letrozole, in another experimental setting, the PAR2 activating peptide (PAR2-AP), SLIGRL-NH_2, (10 μg/10 μl i.pl.) or its reversed inactive form (PAR2-RP), LRGILS-NH_2, (10 μg per 10 μl i.pl.), were injected in the right hind paw. Ten minutes after i.pl. PAR2-AP or PAR2-RP injection, mice received exemestane (10 nmol per 10 μl i.pl.) or letrozole (20 nmol per 10 μl, i.pl.), or their vehicle (5% DMSO), in the plantar surface in the same paw injected with PAR2-AP or PAR2-RP, and the acute nociceptive behaviour was recorded. In another series of experiments H_2O_2 (0.5 μmol per 10 μl, i.pl.) or its vehicle was injected and the acute nocifensor behaviour to H_2O_2, which did not last longer than 5 min, was recorded for 10 min. Ten minutes after vehicle/H_2O_2, exemestane (10 nmol per 10 μl i.pl.) or letrozole (20 nmol per 10 μl, i.pl.) was injected in the same paw injected with H_2O_2 or vehicle and the acute nociceptive behaviour in response to AIs was recorded. Three hours after systemic administration of exemestane (5 mg kg^{-1}, i.p.) or letrozole (0.5 mg kg^{-1}, i.p.), mice were locally injected with H_2O_2 (0.5 μmol per 20 μl, i.pl.) or its vehicle and both acute nocifensor behaviour and mechanical allodynia were recorded.

Acute nocifensive response. AITC (10 nmol per paw), exemestane (10 nmol per paw), letrozole (20 nmol per paw) or their vehicles (5% DMSO), H_2O_2 (0.5 μmol per paw) or its vehicle (isotonic solution) and PAR2-AP or PAR2-RP (10 μg per paw) (10 or 20 μl) were injected into the paw of C57BL/6, *Trpa1*$^{+/+}$ and *Trpa1*$^{-/-}$ mice, and immediately after injection animals were placed in a plexiglas chamber. The total time spent licking and lifting the injected hind paw was recorded for 5 min as previously described[30].

Mechanical stimulation (von frey hair test). Mechanical threshold was measured in C57BL/6, *Trpa1*$^{+/+}$ and *Trpa1*$^{-/-}$ mice after both local (i.pl.) administration of AITC (10 nmol per paw), exemestane (10 nmol per paw), letrozole (20 nmol per paw) or their vehicles (5% DMSO), H_2O_2 (0.5 μmol per paw) or its vehicle (isotonic solution), and systemic (i.p.) administration of exemestane (5 mg kg^{-1}, i.p.) or letrozole (0.5 mg kg^{-1}, i.p.) at different time points by using the up-and-down paradigm[66]. Mechanical nociceptive threshold was determined before (basal level threshold) and after different treatments. The 50% mechanical paw withdrawal threshold response (in g) was then calculated from these scores, as previously described[66,67].

Forelimb grip strength test. The grip strength test was performed with a grip strength meter (Ugo Basile, Varese, Italy), as previously reported[68]. Mice were allowed to grasp a triangular ring attached to a force transducer and gently pulled away by the base of the tail until the grip was broken. The test was repeated four times and the mean peak force values (g) were calculated for each animal. The grip strength was measured in C57BL/6, *Trpa1*$^{+/+}$ and *Trpa1*$^{-/-}$ mice 10 min before and 1, 3, 6 and 24 h post AI administration.

Paw oedema. AITC (10 nmol per paw), exemestane (10 nmol per paw), letrozole (20 nmol per paw) or their vehicles (5% DMSO) (all 20 μl) were injected into the paw of C57BL/6, *Trpa1*$^{+/+}$ and *Trpa1*$^{-/-}$ mice, and paw thickness was measured to determine the development and severity of oedema in the hind paws. Some animals received HC-030031 (100 mg kg^{-1}, i.p.), a combination of L-733,060 and CGRP8-37 (both, 2 μmol/kg, i.v.), or their vehicles (4% DMSO and 4% Tween20 in isotonic solution for HC-030031, and isotonic solution for L-733,060 and CGRP8-37) before stimuli. An engineer's micrometer, with 0.01 mm accuracy (Harvard Apparatus, Kent, UK), was used to measure the paw thickness in millimeters (mm), before and after (60 and 120 min) the i.pl. injection with tested agents by an investigator blinded to treatments. Data were expressed as the increase in mm in paw thickness.

CGRP-like immunoreactivity (LI) assay. For neuropeptide release experiments, 0.4 mm slices of rat and *Trpa1*$^{+/+}$ or *Trpa1*$^{-/-}$ mouse spinal cords were superfused with an aerated (95% O_2 and 5% CO_2) Krebs solution containing (in mM): 119 NaCl, 25 $NaHCO_3$, 1.2 KH_2PO_4, 1.5 $MgSO_4$, 2.5 $CaCl_2$, 4.7 KCl, 11 D-glucose; the solution was maintained at 37 °C, and was added with 0.1% bovine serum albumin, and, to minimize peptide degradation, with the angiotensin converting enzyme inhibitor, captopril (1 μM), and the neutral endopeptidase inhibitor, phosphoramidon (1 μM). Tissues were stimulated with exemestane, letrozole or anastrozole (all 100 μM) or their vehicles (0.05% DMSO) dissolved in the Krebs solution. Some tissues were pre-exposed to capsaicin (10 μM, 20 min) or pretreated with HC-030031 (50 μM). Fractions (4 ml) of superfusate were collected at 10-min intervals before, during and after administration of the *stimulus* and then freeze-dried, reconstituted with assay buffer and analysed for CGRP-like immunoreactivity (LI) by an ELISA assay kit (Bertin Pharma, Montigny le Bretonneux, France). CGRP-LI was calculated by subtracting the mean *pre-stimulus* value from those obtained during or after stimulation. Detection limits of the assays were 5 pg ml^{-1}. Results are expressed as femtomoles of peptide per g of tissue per 10 min.

In another set of experiments, exemestane (5 nmol per 50 μl) and letrozole (10 nmol per 50 μl) or their vehicle (1% DMSO) were i.a. injected in anaesthetized (sodium pentobarbital, 50 mg kg^{-1} i.p.) rats. Ten minutes after injection, rats were killed and the knee joint was dissected[69]. CGRP-LI was measured in the synovial fluid lavage added with captopril (1 μM) and phosphoramidon (1 μM) by using the ELISA assay kit as previously described[69]. Detection limits of the assays were 5 pg ml^{-1}. Results are expressed as femtomoles of peptide per g of tissue per 20 min in the spinal cord experiments or pg ml^{-1} in the rat synovial fluid.

Assay of exemestane and letrozole by liquid chromatography-mass spectrometry. Blood samples (100 μl) were obtained by venepuncture of the tail vein from each mouse at different time points (0.25, 0.5, 1, 3, 6 and 24 h) after i.g. administration of exemestane (10 mg kg^{-1}) or letrozole (0.5 mg kg^{-1}). Blood samples were dropped on a filter paper (903 Whatman GmbH, Dassel, Germany) to obtain dried blood spots (DBS)[70], which were punched, obtaining a 6.0 mm diameter disk, containing ~6 μl of blood. DBS transferred into a 2-ml Eppendorf vial was extracted with 200 μl of methanol:water (95:5, v/v) containing 0.1% acetic acid and the appropriate internal standard (for letrozole and exemestane quantification, extracting solutions contained 5 μg l^{-1} of anastrozole or 2 μg l^{-1} of letrozole, respectively) and after shaking with an orbital shaker for 25 min at 37 °C, solutions were dried under a gentle nitrogen stream. Residues were reconstituted with 40 μl water containing 0.1% of acetic acid.

Samples were measured using a 1290 Infinity liquid chromatograph (LC, Agilent Technologies, Waldbronn, Germany) coupled to a QTRAP 5500 (AB SCIEX, Toronto, Canada) equipped with the Turbo Ion Spray source operating in positive ion mode. The capillary voltage was set to 5 kV. Heated turbo gas (400 °C, air) at a flow rate of 10.0 l min^{-1} was used. The transitions (quantifier and qualifier) recorded in Multiple Reaction Monitoring (MRM) mode were 286.1 > 217.1 and 286.1 > 190.1 for letrozole, 294.1 > 225.1 and 294.1 > 210.1 for anastrozole and 297.1 > 121.0 and 297.1 > 93.1 for exemestane. The LC column was a Gemini C6-Phenyl (100 × 2 mm^2, 3 μm) with the corresponding 4 × 2 mm^2 SecurityGuard™ cartridge (Phenomenex, Torrance, CA), operated at 0.3 ml min^{-1}. Eluent A (water + 0.1% acetic acid) and B (acetonitrile) were used. The gradient elution programme was as follows: 20% B maintained for 2 min, then to 90% B in 7 min, back to 20% B in 1 min and re-equilibrated for a 20 min total run time. Anastrozole, exemestane and letrozole retention times were 6.12, 6.31 and 7.45 min, respectively. Four microlitres of the extracted sample were injected for LC-MS/MS assays. System control and data acquisition were done by Analyst 1.5.1 software, and calibration curves were calculated using the non-weighted linear least-square regression of Analyst Quantitation programme (AB SCIEX, Toronto, Canada).

Calibration curves were constructed for both exemestane and letrozole, using the appropriate internal standard. Whole-blood from control mouse was spiked with different concentrations of exemestane (from 2 to 100 μg l^{-1}) or letrozole (from 10 to 200 μg l^{-1}). A 20 μl volume for each fortified blood sample was spotted on filter paper (DBS) and then treated as described in sample preparation. Each calibration curve was prepared in duplicate. Satisfying linearity was obtained for the two analytes (letrozole, $r = 0.996$; exemestane, $r = 0.998$). Each analytical batch included a double blank sample (without internal standard), a blank sample (with internal standard), five or six standard concentrations for calibration curve, and a set of treated mouse samples (each prepared in duplicate). LC-MS grade acetic acid, methanol, water and acetonitrile were supplied by Sigma Aldrich (Milan, Italy).

Statistical analysis. Data represent mean ± s.e.m. or confidence interval (CI). Statistical analysis was performed by the unpaired two-tailed Student's *t*-test for comparisons between two groups, the ANOVA, followed by the Bonferroni *post-*

hoc test for comparisons between multiple groups. Agonist potency was expressed as half maximal effective concentration (EC_{50}), that is, the molar concentration of agonist producing 50% of the maximum measured effect and 95% confidence interval (CI). $P<0.05$ was considered statistically significant (GraphPadPrism version 5.00, San Diego, CA).

References

1. Gibson, L., Lawrence, D., Dawson, C. & Bliss, J. Aromatase inhibitors for treatment of advanced breast cancer in postmenopausal women. *Cochrane Database Syst. Rev.* **7,** CD003370 (2009).
2. Burstein, H. J. *et al.* American Society of Clinical Oncology clinical practice guideline: update on adjuvant endocrine therapy for women with hormone receptor-positive breast cancer. *J. Clin. Oncol.* **28,** 3784–3796 (2010).
3. Cuzick, J. *et al.* Effect of anastrozole and tamoxifen as adjuvant treatment for early-stage breast cancer: 10-year analysis of the ATAC trial. *Lancet Oncol.* **11,** 1135–1141 (2013).
4. Nabholtz, J. M. Long-term safety of aromatase inhibitors in the treatment of breast cancer. *Ther. Clin. Risk Manag.* **4,** 189–204 (2008).
5. Connor, C. & Attai, D. Adjuvant endocrine therapy for the surgeon: options, side effects, and their management. *Ann. Surg. Oncol.* **20,** 3188–3193 (2013).
6. Mouridsen, H. T. Incidence and management of side effects associated with aromatase inhibitors in the adjuvant treatment of breast cancer in postmenopausal women. *Curr. Med. Res. Opin.* **22,** 1609–1621 (2006).
7. Crew, K. D. *et al.* Prevalence of joint symptoms in postmenopausal women taking aromatase inhibitors for early-stage breast cancer. *J. Clin. Oncol.* **25,** 3877–3883 (2007).
8. Henry, N. L. *et al.* Prospective characterization of musculoskeletal symptoms in early stage breast cancer patients treated with aromatase inhibitors. *Breast Cancer Res. Treat.* **111,** 365–372 (2008).
9. Laroche, F. *et al.* Classification of and risk factors for estrogen deprivation pain syndromes related to aromatase inhibitor treatments in women with breast cancer: a prospective multicenter cohort study. *J. Pain* **15,** 293–303 (2014).
10. Burstein, H. J. & Winer, E. P. Aromatase inhibitors and arthralgias: a new frontier in symptom management for breast cancer survivors. *J. Clin. Oncol.* **25,** 3797–3799 (2007).
11. Presant, C. A. *et al.* Aromatase inhibitor-associated arthralgia and/or bone pain: frequency and characterization in non-clinical trial patients. *Clin. Breast Cancer* **7,** 775–778 (2007).
12. Morales, L. *et al.* Debilitating musculoskeletal pain and stiffness with letrozole and exemestane: associated tenosynovial changes on magnetic resonance imaging. *Breast Cancer Res. Treat* **104,** 87–91 (2007).
13. Henry, N. L. *et al.* Inflammatory cytokines and aromatase inhibitor-associated musculoskeletal syndrome: a case-control study. *Br. J. Cancer* **103,** 291–296 (2010).
14. Mao, J. J. *et al.* Online discussion of drug side effects and discontinuation among breast cancer survivors. *Pharmacoepidemiol. Drug Saf.* **22,** 256–262 (2013).
15. Sestak, I. *et al.* Risk factors for joint symptoms in patients enrolled in the ATAC trial: a retrospective, exploratory analysis. *Lancet Oncol.* **9,** 866–872 (2008).
16. Nilius, B., Owsianik, G., Voets, T. & Peters, J. A. Transient receptor potential cation channels in disease. *Physiol. Rev.* **87,** 165–217 (2007).
17. Clapham, D. E. TRP channels as cellular sensors. *Nature* **426,** 517–524 (2003).
18. Bautista, D. M. *et al.* TRPA1 mediates the inflammatory actions of environmental irritants and proalgesic agents. *Cell* **124,** 1269–1282 (2006).
19. Trevisani, M. *et al.* 4-Hydroxynonenal, an endogenous aldehyde, causes pain and neurogenic inflammation through activation of the irritant receptor TRPA1. *Proc. Natl Acad. Sci. USA* **104,** 13519–13524 (2007).
20. Zhang, X. F., Chen, J., Faltynek, C. R., Moreland, R. B. & Neelands, T. R. Transient receptor potential A1 mediates an osmotically activated ion channel. *Eur. J. Neurosci.* **27,** 605–611 (2008).
21. Bandell, M. *et al.* Noxious cold ion channel TRPA1 is activated by pungent compounds and bradykinin. *Neuron* **41,** 849–857 (2004).
22. Karashima, Y. *et al.* TRPA1 acts as a cold sensor in vitro and in vivo. *Proc. Natl Acad. Sci. USA* **106,** 1273–1278 (2009).
23. del Camino, D. *et al.* TRPA1 contributes to cold hypersensitivity. *J. Neurosci.* **30,** 15165–15174 (2010).
24. Story, G. M. *et al.* ANKTM1, a TRP-like channel expressed in nociceptive neurons, is activated by cold temperatures. *Cell* **112,** 819–829 (2003).
25. Bhattacharya, M. R. *et al.* Radial stretch reveals distinct populations of mechanosensitive mammalian somatosensory neurons. *Proc. Natl Acad. Sci. USA* **105,** 20015–20020 (2008).
26. Geppetti, P. & Holzer, P. *Neurogenic Inflammation* (CRC Press, 1996).
27. Andersson, D. A., Gentry, C., Moss, S. & Bevan, S. Transient receptor potential A1 is a sensory receptor for multiple products of oxidative stress. *J. Neurosci.* **28,** 2485–2494 (2008).
28. Sawada, Y., Hosokawa, H., Matsumura, K. & Kobayashi, S. Activation of transient receptor potential ankyrin 1 by hydrogen peroxide. *Eur. J. Neurosci.* **27,** 1131–1142 (2008).
29. Taylor-Clark, T. E., Ghatta, S., Bettner, W. & Undem, B. J. Nitrooleic acid, an endogenous product of nitrative stress, activates nociceptive sensory nerves via the direct activation of TRPA1. *Mol. Pharmacol.* **75,** 820–829 (2009).
30. Materazzi, S. *et al.* Cox-dependent fatty acid metabolites cause pain through activation of the irritant receptor TRPA1. *Proc. Natl Acad. Sci. USA* **105,** 12045–12050 (2008).
31. Petrus, M. *et al.* A role of TRPA1 in mechanical hyperalgesia is revealed by pharmacological inhibition. *Mol. Pain* **3,** 40 (2007).
32. Eid, S. R. *et al.* HC-030031, a TRPA1 selective antagonist, attenuates inflammatory- and neuropathy-induced mechanical hypersensitivity. *Mol. Pain* **4,** 48 (2008).
33. da Costa, D. S. *et al.* The involvement of the transient receptor potential A1 (TRPA1) in the maintenance of mechanical and cold hyperalgesia in persistent inflammation. *Pain* **148,** 431–437 (2010).
34. McGaraughty, S. *et al.* TRPA1 modulation of spontaneous and mechanically evoked firing of spinal neurons in uninjured, osteoarthritic, and inflamed rats. *Mol. Pain* **6,** 14 (2010).
35. Obata, K. *et al.* TRPA1 induced in sensory neurons contributes to cold hyperalgesia after inflammation and nerve injury. *J. Clin. Invest.* **115,** 2393–2401 (2005).
36. Wei, H., Hamalainen, M. M., Saarnilehto, M., Koivisto, A. & Pertovaara, A. Attenuation of mechanical hypersensitivity by an antagonist of the TRPA1 ion channel in diabetic animals. *Anesthesiology* **111,** 147–154 (2009).
37. Nassini, R. *et al.* Oxaliplatin elicits mechanical and cold allodynia in rodents via TRPA1 receptor stimulation. *Pain* **152,** 1621–1631 (2011).
38. Materazzi, S. *et al.* TRPA1 and TRPV4 mediate paclitaxel-induced peripheral neuropathy in mice via a glutathione-sensitive mechanism. *Pflugers. Arch.* **463,** 561–569 (2012).
39. Trevisan, G. *et al.* Novel therapeutic strategy to prevent chemotherapy-induced persistent sensory neuropathy by TRPA1 blockade. *Cancer Res.* **73,** 3120–3131 (2013).
40. Liu, H. & Talalay, P. Relevance of anti-inflammatory and antioxidant activities of exemestane and synergism with sulforaphane for disease prevention. *Proc. Natl Acad. Sci. USA* **110,** 19065–19070 (2013).
41. Hinman, A., Chuang, H. H., Bautista, D. M. & Julius, D. TRP channel activation by reversible covalent modification. *Proc. Natl Acad. Sci. USA* **103,** 19564–19568 (2006).
42. Macpherson, L. J. *et al.* An ion channel essential for sensing chemical damage. *J. Neurosci.* **27,** 11412–11415 (2007).
43. Brone, B. *et al.* Tear gasses CN, CR, and CS are potent activators of the human TRPA1 receptor. *Toxicol. Appl. Pharmacol.* **231,** 150–156 (2008).
44. McNamara, C. R. *et al.* TRPA1 mediates formalin-induced pain. *Proc. Natl Acad. Sci. USA* **104,** 13525–13530 (2007).
45. Andre, E. *et al.* Cigarette smoke-induced neurogenic inflammation is mediated by alpha,beta-unsaturated aldehydes and the TRPA1 receptor in rodents. *J. Clin. Invest.* **118,** 2574–2582 (2008).
46. Steinhoff, M. S., von Mentzer, B., Geppetti, P., Pothoulakis, C. & Bunnett, N. W. Tachykinins and their receptors: contributions to physiological control and the mechanisms of disease. *Physiol. Rev.* **94,** 265–301 (2014).
47. Reagan-Shaw, S., Nihal, M. & Ahmad, N. Dose translation from animal to human studies revisited. *Faseb J.* **22,** 659–661 (2008).
48. Lintermans, A. *et al.* Aromatase inhibitor-induced loss of grip strength is body mass index dependent: hypothesis-generating findings for its pathogenesis. *Ann. Oncol.* **22,** 1763–1769 (2011).
49. Jin, S. J. *et al.* The pharmacokinetics of letrozole: association with key body mass metrics. *Int. J. Clin. Pharmacol. Ther.* **50,** 557–565 (2012).
50. Jukanti, R., Sheela, S., Bandari, S. & Veerareddy, P. R. Enhanced bioavailability of exemestane via proliposomes based transdermal delivery. *J. Pharm. Sci.* **100,** 3208–3222 (2011).
51. Valle, M. *et al.* A predictive model for exemestane pharmacokinetics/pharmacodynamics incorporating the effect of food and formulation. *Br. J. Clin. Pharmacol.* **59,** 355–364 (2005).
52. Dai, Y. *et al.* Sensitization of TRPA1 by PAR2 contributes to the sensation of inflammatory pain. *J. Clin. Invest.* **117,** 1979–1987 (2007).
53. Wang, S. *et al.* Phospholipase C and protein kinase A mediate bradykinin sensitization of TRPA1: a molecular mechanism of inflammatory pain. *Brain* **131,** 1241–1251 (2008).
54. Vergnolle, N. *et al.* Proteinase-activated receptor-2 and hyperalgesia: A novel pain pathway. *Nat. Med.* **7,** 821–826 (2001).
55. Dalle-Donne, I. *et al.* Actin Cys374 as a nucleophilic target of alpha,beta-unsaturated aldehydes. *Free Radic. Biol. Med.* **42,** 583–598 (2007).
56. Oballa, R. M. *et al.* A generally applicable method for assessing the electrophilicity and reactivity of diverse nitrile-containing compounds. *Bioorg. Med. Chem. Lett.* **17,** 998–1002 (2007).

57. Moran, M. M., McAlexander, M. A., Biro, T. & Szallasi, A. Transient receptor potential channels as therapeutic targets. *Nat. Rev. Drug Discov.* **10,** 601–620 (2011).
58. Kennecke, H. F. *et al.* Late risk of relapse and mortality among postmenopausal women with estrogen responsive early breast cancer after 5 years of tamoxifen. *Ann. Oncol.* **18,** 45–51 (2007).
59. Sies, H. Role of metabolic H2O2 generation: redox signaling and oxidative stress. *J. Biol. Chem.* **289,** 8735–8741 (2014).
60. Spinelli, O. *et al.* Pharmacokinetics (PK) of Aromasin ® (exemestane, EXE) after single and repeated doses in healthy postmenopausal volunteers (HPV). *Eur. J. Cancer* **35,** S295 (1999).
61. Desta, Z. *et al.* Plasma letrozole concentrations in postmenopausal women with breast cancer are associated with CYP2A6 genetic variants, body mass index, and age. *Clin. Pharmacol. Ther.* **90,** 693–700 (2011).
62. Dowsett, M., Cuzick, J., Howell, A. & Jackson, I. Pharmacokinetics of anastrozole and tamoxifen alone, and in combination, during adjuvant endocrine therapy for early breast cancer in postmenopausal women: a sub-protocol of the 'Arimidex and tamoxifen alone or in combination' (ATAC) trial. *Br. J. Cancer* **85,** 317–324 (2001).
63. Kwan, K. Y. *et al.* TRPA1 contributes to cold, mechanical, and chemical nociception but is not essential for hair-cell transduction. *Neuron* **50,** 277–289 (2006).
64. Nassini, R. *et al.* The 'headache tree' via umbellulone and TRPA1 activates the trigeminovascular system. *Brain* **135,** 376–390 (2012).
65. Materazzi, S. *et al.* Parthenolide inhibits nociception and neurogenic vasodilatation in the trigeminovascular system by targeting the TRPA1 channel. *Pain* **3959,** 00438–00437 (2013).
66. Chaplan, S. R., Bach, F. W., Pogrel, J. W., Chung, J. M. & Yaksh, T. L. Quantitative assessment of tactile allodynia in the rat paw. *J. Neurosci. Methods* **53,** 55–63 (1994).
67. Dixon, W. J. Efficient analysis of experimental observations. *Annu. Rev. Pharmacol. Toxicol.* **20,** 441–462 (1980).
68. Doig, J. *et al.* In vivo characterization of the role of tissue-specific translation elongation factor 1A2 in protein synthesis reveals insights into muscle atrophy. *Febs J.* **280,** 6528–6540 (2013).
69. Trevisan, G. *et al.* TRPA1 receptor stimulation by hydrogen peroxide is critical to trigger hyperalgesia and inflammation in a model of acute gout. *Free Radic. Biol. Med.* **72,** 200–209 (2014).
70. la Marca, G. *et al.* Rapid assay of topiramate in dried blood spots by a new liquid chromatography-tandem mass spectrometric method. *J. Pharm. Biomed. Anal.* **48,** 1392–1396 (2008).

Acknowledgements

This work was supported by grants from Associazione Italiana per la Ricerca sul Cancro (AIRC), Milan, Italy (R.N.); Ente Cassa di Risparmio di Firenze, Florence, Italy (S.M.; G.M.); Ministero dell'Istruzione, dell'Università e della Ricerca, PRIN-2010Y4WMCR-007 (S.M.) and Ministero Sviluppo Economico, IMPACT Project, Rome, Italy (P.G.).

Author contributions

C.F., R.N., S.M., P.G., S.B., M.R.D.T., T.S. and T.T. designed experiments, interpreted results and wrote the paper. C.F., S.M. and F.D.L. performed calcium experiments, E.C. performed electrophysiological experiments, R.N., I.M.M., G.T. and D.M. performed *in vivo* experiments, G.M. and G.P. performed mass spectrometry analyses.

Additional information

Supplementary Information accompanies this paper at http://www.nature.com/naturecommunications

Competing financial interests: The authors declare no competing financial interests.

Reprints and permission information is available online at http://npg.nature.com/reprintsandpermissions/

How to cite this article: Fusi, C. *et al.* Steroidal and non-steroidal third-generation aromatase inhibitors induce pain-like symptoms via TRPA1. *Nat. Commun.* 5:5736 doi: 10.1038/ncomms6736 (2014).